SYNTHESIS AND CHARACTERIZATION OF SEVEN THIOPHOSPHATE

ANALOGS OF CYCLIC DIGUANOSINE MONOPHOSPHATE

by

JIANWEI ZHAO

A Dissertation submitted to the

Graduate School-New Brunswick

Rutgers, The State University of New Jersey

in partial fulfillment of the requirements

for the degree of

Doctor of Philosophy

Graduate Program in Chemistry and Chemical Biology

written under the direction of

Professor Roger A. Jones

and approved by

_____

_____

_____

_____

New Brunswick, New Jersey

[May, 2009]

ABSTRACT OF THE DISSERTATION

SYNTHESIS AND CHARACTERIZATION OF SEVEN THIOPHOSPHATE ANALOGS OF CYCLIC DIGUANOSINE MONOPHOSPHATE

by JIANWEI ZHAO

Dissertation Director:

Professor Roger A. Jones

Cyclic diguanosine monophosphate (c-di-GMP) was first identified as an activator of bacterial cellulose synthase in 1987. Since then, it has been recognized as an important second messenger molecule in many bacterial processes, including cellulose synthesis, biofilm formation, and host-pathogen interactions. More recently, it found to stimulate innate immunity in mammals. The monothiophosphate analog was synthesized some years ago and was shown to be a highly potent activator/second messenger with a high stability to enzymatic degradation.

In the work presented here, synthetic methods have been developed to synthesize mono-, di- and trithiophosphate c-di-GMP analogs. All seven diastereomers of these analogs have been separated and purified. Stereochemistry of the two diastereomers of

the monothioate analog was assigned by enzymatic digestion of the linear dimer, as well as direct enzymatic degradation of the cyclic dimers. In addition, the same linear dimer was cyclized to produce a cyclic dimer of known configuration. The correlation between stereochemistry and ^{31}P NMR chemical shifts of the two diastereomers of the monothioate was then used to assign configurations of the di- and trithiophosphate analogs.

1D ^{1}H and ^{31}P NMR, as well as 2D NOSEY and DOSY were used to characterize all seven thiophosphate analogs in both Na$^+$ and K$^+$ forms. It was found that the [*S*] sulfurs, as well as the counterions, display dramatic effects on the equilibrium among five different complexes that can form. It is concluded that: 1) in all cases, the presence of an [*S*] sulfur promotes more extensive complex formation than [*R*]; 2) in both Na$^+$ and K$^+$ forms, two [*S*] sulfurs promote extensive aggregation, forming large aggregates that cannot be observed in the NMR spectra; 3) K$^+$ promotes more extensive complex formation than Na$^+$, with primarily octamolecular complexes in the K$^+$ forms, but tetramolecular complexes in the Na$^+$ forms; and 4) in all the Na$^+$ forms, but not the K$^+$ forms, the presence of one [*S*] sulfur stabilizes *anti* complexes and/or destabilizes *syn* complexes.

DEDICATION

This work is dedicated to my parents, Zhuoyao Zhao and Shufen Liu, my wife,

Yunlin Fu, and my son, Kevin Zhao.

ACKNOWLEDGEMENTS

TABLE OF CONTENTS

Chapter 1

I. Biological background of c-di-GMP 1

II. Synthetic background for c-di-GMP 12

III. Structural properties of c-di-GMP..23

Chapter 3

LIST OF FIGURES

Chapter 1

Chapter 2

Chapter 3

LIST OF SCHEMES

Chapter 1

Chapter 2

LIST OF TABLES

LIST OF ABBREVIATIONS

2D DOSY	two dimensional diffusion ordered spectroscopy
2D NOESY	two dimensional nuclear overhauser effect spectroscopy
A	adenosine
Ad-Cl	adamantanecarbonyl chloride
ATP	adenosine triphosphate
cAMP	cyclic adenosine monophosphate
CD	circular dichroism
CDBGP	c-di-GMP binding protein
c-di-GMP	cyclic diguanosine monophosphate
Cpep	1-(4-chlorophenyl)-4-ethoxypiperidine-4-yl
cGMP	cyclic guanosine monophosphate
DCA	dichloroacetic acid
DGC	diguanylate cyclase
DMT	dimethoxyltrityl
DNA	deoxyribonucleic acid
DPP-H	diphenyl phosphite
DPP-Cl	diphenyl phosphorochloridate
ESI	electrospray ionization
G	guanosine
GTP	guanosine triphosphate
GpG	guanosine linear dimer

GpsG	guanosine linear dimer monothioate
HPLC	high performance liquid chromatography
Ib-Cl	isobutyryl chloride
IMP	imidazolium perchlorate
LC/MS	liquid chromatography/mass spectrometry
m/z	mass/charge ratio
NBS	N-bromosuccinimide
NMI	N-methyl imidazole
NMR	nuclear magnetic resonance
OD	optical density
PDE-A	phosphodiesterase A
Pry	pyridine
Pry·HF	pyridine hydrogen fluoride
Pyr·TFA	pyridinium trifluoroacetate
Pv-Cl	pivaloyl chloride
RNA	ribonucleic acid
RP	reverse phase
S_8	elemental sulfur
TBS	*tert*-butyldimethylsilyl
t-BuMe$_2$SiCl	*tert*-butyldimethylsilyl chloride
t-Bu$_2$Si(OTf)$_2$	di-*tert*-butylsilyl ditriflate
TEA	triethylamine
TEA·3HF	triethylamine trihydrogen fluoride

TEAA	triethylammonium acetate
TMG	tetramethyl guanidine
TPS-Cl	2,4,6-triisopropyl benzenesulfonyl chloride
TPS-NT	2,4,6-triisopropyl benzenesulfonyl-3-nitro-1,2,4-trizaole
UDP	uridine diphosphate
UV	ultraviolet

Chapter 1

Introduction to c-di-GMP

Cyclic diguanosine monophosphate (c-di-GMP), shown in **Figure 1-1**, was first identified as an activator of the synthesis of cellulose in the bacterium *Acetobacter xylinum* (now named *Gluconacetobacter*).[1] More recently, it has been recognized as an important second messenger molecule in many bacterial processes.[2-9] The known roles of c-di-GMP as a signaling molecule include activation of cellulose synthesis, biofilm formation, control of pole morphogenesis, and regulation host-pathogen interactions. Although c-di-GMP only occurs naturally in bacteria, it has very recently been found to stimulate innate immunity in mammals.[10, 11] Monothiophosphate analogs of c-di-GMP, both [R] and [S] diastereomers, were synthesized and used to test the binding affinity to cellulose synthase and phosphodiesterase (PDE-A).[12] It was shown that what was thought to be the [S] monothiophosphate analog, which is highly resistant to enzymatic hydrolysis, bound to cellulose synthase and PDE-A with a similar affinity as unmodified c-di-GMP. The authors proposed that other thiophosphate analogs, with a high stability to enzyme degradation, could be highly potent activator/second messengers.

I. Biological background of c-di-GMP

I1. c-di-GMP regulates cellulose synthesis
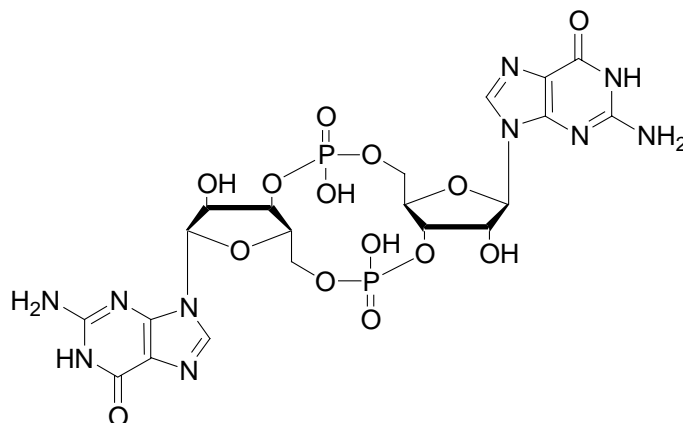
Figure 1-1. Chemical structure of c-di-GMP

Cyclic ribodinucleotides have been an important research topic because of their biological functions since the 1980s, when c-di-UMP was found to act as a potent linear competitive inhibitor of RNA polymerase.[13, 14] However, particular interest was focused on (3'-5')-cyclic diguanosine monophosphate (c-di-GMP) in 1987, when Moshe Benziman[1] first published a landmark paper in *Nature* that demonstrated that cellulose biogenesis in the bacterium *A. xylinum* could be activated by c-di-GMP. The identity of c-di-GMP was first determined in Benziman's work by comparison of the biological material with a chemically synthesized sample, using enzyme activity, NMR and HPLC analysis.

The biological synthesis of cellulose has been postulated to involve several tightly coupled processes, in which glucose is polymerized into polyglucan chains which are then assembled into rigid fibrils.[15] An enzyme called cellulose synthase was identified as being responsible for the polymerization of glucose from UDP-glucose into a β-1,4-linked chain, and the activity of this enzyme was found to be regulated by c-di-GMP.

The allosteric effect of the activator c-di-GMP on cellulose synthase activity is based on its intracellular concentration. Two kinds of enzymes were identified that maintain the cellular level of c-di-GMP.[12] One is diguanylate cyclase (DGC), which catalyzes c-di-GMP formation from two molecules of GTP in a two-step reaction, via the intermediate linear triphosphate pppGpG. The other is a phosphodiesterase (PDE), which degrades the activator, also in a two-step process. First, PDE-A, a membrane-bound phosphodiesterase, degrades c-di-GMP to a linear 5'-phosphoryl dimer, pGpG. This product is then further hydrolyzed to two molecules of 5'-GMP by another phosphodiesterase, PDE-B. A comparison of enzymatic activities of PDE-A and PDE-B shows specific inhibition of PDE-A by low concentrations of Ca^{2+} cations, indicating that cellular Ca^{2+} concentration helps to regulate cellulose synthesis.[12]

From the *A. xylinum* gene that encodes diguanylate cyclase, three *cdg* operons that are involved in c-di-GMP metabolism were isolated using GTP-agarose affinity chromatography, followed by reverse genetics.[16] These three operons, called *cdg*1, *cdg*2, and *cdg*3, were found to encode three different isoforms of diguanylate cyclases and phosphodiesterases. Nucleotide sequence analysis showed that within each operon, a *pde*A gene lay upstream of a *dgc* gene at the C-terminus, with an oxygen sensory domain at the N-terminus. These *dgc* and *pde*A genes encoded multidomain proteins that contained a consensus motif with a central GGDEF domain and a C-terminal EAL domain, which were named after the recurring patterns of amino acids. Disruption of the *cdg* gene, which resulted in no expression of DGC and PDE-A, reduced cellulose

production *in vivo*, indicating that c-di-GMP is essential for cellulose biosynthesis. Since the GGDEF and EAL domains were also found in many other bacterial proteins, it was suggested that c-di-GMP may not only be involved in the activation of cellulose synthase, but may also possess other regulatory functions for different cellular processes, such as cell adhesion and biofilm formation.

I2. c-di-GMP functions in biofilm formation

Bacterial biofilms are formed when free-living bacteria aggregate to create a multicellular complex that is attached to a solid surface and is encased in an exopolysaccharide matrix. Recent studies[17, 18] showed that biofilm formation in different bacteria, such as *Salmonella typhimurium*, *Salmonella enteritidis* and *Escherichia coli*, was characterized by an increased production of extracellular matrix. The formation of biofilms protects the bacteria and allows them to survive even in a challenging environment, such as strong UV exposure, acid exposure, metal toxicity, dehydration, salinity and phagocytosis. Mah and O'Toole's work[19] showed that biofilms have a 10-1000 times increased antibiotic resistance compared to free bacteria. This has an enormous impact on medical treatment, since biofilm can form on many medical implants due to this resistance to antimicrobial agents. The formation of biofilms can also cause serious problems in environmental and industrial fields, such as air conditioning systems and pipelines. The mechanism of the antibiotic resistance of biofilms is not clear. Stewart[20] has proposed three possibilities, all of which are highly dependent on the multicellular nature of the biofilms.

Biofilm formation is influenced by many factors, such as environmental conditions, change of gene expression, and intercellular signaling. The first correlation between biofilm formation and c-di-GMP was reported in 2004, when two important papers were published in the same issue of the journal *Molecular Microbiology*. Camilli's work[21] on virulence gene regulation in *Vibrio cholerae* revealed that the intracellular level of c-di-GMP was down-regulated by protein VieA, and the resulting lowered concentration of c-di-GMP caused repression of exopolysaccharide synthesis, which in turn decreased biofilm formation. Although the mechanism for the influence of c-di-GMP on exopolysaccharide synthesis was not clear, the authors suggested that proteins containing c-di-GMP synthase and phosphodiesterase domains were involved in the regulation of biofilm formation by controlling c-di-GMP concentration.

At the same time, Römling[22] found that in the bacterium *Salmonella typhimurium*, two proteins called AdrA and YhjH were involved in the turnover of c-di-GMP *in vivo*, thereby regulating cellulose synthesis. AdrA, containing a GGDEF domain, was responsible for the production of c-di-GMP, and YhjH, containing an EAL domain, reduced its intracellular concentration. Further study of multicelluar behaviors of *S. typhimurium*, including biofilm formation and transition from sessility to motility, confirmed that these two proteins had opposite effects. Group swarming of *S. typhimurium* was dramatically stimulated by YhjH, which was correlated with lower c-di-GMP concentration, but inhibited by AdrA, which was correlated with higher c-di-GMP concentration. The same opposing effects were found on independent swimming of *S.*

typhimurium, which was stimulated by YhjH, but significantly inhibited by AdrA. Furthermore, biofilm formation in two other bacterial systems, the pathogen *Pseudomonas aeruginosa* and the commensal *Escherichia coli*, was enhanced by the expression of AdrA and repressed by YhjH.

I3. c-di-GMP functions in mammals

More strikingly, c-di-GMP was recently found to possess "drug-like" properties.[10, 11, 23, 24] In 2005, Karaolis[23] reported that at a non-lethal cytotoxic concentration (≤50 μM), c-di-GMP inhibited both basal and growth factor-stimulated human colon cancer cell proliferation *in vitro*. They found that c-di-GMP inhibited *Staphylococcus aureus* cell-cell interactions and biofilm formation, and reduced the *S. aureus* infection in a mouse mastitis model.[24] A second study by Karaolis[10] reported that pretreatment of mice with c-di-GMP had significant protective and prophylactic effects against *S. aureus* infection. Furthermore, c-di-GMP stimulated the maturation of human immature dendritic cells. In addition, they recently reported that administration of c-di-GMP stimulated protective innate immunity against *Klebsilla pneumonia* infection in mice.[11] These authors have proposed a significant clinical potential for c-di-GMP as an immunomodulator, immune enhancer and vaccine adjuvant against respiratory infection and pneumonia.

I4. GGDEF and EAL domains control c-di-GMP concentration

As discussed in section **I1**, proteins containing GGDEF and EAL domains are found to be involved in the turnover of c-di-GMP, which acts as a second messenger in regulation of cellulose synthesis and biofilm formation. However, it took some time to verify the precise role of GGDEF and EAL domains in the control of c-di-GMP. The DGC and PDE-A proteins in *A. xylinum* were found to contain similar domain structures with highly homologous GGDEF and EAL motifs, which were later predicted to possess the enzymatic activities of cyclase and phosphodiesterase, respectively.[16] More recently, the functions of these two domains were more fully verified in different bacterial systems.[25-34]

The first biochemical demonstration of cyclase activity of a GGDEF domain was reported in 2004, by Jenal.[25] PleD, a C-terminal GGDEF domain-containing protein was found to be responsible for pole development in the *Caulobacter crescentus* cell cycle. Dynamic localization of PleD to the cell pole was correlated with phosphorylation of the N-terminal receiver domain in the protein, resulting in catalysis of the synthesis of c-di-GMP. Further study of the role of GGDEF domain proteins was published by Gomelsky [26] Six GGDEF domain-encoding genes from randomly chosen bacterial systems were cloned and overexpressed, and all resulting recombinant proteins were found to efficiently encode DGC. However, the overexpressed individual GGDEF domains showed only low activities, which indicates that the adjacent sensory protein domains were essential for full enzymatic activity of the GGDEF domains. These results are consistent with a previous report that the DGC activity of a GGDEF domain was dependent on the phosphorylation status of its N-terminal domain, which stimulated the

cyclase activity by two orders of magnitude. More recently, a GGDEF domain protein in *Pseudomonas putida*, YedQ, was shown to possess diguanylate cyclase activity, which up-regulated the intracellular concentration of c-di-GMP, resulting in increased biofilm formation.[28] WspR, a GGDEF domain protein in *Pseudomonas fluorescens*, was also found to control the cellular level of c-di-GMP, thereby regulating the overproduction of acetylated cellulose and cell attachment.[29] Mutational analysis showed that the RYGGDEF motif of WspR was highly conserved, since every mutation abolishes its cyclase function.

It has been found that DGC needs to be assembled into a dimer or trimer before it can regulate c-di-GMP production.[26, 35] A very recent report[36] that focused on the crystal structure of PleD, a GGDEF domain protein, confirmed that its dimerization was required for c-di-GMP synthesis. BeF_3^- modification of the PleD receiver domain was used to study the structural changes of PleD. The results showed that BeF_3^- promoted the dimer formation by facilitating an efficient encounter of two symmetric catalytic domains.

Phosphodiesterase activity has recently been assigned to the EAL domain.[4, 31-34] The biochemical characterization of this activity was first identified in 2005,[31] when CC3396, a GGDEF-EAL composite protein from *Caulobacter crescentus* was found to be a soluble PDE. The C-terminal EAL domain was shown to possess the PDE-A activity, which rapidly converted c-di-GMP into the linear dinucleotide pGpG. Instead of detectable DGC activity, the GGDEF domain of this protein was found to bind GTP and be responsible for activation of the neighboring EAL domain for the PDE-A activity.

Detailed study of YahA, an EAL domain-containing protein in *E. coli*, showed that both the full-length protein and the isolated EAL domain were able to hydrolyze c-di-GMP into linear pGpG.[32] Both reports showed that the phosphodiesterase activity of an EAL domain required Mg^{2+} or Mn^{2+}, but was strongly inhibited by Ca^{2+} and Zn^{2+}. A very recent example[34] of regulation of the swarming and sticking multicellular behavior of *Vibrio parahaemolyticus* by c-di-GMP showed that ScrG, an EAL domain protein, was sufficient to induce lateral flagellar gene expression, and decrease biofilm formation.

As with the GGDEF domain, N-terminal signaling and sensing domains were shown to be essential for enzymatic activity of the EAL domain, and function by modulating its substrate affinity. The stimulation of DGC by N-terminal phosphorylation, along with PDE-A modulation by the sensory domain, ensures the dynamic adjustment of c-di-GMP intracellular levels.

I5. c-di-GMP binds proteins and receptors

The cellular concentration of c-di-GMP in *A. xylinum* was estimated to be 5-10 μM.[37] However, it was found that only a small amount of c-di-GMP seemed to be free within the cell, with most of it being membrane-bound and also associated with c-di-GMP-binding protein (CDGBP), which was first found in *A. xylinum* in 1997.[38] This membrane-bound binding protein demonstrated high affinity, specificity, reversibility and saturability for the c-di-GMP substrate. The c-di-GMP generated by diguanylate cyclase bound to CDGBP, and was thereby protected from degradation by PDE-A. The cellular

level of free c-di-GMP released from the CDGBP controlled the pace of the glucose polymerization process. In addition, K^+ was found to be the only metal to increase the binding rate of c-di-GMP to CDGBP by 2~3 fold, from all the cations studied, including Li^+, Na^+, K^+, Rb^+, Cs^+. Thus, the cellular concentration of K^+ appears to help regulate cellulose synthesis by controlling the level of available c-di-GMP through its binding to CDGBP. It was confirmed that when K^+ was replaced by Na^+, cellulose synthesis was inhibited by ~ 90%.

Sequence analysis has shown that the PilZ domain is encoded in numerous bacterial genomes, including cellulose synthases, alginate biosynthesis protein Alg44, and firmicute YpfA families. The encoding pattern of the PilZ domain was reported to be similar to those of GGDEF (DGC) and c-di-GMP-specific EAL (PDE-A) domains.[39] It was therefore suggested that the PilZ domain serves as a c-di-GMP binding protein.[39] This hypothesis was later verified by Römling[40] who used YcgR from *E. coli*, a PilZ domain protein, to test its c-di-GMP binding activity both *in vivo* and *in vitro*. The full length YcgR bound to c-di-GMP tightly and specifically, with a K_d of 0.84 ± 0.16 μM. The isolated PilZ domain from YcgR also bound to c-di-GMP but with a lower affinity. Site-directed mutagenesis of YcgR confirmed that the conserved PilZ domain bound c-di-GMP directly, and was the only binding site within the YcgR protein. In late 2007, several c-di-GMP receptor-binding proteins were reported to be essential for controlling multicellular behavior in different bacterial systems. Alg44, a PilZ domain-containing protein, was found to bind c-di-GMP specifically, thereby regulating alginate biosynthesis in *Pseudomonas aeruginosa*.[41] Using affinity chromatography, Jenal[42] has

isolated several c-di-GMP binding proteins from *Caulobacter crescentus*. Among them, DgrA, a PilZ homolog, was proven to be a diguanylate receptor, which controlled cell motility by means of c-di-GMP motility.

PleD, a protein required for exopolysaccharide production in *Pseudomonas aeruginosa*, was also found to bind c-di-GMP.[43] The binding affinity of PleD to c-di-GMP was determined to be K_d 1 μM, suggesting one binding site per PleD protein. Sequence analysis demonstrated that no recognizable PilZ domain was present in this protein, but a different highly conserved motif was found to be responsible for the binding activity. Results from mutagenesis indicated that PleD is a novel c-di-GMP receptor that mediates c-di-GMP regulation of exopolysaccharide biosynthesis.

I6. c-di-GMP functions in different bacteria

From the first discovery of the novel regulator c-di-GMP in cellulose biosynthesis in *A. xylinum*,[1] the function of this cyclic dinucleotide in activation of cellulose synthase has been established in numerous bacterial systems, including *Agrobacterium tumefaciens*, *Rhizobium leguminosarum bv. trifolii*, *Escherichia coli*, and *Klebsiella pneumoniae*.[2, 18, 37, 44, 45] In all these species, a cellulose synthase has been identified that is regulated by intracellular c-di-GMP.

c-di-GMP was also found to function in various multicellular behaviors in different bacterial species, including transition from swarming to swimming, motility to sessility,

and biofilm formation.[28, 34, 46-50] GGDEF and EAL domain-containing proteins have been characterized and identified as diguanylate cyclases and phosphodiesterases, respectively, which together control the concentration of c-di-GMP in the cell. These results support the theory that c-di-GMP is a second messenger molecule, which regulates many different bacterial functions.

The Jones lab has provided authentic samples of chemically synthesized c-di-GMP for other studies. In one of them, c-di-GMP has been found to enhance the ability of *Salmonella* to kill mouse macrophage cells, and promote resistance to hydrogen peroxide.[5] The results indicated that bacterial c-di-GMP, as a second messenger, regulated host-pathogen interactions. In another study, Miller found that c-di-GMP was essential for the regulation of biofilm formation that is induced by aminoglycoside antibiotics (tobramycin) in *Pseudomonas aeruginosa*.[51] Since these biofilms are associated with increased antibiotic resistance, the EAL domain proteins present in the system were verified to be the determinant of biofilm-mediated antibiotic resistance. This finding suggests the therapeutic possibility of manipulating c-di-GMP metabolism.

II. Synthetic background for c-di-GMP

II1. Synthesis of unmodified c-di-GMP

In the early 1980's, cyclic ribodinucleotides were shown to act as inhibitors for the DNA dependent RNA polymerase of *E. coli*.[13, 52] Further study of this biological property

largely relied on a continuous supply of cyclic dinucleotides. However, the original method, in which cyclic nucleotides were isolated as side products from the complex mixtures of homopolymerization reactions,[53-56] turned out to be extremely inefficient. A series of new synthetic pathways was developed by different research groups during the past two decades, including phosphotriester[14, 57, 58] and H-phosphonate methods.[59] In 1985, the Jones[14] group developed a phosphotriester method to synthesize cyclic-di-AMP, c-di-UMP and c-AMP-UMP. In this method, a phosphotriester condensation was utilized in both intermolecular and intramolecular couplings, as shown in **Scheme 1-1.** In both steps, 2,4,6-triisopropylbenzenesulfonyl chloride (TPSCl) was used as a condensing reagent, along with tetrazole as a catalyst. Unblocking of base and 2'-OH protection gave final cyclic dinucleotides **7**. Later in the 1990s, a modified phosphotriester method[1, 12] was used by van Boom to synthesize c-di-GMP and several of its analogs. These compounds were used to explore the regulatory effects of c-di-GMP on cellulose synthase in *A. xylinum*. In this modified method, a bifunctional phosphorylating reagent was used to condense two nucleoside units into a linear dimer in a two-step phosphorylation process, followed by cyclization (shown in **Scheme 1-6**, along with the method for the thiophosphate analog).
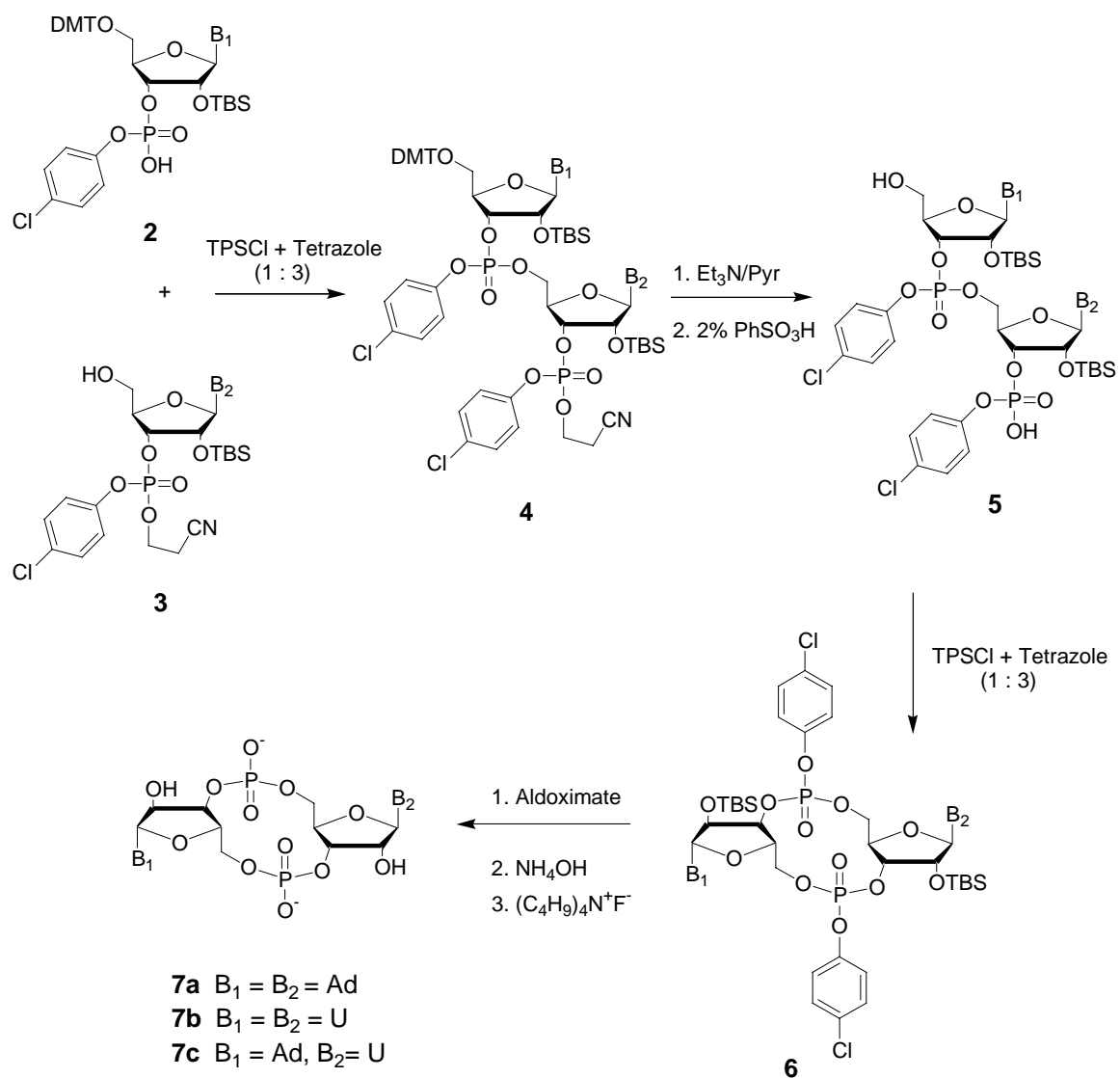
Scheme 1-1. Jones phosphotriester method[14]
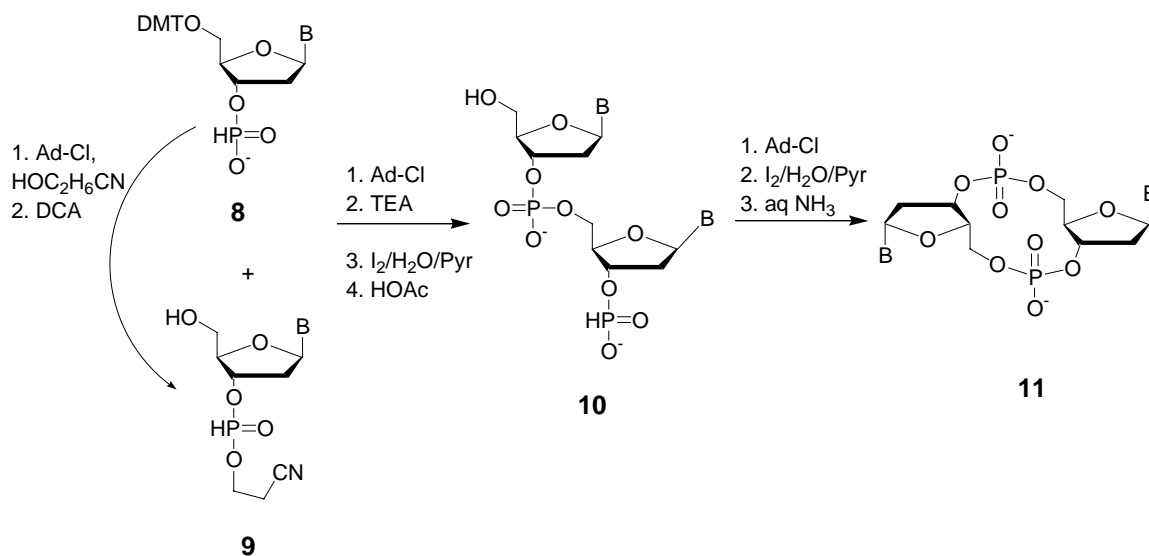
Scheme 1-2. Jones H-phosphonate method[59]

In 1996, an H-phosphonate method[59] was used for the first time to synthesize all ten of the natural cyclic deoxydinucleotides by the Jones group. As shown in **Scheme 1-2**, H-phosphonate couplings were applied to both intermolecular and intramolecular reactions. This P(III) chemistry gave significantly better yields than the P(V) chemistry of the triester method.
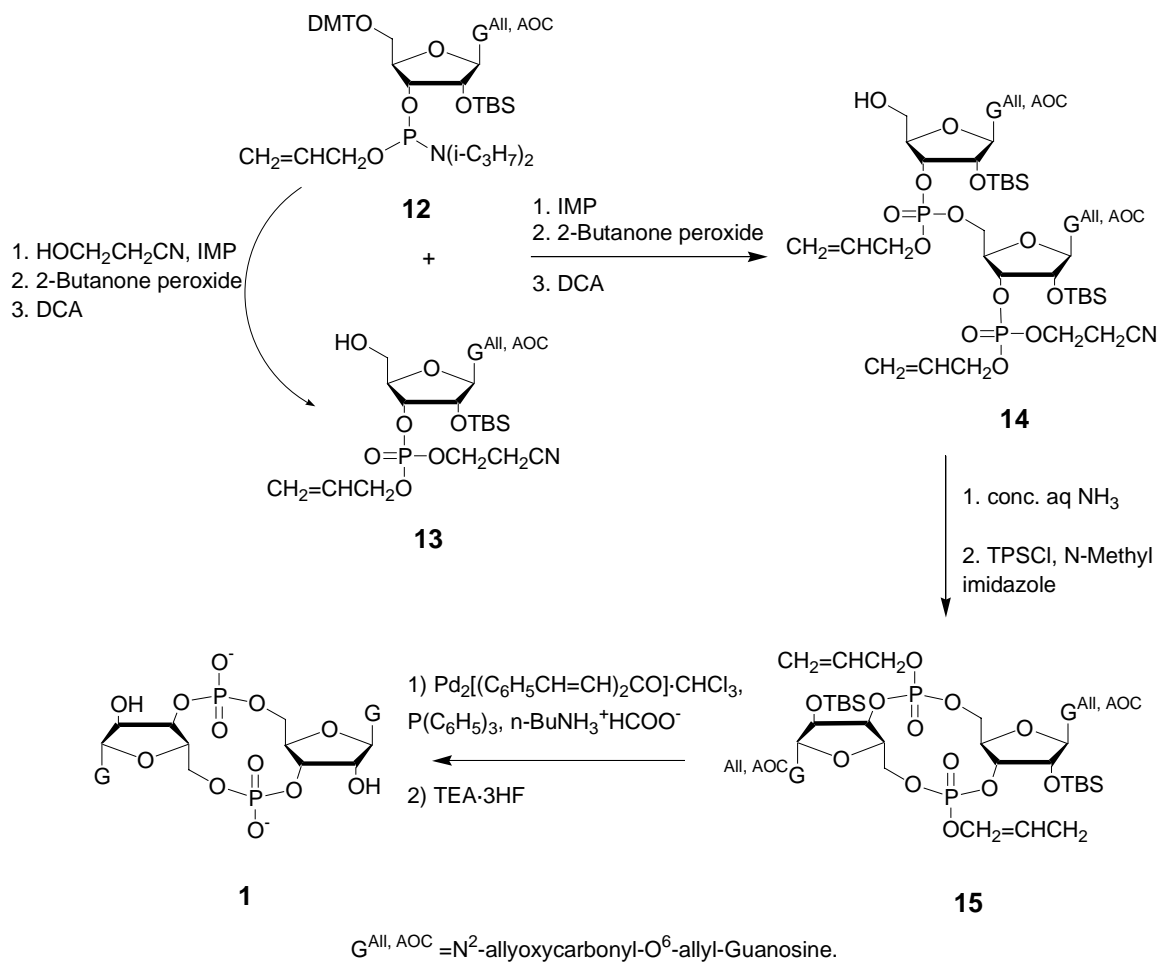
Scheme 1-3. Hayakawa's amidite/triester method[60]

In 2003, Hayakawa[60] reported a mixed method to synthesize c-di-GMP, in which a phosphoramidite coupling was utilized to give the linear dimer **14**, with a higher yield in a shorter reaction time than with the old triester method. However, as illustrated in **Scheme 1-3**, the phosphotriester method was still used for the cyclization, which took a long time. Another shortcoming of this method was the use of allyl groups to protect the guanine O6 and phosphates, for which deblocking was accomplished using a palladium complex as a catalyst.
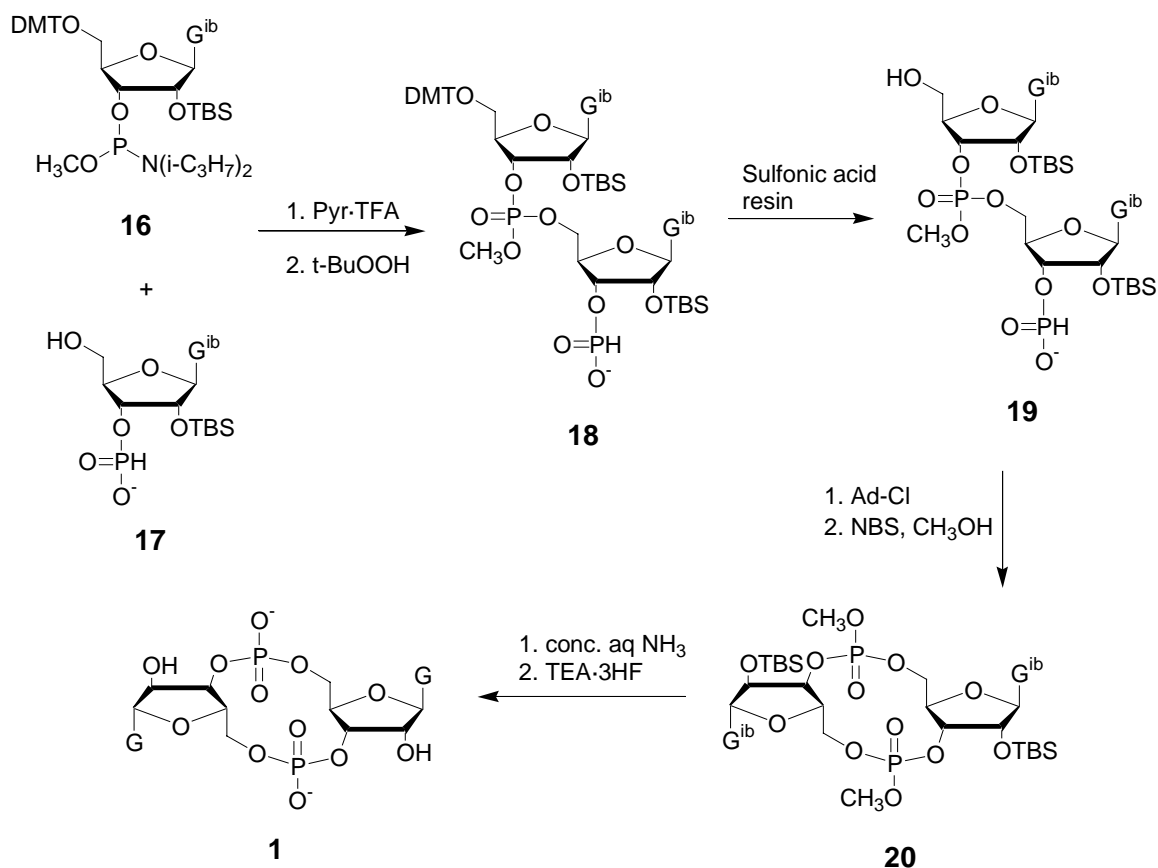
Scheme 1-4. Jones amidite/H-phosphonate method[61]

These disadvantages were avoided in a new method that was being developed by Zhaoying Zhang in the Jones group when Hayakawa's report appeared. This new method[61] combined a phosphoramidite coupling to obtain the linear dimer and an H-phosphonate cyclization to give the cyclic dimer. As shown in **Scheme 1-4**, the H-phosphonate at the 3' position in **17** acts as a protecting group during the linear dimer coupling, and then cyclizes with the free 5'-OH in **19**. Use of *tert*-butyl hydroperoxide as the oxidant after the linear coupling allowed selective oxidation of the center phosphite,
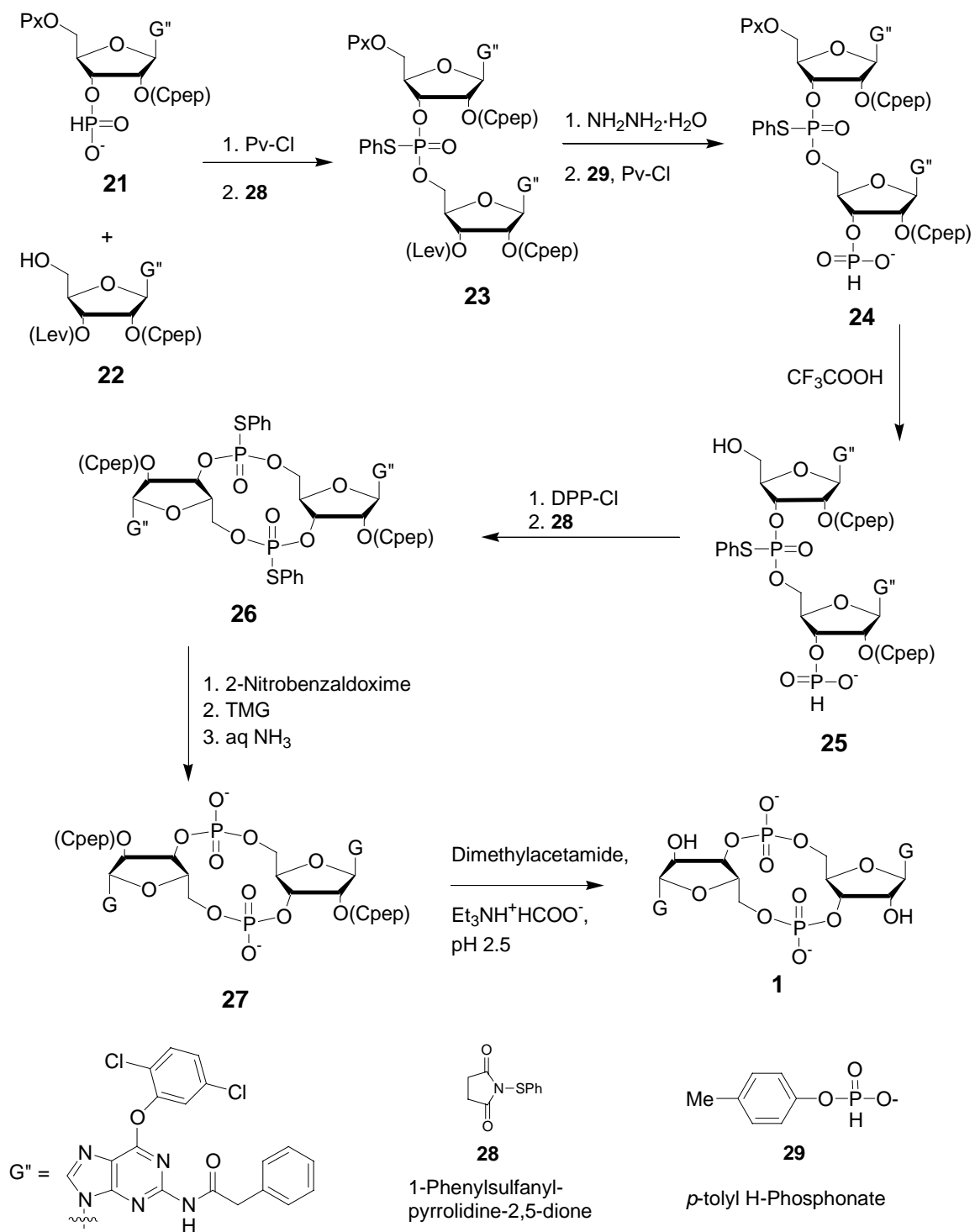
Scheme 1-5. Yan's H-phosphonate method[62]

but not the phosphonate monoester. Use of NBS/CH$_3$OH as oxidant after the cyclization allowed formation of a symmetrical product.

Several new synthetic methods for c-di-GMP have been developed in recent years, including one reported by Giese *et al.* in 2006.[63] In this method, a cyclic sugar backbone was constructed first, and the guanines were introduced in the final step of the synthetic process.

The most recent synthetic procedure for c-di-GMP was introduced by Yan and Aguilar in 2007,[62] in which an H-phosphonate coupling was utilized in both steps of inter- and intramolecular reactions, as illustrated in **Scheme 1-5**. A new feature of this method was that 1-(4-chlorophenyl)-4-ethoxypiperidine-4-yl (Cpep) was used as a 2'-OH protecting group instead of the commonly used TBS group. This Cpep group had the advantage of easy deprotection under mild acidic conditions (pH 4, 35-40 °C, 5 hours). Also, O6 and N2 double protection increased the solubility of guanosine and prevented side reactions with phosphorylating agents.

II2. Synthesis of c-di-GMP thiophosphate analogs
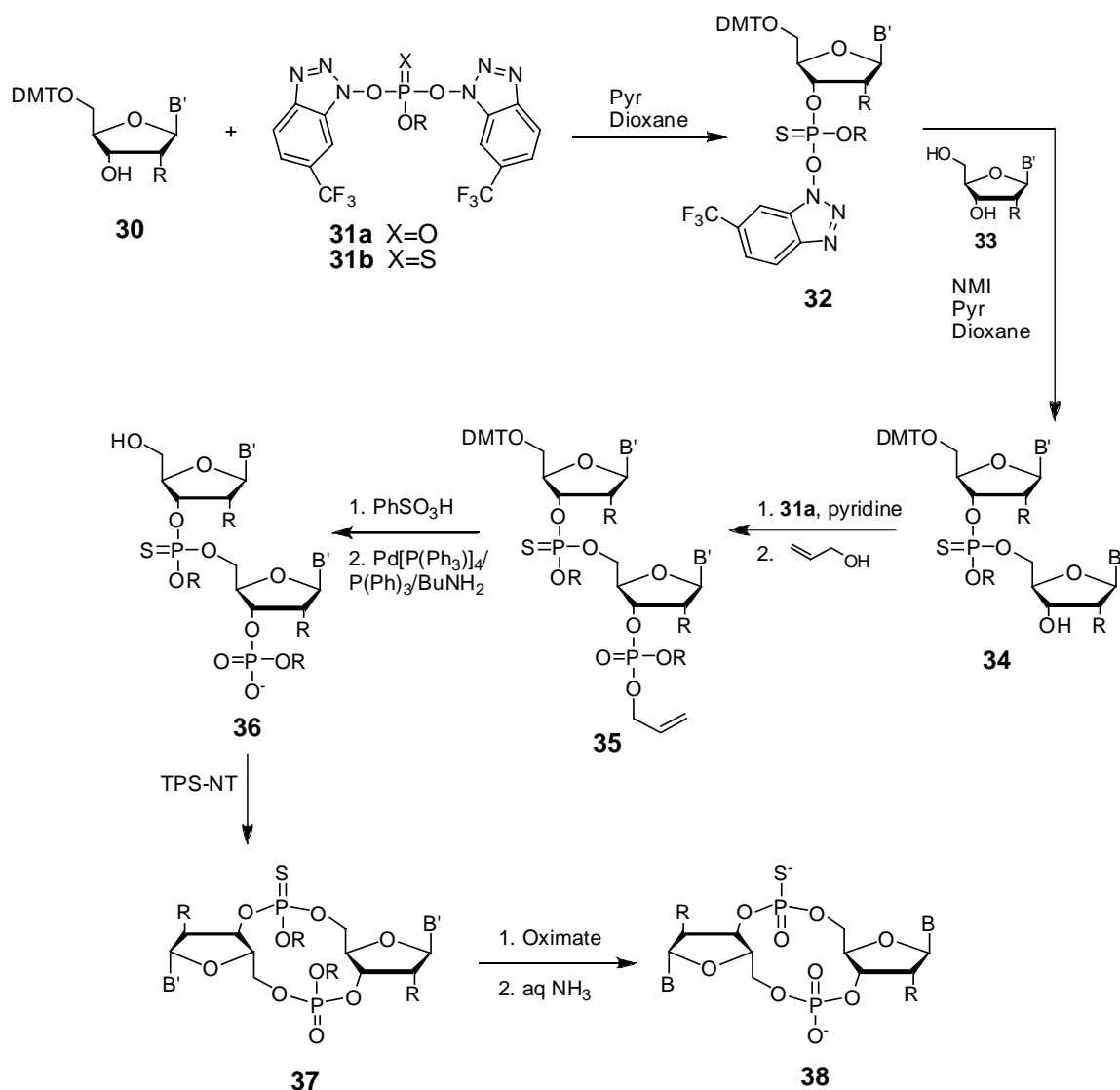
Scheme 1-6. van Boom's phosphotriester method[12]

The first thiophosphate analog of c-di-GMP was synthesized by van Boom in 1990,[12] using a modified phosphotriester method. As illustrated in **Scheme 1-6**, a 5' protected nucleoside, with a free 3' hydroxyl group was reacted with 2-chlorophenyl-*O,O*'-bis(1-benzotriazolyl) thiophosphate triester (**31a**) to give an initial nucleotide phosphotriester, which further reacted with the 5'-OH of another nucleoside to give the linear dimer **34**. The thiophosphate triester reagent was critical for introducing the non-bridging

thiophosphate linkage. This initial dimer was then treated with phosphorylating reagent (**31b)** and allyl alcohol to give the tritylated phosphorylated compound **35**. Following detritylation using acid, the linear dimer was cyclized using triisopropyl benzenesulfonyl nitrotriazole (TPS-NT) as a condensing reagent. Using this method, several cyclic dinucleotide analogs, including unsymmetrical dimers, trimers, and thiophosphate derivatives were prepared. All of these analogs were tested for binding affinity to both cellulose synthase and c-di-GMP phosphodiesterase in *A. xylinum*.
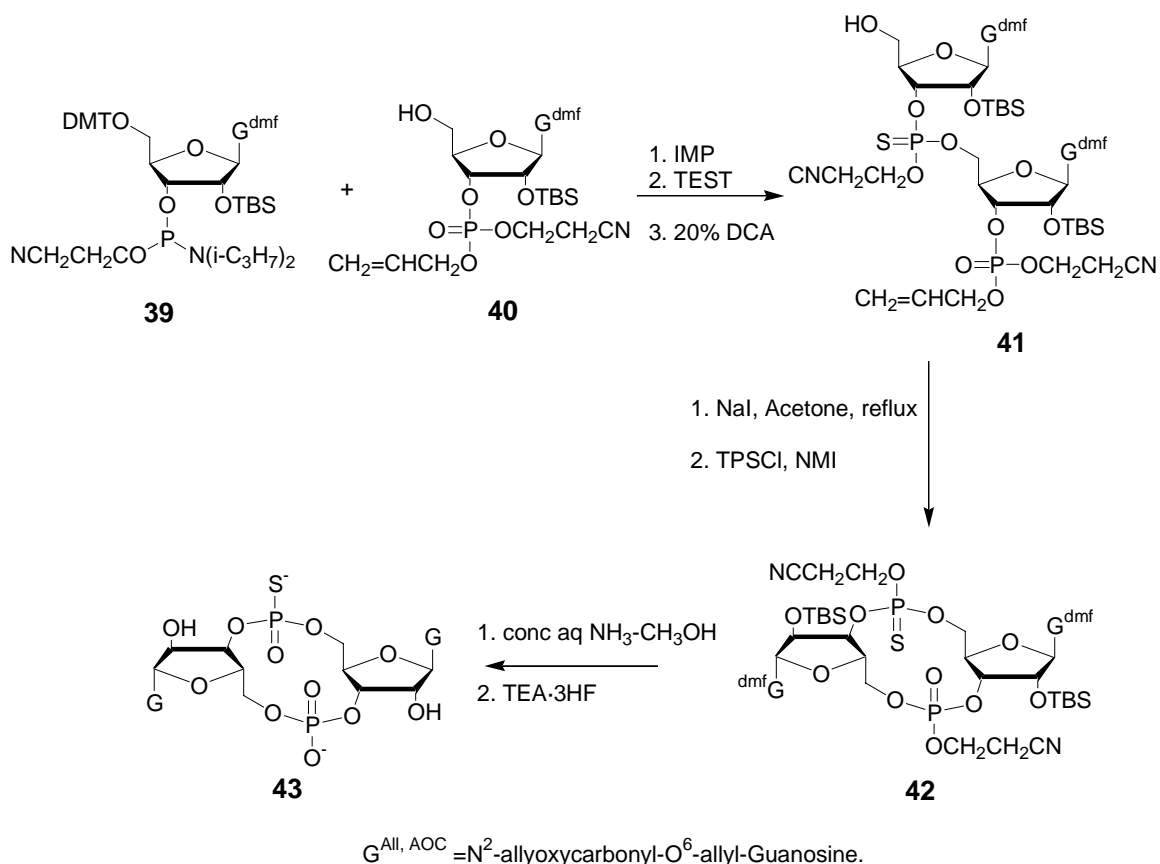
Scheme 1-7. Hayakawa's amidite/triester method[64]

Another method to synthesize c-di-GMP thiophosphate analogs was developed by Hayakawa in 2006,[64] shown in **Scheme 1-7**. A phosphoramidite coupling was utilized to

form a linear dimer, followed by sulfurization using bis[3-(triethoxysilyl)propyl] tetrasulfide(TEST). The linear dimer was then cyclized using the phosphotriester method, using TPSCl and NMI as condensing agent and catalyst, respectively. This was followed by a series of deprotecting procedures to give c-di-GMP thiophosphate. A drawback of the two methods described above is that they can only give mono-modified thiophosphate analogs, with only one sulfur.
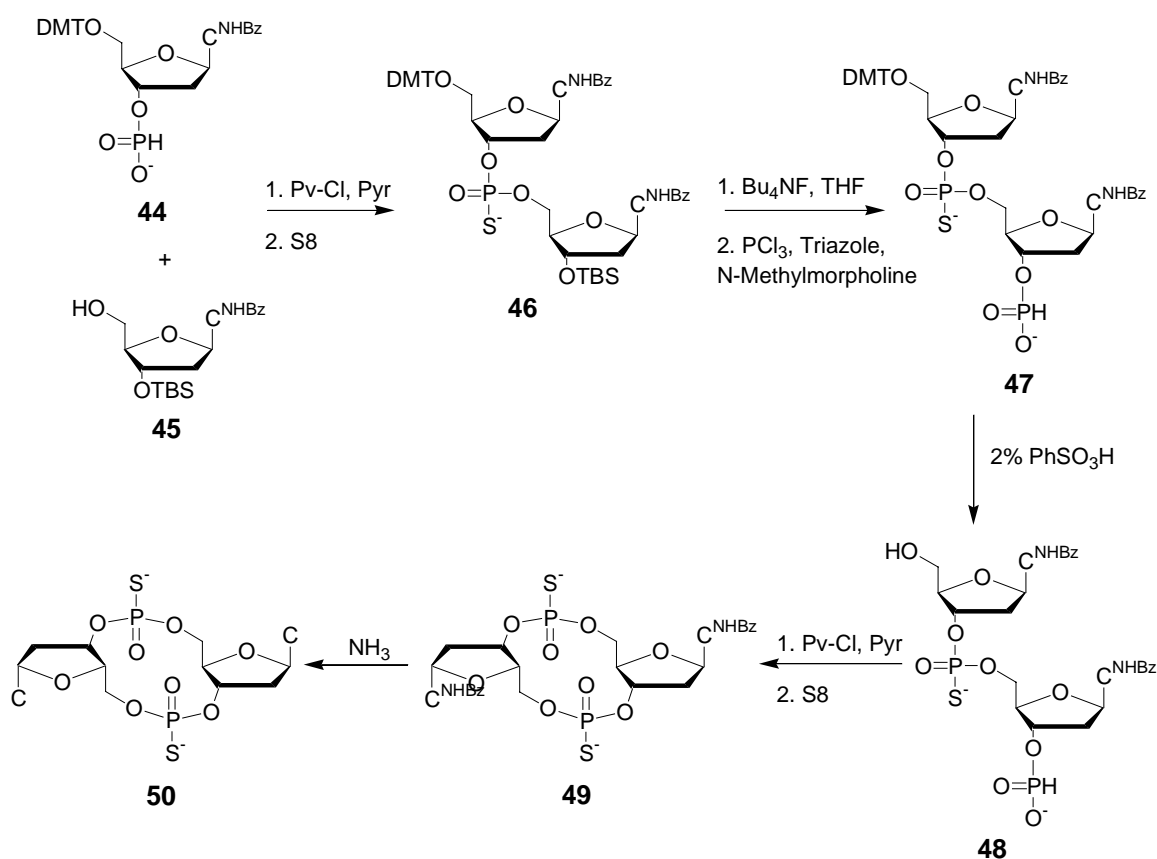
Scheme 1-8. Battistini's H-phosphonate method[65]

In 1993, the first cyclic dideoxycytosine dithiophosphate was synthesized by the Battistini group in Italy,[65] as shown in **Scheme 1-8**. An H-phosphonate method was used

for both inter- and intramolecular couplings, followed in each step by direct sulfurization using elemental sulfur (S_8). The H-phosphonate method with S_8 sulfurization combination had previously been used for the synthesis of linear dinucleotide thiophosphates and other analogs.[66-69] The linear dimer **47** was obtained as a mixture of two diastereomers, which were separated and purified in a ratio of 35:65, *R*:*S*. The configurations were determined using a snake venom phosphodiesterase[70, 71] degradation method. ^{31}P NMR spectra were obtained for each diastereomer, which showed a larger chemical shift for the [*S*] diastereomer than the [*R*]. The two diastereomers of **48** were then independently cyclized, sulfurized, and deprotected to give the corresponding cyclic dinucleotide dithiophosphates **50**, which were also characterized by ^{31}P NMR. Interestingly, H-phosphonate cyclization followed by S_8 sulfurization gave only the [*R*] configuration at the newly formed phosphorus chiral center, which means that only the (*R, R*) and (*R, S*) diastereomers of c-di-CMP thiophosphates were obtained by this method.

III. Structural properties of c-di-GMP

III1. Crystal structure

In the early 1990's, Alexander Rich[72] and Andrew Wang[73] independently reported the crystal structure of c-di-GMP using X-ray. As illustrated in **Figure 1-2**, the structure contains two c-di-GMP molecules that form a self-intercalated unit stabilized by the partial stacking of four guanines and hydrogen bonding. The two molecules have almost identical conformations, both in *anti* conformation. In each c-di-GMP molecule, there are

two phosphodiester linkages, that are part of a fairly rigid 12-membered ring. In Wang's work, two different structures were obtained in the presence of Co^{2+} or Mg^{2+}. A trigonal crystal formed in the presence of Mg^{2+}, in which the rigid 12-membered ring kept the two guanines in parallel planes 6.8 Å apart. However, in a tetragonal crystal, Co^{2+} was located between the two central guanines and coordinated to their N7 atoms, thereby destacking them with a dihedral angle of 29°, with the two outer guanines almost in parallel planes. A similar destacked structure was obtained in Rich's work, with Mg^{2+} coordinated to the central guanines.
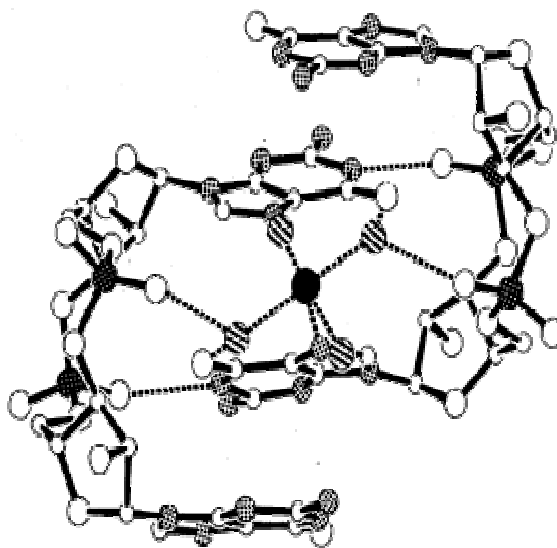
Figure 1-2. Crystal structure of c-di-GMP[72, 73]

III2. UV and CD of c-di-GMP at low concentration

Zhaoying Zhang[61] in the Jones lab used ultraviolet (UV) and circular dichroism (CD) spectroscopies to study the structure and behavior of various salt forms of c-di-GMP in solution at low concentrations (less than 0.4 mM). UV melting curves showed different

properties for the Li^+/Na^+ vs. K^+ forms. In both Li^+ and Na^+, there was only one thermal transition, which indicated that intermolecular aromatic stacking was dominant. A single molecule of c-di-GMP or a bimolecular complex was proposed to be the major form in both Li^+ and Na^+. However, a second transition in the UV melting curve of the K^+ form indicated the existence of an additional structure. Consistent with UV data, the CD spectra of the K^+ form had a different pattern than the Li^+ and Na^+ forms, supporting the presence of a second structure. Because it is well known that K^+ provides specific stabilization of guanine quartets,[74-78] the second structure in the K^+ form was suggested to involve the formation of a G-quartet.

III3. NMR of c-di-GMP at high concentration

III3.1. 1D and 2D ^{1}H NMR of different salt forms

Zhaoying Zhang also used 1D and 2D nuclear magnetic resonance (NMR) spectroscopy to study the structures of c-di-GMP in solution at high concentrations (30-40 mM).[79] Surprisingly, c-di-GMP in both Li^+ and K^+ was shown to form five different complexes, but in different amounts. These include bimolecular with an all-*anti* conformation of the glycosidic bond, tetramolecular with all-*syn* or all-*anti* arrangements, and octamolecular with all-*syn* or all-*anti* arrangements. Cartoons of these complexes are shown in **Figure 1-3**, with the structures of *syn* and *anti* conformations of guanosine shown in **Figure 1-4**. The equilibrium among these different complexes was found to depend on the cations, with K^+ favoring the higher order ones.
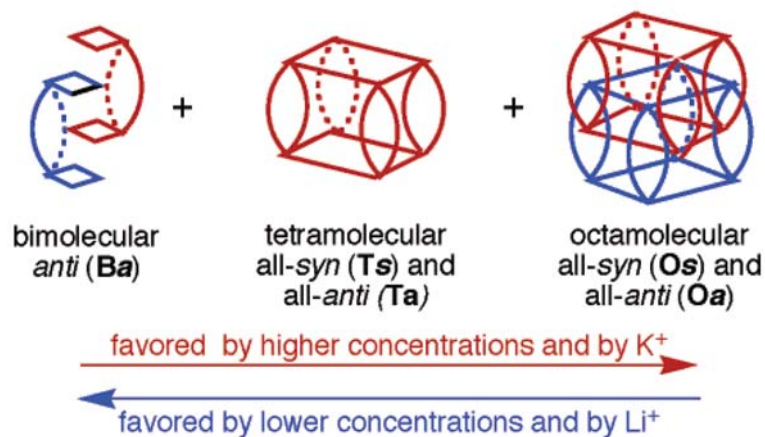
Figure 1-3. Cartoons of different complexes of c-di-GMP[79]
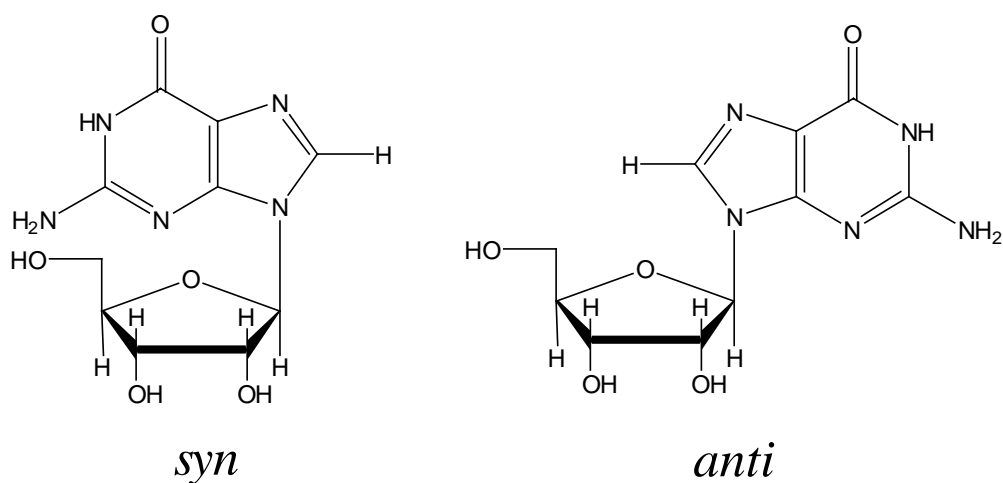
Figure 1-4. Structures of *syn/anti* conformations of guanosine

The 1D ^{1}H NMR spectra of different salt forms of c-di-GMP are shown in **Figure 1-5**. Consistent with the literature,[80-82] the resonances near 11 ppm were assigned to the hydrogen-bonded H1s, and the broad resonances around 9.0 and 6.5 ppm were assigned to hydrogen-bonded and non-hydrogen-bonded amino protons, respectively. ^{1}H-^{1}H NOESY spectra (2D spectra not shown) were used to assign the *syn* and *anti* conformations, since *syn* guanines are known to give stronger H8 to H1' cross peaks than

anti guanines.[83, 84] As shown in **Figure 1-4**, the distance between these two protons in the *syn* conformation is shorter than that in the *anti* conformation. ^{1}H-^{13}C HMBC/HMQC spectra were used to confirm these *syn/anti* assignments, since the H1' of a *syn* guanine is known to show a stronger cross-peak to the C4 than to the C8 resonances, while an *anti* guanine shows a stronger cross-peak to C8.[85]
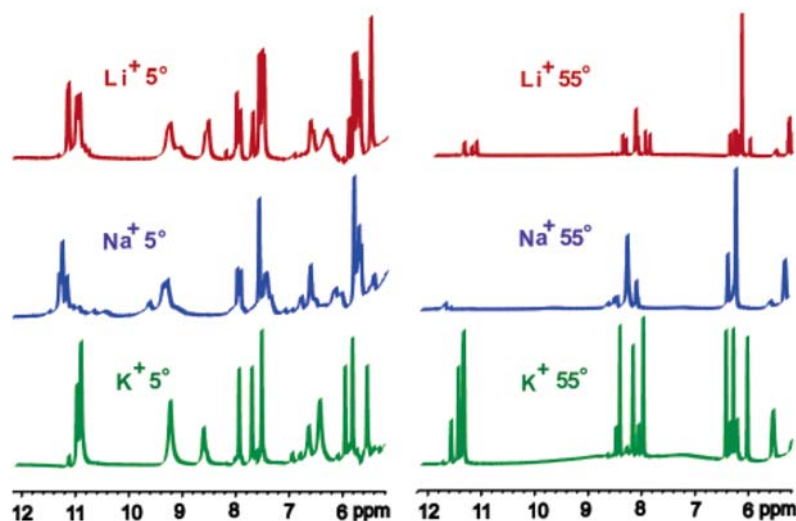
Figure 1-5. 1D ^{1}H NMR spectra of different salt forms of c-di-GMP[61]

III3.2. ^{31}P NMR of different salt forms

The *syn/anti* assignments were correlated to the ^{31}P NMR spectra of the Li^{+} and K^{+} forms, shown in **Figure 1-6**, along with the Na^{+} form. In the Li^{+} form at 55 °C, the dominant central peak near –0.8 ppm moved to –1.5 ppm and diminished upon cooling to 5 °C. This central peak was assigned to the unstructured molecule in fast equilibrium with the bimolecular complex. Two clusters of new signals appeared at the same time during the cooling process. One set had an upfield chemical shift, and was correlated with

the all-*anti* tetra- and octamolecular complexes. The other set had a downfield chemical shift, and was correlated with the all-*syn* complexes. On the other hand, the ^{31}P NMR spectra of the K$^+$ form displayed no central signal at –1.5 ppm at 5 °C, and a very small one even at 55 °C, with the upfield and downfield resonances being dominant. These results showed that K$^+$ provides significant stabilization for the tetra/octamolecular complexes, consistent with the previous UV and CD.
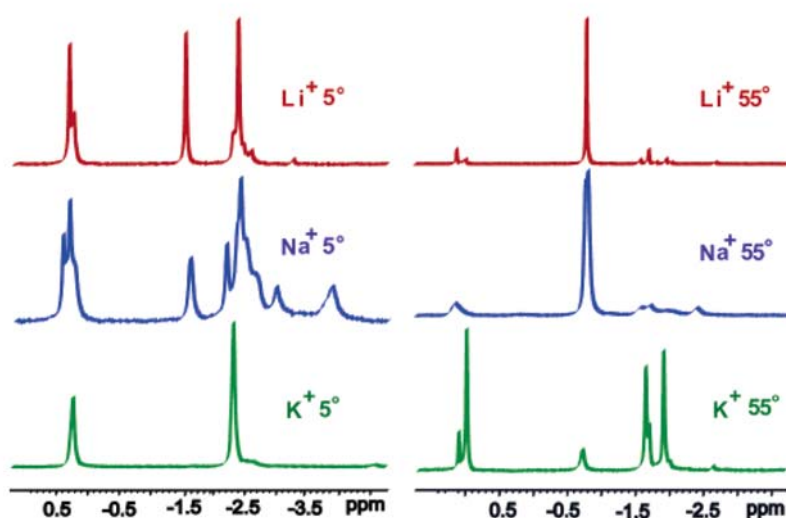
Figure 1-6. ^{31}P NMR spectra of different salt forms of c-di-GMP[61]

No NMR data have been reported so far for thiophosphate analogs of c-di-GMP. The work presented in this thesis describes the synthesis of a variety of thiophosphate analogs of c-di-GMP, and a NMR study of the effects of the substitutions on the equilibrium among the different complexes in Na$^+$ and in K$^+$.

IV. References

1.   Ross, P., Weinhouse, H., Aloni, Y., Michaeli, D., Weinberger-Ohana, P., Mayer, R., Braun, S., de Vroom, E., van der Marel, G.A., van Boom, J.H., and Benziman, M., "Regulation of cellulose synthesis in *Acetobacter xylinum* by cyclic diguanylic acid". *Nature*, **1987**, 325, 279-281.

2.   Römling, U., "Molecular biology of cellulose production in bacteria". *Research in Microbiology*, **2002**, 153, 205-212.

3.   Aldridge P. and Jenal, U., "Cell cycle-dependent degradation of a flagellar motor component requires a novel-type response regulator". *Mol. Microbiol.*, **1999**, 32(2), 379-391.

4.   Kazmierczak, B.I., Lebron, M.B., and Murray, T.S., "Analysis of FimX, a phosphodiesterase that governs twitching motility in Pseudomonas aeruginosa". *Mol. Microbiol.*, **2006**, 60, 1026-1043.

5.   Hisert, K.B., MacCoss, M., Shiloh, M., Darwin, K., Singh, S., Jones, R., Ehrt, S., Zhang, Z., Gaffney, B., Gandotra, S., Holden, D., Murray, D., and Nathan, C., "A glutamate-alanine-leucine (EAL) domain protein of Salmonella controls bacterial survival in mice, antioxidant defense and killing of macrophages: role of cyclic diGMP". *Mol. Microbiol.*, **2005**, 56(5), 1234-1245.

6.   Jenal, U., "Cyclic di-guanosine-monophosphate comes of age: a novel secondary messenger involved in modulating cell surface structures in bacteria?" *Curr. Opin. Microbiol.*, **2004**, 7, 185-191.

7.   Römling, U. and Amikam, D., "Cyclic di-GMP as a second messenger". *Curr. Opin. Microbiol.*, **2006**, 9, 218-228.

8.   Cotter, P.A. and Stibitz, S., "c-di-GMP-mediated regulation of virulence and biofilm formation". *Curr. Opin. Microbiol.*, **2007**(10), 17-23.

9.   Tamayo, R., Pratt, J.T., and Camilli, A., "Roles of cyclic diguanylate in the regulation of bacterial pathogenesis". *Annu. Rev. Microbiol.*, **2007**, 61(131-148).

10. Karaolis, D.K.R., Means, T.K., Yang, D., Takahashi, M., Yoshimura, T., Muraille, E., Philpott, D., Schroeder, J.T., Hyodo, M., Hayakawa, Y., Talbot, B.G., Brouillette, E., and Malouin, F., "Bacterial c-di-GMP is an immunostimulatory molecule". *J. Immunol.*, **2007**, 178, 2171-2181.

11. Karaolis, D.K.R., Newstead, M.W., Zeng, X., Hyodo, M., Hayakawa, Y., Bhan, U., Liang, H., and Standiford, T.J., "Cyclic di-GMP stimulates protective innate immunity in bacterial pneumonia*". INFECT. IMMUN*, **2007**, 75, 4942-4950.

12. Ross, P., Mayer, R., Weinhouse, H., Amikam, D., Huggirat, Y., Benziman, M., Vroom, E.d., Fidder, A., Paus, P.D., Sliedregt, L.A.J.M., Marel, G.A.v.d., and van Boom, J.H., "The cyclic diguanylic acid regulatory system of cellulose synthesis in *Acetobacter xylinum*. Chemical synthesis and biological activity of cyclic nucleotide dimer, trimer, and phosphothioate derivatives*". J. Biol. Chem.*, **1990**, 265, 18933-18943.

13. Hsu, C.-Y. and Dennis, D., "RNA polymerase: linear competitive inhibition by bis-(3' to 5')-cyclic dinucleotides, NpNp*". Nucleic Acids Res.*, **1982**, 10, 5637-5647.

14. Hsu, C.-Y., Dennis, D., and Jones, R.A., "Synthesis and physical characterization of *bis* 3',5' cyclic dinucleotides: RNA Polymerase inhibitors*". Nucleosides & Nucleotides*, **1985**, 4, 377-389.

15. Benziman, M., Haigler, C.H., Brown, R.M., Jr., White, A.R., and Cooper, K.M., "Cellulose biogenesis: polymerization and crystallization are coupled processes in Acetobacter xylinum*". Proc. Natl. Acad. Sci. USA*, **1980**, 77, 6678-6682.

16. Tal, R., Wong, H.C., Calhoon, R., Gelfand, D., Fear, A.L., Volman, G., Mayer, R., Ross, P., Amikam, D., Weinhouse, H., Cohen, A., Sapir, S., Ohana, P., and Benziman, M., "Three cdg operons control cellular turnover of cycli-di-GMP in Acetobacter xylinum: genetic organization and occurrence of conserved domains in isoenzymes*". J. Bacteriol.*, **1998**, 180, 4416-4425.

17. Solano, C., Garcia, B., Valle, J., Berasain, C., Ghigo, J., Gamazo, C., and Lasa, I., "Genetic analysis of Salmonella enteritidis biofilm formation: critical role of cellulose*". Mol. Microbiol.*, **2002**, 43, 793-808.

18. Zogaj, X., Nimtz, M., Rohde, M., Bokranz, W., and Romling, U., "The multicellular morphotypes of Salmonella typhimurium and Escherichia Coli produce cellulose as the second component of the extracellular matrix*". Mol. Microbiol.*, **2001**, 39, 1452-1463.

19. Mah, T.-F.C. and O'Toole, G.A., "Mechanisms of biofilm resistance to antimicrobial agents*". Trends Microbiol.*, **2001**, 9, 34-39.

20. Stewart, P.S. and Costerton, J.W., "Antibiotic resistance of bacteria in biofilms*". Lancet*, **2001**, 358, 135-138.

21. Tischler, A.D. and Camilli, A., "Cyclic diguanylate (c-di-GMP) regulates *Vibrio cholerae* biofilm formation*". Mol. Microbiol.*, **2004**, 53, 857-869.

22. Simm, R., Morr, M., Kader, A., Nimtz, M., and Romling, U., "GGDEF and EAL domains inversely regulate cyclic di-GMP levels and transition from sessility to motility*". Mol. Microbiol.*, **2004**, 53, 1123-1134.

23. Karaolis, D.K.R., Cheng, K., Lipsky, M., Elnabawi, A., Catalano, J., Hyodo, M., Hayakawa, Y., and Raufman, J.-P., "3',5'-Cyclic diguanylic acid (c-di-GMP) inhibits basal and growth factor-stimulated human colon cancer cell proliferation*". Biochem. Biophys. Res. Commun.*, **2005**, 329, 40-45.

24. Karaolis, D.K.R., Rashid, M.H., Rajanna, C., Luo, W., Hyodo, M., and Hayakawa, Y., "c-di-GMP (3'-5'-cyclic diguanylic acid) inhibits Staphylococcus aureus cell-cell interactions and biofilm formation*". Antimicrob. Agents Chemother.*, **2005**, 49, 1029-1038.

25. Paul, R., Weiser, S., Amiot, N.C., Chan, C., Schirmer, T., Giese, B., and Jenal, U., "Cell cycle-dependent dynamic localization of a bacterial response regulator with a novel di-guanylate cyclase output domain*". Genes Dev.*, **2004**, 18, 715-727.

26. Ryjenkov, D.A., Tarutina, M., Moskvin, O.V., and Gomelsky, M., "Cyclic diguanylate is a ubiquitous signaling molecule in bacteria: insights into biochemistry of the GGDEF protein domain*". J. Bacteriol.*, **2005**, 187, 1792-1798.

27. Jenal, U. and Malone, J., "Mechanisms of cyclic-di-GMP signaling in bacteria*". Annu. Rev. Genet.*, **2006**, 40, 385-407.

28. Gjermansen, M., Ragas, P., and Tolker-Nielsen, T., "Proteins with GGDEFand EAL domains regulate Pseudomonas putida biofilm formation and dispersal*". FEMS Microbiol. Lett.*, **2006**, 265, 215-224.

29. Malone, J.G., Williams, R., Christen, M., Jenal, U., Spiers, A.J., and Rainey, P.B., "The structure–function relationship of WspR, a Pseudomonas fluorescens response regulator with a GGDEF output domain*". Microbiology*, **2007**, 153, 980-994.

30. Bobrov, A.G., Kirillina, O., and Perry, R.D., "The phosphodiesterase activity of the HmsP EAL domain is required for negative regulation of biofilm formation in Yersinia pestis*". FEMS Microbiol. Lett.*, **2005**, 247, 123-130.

31. Christen, M., Christen, B., Folcher, M., Schauerte, A., and Jenal, U., "Identification and characterization of a cyclic di-GMP-specific phosphodiesterase and its allosteric control of GTP*". J. Biol. Chem.*, **2005**, 280, 30829-30837.

32. Schmidt, A.J., Ryjenkov, D.A., and Gomelsky, M., "The ubiquitous protein domain EAL is a cyclic diguanylate-specific phosphodiesterase: enzymatically active and inactive EAL domains*". J. Bacteriol.*, **2005**, 187, 4774-4781.

33. Simm, R., Lusch, A., Kader, A., Andersson, M., and Römling, U., "Role of EAL-containing proteins in multicellular behavior of Salmonella enterica Serovar Typhimurium*". J. Bacteriol.*, **2007**, 189, 3613-3623.

34. Kim, Y.-K. and McCarter, L.L., "ScrG, a GGDEF-EAL protein, participates in regulating swarming and sticking in Vibrio parahaemolyticus*". J. Bacteriol.*, **2007**, 189, 4094-4107.

35. Chan, C., Paul, R., Samoray, D., Amiot, N.C., Giese, B., Jenal, U., and Schirmer, T., "Structure basis of activity and allosteric control of diguanylate cyclase*". Proc. Natl. Acad. Sci. USA*, **2004**, 101, 17084-17089.

36. Wassmann, P., Chan, C., Paul, R., Beck, A., Heerklotz, H., Jenal, U., and Schirmer, T., "Structure of BeF3--modified response regulator PleD: Implications for diguanylate cyclase activation, catalysis, and feedback inhibition*". Structure*, **2007**, 15, 915-927.

37. Ross, P., Mayer, R., and Benziman, M., "Cellulose biosynthesis and function in bacteria*". Microbiol. Rev.*, **1991**, 55, 35-58.

38. Weinhouse, H., Sapir, S., Amikam, D., Shilo, Y., Volman, G., Ohana, P., and Benziman, M., "c-di-GMP-binding protein, a new factor regulating cellulose synthesis in *Acetobacter xylinum". FEBS Lett.*, **1997**, 416, 207-211.

39. Amikam, D. and Galperin, M.Y., "PilZ domain is part of the bacterial c-di-GMP binding protein*". Bioinformatics*, **2006**(22), 3-6.

40. Ryjenkov, D.A., Simm, R., Römling, U., and Gomelsky, M., "The PilZ domain is a receptor for the second messenger c-di-GMP. The PilZ domain protein YcgR controls motility in enterobacteria". *J. Biol. Chem.*, **2006**, 281, 30310-30314.

41. Merighi, M., Lee, V.T., Hyodo, M., Hayakawa, Y., and Lory, S., "The second messenger bis-(3',-5')-cyclic-GMP and its PilZ domain-containing receptor Alg44 are required for alginate biosynthesis in Pseudomonas aeruginosa". *Mol. Microbiol.*, **2007**, 65, 876-895.

42. Christen, M., Christen, B., Allan, M.G., Folcher, M., Jenö, P., Grzesiek, S., and Jenal, U., "DgrA is a member of a new family of cyclic diguanosine monophosphate receptors and controls flagellar motor function in Caulobacter crescentus". *Proc. Natl. Acad. Sci. USA*, **2007**, 104, 4112-4117.

43. Lee, V.T., Matewish, J.M., Kessler, J.L., Hyodo, M., Hayakawa, Y., and Lory, S., "A cycli-di-GMP receptor required for bacterial exopolysaccharide production". *Mol. Microbiol.*, **2007**, 65, 1474-1484.

44. Matthysse, A.G., White, S., and Lightfoot, R., "Genes required for cellulose synthesis in Agrobacterium tumefaciens". *J. Bacteriol.*, **1995**, 177, 1069-1075.

45. Ausmees, N., Jonsson, H., Holglund, S., Ljunggren, H., and Lindberg, M., "Structural and putative regulatory genes involved in cellulose synthesis in Rhizobium leguminosarum bv. trifolii". *Microbiology*, **1999**, 145, 1253-1262.

46. Spiers, A.J., Bohannon, J., Gehrig, S.M., and Rainey, P.B., "Biofilm formation at the air-liquid interface by the Pseudomonas fluorescens SBW25 wrinkly spreader requires an acetylated form of cellulose". *Mol. Microbiol.*, **2003**, 50, 15-27.

47. Rashid, M.H., Rajanna, C.A.A., and Karaolis, D.K.R., "Identification of genes involved in the switch between the smooth and rugose phenotypes of Vibrio cholerae". *FEMS Microbiol. Lett.*, **2003**, 227, 113-119.

48. Rahman, M., Simm, R., Kader, A., Basseres, E., Römling, U., and Möllby, R., "The role of c-di-GMP signaling in an Aeromonasveronii *biovar sobriastrain*". *FEMS Microbiol. Lett.*, **2007**, 273, 172-179.

49. Kobayashi, K., "Gradual activation of the response regulator DegU controls serial expression of genes for flagellum formation and biofilm formation in Bacillus subtilis". *Mol. Microbiol.*, **2007**, 66, 395-409.

50. Ryan, R.P., Fouhy, Y., Lucey, J.F., Jiang, B., He, Y., Feng, J., Tang, J., and Dow, J.W., "Cyclic di-GMP signaling in the virulence and environmental adaptation of Xanthomonas campestris". *Mol. Microbiol.*, **2007**, 63, 429-442.

51. Hoffman, L.R., D'Argenio, D.A., MacCoss, M.J., Zhang, Z., Jones, R.A., and Miller, S.I., "Aminoglycoside antibiotics induce bacterial biofilm formation". *Nature (London)*, **2005**, 436, 1171-1175.

52. Dennis, D. and Sylvester, J.E., "RNA Polymerase: a model for rotational translocation". *FEBS Lett.*, **1981**, 124, 135-139.

53. Rammler, D.H., Lapidot, Y., and Khorana, H.G., "Studies on Polynucleotides. XIX. The Specific Synthesis of C3-C5 Inter-ribonucleotidic Linkage. A New Approach and its Use in the Synthesis of C3-C5-Linked Uridine Oligonucleotides". *J. Am. Chem. Soc.*, **1963**, 85(13), 1989-97.

54. Coutsogeorgopoulos, C. and Khorana, H.G., "Studies on Polynucleotides. XXXI. The Specific Synthesis of C3'-C5'-Linked Ribopolynucleotides (6). A Further Study of the Synthesis of Uridine Polynucleotides". *J. Am. Chem. Soc.*, **1964**, 86(14), 2926-31.

55. Tener, G.M., Khorana, H.G., Markham, R., and Pol, E.H., "Studies on Polynucleotides. II.1 The Synthesis and Characterization of Linear and Cyclic Thymidine Oligonucleotides2". *J. Am. Chem. Soc*, **1958**, 80(23), 6223-6230.

56. Ohtsuka, E., Tsuji, H., and Ikehara, M., "Transfer ribonucleic acids and related compounds VII. Synthesis and properties of cyclic oligoadenylic acids". *Chem. Pharm. Bull.*, **1974**, 22, 1022-1028.

57. Rao, M.V. and Reese, C.B., "Synthesis of cyclic oligodeoxyribonucleotides via the 'filtration' approach". *Nucleic Acids Res.*, **1989**, 17(20), 8221-8239.

58. Capobianco, M.L., Carcuro, A., Tondelli, L., Garbesi, A., and Bonora, G.M., "One pot solution synthesis of cyclic oligodeoxyribonucleotides". *Nucleic Acids Res.*, **1990**, 18, 2661-2669.

59. Zeng, F. and Jones, R.A., "Synthesis of cyclic dinucleotides by an H-phosphonate method in solution". *Nucleosides & Nucleotides*, **1996**, 15, 1679-1686.

60. Hayakawa, Y., Nagata, R., Hirata, A., Hyodo, M., and Kawai, R., "A facile synthesis of cyclic bis(3'-5')diguanylic acid". *Tetrahedron*, **2003**, 59, 6465-6471.

61. Zhang, Z., Gaffney, B.L., and Jones, R., "c-di-GMP displays a monovalent metal ion-dependent polymorphism". *J. Am. Chem. Soc*, **2004**, 126, 16700-16701.

62. Yan, H. and Aguilar, A.L., "Synthesis of 3',5'-cyclic diguanylic acid (cdiGMP) using 1-(4-chlorophenyl)-4-ethoxypiperidin-4-yl as a protecting group for 2'-hydroxy functions of ribonucleosides". *Nucleosides, Nucleotides, and Nucleic Acids*, **2007**, 26, 189-204.

63. Amiot, N., Heintz, K., and Giese, B., "New approach for the synthesis of c-di-GMP and its analogues". *Synthesis*, **2006**, 24, 4230-4236.

64. Hyodo, M., Sato, Y., and Hayakawa, Y., "Synthesis of cyclic bis(3'-5')diguanylic acid (c-di-GMP) analogs". *Tetrahedron*, **2006**, 62, 3089-3094.

65. Battistini, C., Fustinoni, S., Brasca, M.G., and Borghi, D., "Stereoselective synthesis of cyclic dinucleotide phosphorothioates". *Tetrahedron*, **1993**, 49, 1115-1132.

66. Stawinski, J., Thelin, M., and Zain, R., "Nucleoside H-phosphonates. X. Studies on nucleoside hydrogenphosphonothioate diester synthesis". *Tetrahedron Lett.*, **1989**, 30, 2157-2160.

67. Stawinski, J., Strömberg, R., and Thelin, M., "Synthesis of diribonucleoside phosphorothioates via stereospecific sulfurization of H-phosphonate diesters". *J. Org. Chem.*, **1992**, 57, 6163-6169.

68. Seela, F. and Kretschmer, U., "Diastereomerically pure R_p and S_p dinucleoside H-phosphonates: the stereochemical course of their conversion into p-methylphosphonates, phosphorothioates, and [^{18}O] chiral phosphates". *J. Org. Chem.*, **1991**, 56, 3861-3869.

69. Seela, F. and Kretschmer, U., "Stereospecific oxidation of R_p- and S_p-dinucleoside H-phosphonates to phosphorothioates". *Nucleosides & Nucleotides*, **1991**, 10, 711-712.

70. Burgers, P.M.J. and Eckstein, F., "Absolute configuration of the diastereomers of adenosine 5'-O-(1-thiotriphosphate): consequences for the stereochemistry of polymerization by DNA-dependent RNA polymerase from Escherichia coli". *Proc. Natl. Acad. Sci. USA*, **1978**, 75, 4798-4800.

71. Chen, Y., Qu, F., and Zhang, Y., "Diuridine 3',5'-boranophosphate: preparation and properties". *Tetrahedron Lett.*, **1995**, 36, 745-748.

72. Egli, M., Gessner, R.V., Williams, L.D., Quigley, G.J., van der Marel, G.A., van Boom, J.A., Rich, A., and Frederick, C.A., "Atomic-resolution structure of the cellulose synthase regulator cyclic diguanylic acid". *Proc. Natl. Acad. Sci. U.S.A.*, **1990**, 87, 3235-3239.

73. Guan, Y., Gao, Y.G., Liaw, Y.C., Robinson, H., and Wang, A.H.J., "Molecular Structure of Cyclic Diguanylic Acid at 1 Å Resolution of Two Crystal Forms: Self-association, Interactions with Metal Ion/Planar Dyes and Modeling Studies". *J Biomol Struct Dynam*, **1993**, 11(2), 253-277.

74. Pinnavaia, T.J., Marshall, C.L., Mettler, C.M., Fisk, H.T., Miles, H.T., and Becker, E.D., "Alkali metal ion specificity in the solution ordering of a nucleotide, 5'-guanosine monophosphate". *J. Am. Chem. Soc*, **1978**, 100, 3625-3627.

75. Williamson, J.R., Raghuraman, M.K., and Cech, T.R., "Monovalent cation-induced structure of telomeric DNA: The G-quartet model". *Cell*, **1989**, 59, 871-880.

76. Williamson, J.R., "Guanine quartets". *Curr. Opin. Struct. Biol.*, **1993**, 3, 357-362.

77. Detellier, C.D. and Laszlo, P., "Role of alkali metal and ammonium cations in the self-assembly of 5'-guanosine monophosphate dianion". *J. Am. Chem. Soc*, **1980**, 102, 1135-1141.

78. Fukushima, K. and Iwahashi, H., "1:1 complex of guanine quartet with alkali metal cations detected by electrospray ionization mass spectrometry". *Chem. Commun.*, **2000**, 895-896.

79. Zhang, Z., Kim, S., Gaffney, B.L., and Jones, R.A., "Polymorphism of signaling molecule c-di-GMP". *J. Am. Chem. Soc*, **2006**, 128, 7015-7024.

80. Pinnavaia, T.J., Miles, H.T., and Becker, E.D., "Self-assembled 5'-guanosine monophosphate. Nuclear magnetic resonance evidence for a regular, ordered structure and slow chemical exchange". *J. Am. Chem. Soc*, **1975**, 97, 7198-7200.

81. Wang, Y. and Patel, D.J., "Guanine residues in d(T2AG3) and d(T2G4) form parallel-stranded potassium cation stabilized G-quadruplexes with anti glycosidic torsion angles in solution". *Biochemistry*, **1992**, 31, 8112-8119.

82. Smith, F.W. and Feigon, J., "Strand orientation in the DNA quadruplex formed from the Oxytricha telomere repeat oligonucleotide d(G4T4G4) in solution". *Biochemistry*, **1993**, 32, 8682-8692.

83. Smith, F.W. and Feigon, J., "Quadruplex structure of Oxytricha telomeric DNA oligonucleotides". *Nature (London)*, **1992**, 356, 164-168.

84. Wang, K.Y., McCurdy, S., Shea, R.G., Swaminathan, S., and Bolton, P.H., "A DNA aptamer which binds to and inhibits thrombin exhibits a new structural motif for DNA". *Biochemistry*, **1993**, 32, 1899-1904.

85. Zhu, G., Live, D., and Bax, A., "Analysis of sugar puckers and glycosidic torsion angles in a DNA G-tetrad structure by heteronuclear three-bond J couplings". *J. Am. Chem. Soc*, **1994**, 116, 8370-8371.

Chapter 2

Synthesis of Thiophosphate Analogs of c-di-GMP

I. Introduction

In 1990, van Boom synthesized a series of analogs of c-di-GMP, and Benziman tested their ability to mimic standard c-di-GMP as activators of cellulose synthase and as substrates for phosphodiesterase A (PDE-A).[1] These analogs included the monothiophosphate of c-di-GMP, both [*R*] and [*S*] diastereomers. The interesting results showed that what they thought was the [*S*] monothiophosphate analog, which was highly resistant to PDE-A degradation, had a binding affinity similar to that of standard c-di-GMP for both cellulose synthase and PDE-A.[1] This finding raises the prospect of synthesizing a family of different thiophosphate analogs of c-di-GMP, some of which may be highly potent activators/second messengers, but with a high stability to enzymatic degradation.

As discussed in Chapter 1, in 1987, van Boom's group[2] was the first to chemically synthesize c-di-GMP, using a modified phosphotriester method. Since then, several methods have been developed to synthesize this molecule more efficiently, including the amidite/H-phosphonate monoester method developed in the Jones lab.[3] However, the synthetic approaches for thiophosphate analogs of c-di-GMP have been limited, with only

two methods reported so far. The first approach reported by van Boom[1] utilized the modified phosphotriester method, which is extremely time consuming and gives poor yields (**Scheme 1-6**). The second is Hayakawa's method,[4] in which a phosphoramidite coupling was used to give the linear dimer, followed by sulfurization to introduce one sulfur at the central phosphorus (**Scheme 1-7**). He then used a phosphotriester method for the cyclic coupling, in spite of its major disadvantages. Furthermore, for both the van Boom and Hayakawa methods, only monothiophosphates can be synthesized, which limits the application of those methods. Clearly, new approaches are needed.

II. Results and Discussion

This thesis reports the development of new approaches to the synthesis of a family of thiophosphate analogs of c-di-GMP, including mono-, di- and trithiophosphates. In these methods, which will be described in the following sections, various monomers have been utilized, including guanosine phosphoramidite, H-phosphonate mono-/di-esters and H-thiophosphonate monoester. Their preparation will be described first.

II1. Synthesis of monomers

Protected guanosine **4** was prepared according to Beigelman[5] and Katsura.[6] As shown in **Scheme 2-1**, the 3' and 5' hydroxyl groups of guanosine **1** were reacted with bis(*tert*-butyl)silylditriflate to give **2**, which was then reacted with *tert*-butyldimethylsilyl

chloride to protect the 2'-OH. *N*-acylation was carried out using isobutyryl chloride to protect the 2-amino group. The product **3** was then reacted with pyridine·HF, resulting in selective desilylation of the silylene, followed by selective tritylation of the 5'-OH using dimethoxytrityl chloride to give protected guanosine **4**.

Scheme 2-1. Guanosine protection and synthesis of monomers

One portion of the protected guanosine **4** was then phosphitylated using 2-cyanoethyltetraisopropylphosphoramidite **5**, activated by pyridinium trifluoroacetate,[7] to give guanosine phosphoramidite **6**. This product was then hydrolyzed, also with Pyr·TFA

activation, to give an H-phosphonate diester intermediate, followed by detritylation catalyzed by sodium bisulfate adsorbed to silica gel (NaHSO$_4$/SiO$_2$)[8] to give compound **7**. This newly reported detritylation method has been adapted here to give a particularly efficient procedure for most tritylated compounds described in this thesis. The 5'-DMT compound was dissolved in CH$_2$Cl$_2$, and 0.6 equivalents of the bisulfate/silica gel and two equivalents of water were added. Thirty minutes of shaking gave a fully detritylated product, and the silica gel was quickly removed by filtration. Addition of toluene and evaporation of CH$_2$Cl$_2$ allowed deposition of the product on the inside of the round bottom flask, while tritanol remained in the toluene. Compared to other detritylation methods, such as those using dichloroacetic acid, acetic acid or sulfonic acid resin, this detritylation method and the use of toluene have the advantages of a fast reaction, fast and easy removal of the acidic silica gel, and convenient separation of the product from tritanol.

Another portion of the protected guanosine **4** was allowed to react with 2-chloro-4*H*-1,3,2-benzodioxaphosphorin-4-one **8**,[3, 9] followed by hydrolysis to make the H-phosphonate monoester **9a**. Another method, in which **4** was reacted with diphenyl phosphite,[10] followed by hydrolysis or sulfide treatment gave the H-phosphonate monoester **9a** or the H-thiophosphonate monoester **9b,** respectively. This second method with hydrolysis gave a similar yield of **9a** as that using 2-chloro-4*H*-1,3,2-benzodioxaphosphorin-4-one. Detritylation was accomplished for both compounds using NaHSO$_4$/SiO$_2$ to give monomers **10a** and **10b**.

II2. Synthesis of monothiophosphate c-di-GMP and configuration assignment

Introduction of only one sulfur at a non-bridging position of a phosphate creates one new chiral center, which can theoretically exist as two diastereomers, [*R*] and [*S*]. However, as described in Battistini's method[11] in Chapter 1, direct sulfurization during H-phosphonate cyclization was stereospecific, and produced only the[*R*] configuration at the new chiral center.

II2.1. Synthesis of monothiophosphate analogs

The first method used here was modified from the published Jones amidite/H-phosphonate monoester method,[3] and sulfurization using elemental sulfur (S_8) was performed during cyclization, rather than oxidation using I_2/H_2O. As shown in **Scheme 2-2**, phosphoramidite **6** was reacted with H-phosphonate monoester **10a**, activated by pyridinium trifluoroacetate,[12] followed by a selective *tert*-butyl hydroperoxide oxidation to give linear dimer **11**. After detritylation, compound **12** was cyclized using pivaloyl chloride as a condensing reagent, and then sulfurized using S_8 to give compound **13**. Because the Beaucage reagent (3H-1,2-benzodithiol-3-one 1,1-dioxide)[13, 14] is used as a standard sulfurizing reagent in solid-phase synthesis, it was also tested for this sulfurization for comparison. It required much stricter anhydrous conditions, and gave a poorer yield because of partial desulfurization. Methylamine (40%) in H_2O was used to

remove the N2-isobutyryl and P-O cyanoethyl protecting groups, followed by 2'

desilylation using triethylamine/trihydrogen fluoride (TEA•3HF) to give the fully

deprotected monothiophosphate c-di-GMP **14**. Only one diastereomer was isolated, and

its assignment is described in section **II2.2**. Consistent with Battistini's results,[11] direct

sulfurization during H-phosphonate cyclization gave only the [*R*] diastereomer.
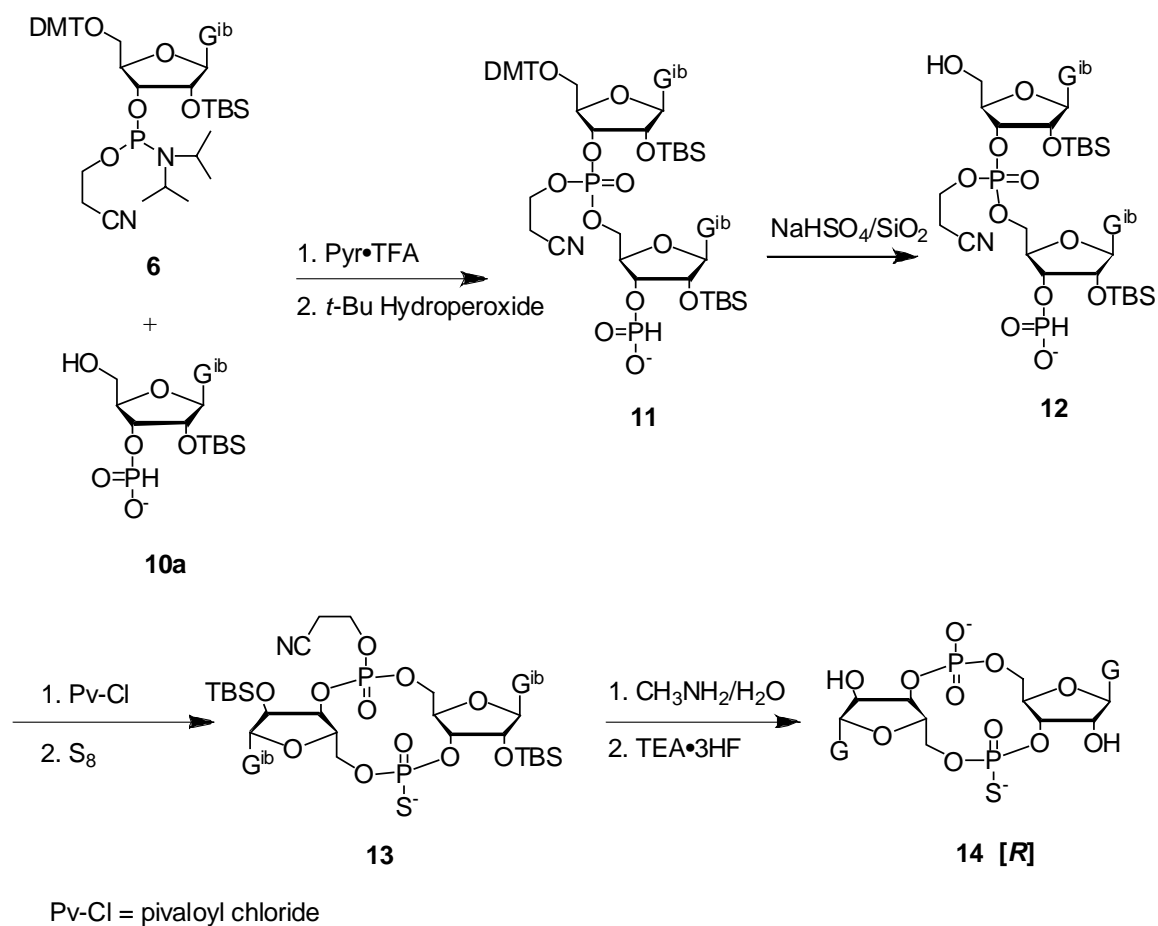
Scheme 2-2. Synthesis of monothiophosphate c-di-GMP by amidite/H-phosphonate
monoester method with sulfurization during cyclization
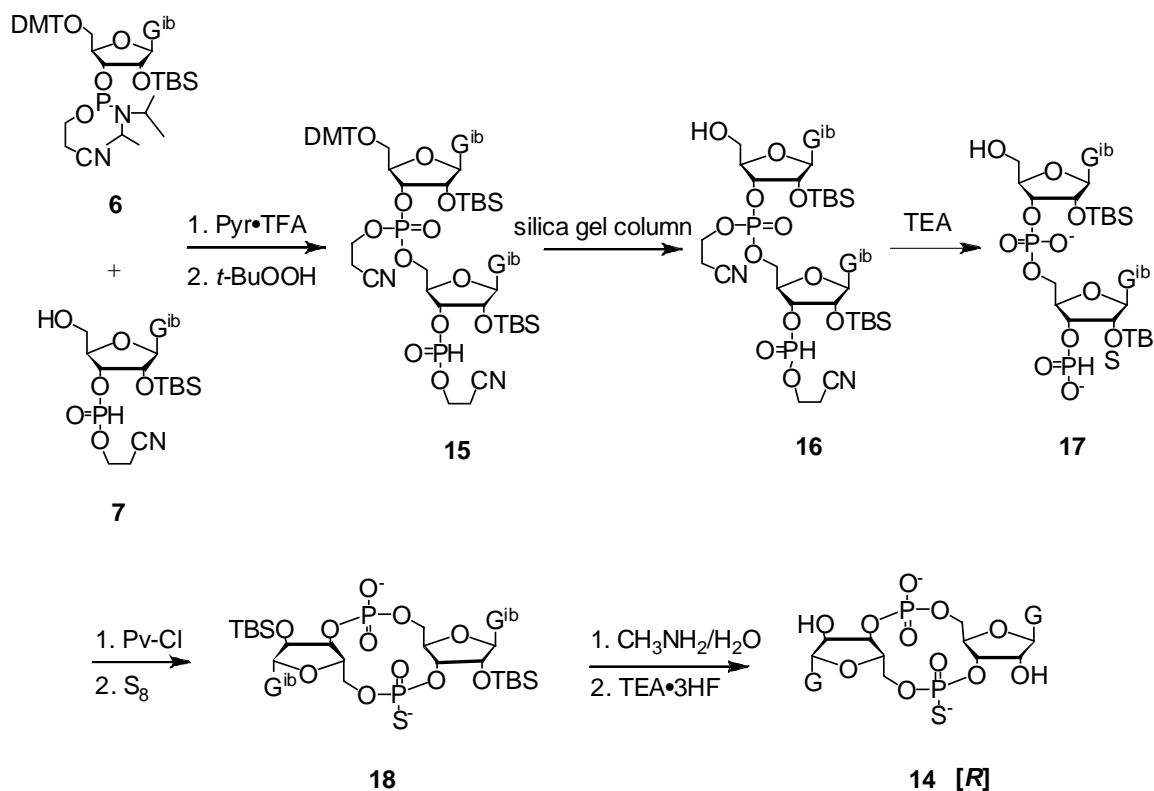
Scheme 2-3. Synthesis of monothiophosphate c-di-GMP by amidite/H-phosphonate
diester method with sulfurization during cyclization

Recently, another method for both the oxygen version of c-di-GMP and the [R]
monothiophosphate c-di-GMP was developed, called the amidite/H-phosphonate diester
method, shown in **Scheme 2-3**. Detritylated H-phosphonate diester **7**, instead of the
monoester **10a**, was reacted with phosphoramidite **6**, followed by a selective *tert*-butyl
hydroperoxide oxidation to give compound **15**. Silica gel chromatography in the presence
of excess Pyr·TFA was found to cause complete detritylation of **15** as well as purification
of the resulting compound **16**. TEA was then used to remove the cyanoethyl groups to
give linear dimer **17**. This intermediate was then cyclized and sulfurized to give only one
diastereomer of cyclic dimer **18**, which was partially purified by silica gel
chromatography and then crystallized. If I$_2$/H$_2$O had been used, unmodified protected c-

di-GMP would have been obtained. After the same deprotection procedures described in the previous method, monothiophosphate c-di-GMP **14** was obtained. Again, as discussed for the previous method, only the [*R*] diastereomer was obtained by cyclization of the H-phosphonate followed by sulfurization. However, it was found that a significant amount of dephosphorylated linear dimer was formed as a side product. Thus, this method has not been pursued.

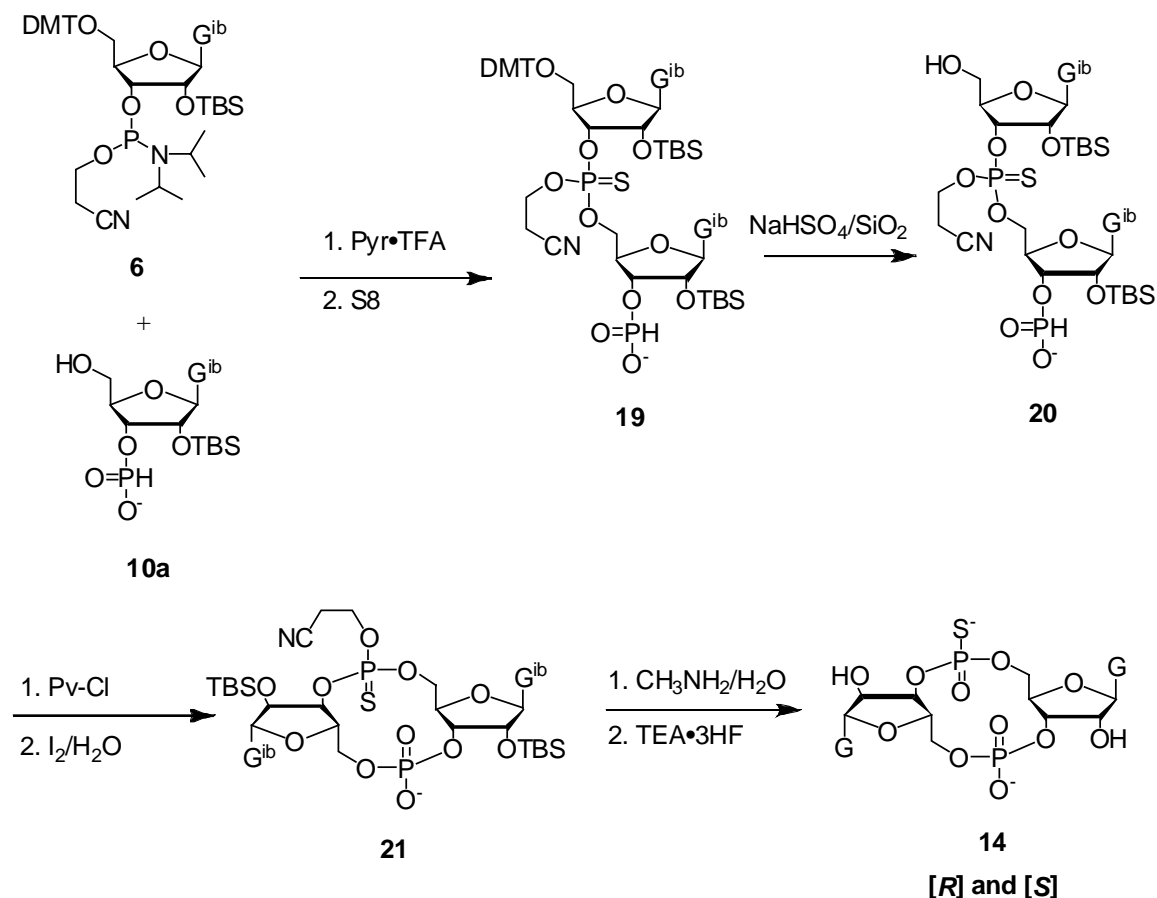**Scheme 2-4.** Synthesis of monothiophosphate c-di-GMP by amidite/H-phosphonate monoester method with sulfurization during linear coupling

In order to get the [*S*] monothiophosphate c-di-GMP, a new strategy was used, in which the sulfurization takes place during the linear coupling rather than during the cyclization. Although this reaction is not selective and gives a mixture of [*R*] and [*S*]

diastereomers, the final products can be separated. Therefore, the amidite/H-phosphonate monoester approach was modified, as illustrated in **Scheme 2-4**. The amidite **6** and the monoester **10a** were reacted, after which one sulfur was introduced using S_8, giving a mixture of diastereomeric thiophosphate triesters **19**. The purification of linear dimer **19** was carried out on silica gel, with poor separation between **19** and a side-product obtained from sulfurization of excess phosphoramidite. It was also very difficult to remove S_8, which eluted throughout the gradient. Detritylation of **19** produced the linear dimer **20**, which was cyclized using pivaloyl chloride and oxidized using I_2/H_2O to give cyclic dimer **21**. The same deprotection procedures were utilized to give fully deprotected monothiophosphate c-di-GMP **14**, as about equal amounts of the [*R*] and [*S*] diastereomers, which were separated and purified using semi-preparative RP HPLC. Unfortunately, the separation and purification of these diastereomers turned out to be very difficult.

It has been reported that RP HPLC can be used to separate the two diastereomers of linear dimers d(TpsT) and d(TpsA), but only at small scales (~ 1-2 µmol) range.[15, 16] Fairly large scale (250 µmol) mixtures of diastereomers of linear DNA dimer TpsT could be separated and purified up to 80% purity, using a DEAE-Sephadex A-25 resin, with a shallow gradient of TEAB.[17] These 80% enriched diastereomers were then further purified by semi-preparative RP-HPLC to give a 95% pure product.

For the work here, the [*R*] and [*S*] diastereomers of the monothioate analog could be well separated by semi-preparative RP-HPLC at ~ 300 µmol. However, a major problem

that resulted in low yields was the separation of each diastereomer from other impurities due to several reasons. First, linear dimers GpsG and GpsGp, both with [R] and [S] diastereomers, were the main side products of the cyclization and deprotection steps, and eluted from the RP column at a similar rate as c-di-GMP due to structural similarity. A second problem was complex formation of the products and side products, since guanosine is well known to form quartets in the presence of Na^+ or K^+.[18] As will be discussed in Chapter 3, the monothiophosphate c-di-GMP, as well as the linear impurities tended to form various kinds of complexes at the high HPLC sample concentrations, which made purification very difficult. To obtain pure diastereomers, several columns had to be run for each sample, resulting in a large loss of final product. The effect of aggregation was more pronounced for the [S] diastereomer, since it forms complexes to a higher extent than the [R] diastereomer, as discussed in Chapter 3. These problems also occurred for the purification of the di- and trithiophosphate c-di-GMP analogs. The [R] and [S] configuration assignment of the monothioate is described in the next section using synthetic and enzymatic methods.

II2.2. Configuration assignment of monothiophosphate c-di-GMP

The configuration of the two diastereomers of monothiophosphate c-di-GMP **14** was assigned in two different ways, first by enzymatic degradation of the linear dimers that were also cyclized, and second by direct digestion of the cyclic dimers. In order to assign the configuration by the first method, the linear dimer intermediate **19**, described in the previous section, was separated and purified to > 80% enrichment of each diastereomer.

For each of these individual diastereomers, one portion was cyclized to give c-di-GMP **14**, and another portion was subjected to a series of deprotecting and purification steps to give the pure linear dimer diastereomers, shown in **Figure 2-1**. This process is illustrated by HPLC chromatograms in **Figure 2-8** in the Appendix of this chapter. As can be seen in these chromatograms, the diastereomer of **14** with the longer retention time (6.1 min) must have the same configuration as the linear dimer with a retention time of 5.1 min. The other diastereomer with a shorter retention time (4.7 min) must have the same configuration as the linear dimer with a retention time of 5.8 min. The configuration of the linear dimers was then assigned as described below using enzymatic digestion, and the results were correlated to the corresponding cyclic dimers.

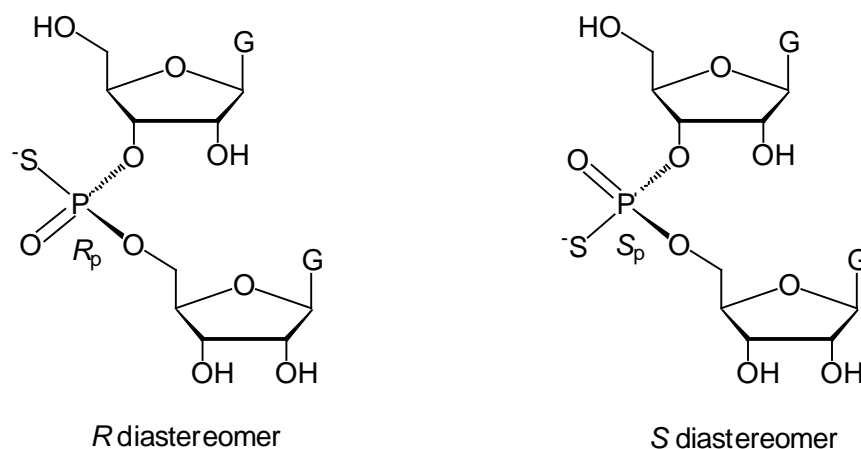**Figure 2-1.** Schematic structures of the two diastereomers of linear dimer (GpsG)

Snake venom phosphodiesterase (SVPDE) has been used by others to determine the configuration of linear dinucleotide analogs, including thiophosphates and boranophosphates.[17, 19, 20] To determine the specificity of the SVPDE degradation of the phosphorothioate linkage, Eckstein[17] has used the two diastereomers of linear UpsA as

substrates for two enzymes, ribonuclease A (RNase A) and SVPDE. The diastereomer of UpsA with a shorter retention time on reverse phase was digested by RNase A to form uridine 2',3'-cyclic phosphorothioate (U>pS) as an *endo* isomer, and the one with a longer retention time was digested to form an *exo* isomer. According to their earlier X-ray crystal structure study of RNase A mechanism,[21, 22] hydrolysis of the linear thiophosphate with [R] configuration specifically gives the *endo* isomer. The stereochemistry of UpsA was thus established by RNase A, relative to the HPLC elution order. The known diastereomers of UpsA were then subjected individually to SVPDE degradation, and it was found that the [R] diastereomer was digested much faster than the [S] diastereomer.

The two diastereomers of the linear dimer GpsG described above were then digested individually using SVPDE at the same substrate-to-enzyme ratio and the digestion was followed by LC-MS. A plot of disappearance of GpsG against time is shown in **Figure 2-2**, which was obtained by integration of the HPLC peaks in the chromatograms shown in **Figure 2-9** in the Appendix. The HPLC chromatograms and the plot illustrate the fast disappearance of the linear dimer with a retention time of 5.1 min, which is therefore assigned as the [R] diastereomer. The other linear dimer with a retention time of 5.7 min showed negligible digestion over three days and was assigned as the [S] diastereomer. These configurations were then assigned to their corresponding cyclic dimers, with the one with longer retention time (6.1 min) as the [R] diastereomer, and the one with shorter retention time (4.7 min) as the [S] diastereomer.
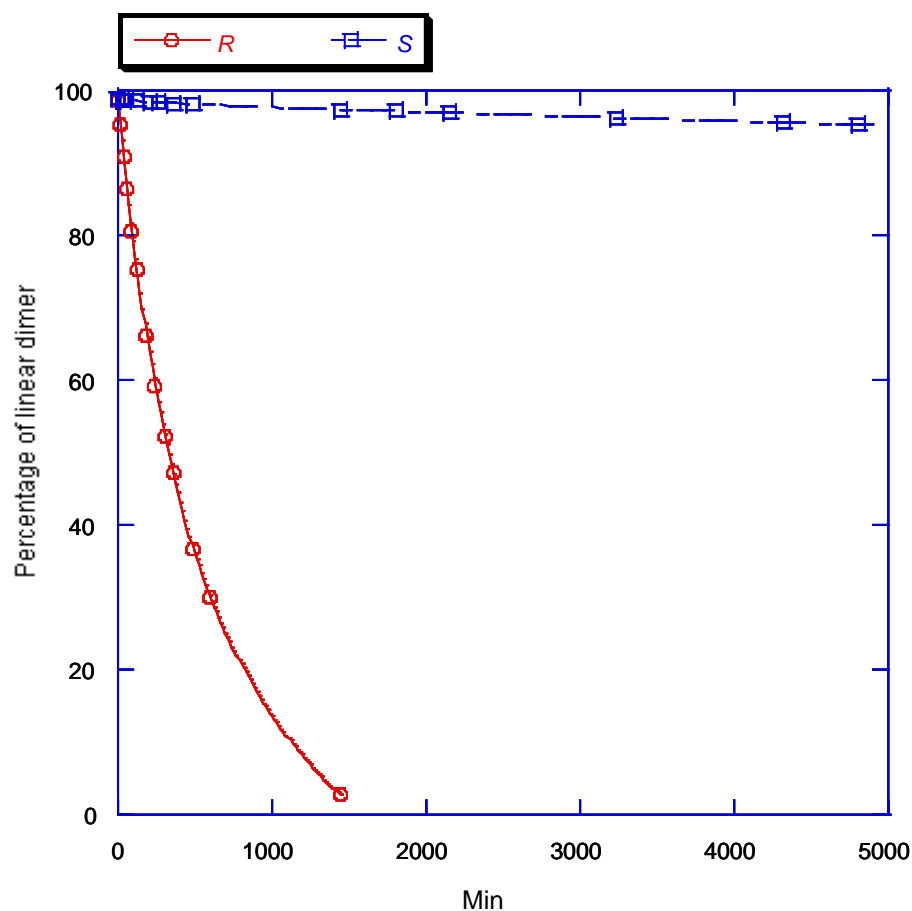
Figure 2-2. SVPDE digestion of two diastereomers of synthetic linear dimer GpsG

Direct enzymatic digestion to assign the configuration of monothiophosphate c-di-GMP by the second method was carried out using three different enzymes. Since SVPDE is an exonuclease and cannot open the closed ring of a cyclic dimer, nuclease P1, an endonuclease, was initially used to individually hydrolyze the two diastereomers of monothio c-di-GMP at the unmodified phosphate to give linear dimers with 5'-phosphates (pGpsG). According to the HPLC chromatograms in **Figure 2-10** in the Appendix, the cyclic dimer with the longer retention time gave the linear dimer with the longer retention time. The elution order of these phosphorylated linear dimers (pGpsG) is

opposite to that of unphosphorylated linear dimers (GpsG), as a result of the 5'-phosphate.
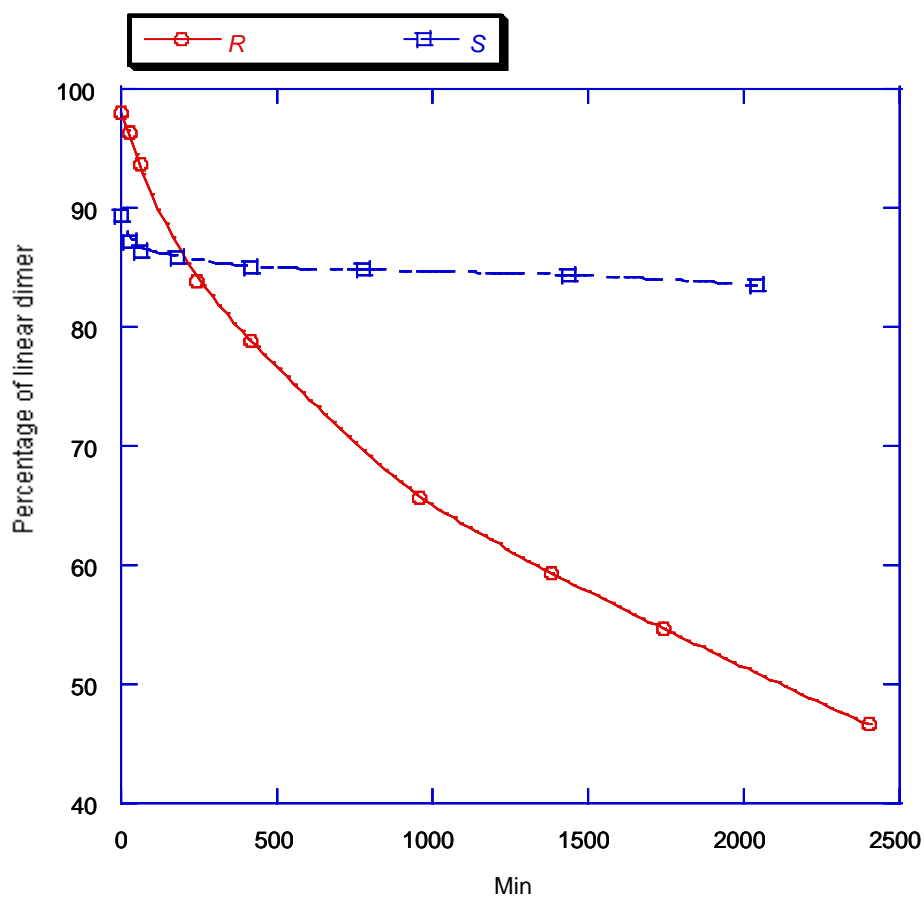
Figure 2-3. SVPDE digestion of linear dimer products without 5'-phosphate. Ring opened by nuclease P1 and dephosphorylated by phosphatase

After denaturation of the P1 by heating at 95 °C for 30 min, alkaline phosphatase was added to the solution to remove the 5'-phosphate. The solution was heated at 37 °C for 4 hrs, at which point HPLC showed complete removal of the 5'-phosphate to give linear GpsG. After 30 min denaturation of the phosphatase at 95 °C, SVPDE was added to the solution to digest the linear dimer GpsG. During the whole process, the ratio of enzymes

to substrates was kept the same for both samples. The SVPDE degradation was monitored by HPLC-MS, with the % GpsG remaining obtained by integration of HPLC peaks in the chromatograms shown in **Figure 2-10** in the Appendix. A plot of % GpsG remaining against time is shown in **Figure 2-3**. Consistent with the first method described above, the cyclic dimer with a longer retention time degraded faster with SVPDE and was assigned as the [*R*] diastereomer, while the c-di-GMP with a shorter retention time degraded much slower and was assigned as the [*S*] diastereomer.
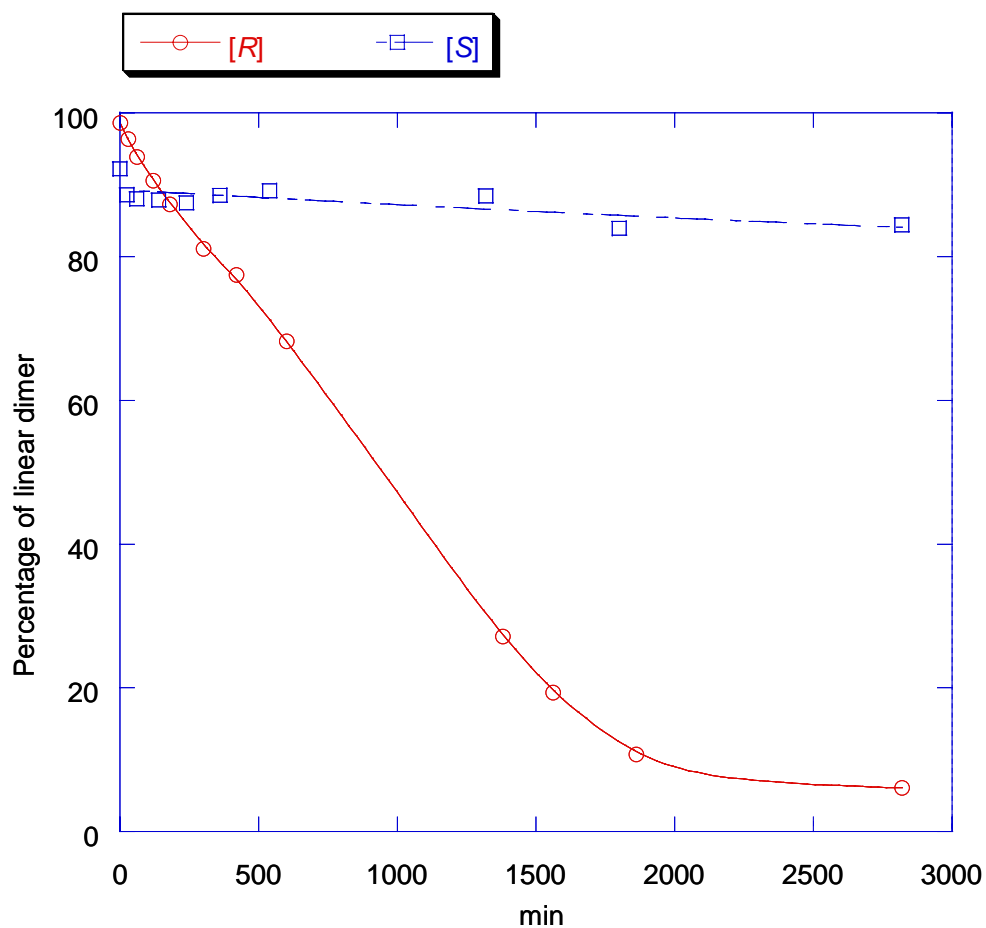

Figure 2-4. SVPDE digestion of linear dimer products containing 5'-phosphate. Ring opened by nuclease P1

This same method was also carried out without removal of the 5'-phosphate by phosphatase to determine whether or not it made a difference. The two diastereomers were separately subjected to nuclease P1 for the ring opening, to give linear dimer pGpsG, as before. After denaturation of P1 by heating at 95 °C, the phosphorylated linear dimers were directly digested by addition of SVPDE. The percentage of linear dimer remaining was obtained by integration of HPLC peaks in the chromatograms shown in **Figure 2-11,** and a plot of the disappearance of pGpsG against time is shown in **Figure 2-4**. Again, the monothio c-di-GMP with a longer retention time gave a linear product that was almost completely degraded after 47 hrs and was therefore assigned as the [*R*] diastereomer. The linear dimer from the other diastereomer was only slightly digested by SVPDE after 47 hrs and was therefore assigned as the [*S*] diastereomer.

To compare these SVPDE results to a different enzyme, an alternative method using nuclease P1 to degrade the linear dimer, as well as cleave the cyclic dimer, was applied to both diastereomers. Nuclease P1 has been used by others to assign the configuration of monothiophosphate substituted linear oligonucleotides.[17, 23] They found that for linear oligonucleotides, the [*S*] thiophosphates were digested faster by this enzyme than the corresponding [*R*] thiophosphates, opposite to the pattern with SVPDE. For this work, the cyclic dimer was again initially hydrolyzed by nuclease P1 in pH 7.0 TEAA buffer, to give linear dimer pGpsG. The solution was heated at 95 °C for 30 min to denature the enzyme, and the pH was then adjusted to about 5.9, which is the optimal pH for nuclease P1,[24] by addition of acetic acid. A smaller portion of fresh nuclease P1 was then added, and the progress of the subsequent cleavage at the thiophosphate was monitored by LC-

MS. Phosphatase was not used because it was shown in the previous section that the 5'-phosphate did not affect the results. A plot of disappearance of pGpsG against time is shown in **Figure 2-5**, with the data having been derived from integration of the HPLC peaks in the chromatograms shown in **Figure 2-12** in the Appendix. The results show that the diastereomer with the longer retention time degrades slower while the diastereomer with the shorter retention time degrades faster. According to the literature, the dimer with the faster degradation rate was assigned as the [*S*] diastereomer. The other dimer, which had almost no degradation over two days, was assigned as the [*R*] diastereomer. These results are consistent with all the methods described above, that the diastereomer of monothiophosphate c-di-GMP with the longer retention time is [*R*] and diastereomer with shorter retention time is [*S*].

After this determination of the stereochemistry of the monothiophosphate c-di-GMP, samples were prepared for ^{31}P NMR at low concentration to obtain chemical shifts for both the [*R*] and [*S*] thiophosphates. These chemical shifts were then used to assign the configurations of the di- and trithiophosphate analogs, as discussed in Chapter 3, section **II**.
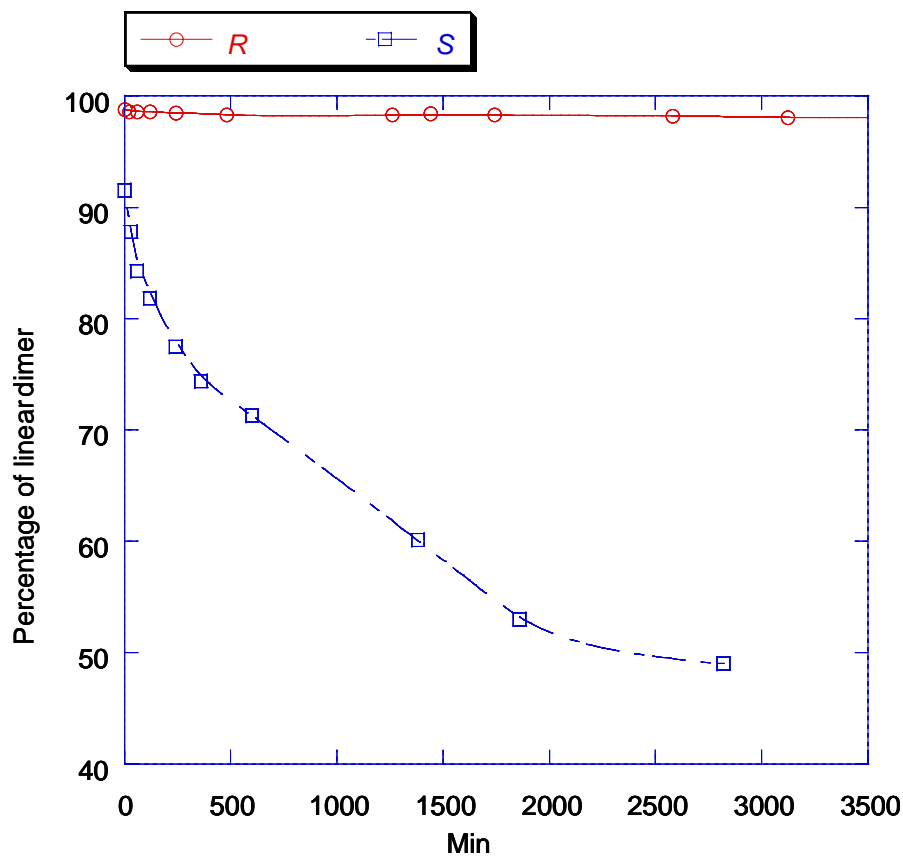
Figure 2-5. Nuclease P1 digestion of linear dimer products containing 5'-phosphate. Ring opened by Nuclease P1

II3. Synthesis of dithiophosphate c-di-GMP
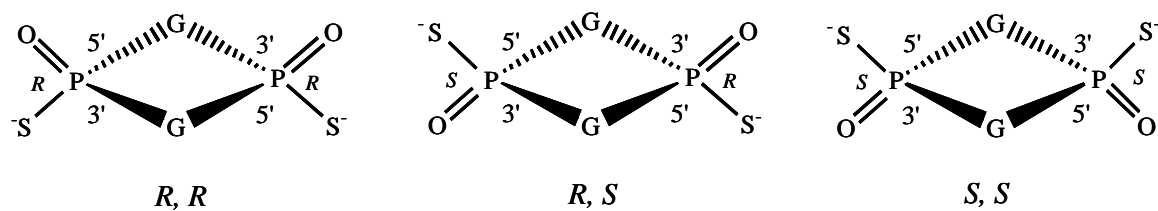
Figure 2-6. Schematic structures of the three diastereomers of dithioate c-di-GMP

The three possible diastereomers of dithiophosphate c-di-GMP are shown schematically in **Figure 2-6**. Because of the symmetry of the molecule, there are three rather than four diastereomers. However, until now, synthesis of any dithiophosphate c-di-GMP has not been reported.
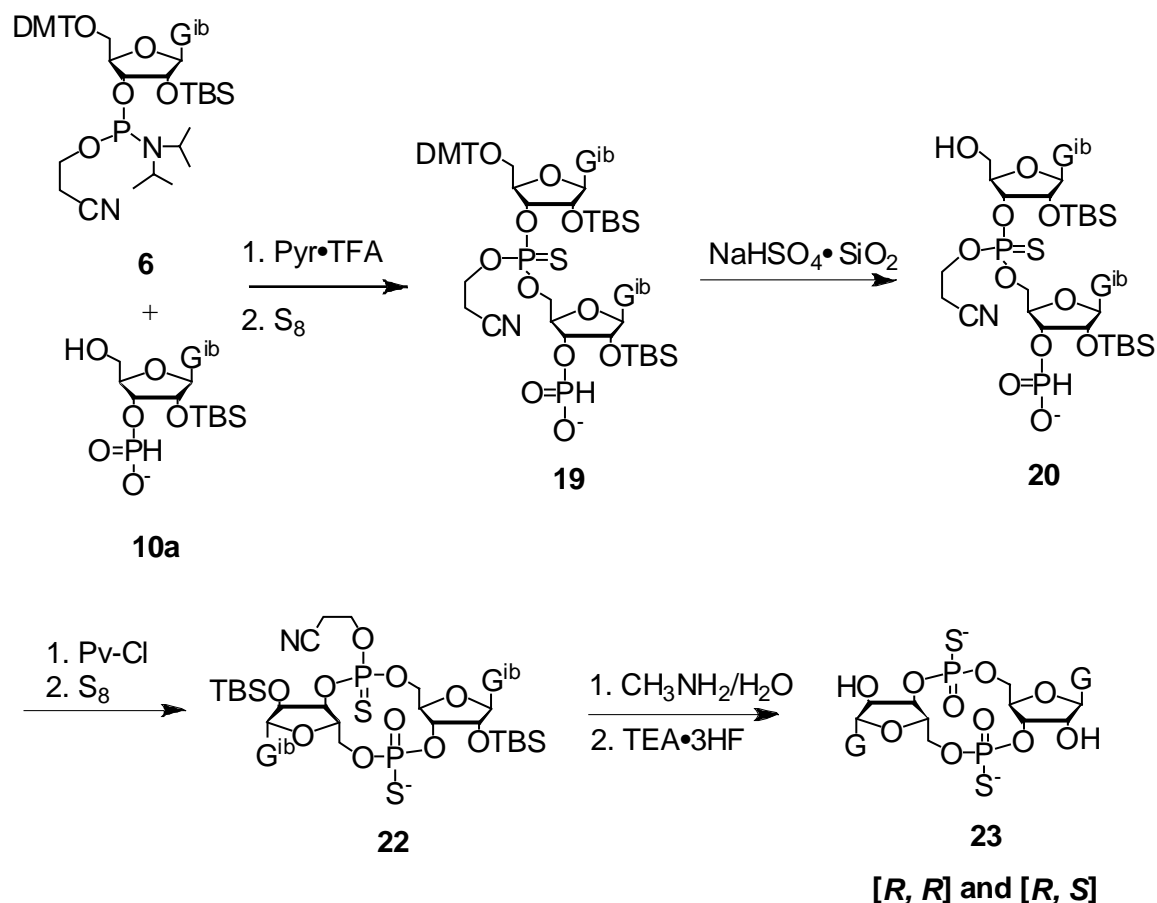
Scheme 2-5. Synthesis of dithiophosphate c-di-GMP by amidite/H-phosphonate monoester method

The first approach used to synthesize dithiophosphate c-di-GMP was modified from the previous amidite/H-phosphonate monoester method. As shown in **Scheme 2-5**, during the linear coupling step using an amidite reaction, S_8 was used to introduce the first sulfur

at the internal phosphorus center, as described in **Scheme 2-4** for the first part of the monothiophosphate synthesis. After detritylation, dimeric compound **20** was cyclized using pivaloyl chloride as before, but then sulfurized again using S_8 to give cyclic dimer **22**. After deblocking to give fully deprotected dithiophosphate c-di-GMP **23**, only two diastereomers were obtained. As before, the stereospecificity of cyclization and sulfurization allowed only formation of the [*R*] configuration at the second chiral center. As a result, only two out of three possible diastereomers were obtained, with configurations of [*R, R*] and [*R, S*].
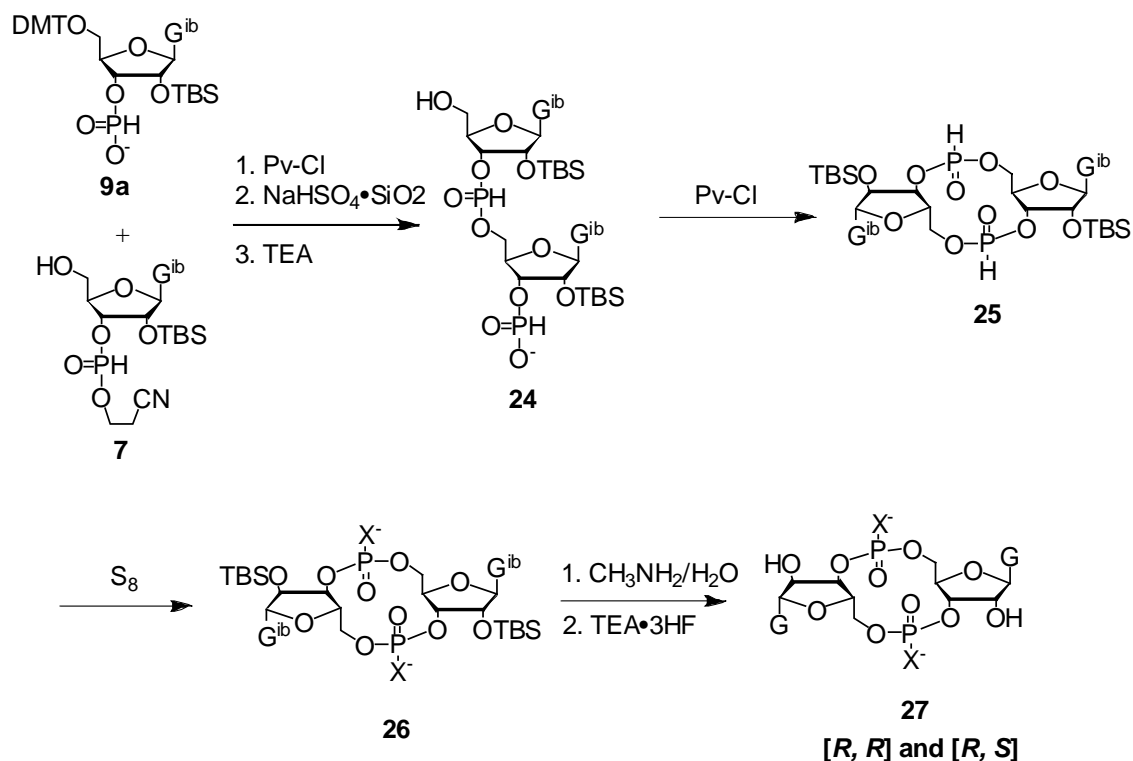
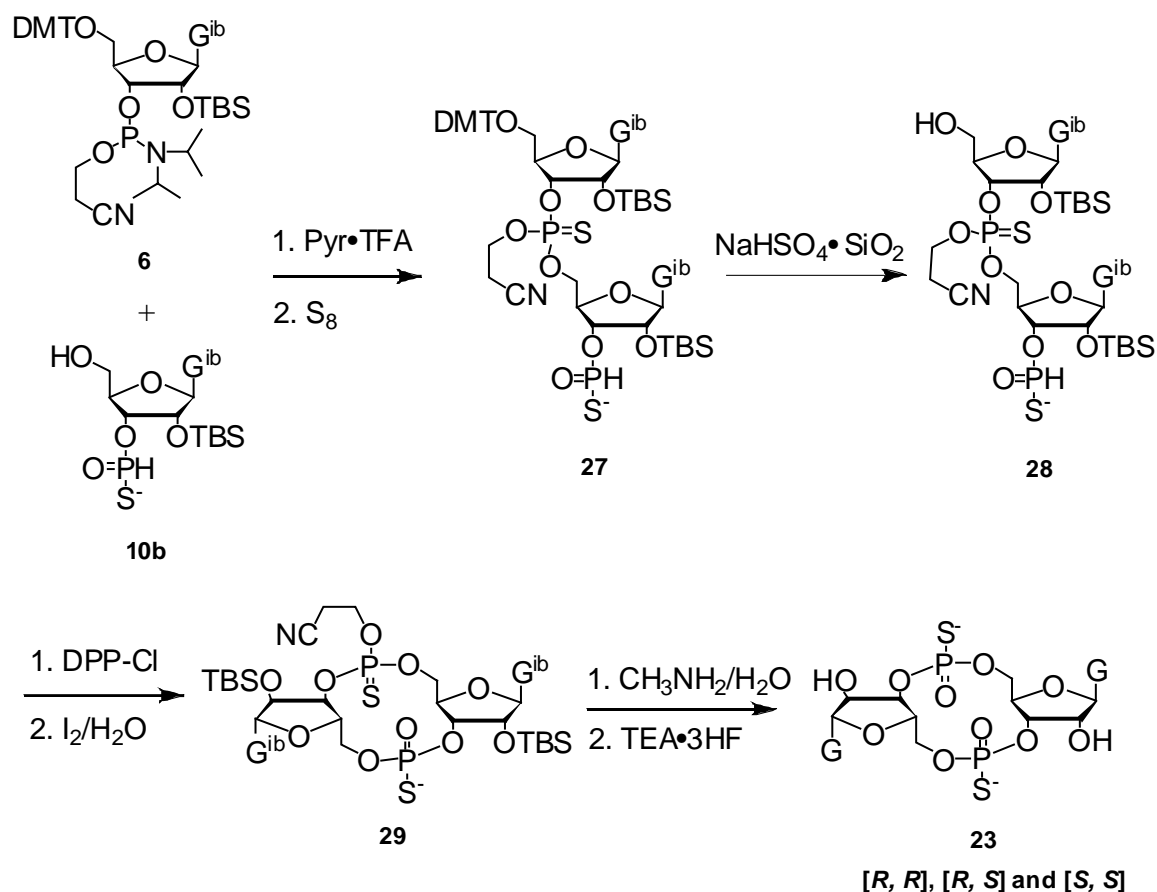**Scheme 2-6.** Synthesis of dithiophosphate c-di-GMP by H-phosphonate mono-/di-ester method

A new approach using H-phosphonate coupling in both steps was then developed to synthesize dithiophosphate c-di-GMP, with the hope of obtaining some of the [*S, S*]

diastereomer. This H-phosphonate mono-/diester method is illustrated in **Scheme 2-6**. Tritylated H-phosphonate monoester **9a** was coupled with H-phosphonate diester **7**, followed by detritylation and TEA treatment to give linear dimer **24**. This compound was immediately cyclized without oxidation to give intermediate **25**, which contains two H-phosphonate diesters. Cyclic dimer **25** was sulfurized at both H-phosphonates to give dithiophosphate **26**, and then fully deprotected as before. However, once again, this new method only produced two diastereomers of dithiophosphate c-di-GMP **23**, the [*R, R*] and the [*R, S*], presumably because of the same constraints of the cyclization process.

One advantage of this approach is that both sulfurizations could be done in one reaction. Furthermore, there was no silica column purification after the intermolecular coupling. Although the only normal phase chromatography was done on cyclic compound **25**, which was a neutral molecule, partial decomposition of compound **25** occurred, resulting in much lower yield. Therefore, this method was not pursued.

As discussed above, both previously described methods only gave [*R, R*] and [*R, S*] diastereomers of dithiophosphate c-di-GMP. Thus, it was necessary to develop a new method to synthesize the third diastereomer [*S, S*]. A new strategy was devised using an amidite/H-thiophosphonate monoester method. Use of a H-phosphonate monoester already containing a sulfur, **10b**, should allow formation of the [*S*] diastereomer during the cyclization, which is followed by oxidation with I_2/H_2O. As shown in **Scheme 2-7**, intermolecular coupling between the phosphoramidite **6** and the H-thiophosphonate monoester **10b**, followed by S_8 sulfurization, produced the linear dimer **27**, already

containing two sulfurs. In this step, elemental sulfur was chosen over the Beaucage reagent because of the desulfurization problem with Beaucage that was discussed before in the synthesis of monothiophosphate c-di-GMP. In addition, the Beaucage reagent would react with H-thiophosphonate, while S_8 does not. The detritylated intermediate **28** was then cyclized using diphenyl chlorophosphate (DPP-Cl) and oxidized using I_2/H_2O to give cyclic compound **29**. DPP-Cl was used as condensing reagent during cyclization instead of Pv-Cl to avoid desulfurization. An H-thiophosphonate can react with a condensing agent either through its sulfur or its oxygen to form a mixed anhydride.

Scheme 2-7. Synthesis of dithiophosphate c-di-GMP by amidite/H-thiophosphonate monoester method

With Pv-Cl, it reacts through its sulfur, which is then lost during cyclization. However, according to Stawinski,[25] it reacts with DPP-Cl through its oxygen, which is more nucleophilic than sulfur towards a phosphorus center, thereby retaining the sulfur. The subsequent oxidation using I_2/H_2O is known not to be stereospecific,[26, 27] so both [*R*] and [*S*] configurations were produced at the new chiral center. Since the first chiral center already had both configurations, the cyclized dimer **29** was a mixture of all three diastereomers. During this oxidation of the newly formed H-thiophosphonate diester, other oxidants were tested, but none was as good as I_2/H_2O. *t*-Bu hydroperoxide was not able to oxidize the P(III) to P(V), and H_2O_2 and *m*-chloroperbenzoic acid gave partially oxidized ring-opened linear products. At this point, this new method is the only way to synthesize the [*S, S*] diastereomer of dithiophosphate c-di-GMP. Unfortunately, this mixture requires multiple columns for initial diastereomer separation and further purification, because of the enhanced tendency of the [*S, S*] diastereomer to aggregate, as described in Chapter 3. The final yields are therefore poor.
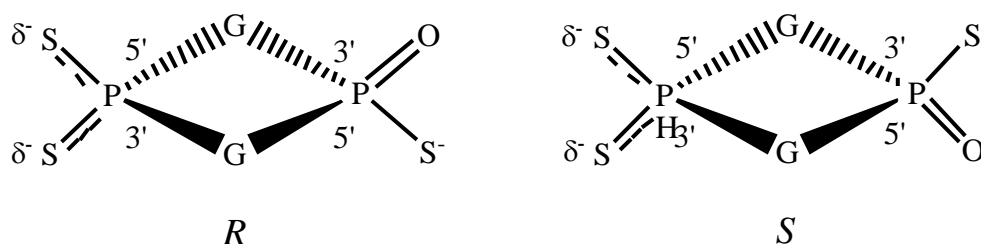
II4. Synthesis of trithiophosphate c-di-GMP

Figure 2-7. Schematic structures of two diastereomers of trithioate c-di-GMP

Trithiophosphate c-di-GMP exists as only two diastereomers, [R] and [S], as shown in **Figure 2-7**. Both of these diastereomers have sulfur atoms in the [R] and [S] positions at the non-chiral phosphate, and so may have interesting properties.
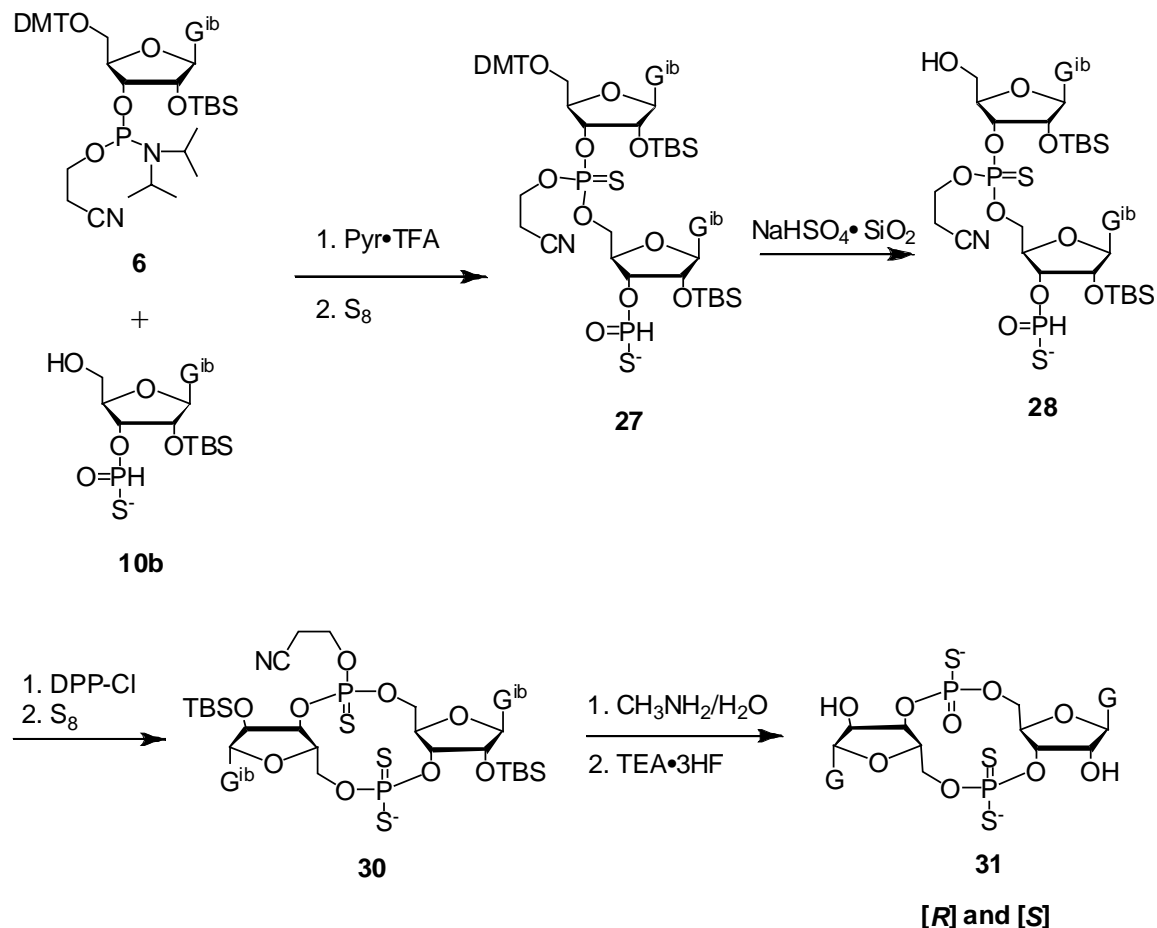
Scheme 2-8. Synthesis of trithiophosphate c-di-GMP by amidite/H-thiophosphonate monoester method

The third amidite/H-thiophosphonate method used for the synthesis of dithiophosphate c-di-GMP can also be used for synthesis of trithiophosphate c-di-GMP, but with a final sulfurization. The same procedures described earlier were utilized to make linear compound **28**, then S_8 was used to introduce the third sulfur after the cyclization step with DPP-Cl. After deprotection, cyclic trithiophosphate **31** was obtained

as a mixture of both [*R*] and [*S*] diastereomers. Again, because of their tendency to aggregate, extensive separation and purification were required during the final semi-preparative HPLC.

III. Experimental procedures

III1. General methods

Guanosine hydrate, di-*tert*-butylsilyl ditriflate, *tert*-butyldimethylchlorosilane, hydrogen fluoride-pyridine, pyridinium trifluroacetate, diphenyl phosphite, diphenyl chlorophosphate, lithium sulfide, *tert*-butylhydroperoxide, methylamine in water, TEA•3HF and elemental sulfur were purchased from Aldrich. Pivaloyl chloride was purchased from Aldrich, and freshly distilled before each use. Snake venom phosphodiesterase (Type IV from *Crotalus atrox*) and nuclease P1 phosphodiesterase were purchased from Sigma. Analytical reverse phase HPLC was carried out on a Waters 2960 system, with an Atlantis analytical column (dC18 column, 100Å, 4.6 mm × 50 mm, 3.0 μm). Binary mobile phase gradients of acetonitrile and 0.1 M triethylammonium acetate (TEAA) buffer (pH 6.8) were used with a flow rate of 1.0 mL/min. ESI-MS was acquired using a Waters Micromass single quadropole LCZ system. Semi-preparative reverse phase HPLC was performed on a Waters Novapak C18 19 × 300 mm column or a Beckman ultrapore RPSC C3 10 × 250 mm column. Preparative silica gel chromatography was carried out on pre-packed silica gel flash columns from AnaLogix.

III2. Synthesis of monomers

III2.1. Protection of guanosine

Guanosine hydrate **1** (15.05 g, 50 mmol) was dried three times by coevaporation with pyridine and suspended in DMF. Di-*tert*-butylsilyl ditriflate (18.0 mL, 55 mmol, 1.1 equivalent) was added dropwise and allowed to react for 0.5 hr at 0 ºC. This was followed by addition of imidazole (17.0 g, 250 mmol, 5 eq), which was stirred for 0.5 hr at room temperature, and then *tert*-butyldimethylchlorosilane (9.06 g, 60 mmol, 1.2 eq), which was stirred for 2 hrs in a 60 °C oil bath. After chilling, product **2** was collected by filtration, washed with cold methanol and dried in a desiccator over P_2O_5. Compound **2** (22.0 g, 41 mmol) was next reacted with isobutyryl chloride (8.6 mL, 82 mmol, 2 eq) in 3:1 methylene chloride:pyridine to protect the 2-amino group. The reaction was allowed to proceed for 3 hrs at room temperature, then diluted with 32 mL methanol to quench the excess isobutyryl chloride and cooled in an ice bath. A solution of methylamine in ethanol (21 mL, 205 mmol, 5 eq) was then added to the reaction mixture to remove the second isobutyryl group on the guanine amino. After 0.5 hr, the mixture was concentrated to a slurry and suspended in methanol in an ice bath for 2 hrs. Product **3** (25.3 g, 41 mmol) was collected by filtration and washed with cold methanol. Hydrogen fluoride-pyridine (4.9 mL, 189 mmol, 4.6 eq) was added to a suspension of **3** in dry methylene chloride for 2 hrs in an ice bath. Then a saturated sodium bicarbonate solution was used to wash the reaction mixture, and the organic layer was concentrated and coevaporated with pyridine three times, the last time leaving about 100 mL. Dimethoxytrityl chloride (15.3 g, 45.1 mmol, 1.1 eq) was then added to the solution at 0 ºC. The reaction mixture

was kept in a refrigerator overnight, then quenched with addition of 0.5 mL methanol. Most of the pyridine was removed by evaporation and the residue was then dissolved in CH_2Cl_2, which was washed with saturated sodium bicarbonate. The organic layer was then concentrated, evaporated with toluene three times, and dissolved in CH_2Cl_2. The product was crystallized in 10% CH_2Cl_2 in ethyl ether to give the protected guanosine **4** (28.1 g, 36.5 mmol) in 73% yield from guanosine hydrate **1**.

III2.2. Synthesis of guanosine monomers

Guanosine phosphoramidite (6). Protected guanosine **4** (3.85 g, 5.0 mmol) was dried by coevaporation with CH_3CN, and then bis(diisopropylamino)cyanoethylphosphoramidite (1.9 mL, 6.0 mmol, 1.2 eq) was added. Pyridinium trifluoroacetate (1.16 g, 6.0 mmol, 1.2 eq) was first dried with CH_3CN and then slowly added to the solution of **4**. The reaction was allowed to proceed overnight at room temperature and was then checked by HPLC/MS. The mixture was concentrated and directly purified by silica gel chromatography using a gradient of ethyl acetate in hexane to give protected guanosine phosphoramidite **6** (4.16 g, 4.3 mmol) in 86% yield. The LC-MS profile shown in **Figure 2-13** confirmed the correct product with an m/z (M-1) of 968.8 (calculated for $C_{50}H_{67}N_7O_9PSi^-$: 968.5) in negative mode.

Detritylated guanosine H-phosphonate diester (7). Guanosine phosphoramidite **6** (1.94 g, 2.0 mmol) was dissolved in 20 mL CH_3CN, and water (72 μL, 4.0 mmol, 2 eq) was added. Pyridinium trifluroacetate (0.39 g, 2.0 mmol, 1 eq) was added to the solution,

which was left for 10 min to complete hydrolysis, and checked by LC-MS. The reaction mixture was then concentrated and evaporated with 10 mL toluene, followed by 10 mL CH_3CN to make a dry foam. It was dissolved in 100 mL CH_2Cl_2 and water (72 μL, 4.0 mmol, 2 eq) was added, along with sodium bisulfate adsorbed to silica gel ($NaHSO_4/SiO_2$, 0.55 g, 1.2 mmol H^+, 0.6 eq). The mixture was shaken for 0.5 hr to complete detritylation. The detritylated product was filtered to remove the silica gel, which was washed three times with CH_2Cl_2. To remove the tritanol, the filtrate was evaporated with frequent additions of toluene (50 mL × 3), the last time with about 100 mL liquid left. The H-phosphonate diester was deposited on the inside wall of the flask, leaving tritanol in the toluene solution. Hexane (15 mL) was added to the solution, which was allowed to sit for 30 min. The liquid was decanted and the residue was washed with 20 mL 15% hexane in toluene. The residue was then dissolved in CH_2Cl_2, made into a dry foam, and dried in a desiccator over P_2O_5 to give product **7** (1.33 g, 1.66 mmol) in 83% yield. The product was confirmed by LC-MS in negative mode as shown in **Figure 2-14**, with a major MS peak at 530.5, which is believed to be a fragment of the molecular ion. The molecular ion with an m/z (M-1) of 583.5 (calcd for $C_{23}H_{36}N_6O_8PSi^-$: 583.2), was also shown in the MS spectrum but with low intensity.

Detritylated guanosine H-phosphonate (10a). Diphenyl phosphite (DPP-H, 1.9 mL, 10 mmol, 2 eq) was dissolved in dry pyridine in a 100 mL round bottom flask. Protected guanosine **4** (3.85 g, 5.0 mmol) was evaporated with pyridine three times, the last time with 15 mL left. This solution was immediately transferred to the flask with DPP-H, and allowed to react for 15 min at room temperature. The reaction mixture was poured into

saturated NaHCO$_3$ and extracted with CH$_2$Cl$_2$ (50 mL × 3). The organic layers were concentrated, and the product was purified by silica gel chromatography using a gradient of methanol in methylene chloride with 0.5% pyridine. Pure product fractions were combined and then detritylated using NaHSO$_4$/SiO$_2$ (1.36 g, 3.0 mmol, 0.6 eq). The resulting product was then separated from tritanol using a procedure similar to that described for **7** to give guanosine H-phosphonate **10a** (2.25 g, 3.7 mmol, 74%), which was characterized by LC-MS in negative mode, showing m/z (M-1) 530.5 (calcd for C$_{20}$H$_{33}$N$_5$O$_8$PSi$^-$: 530.2) (**Figure 2-15**)

Detritylated guanosine H-thiophosphonate (10b). Protected guanosine **4** (3.21 g, 4.1 mmol) and DPP-H (1.6 mL, 8.2 mmol, 2 eq) were reacted as described for **10a**. After the reaction was stirred for 15 min, lithium sulfide (Li$_2$S, 0.94 g, 20.5 mmol, 5 eq) was added to the reaction. After 40 min, the solution was extracted with aqueous NaHCO$_3$, and the organic layers were concentrated and purified by silica gel chromatography using a gradient of methanol in methylene chloride with 0.5% pyridine. Product fractions were pooled, concentrated to dryness and then dissolved in CH$_2$Cl$_2$ for overnight self-detritylation. The product was separated from tritanol as described for **7** to give guanosine H-thiophosphonate **10b** (1.81 g, 2.9 mmol) in 71% yield. The product was confirmed by LC-MS with m/z (M-1) of 546.4 (calcd for C$_{20}$H$_{33}$N$_5$O$_7$PSSi$^-$: 546.2) (**Figure 2-16**).

III3. Synthesis of monothiophosphate c-di-GMP

III3.1. Amidite/H-phosphonate monoester method with sulfurization during cyclization

Detritylated linear dimer (12). Guanosine phosphoramidite **6** (1.45 g, 1.5 mmol, 1.5 eq) and H-phosphonate **10a** (0.61g, 1.0 mmol) were dried together overnight in a desiccator over P_2O_5. The mixture was dissolved at room temperature under argon in 20 mL CH_3CN that had been dried over molecular sieves, and then pyridinium trifluroacetate (0.58 g, 3 mmol, 2 eq relative to amidite) that had been dried by evaporation of CH_3CN was added. The reaction mixture was stirred for 30 min, followed by addition of anhydrous *tert*-butylhydroperoxide (0.87 mL, 6.25 mmol, 6.25 eq) in decane over molecular sieves. After 30 min, the mixture was poured into aqueous $NaHCO_3$ and extracted with ethyl acetate. The organic layers were then concentrated and purified by silica gel chromatography using a gradient of methanol in CH_2Cl_2 with 0.5% pyridine to give partially purified linear dimer **11**. $NaHSO_4/SiO_2$ (0.91 g, 2 eq) was then used for detritylation of **11**, which was isolated as described for **7** to give 5'-OH linear dimer **12** (0.64 g, crude). The two diastereomers of **12** were too close to be separated during analytical HPLC, and the ESI-MS showed m/z (M-1) of 1113.0 (calcd for $C_{43}H_{68}N_{11}O_{16}P_2Si_2^-$: 1112..4), confirming the product (**Figure 2-17**).

Protected monothiophosphate c-di-GMP (13). Linear dimer **12** (0.28 g, crude) was dried three times with pyridine, the last time with 15 mL left, and freshly distilled pivaloyl chloride (Pv-Cl, 0.12 mL, 1.0 mmol, 4 eq) was added quickly under argon at room temperature. After 3 min, elemental sulfur (40 mg, 1.25 mmol, 5 eq) was added to the reaction mixture directly as a solid. After 40 min, the mixture was concentrated and

evaporated with toluene three times to remove pyridine. The resulting residue was evaporated with CH_3CN three times, the last time leaving about 5 mL and filtered to remove excess sulfur to give **13** (0.25 g, crude). It was deprotected as described in the following section without further purification and its yield was not calculated due to the presence of impurities. The crude product was analyzed by LC-MS and showed m/z (M-1) of 1127.1 (calcd for $C_{43}H_{66}N_{11}O_{15}P_2SSi_2^-$: 1126.4) (**Figure 2-18**). The HPLC chromatogram showed the major peaks for two diastereomers.

Monothiophosphate c-di-GMP [*R*] (14). The crude mixture of **13** (0.25 g, crude) described above was first treated with a large excess (4 mL) of methylamine in water (40%) for 40 min. The mixture was then concentrated and evaporated with pyridine three times to remove any water. TEA•3HF (2.2 mL, 13.3 mmol, 100 eq to TBS) with additional 1.5 mL TEA was added, and the mixture was kept at 50 °C for 4 hrs. The reaction was quenched with 7 mL isopropyl trimethylsilyl ether, followed by 10 mL ethyl ether to fully precipitate. The mixture was allowed to sit overnight, and the liquid was decanted. The crude product was purified by semi-preparative reverse phase HPLC on Waters Novapak C18 column using a gradient of 2-20% CH_3CN in 0.1 M TEAA over 90 min. The pure fractions were pooled, lyophilized and desalted by RP-HPLC using a gradient of CH_3CN in 0.1 M ammonium bicarbonate to give pure product **14 [*R*]** (12.0 μmol) in 2.7 % yield from H-phosphonate **10a**. To determine the yield, UV optical density (OD) measurements were carried out at wavelength of 260 nm, assuming the extinction coefficient of this analog is same as the unmodified c-di-GMP. This OD method was applied to all the other analogs as well to determine the amount of products.

The product was characterized by LC-MS, showed a single peak with m/z (M-1) of 705.3

(calcd for $C_{20}H_{23}N_{10}O_{13}P_2S^-$: 705.1) and retention time of 6.0 min as shown in **Figure 2-19**, clearly showed that only single diastereomer was obtained. Sodium and potassium

forms were obtained by ion exchange using 10 mL of AG 50W-X2 sulfonic acid resin,

which had previously been converted to the Na^+ or K^+ forms, respectively.

III3.3. Amidite/H-phosphonate monoester method with sulfurization during linear coupling

Monothiophosphate linear dimer (20). A pre-dried mixture of guanosine

phosphoramidite **6** (1.45 g, 1.5 mmol, 1.7 eq) and H-phosphonate **10a** (0.54 g, 0.90

mmol) was dissolved in 20 mL CH_3CN at room temperature, and pyridinium

trifluroacetate (0.58 g, 3.0 mmol, 2.2 eq to amidite) that had been dried by evaporation of

CH_3CN was added. After 30 min, elemental sulfur (0.16 g, 5.0 mmol, 5.6 eq) dissolved in

30 mL 1:1 pyridine : CH_2Cl_2 was added, and the mixture was stirred for 40 min. The

resulting mixture was then concentrated, evaporated with toluene three times and CH_3CN

three times, and then filtered to remove excess solid sulfur. The product was purified by

silica gel chromatography using a gradient of methanol in CH_2Cl_2 to give linear dimer **19**.

It was then detritylated with $NaHSO_4/SiO_2$ (0.91 g, 2.2 eq) and separated from tritanol as

described for **7** to give the 5'-OH linear dimer **20** (0.72 g, crude) with an m/z (M-1) of

1128.9 shown in LC-MS in **Figure 2-20**. (calcd for $C_{43}H_{68}N_{11}O_{15}P_2SSi_2^-$: 1128.4)

Protected monothiophosphate c-di-GMP as a mixture of two diastereomers (21).

Linear dimer **20** (0.41 g, crude) was dried three times with pyridine, the last time with 15

mL left, and freshly distilled Pv-Cl (0.17 mL, 1.4 mmol, 3 eq) was added at room temperature. After 3 min, water (0.10 mL, 5.6 mmol, 4 eq to Pv-Cl) was added to quench the reaction, followed by addition of iodine (0.432 g, 1.7 mmol, 5 eq) for 5 min. The mixture was then poured into aqueous $NaHCO_3$ with two equivalents of Na_2SO_3 (0.34 g) and extracted using CH_2Cl_2. The organic layers were concentrated and purified by silica gel chromatography using a gradient of methanol in CH_2Cl_2. The pure fractions were pooled to give cyclic dimer **21** (0.14 g, crude) as a mixture of two diastereomers, which were characterized by LC-MS, showing m/z (M-1) 1126.7 (calcd for $C_{43}H_{66}N_{11}O_{15}P_2SSi_2^-$: 1126. 4) (**Figure 2-21**)

Monothiophosphate c-di-GMP (14) [*R*] and [*S*]. The deprotection procedure for the cyclic dimer **21** mixture (0.14 g, crude) of two diastereomers was the same as for **14 [*R*]**. The mixture was separated during semi-preparative RP-HPLC into two main peaks, each containing one of the two diastereomers as a major component. Fractions from each peak were combined and then further purified by RP-HPLC using a different gradient. Final products were obtained in 3.1% yield for the [*R*] diastereomer (17.6 μmol) and 1.8% for the [*S*] diastereomer (9.9 μmol) from H-phosphonate **10a**. The [*R*] diastereomer showed the same LC-MS profile as shown in **Figure 2-19.** The [*S*] diastereomer showed a m/z (M-1) 705.3 (calcd for $C_{20}H_{23}N_{10}O_{13}P_2S^-$: 705.1) and a retention time of 4.8 min in the LC-MS in **Figure 2-22.**

III4. Synthesis of dithiophosphate c-di-GMP

III4.1. Amidite/H-phosphonate monoester method

This method utilized the same starting materials and early synthetic steps up to the linear dimer intermediate **20**, followed by direct sulfurization using elemental sulfur. The experimental details described below used this linear dimer as a starting point.

Protected dithiophosphate c-di-GMP as a mixture of two diastereomers (22). Linear dimer **20** (0.29 g, crude) was dried three times by evaporation of pyridine, the last time with 15 mL left. Freshly distilled Pv-Cl (0.10 mL, 0.8 mmol, 4 eq) was added at room temperature. After 3 min, elemental sulfur (25.6 mg, 0.8 mmol, 4 eq) was added and the reaction was stirred for 40 min. The mixture was then concentrated and evaporated with CH_3CN three times, then filtered to remove excess sulfur to give cyclic dimer **22** (0.22 g, crude) as a mixture of two diastereomers, which was confirmed by LC-MS, which showed m/z (M-1) of 1142.9 (calcd for $C_{43}H_{66}N_{11}O_{14}P_2S_2Si_2^-$: 1142.3) (**Figure 2-23**). This crude mixture was then deprotected without further purification.

Dithiophosphate c-di-GMP (23) [*R, R*] and [*R, S*]. The protected cyclic dimer mixture of two diastereomers was deblocked as described for **14**. The crude mixture (0.22 g) was separated during semi-preparative RP-HPLC using 0.1 M TEAA buffer and CH_3CN into two major peaks, each containing either the [*R, R*] or the [*R, S*] diastereomer as the major component. The fractions for each diastereomer were pooled, lyophilized and individually further purified by C18 RP-HPLC using a different gradient to give 28.9

μmol (3.4%) [*R, R*] and 16.2 μmol (1.9%) [*R, S*] from H-phosphonate **10a**. These two diastereomers were characterized by LC-MS, which showed different retention times at 8.0 min with a m/z (M-1) of 721.6 for the [*R, R*], and 6.2 min with a m/z (M-1) of 721.5 for the [*R, S*] (calcd for $C_{20}H_{23}N_{10}O_{12}P_2S_2^-$: 721.0) (**Figure 2-24 and Figure 2-25**). Desalting and ion exchange followed the same procedure as described for **14**.

III4.2. Amidite/H-thiophosphonate monoester method

Linear dimer with two sulfurs (28). Guanosine phosphoramidite **6** (5.81 g, 6.0 mmol, 1.5 eq) and H-thiophosphonate **10b** (2.52 g, 4.0 mmol,) were dried together overnight in a desiccator over P_2O_5. The mixture was then dissolved at room temperature under argon in 40 mL CH_3CN that had been dried over molecular sieves. Pyridinium trifluroacetate (2.31 g, 12.0 mmol, 2 eq relative to amidite) was dried by evaporation of CH_3CN three times and then added into the guanosine mixture. The reaction was stirred for 30 min, followed by addition of elemental sulfur (0.384 g, 12.0 mmol, 3 eq) dissolved in 30 mL 1:1 pyridine:CH_2Cl_2. The reaction was stirred for 40 min, and the resulting mixture was concentrated and evaporated three times with toluene to remove pyridine, and then with CH_3CN three times. The remaining sulfur residue was filtered off and the organic filtrate was concentrated and evaporated with CH_2Cl_2 several times. Silica gel chromatography using a gradient of methanol in CH_2Cl_2 with 0.5% pyridine was then carried out to give linear dimer **27**, with small amount of unidentified impurities. NaHSO₄/SiO₂ (2.73 g, 1.5 eq) was then used to detritylate **27**, and the product was separated from tritanol as described for monomer **7**, to give 5'-OH linear dimer **28** (2.33 g, crude), which was

deprotected without further purification. The LC-MS shown in **Figure 2-26** gave a m/z (M-1) of 1144.8 for the protected cyclic dimer **28** (calcd for $C_{43}H_{68}N_{11}O_{14}P_2S_2Si_2^-$: 1144.3).

Protected dithiophosphate c-di-GMP as a mixture of three diastereomers (29). The linear dimer **28** (0.41 g, crude) was evaporated three times with pyridine, the last time leaving about 20 mL. In a separate pear-shaped flask, diphenyl chlorophosphate (DPP-Cl, 0.1 mL, 0.5 mmol, 1.5 eq) was dissolved in about 3 mL pyridine, and then added to the reaction mixture. After 20 min, H_2O (12 µL, 0.66 mmol, 2 eq) was added, followed by I_2 (0.42 g, 1.65 mmol, 5eq). The mixture was stirred for 5 min, and then quenched by a $NaHCO_3$ solution containing two equivalents (0.34 g, relative to remaining I_2) of Na_2SO_3. This mixture was then extracted with CH_2Cl_2, and the organic layers were concentrated and evaporated with 10 mL toluene three times to remove pyridine. The residue was evaporated with CH_2Cl_2 and then purified by silica gel chromatography using a gradient of methanol in CH_2Cl_2 to give cyclic dimer **29** (0.21 g, crude) as a mixture of three diastereomers, which was then deprotected without further separation. The LC-MS profiles of **29** showed several overlapped peaks, each with a m/z (M-1) of 1142.3 (calcd for $C_{43}H_{66}N_{11}O_{14}P_2S_2Si_2^-$: 1142.3) as shown in **Figure 2-27**.

Dithiophosphate c-di-GMP (23) [*R, R*], [*R, S*] and [*S, S*]. The protected cyclic dimer mixture of three diastereomers **29** (0.21 g, crude) was deprotected by the same two-step procedure described for **14**. The crude products were separated by semi-preparative RP-HPLC using 0.1 M TEAA buffer and CH_3CN to give three major peaks, each containing

the [*R, R*], [*R,* S] or [*S, S*] diastereomer as the major component. These were then confirmed by LC-MS with m/z (M-1) 721.2 for all diastereomers, with various retention times. Further purification by C18 RP-HPLC was necessary for each component using a different gradient. For the [*S, S*] diastereomer purification, a Beckman ultrapore RPSC C3 10×250 mm column and diisopropylethylammonium acetate (DIPEAA) buffer was used. All diastereomers were converted to appropriate ion forms after desalting using the ion exchange process described above. The final yields were 3.6% (24.8 µmol), 1.8% (12.2 µmol) and 0.6% (4.2 µmol) for [*R, R*], [*R,* S] and [*S, S*] diastereomers, respectively, from H-thiophosphonate **10b**. The [*R, R*] and [*R,* S] diastereomers showed the same LC-MS profiles as shown in **Figure 2-24** and **Figure 2-25**. The [*S, S*] diastereomer was also characterized by LC-MS, with a m/z of 721.4, but a shorter retention time at 5.3 min. (**Figure 2-28**)

III5. Synthesis of trithiophosphate c-di-GMP

The synthesis of trithiophosphate c-di-GMP was carried out using the linear dimer **28** described above, which was used in the amidite/H-thiophosphonate method described for the dithiophosphate analog **23**.

Protected trithiophosphate c-di-GMP as a mixture of two diastereomers (30). The linear dimer **28** (0.88 g, crude) was evaporated three times with pyridine, the last time leaving about 20 mL. In a separate pear-shaped flask, DPP-Cl (0.22 mL, 1.05 mmol, 1.5 eq) was dissolved in about 3 mL dry pyridine, and then added to the reaction mixture.

After 20 min, elemental sulfur (0.068 g, 2.1 mmol, 3 eq) was added, and the mixture was stirred for 40 min. The mixture was then concentrated and evaporated with 10 mL toluene three times to remove pyridine, then three times with CH_3CN. Excess sulfur was removed by filtration, and the filtrate was evaporated with CH_2Cl_2. The residue was purified by silica gel chromatography using a gradient of methanol in CH_2Cl_2 to give cyclic dimer **30** (0.85 g, crude) in 66% yield (HPLC integration with small amount of impurities) from linear dimer **28**, as a mixture of two diastereomers, which were confirmed by LC-MS with m/z (M-1) 1158.7 (calcd for $C_{43}H_{66}N_{11}O_{13}P_2S_3Si_2^-$: 1158.3) (**Figure 2-29**). The mixture was deprotected without further purification.

Trithiophosphate c-di-GMP (31) [*R*] and [*S*]. The protected cyclic dimer mixture **30** (0.52 g, crude) was deprotected by the same two-step procedures described for **14** to give trithiophosphate c-di-GMP **31**. The crude products were separated by semi-preparative RP-HPLC using 0.1 M TEAA buffer and CH_3CN to give two major peaks, each containing the [*R*] or the [*S*] diastereomer as the major component. The [*R*] containing fractions were lyophilized and further purified by RP-HPLC using TEAA and CH_3CN by a different gradient. The [*S*] diastereomer containing fractions were further purified on a Beckman ultrapore RPSC C3 column using 0.1 M diisopropylethylammonium acetate buffer and CH_3CN. Desalting and ion exchange was carried out as described for **14**, to give final trithiophosphate c-di-GMP **31** in 3.6% (31.5 μmol) and 0.7% (6.4 μmol) yield from H-thi**ophosphonate 10b** for the [*R*] and [*S*] diastereomers, respectively. The LC-MS profiles of both diastereomers showed different retention time at 9.1 min with a m/z

(M-1) of 737.4 for [*R*], and 8.0 min with a m/z of 737.1 for [*S*] (calcd for C$_{20}$H$_{23}$N$_{10}$O$_{11}$P$_2$S$_3$: 737.0) (**Figure 2-30 and Figure 2-31**).

IV. References

1. Ross, P., Mayer, R., Weinhouse, H., Amikam, D., Huggirat, Y., Benziman, M., Vroom, E. d., Fidder, A., Paus, P. d., Sliedregt, L. A. J. M., Marel, G. A. v. d., and Boom, J. H. v., "The cyclic diguanylic acid regulatory system of cellulose synthesis in *Acetobacter xylinum*. Chemical synthesis and biological activity of cyclic nucleotide dimer, trimer, and phosphothioate derivatives" *J. Biol. Chem.*, **1990**, 265, 18933-18943

2. Ross, P., Weinhouse, H., Aloni, Y., Michaeli, D., Weinberger-Ohana, P., Mayer, R., Braun, S., de Vroom, E., van der Marel, G. A., van Boom, J. H., and Benziman, M., "Regulation of cellulose synthesis in *Acetobacter xylinum* by cyclic diguanylic acid" *Nature*, **1987**, 325, 279-281

3. Zhang, Z., Gaffney, B. L., and Jones, R., "c-di-GMP displays a monovalent metal ion-dependent polymorphism" *J. Am. Chem. Soc*, **2004**, 126, 16700-16701

4. Hyodo, M., Sato, Y., and Hayakawa, Y., "Synthesis of cyclic bis(3'-5')diguanylic acid (c-di-GMP) analogs" *Tetrahedron*, **2006**, 62, 3089-3094

5. Serebryany, V. and Beigelman, L., "An efficient preparation of protected ribonucleosides for phosphoramidite RNA synthesis" *Tetrahedron Lett.*, **2002**, 43, 1983-1985

6. Furusawa, K., Ueno, K., and Katsura, T., "Synthesis and restricted conformation of 3',5'-*O*-(di-*t*-butylsilanediyl)ribonucleosides" *Chem. Lett.*, **1990**, 97-100

7. Sanghvi, Y. S., Guo, Z., Pfundheller, H. M., and Converso, A., "Improved process for the preparation of nucleosidic phosphoramidites using a safer and cheaper activator" *Org. Process Res. Dev.*, **2000**, 4, 175-181

8. Das, B., Mahender, G., Kumar, V. S., and Chowdhury, N., "Chemoselective deprotection of trityl ethers using silica-supported sodium hydrogen sulfate" *Tetrahedron Lett.*, **2004**, 45, 6709-6711

9. Marugg, J. E., Tromp, M., Kuyl-Yeheskiely, E., Marel, G. A. v. d., and Boom, J. H. v., "A Convenient and general approach to the synthesis of properly protected d-nucleoside-3'-hydrogenphosphonates via phosphite intermediates" *Tetrahedron Lett.*, **1986**, 27, 2661-2664

10. Kers, I., Kers, A., and Stawinski, J., "A H-phosphonates. 8. Simple and efficient method for the preparation of nucleoside H-Phosphonothioate monoesters" *Tetrahedron Lett.*, **1999**, 40, 3945-3948

11. Battistini, C., Fustinoni, S., Brasca, M. G., and Borghi, D., "Stereoselective synthesis of cyclic dinucleotide phosphorothioates" *Tetrahedron*, **1993**, 49, 1115-1132

12. Eleuteri, A., Capaldi, D. C., Krotz, A. H., Cole, D. L., and Ravikumar, V. T., "Pyridinium trifluoroactate/N-methylimidazole as an efficient activator for oligonucleotide synthesis via the phosphoramidite method" *Org. Process Res. Dev.*, **2000**, 4, 182-189

13. Regan, J. B., Phillips, L. R., and Beaucage, S. L., "Large-scale preparation of the sulfur-transfer reagent 3*H*-1,2-benzodithiol-3-one 1,1-dioxide" *Org. Prep. Proc. Int.*, **1992**, 24, 488-492

14. Iyer, R. P., Phillips, L. R., Egan, W., Regan, J. B., and L., B. S., "The automated synthesis of sulfur-containing oligodeoxyribonucleotides using 3H-1,2-benzodithiol-3-one 1,1-dioxide as a sulfur-transfer reagent" *J. Org. Chem.*, **1990**, 55, 4693-4698

15. Romaniuk, P. J. and Eckstein, F., "A study of the mechanism of T4 DNA polymerase with diastereomeric phosphorothioate analogues of deoxyadenosine triphosphate" *J. Biol. Chem.*, **1982**, 257, 7684-7688

16. Bartlett, P. A. and Eckstein, F., "Stereochemical course of polymerization catalyzed by avian myeloblastosis virus reverse transcriptase" *J. Biol. Chem.*, **1982**, 257, 8879-8884

17. Potter, B. V. L., Connolly, B. A., and Eckstein, F., "Synthesis and conformational analysis of a dinucleoside phosphate isotopically chiral at phosphorus. Stereochemical course of *Penicillium citrum* nuclease P1 reaction" *Biochemistry*, **1983**, 22, 1369-1377

18. Williamson, J. R., "Guanine quartets" *Curr. Opin. Struct. Biol.*, **1993**, 3, 357-362

19. Burgers, P. M. J. and Eckstein, F., "Absolute configuration of the diastereomers of adenosine 5'-O-(1-thiotriphosphate): consequences for the stereochemistry of polymerization by DNA-dependent RNA polymerase from Escherichia coli" *Proc. Natl. Acad. Sci. USA*, **1978**, 75, 4798-4800

20. Chen, Y., Qu, F., and Zhang, Y., "Diuridine 3',5'-boranophosphate: preparation and properties" *Tetrahedron Lett.*, **1995**, 36, 745-748

21. Saenger, W., Suck, D., and Eckstein, F., "On the mechanism of ribonuclease A. Crystal and molecular structure of uridine 3'-*O*-thiophosphate methyl ester triethylammonium salt" *Eur. J. Biochem.*, **1974**, 46, 559-567

22.   Usher, D. A., Erenrich, E. S., and Eckstein, F., "Geometry of the first step in the action of ribonuclease-A" *Proc. Natl. Acad. Sci. USA*, **1972**, 69, 115-118

23.   Slim, G. and Gait, M. J., "Configurationally defined phosphorothioate-containing oligoribonucleotides in the study of the mechanism of cleavage of hammerhead ribozymes" *Nucleic Acids Res.*, **1991**, 19, 1183-1188

24.   Blaho, J. A., Larson, J. E., McLean, M. J., and Wells, R. D., "Multiple DNA secondary structures in perfect inverted repeat Inserts in plasmids. Right-handed B-DNA, Cruciforms, and Left-handed Z-DNA" *J. Biol. Chem.*, **1988**, 263, 14446-14455

25.   Stawinski, J., Thelin, M., and Zain, R., "Nucleoside H-phosphonates. X. Studies on nucleoside hydrogenphosphonothioate diester synthesis" *Tetrahedron Lett.*, **1989**, 30, 2157-2160

26.   Seela, F. and Kretschmer, U., "Diastereomerically pure R_p and S_p dinucleoside H-phosphonates: the stereochemical course of thier conversion into p-methylphosphonates, phosphorothioates, and [^{18}O] chiral phosphates" *J. Org. Chem.*, **1991**, 56, 3861-3869

27.   Seela, F. and Kretschmer, U., "Stereospecific oxidation of R_p- and S_p-dinucleoside H-phosphonates to phosphorothioates" *Nucleosides & Nucleotides*, **1991**, 10, 711-712

Appendix
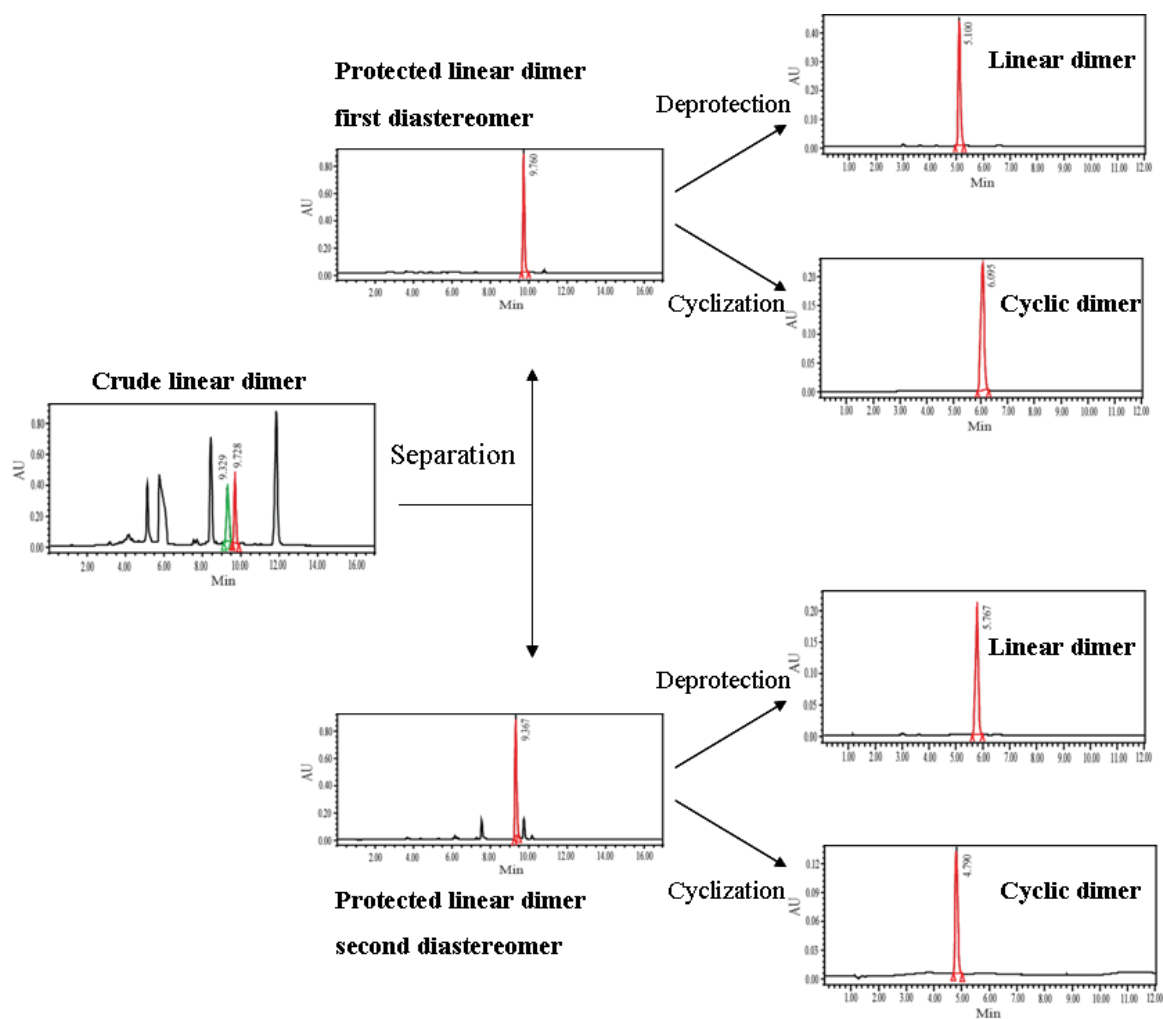
Figure 2-8. HPLC chromatograms showing first method to assign stereochemistry of the monothiophosphate c-di-GMP

[*R*] diastereomer
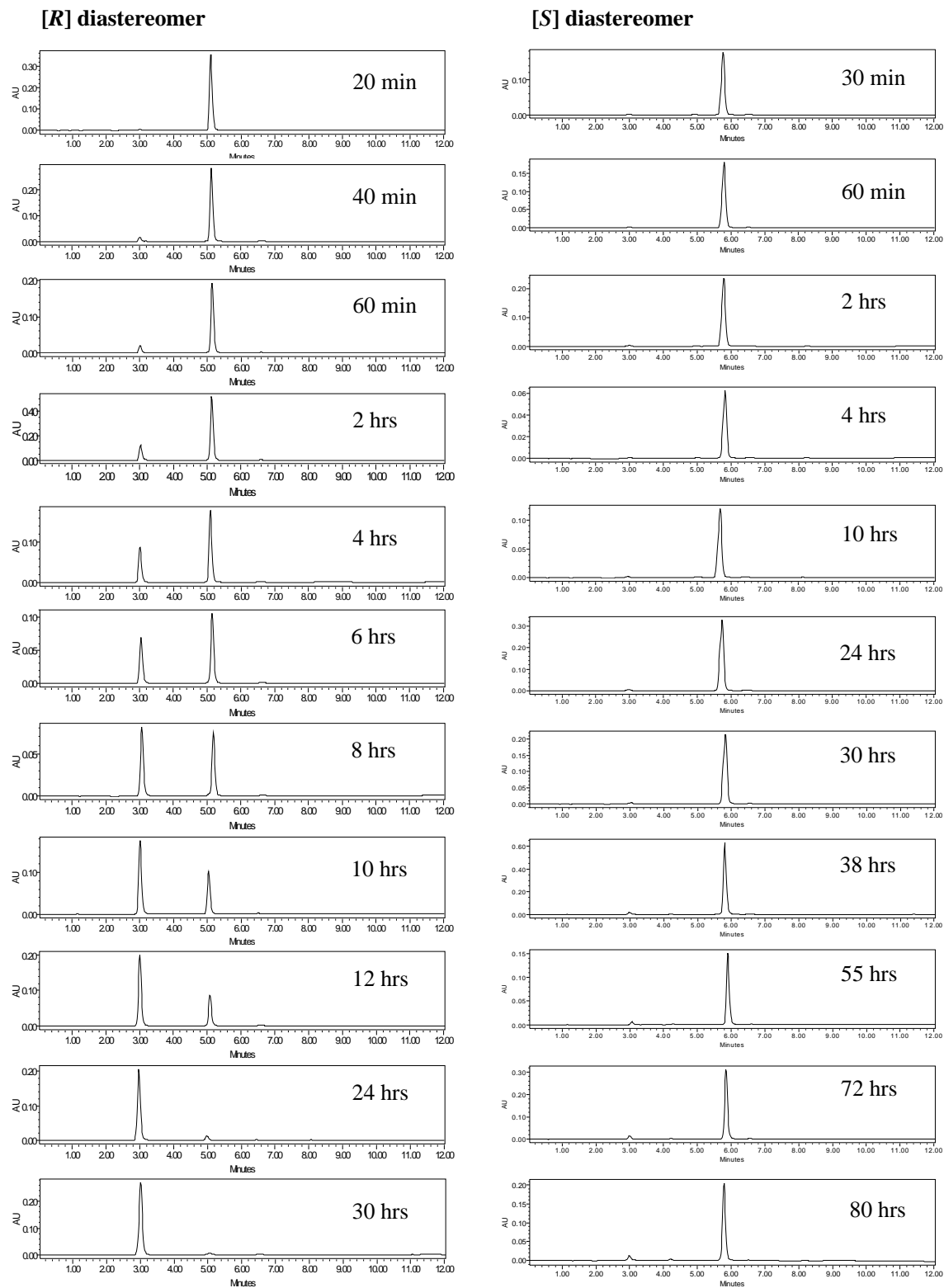
[*S*] diastereomer

Figure 2-9. HPLC monitoring SVPDE digestion of two diastereomers of liner dimer

[*R*] diastereomer
longer retention time

[*S*] diastereomer
shorter retention time

Nuclease P1

30 min

2 hrs

Nuclease P1

30 min

2 hrs

Phosphatase

30 min

60 min

2 hrs

4 hrs

Phosphatase

30 min

60 min

2 hrs

4 hrs

SVPDE

30 min

60 min

2 hrs

4 hrs

7 hrs

16 hrs

23 hrs

29 hrs

40 hrs

SVPDE

30 min

60 min

2 hrs

4 hrs

7 hrs

14 hrs

24 hrs

35 hrs

61 hrs
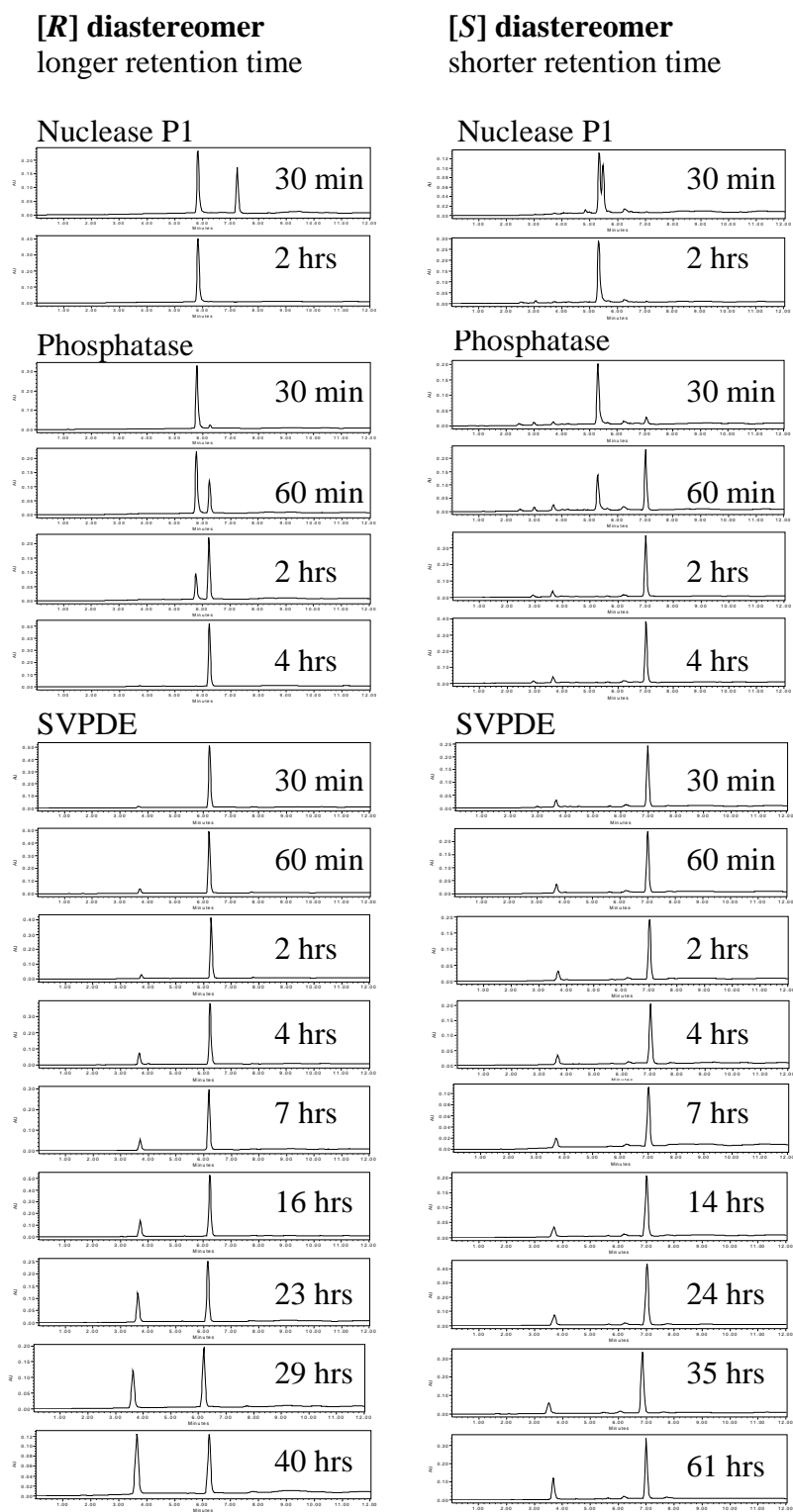
Figure 2-10. HPLC monitoring P1/phosphatase/SVPDE digestion of monothioate c-di-GMP

[*R*] diastereomer
longer retention time

[*S*] diastereomer
shorter retention time

Nuclease P1
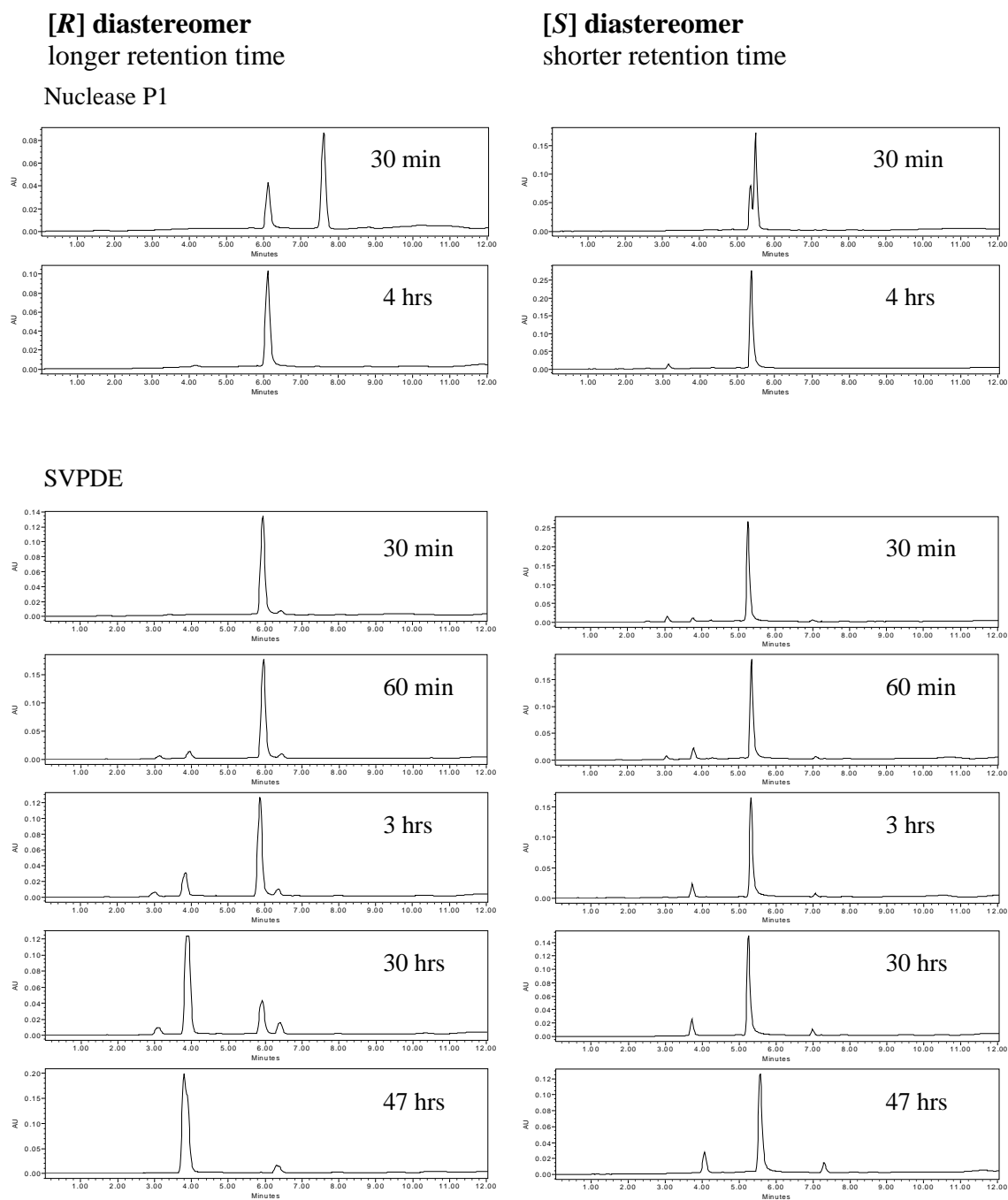
SVPDE

Figure 2-11. HPLC monitoring P1/SVPDE digestion monothioate c-di-GMP

[*R*] diastereomer
longer retention time

[*S*] diastereomer
shorter retention time

Nuclease P1

Nuclease P1
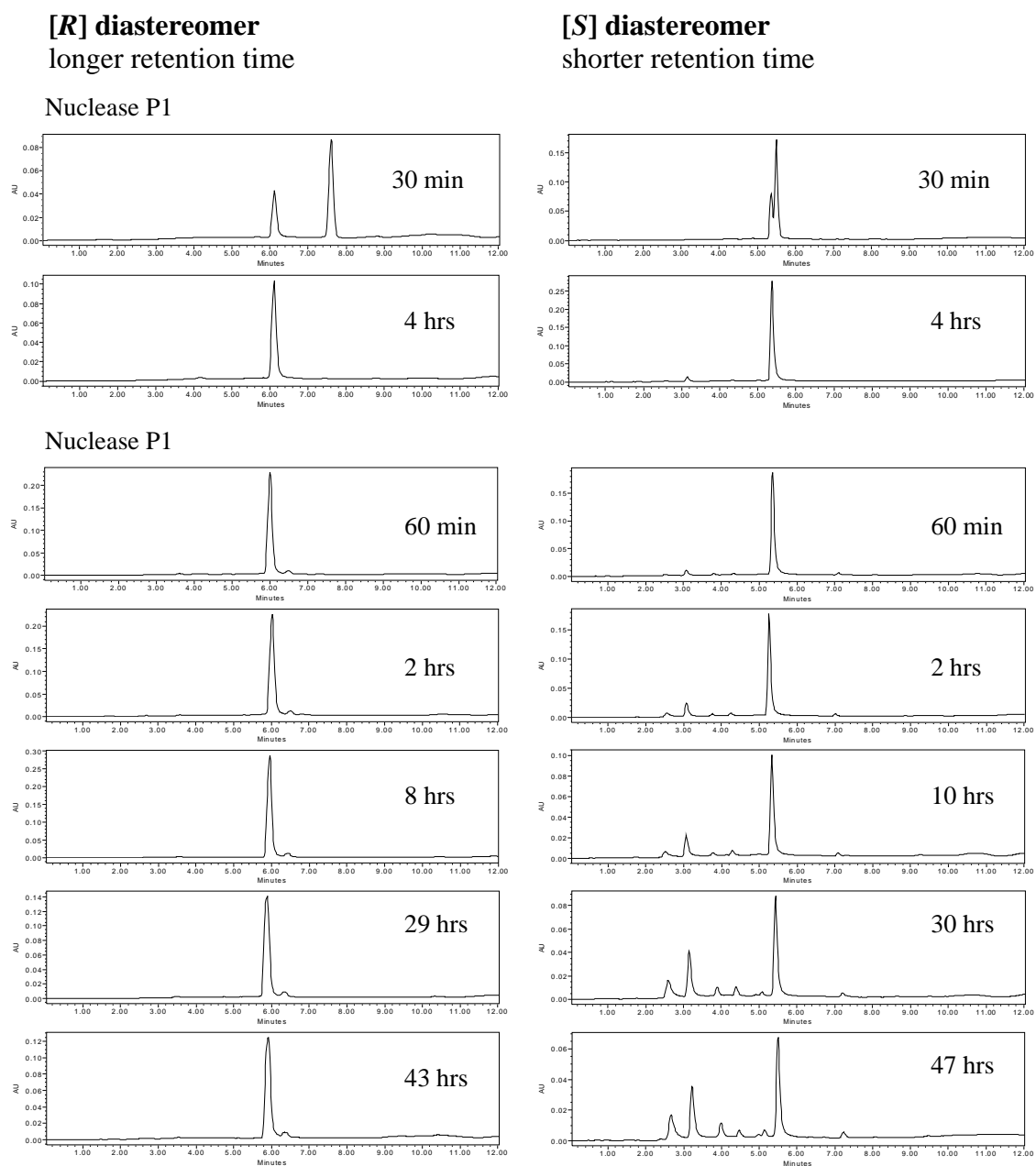
Figure 2-12. HPLC monitoring P1/P1 digestion monothioate c-di-GMP
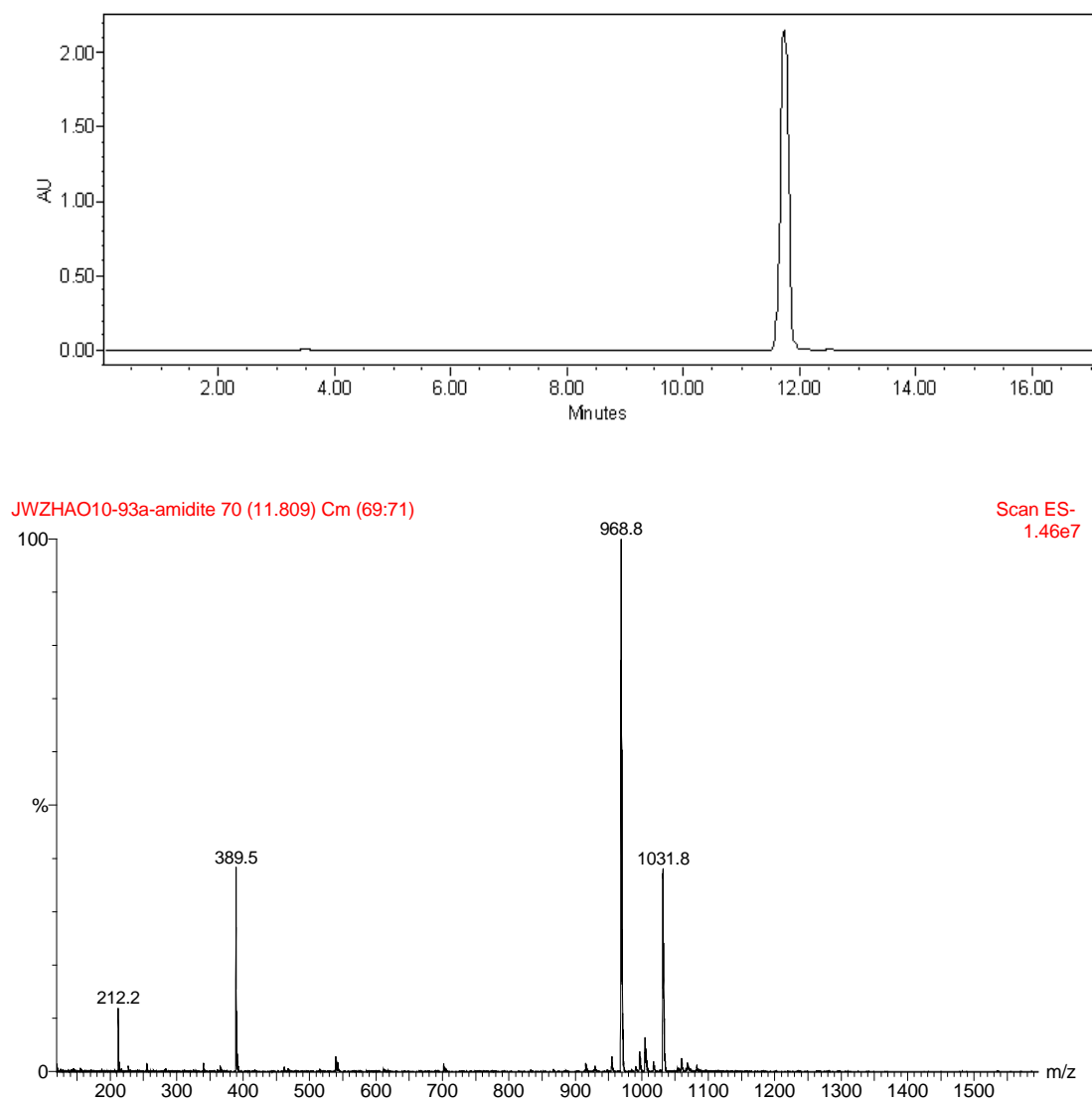
Figure 2-13. LC-MS of phosphoramidite **6**
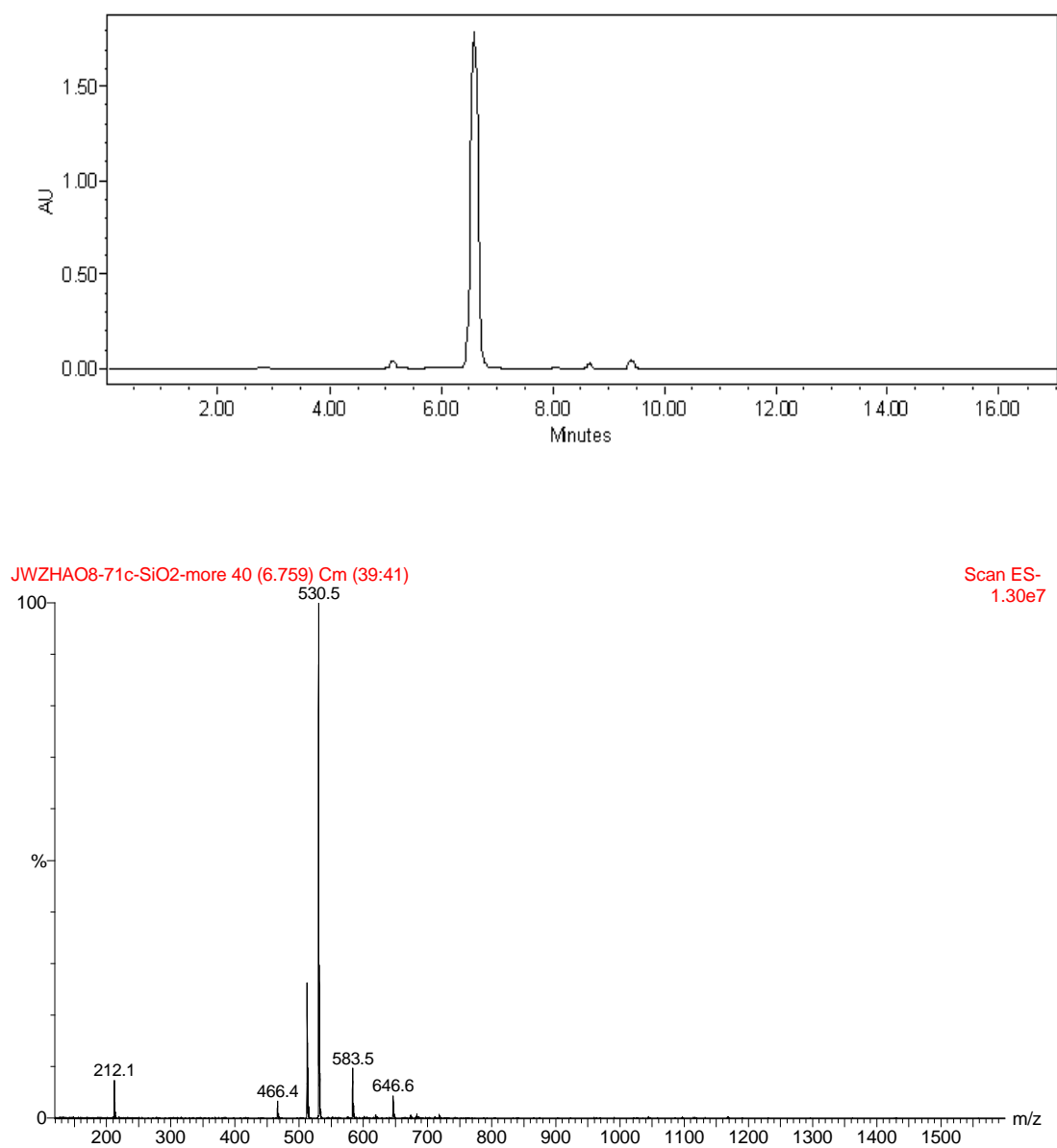
Figure 2-14. LC-MS of detritylated H-phosphonate diester **7**
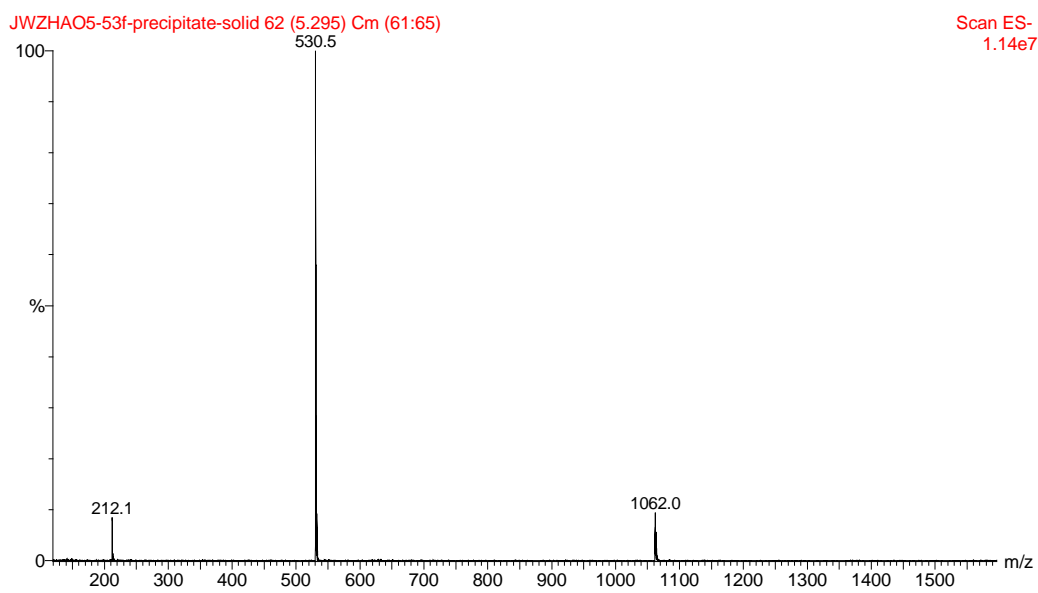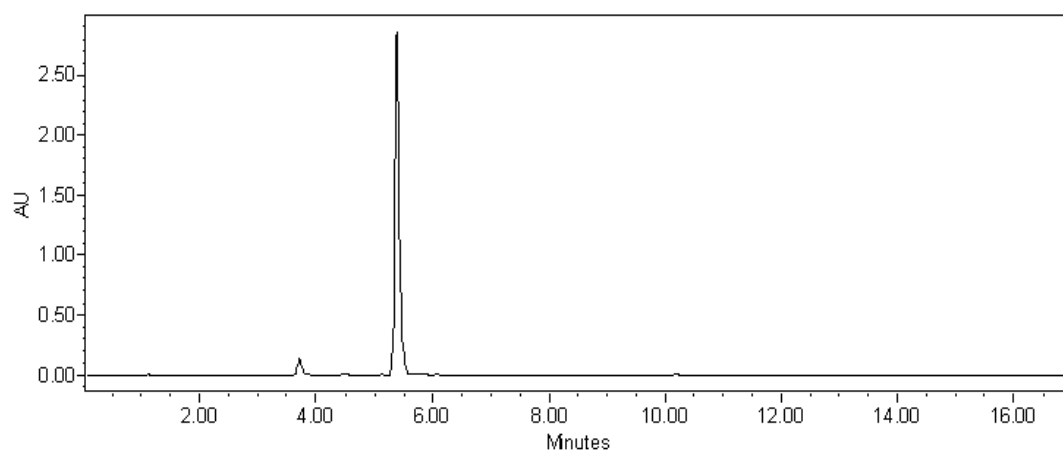
Figure 2-15. LC-MS of detritylated H-phosphonate monoester **10a**
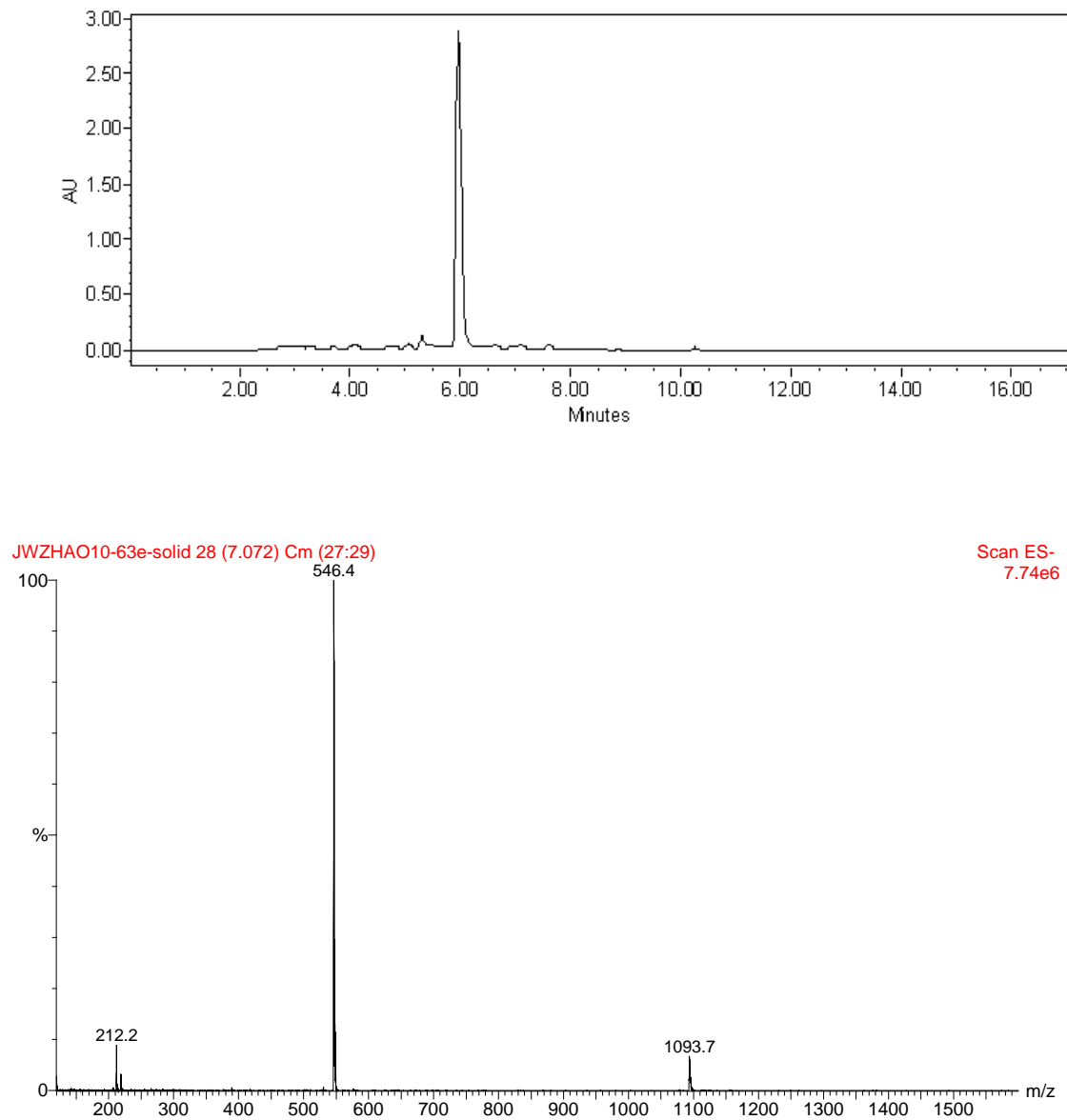
Figure 2-16. LC-MS of detritylated H-thiophosphonate monoester **10b**
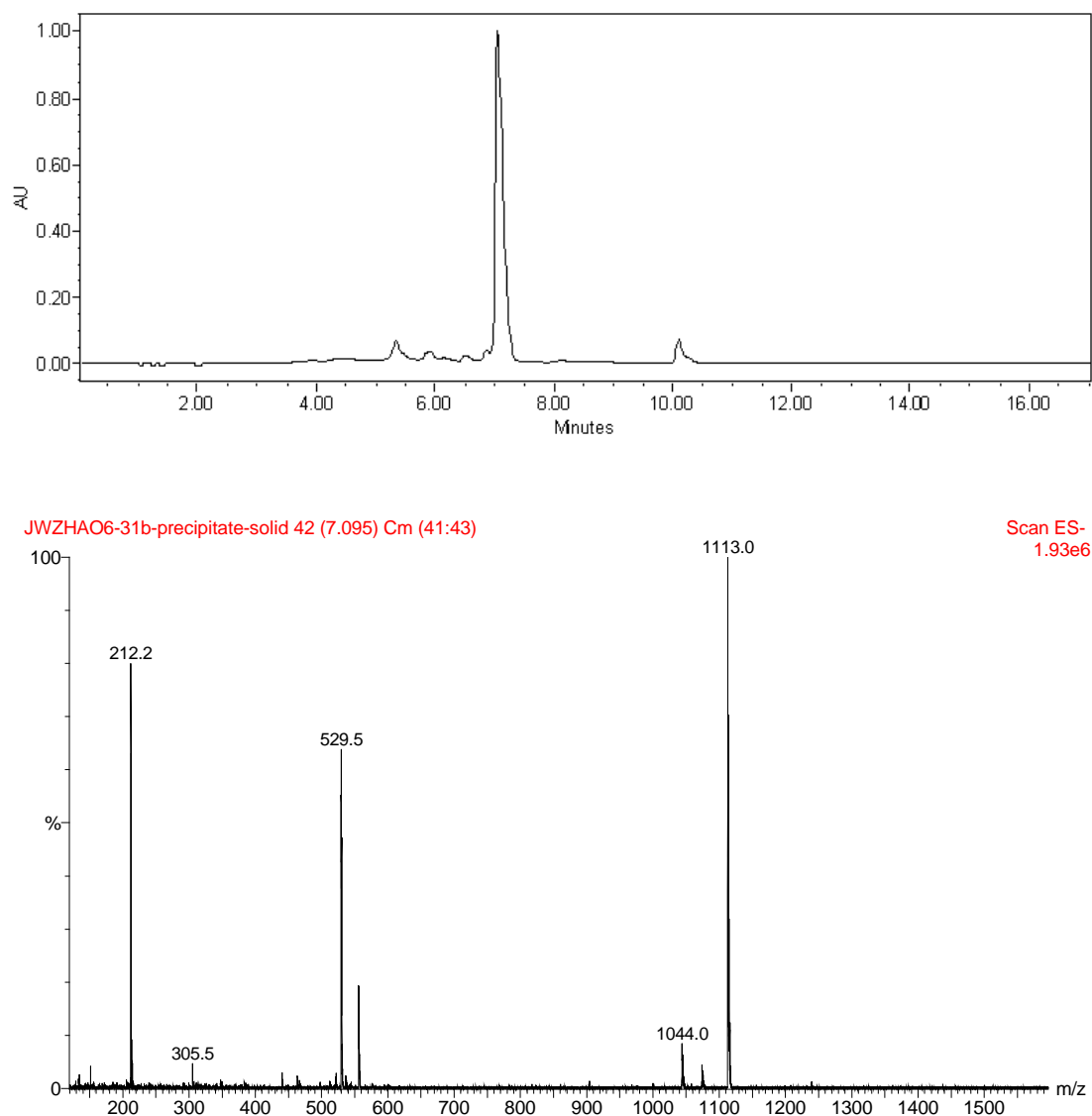
Figure 2-17. LC-MS of detritylated linear dimer **12** by amidite/H-phosphonate monoester method
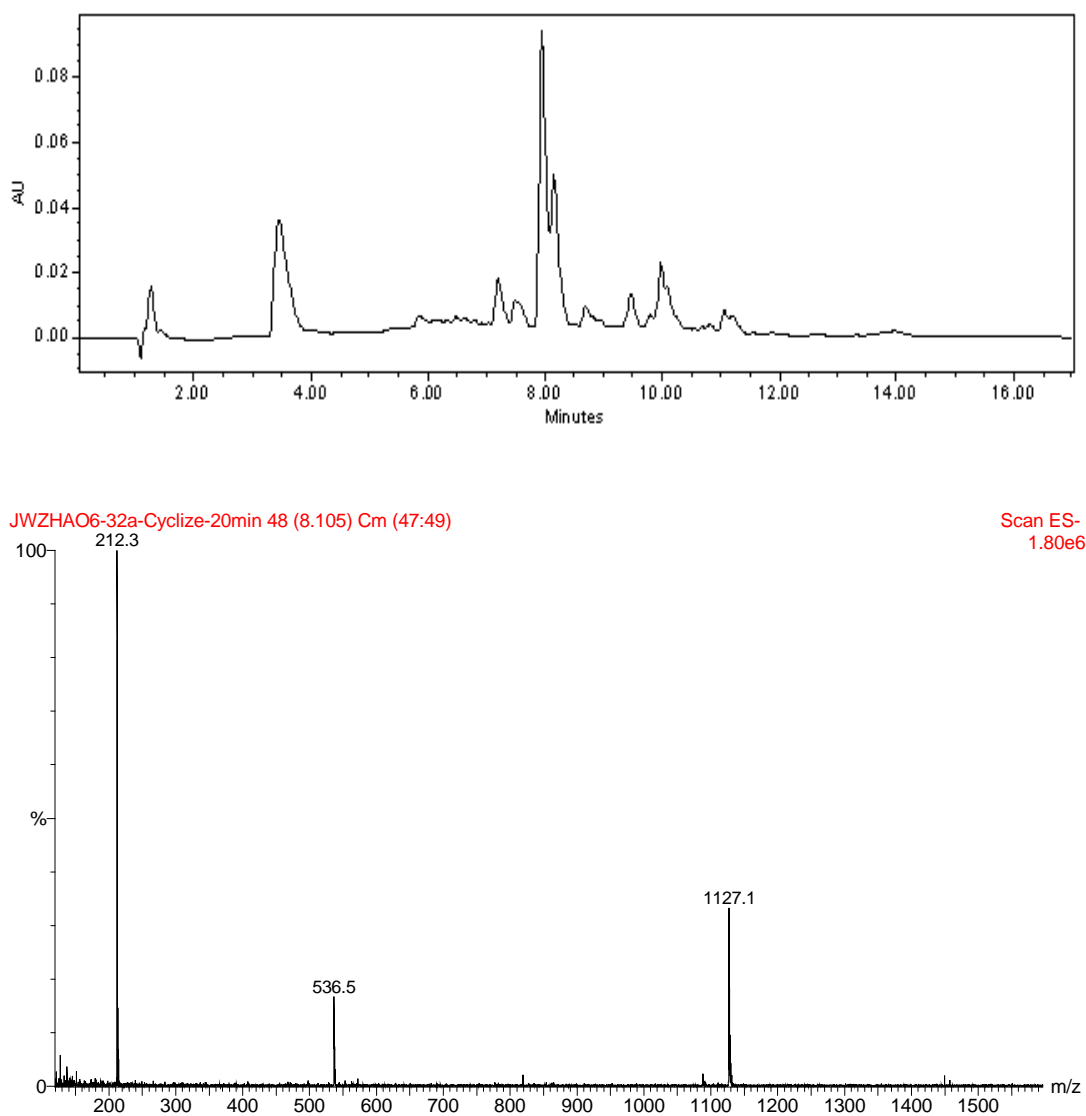
Figure 2-18. LC-MS of crude protected cyclic dimer **13** from method of amidite/H-phosphonate monoester, sulfurizing during cyclization
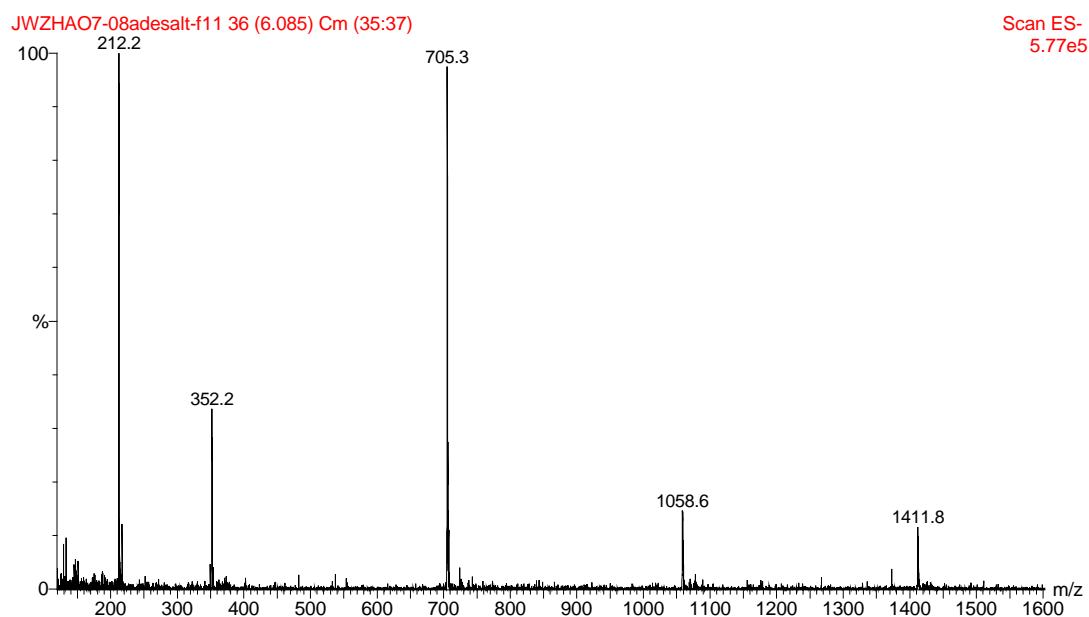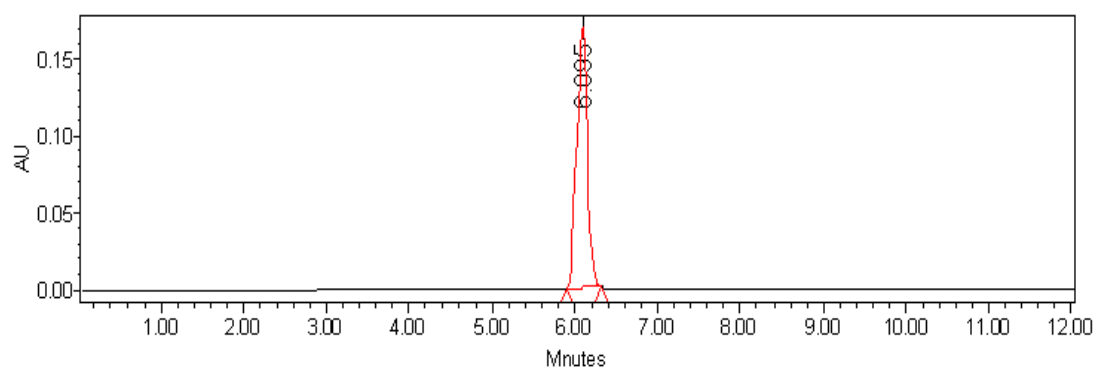
Figure 2-19. LC-MS profile of cyclic dimer **14 [*R*]**
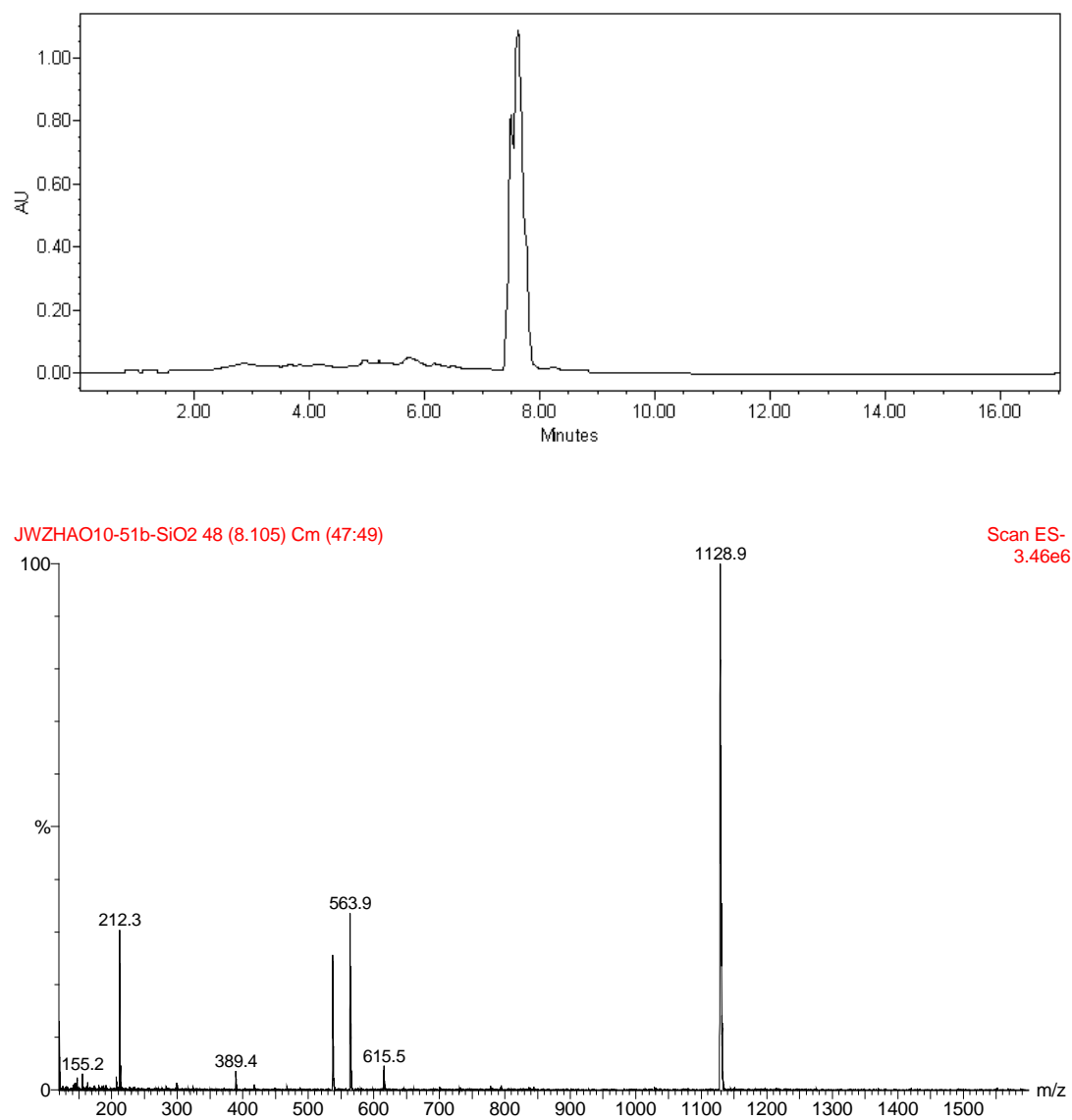
Figure 2-20. LC-MS of linear dimer **20** using amidite/H-phosphonate monoester method sulfurizing during linear coupling
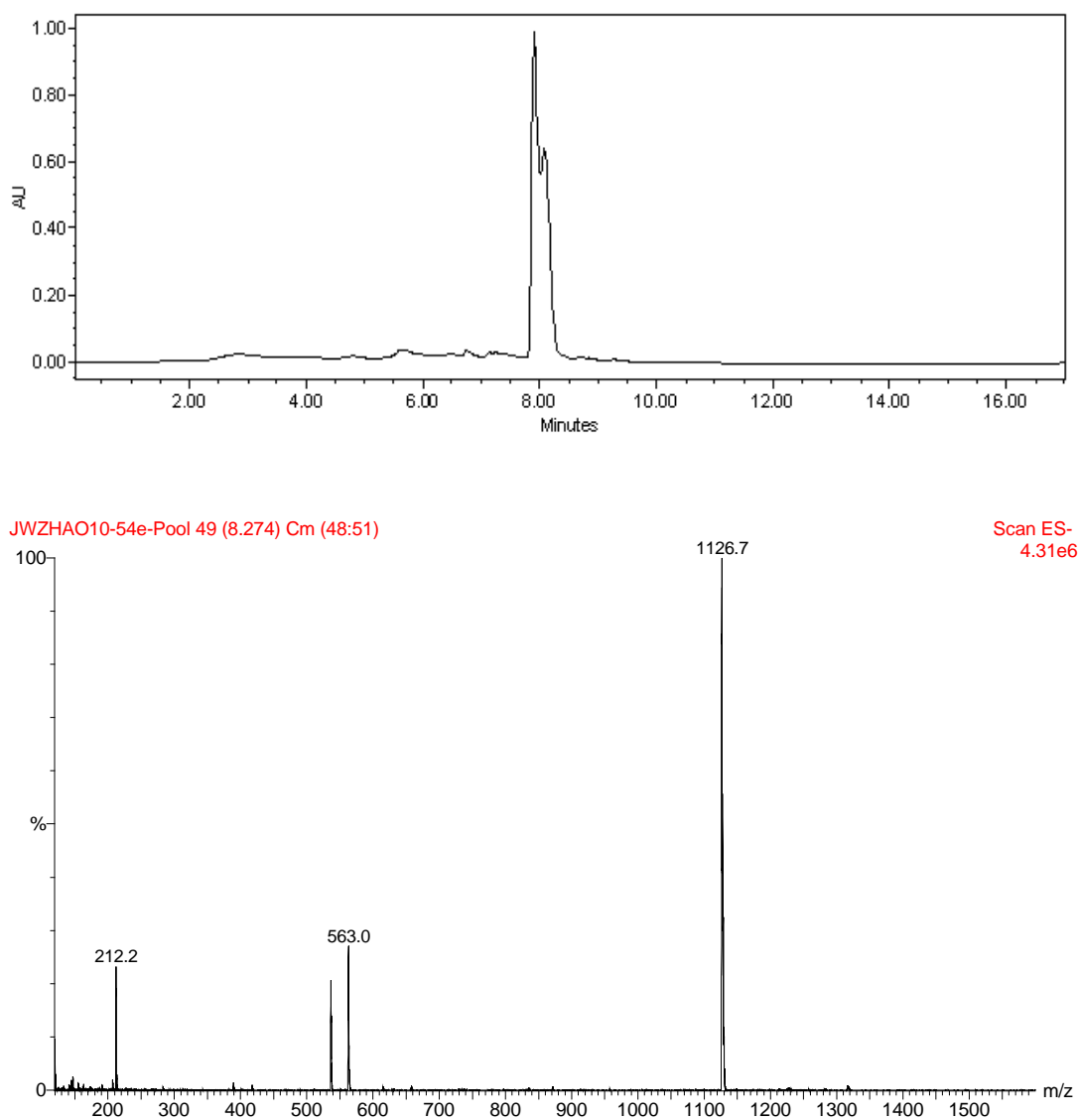
Figure 2-21. LC-MS of protected cyclic dimer **21** from amidite/H-phosphonate monoester method sulfurizing during linear coupling
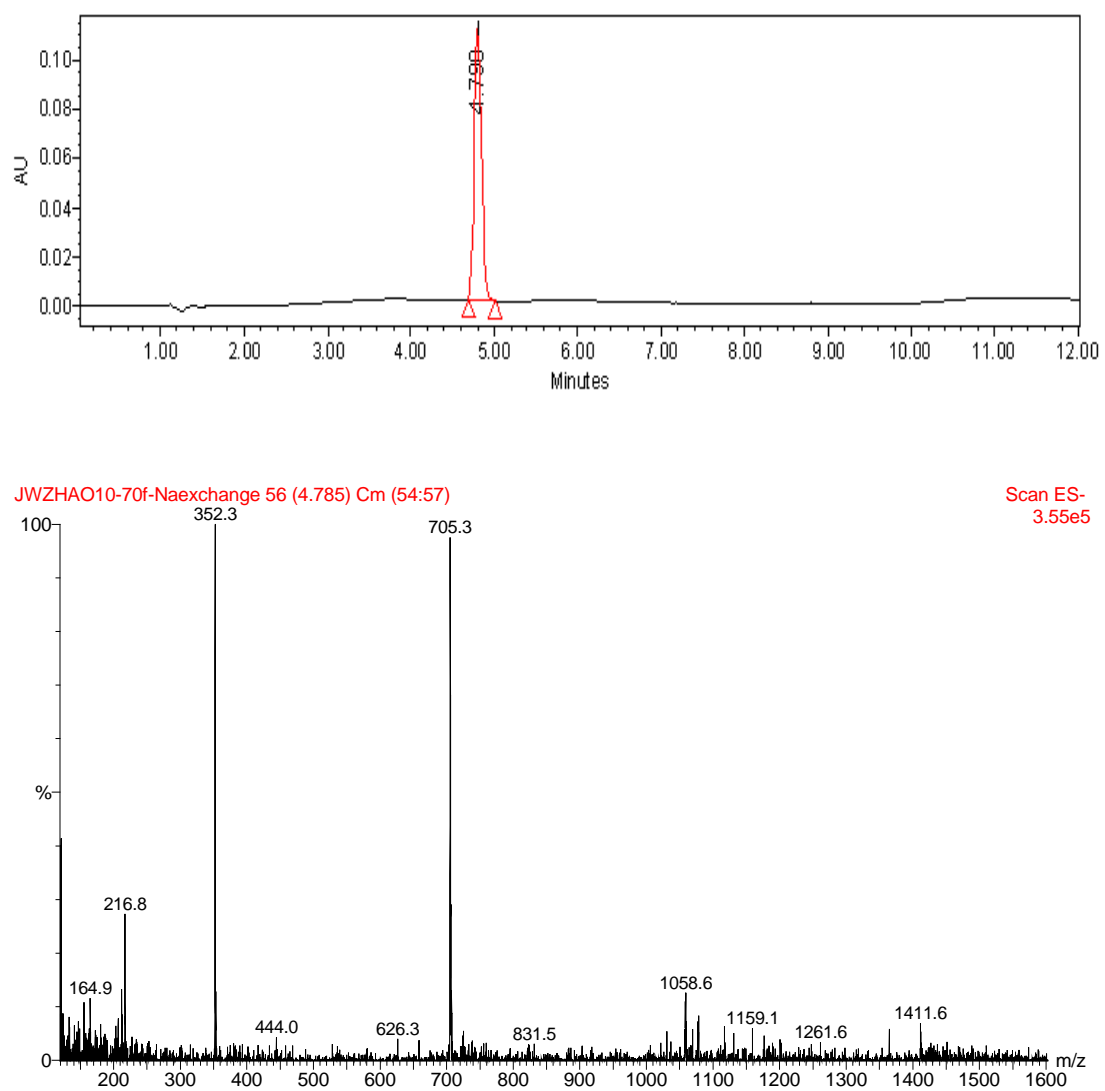
Figure 2-22. LC-MS profile of cyclic dimmer **14** [*S*]
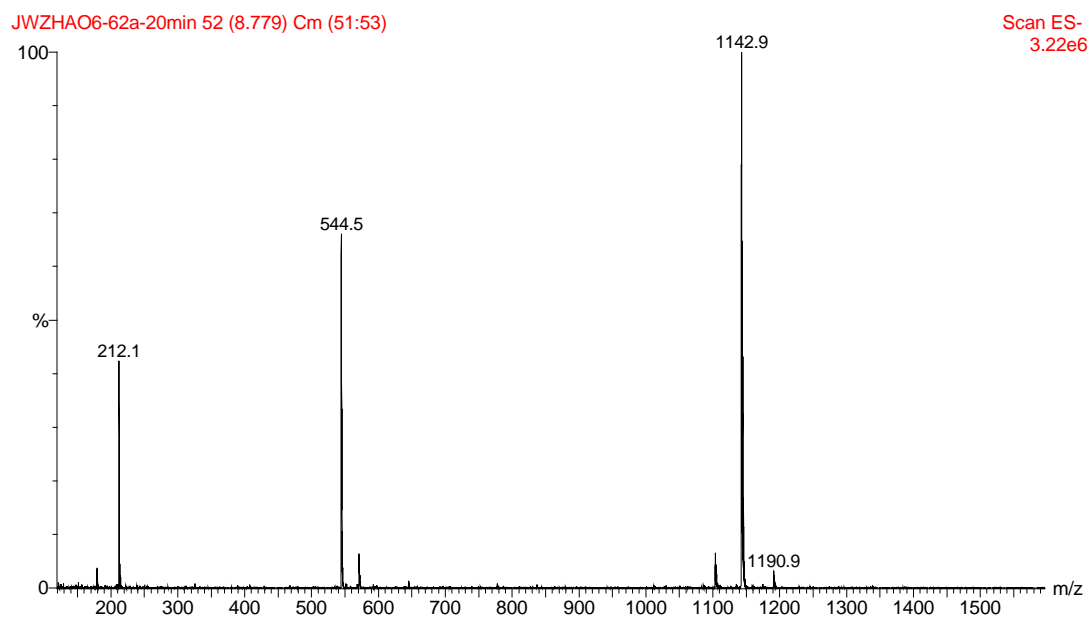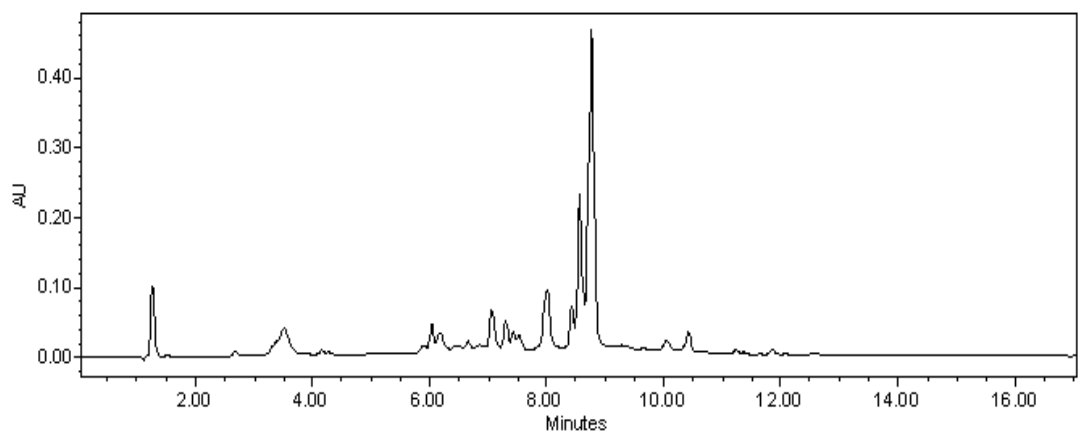
Figure 2-23. LC-MS of crude protected cyclic dimer **22** using amidite/H-phosphonate monoester method
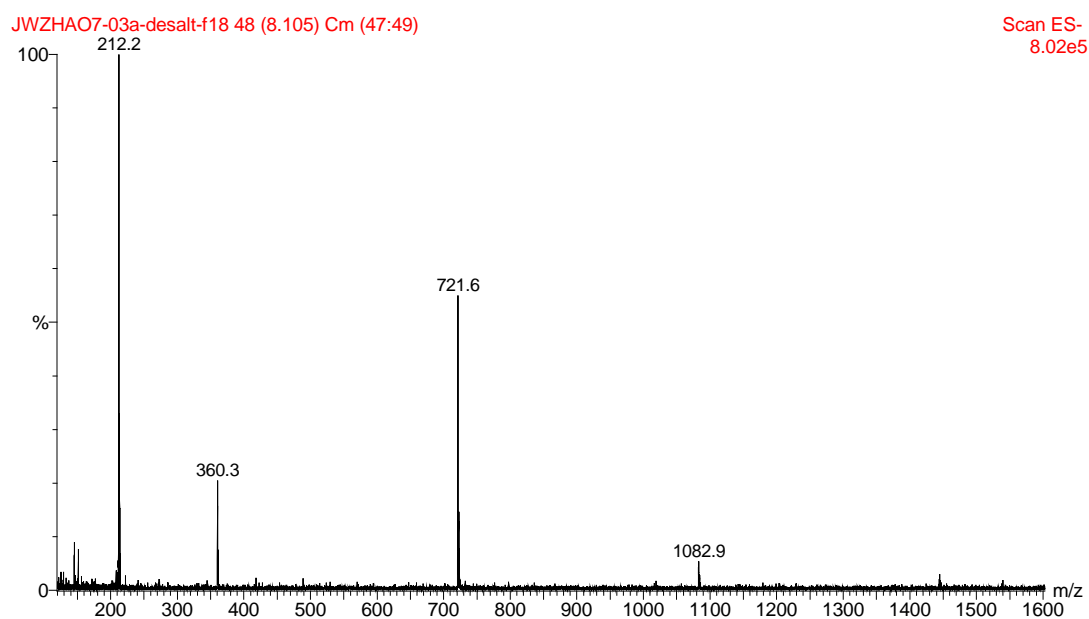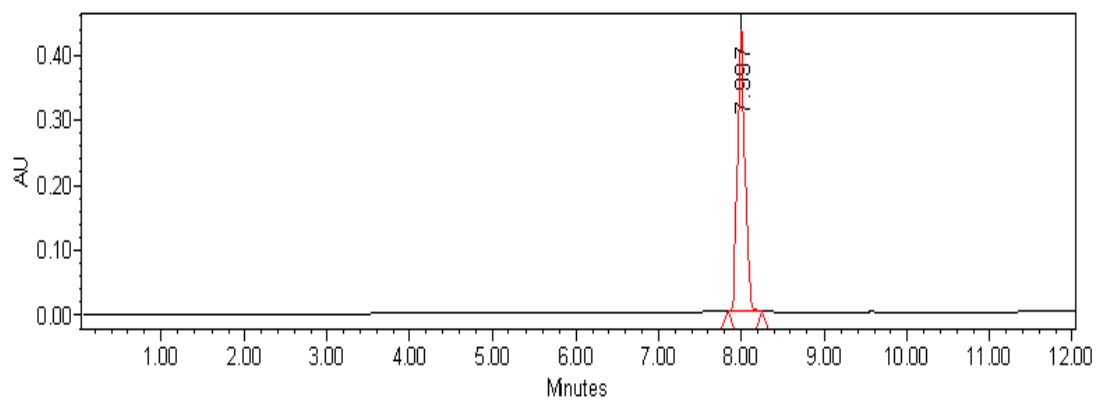
Figure 2-24. LC-MS of dithiophosphate c-di-GMP **23** [*R, R*]
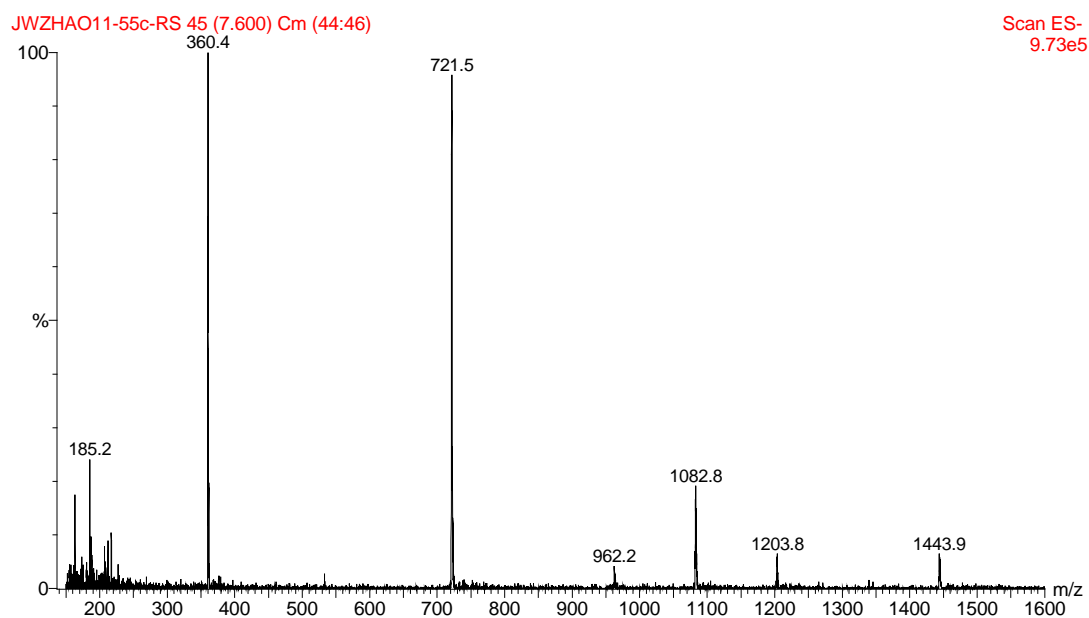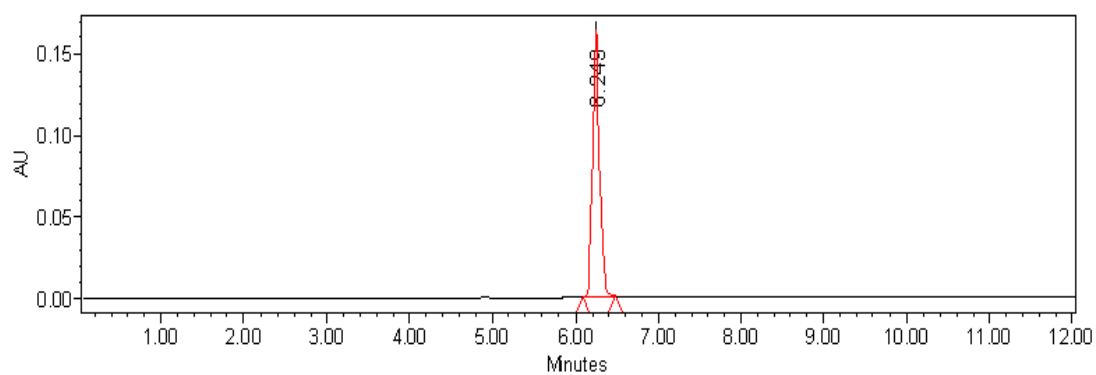
Figure 2-25. LC-MS of dithiophosphate c-di-GMP **23** [*R, S*]
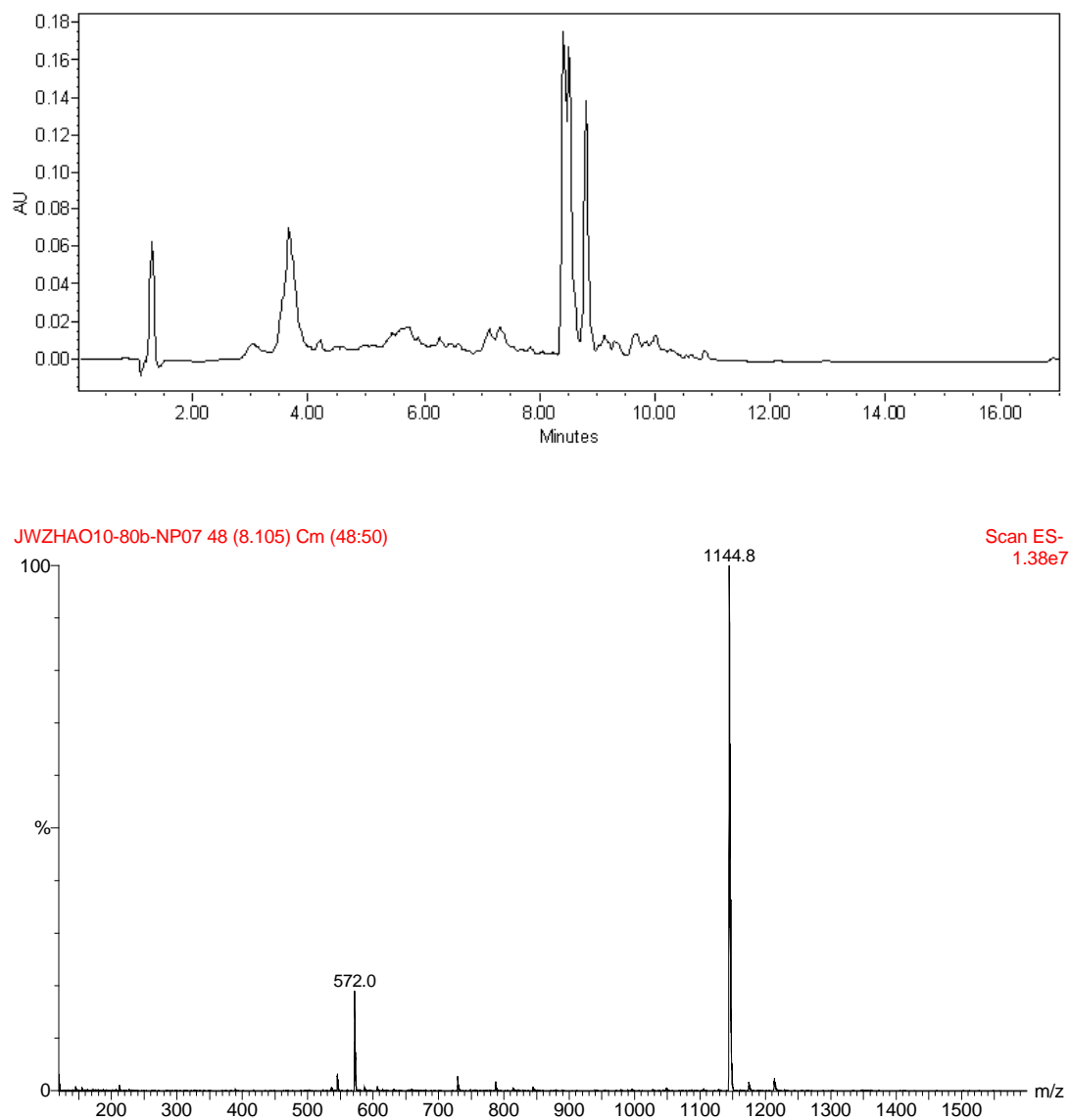
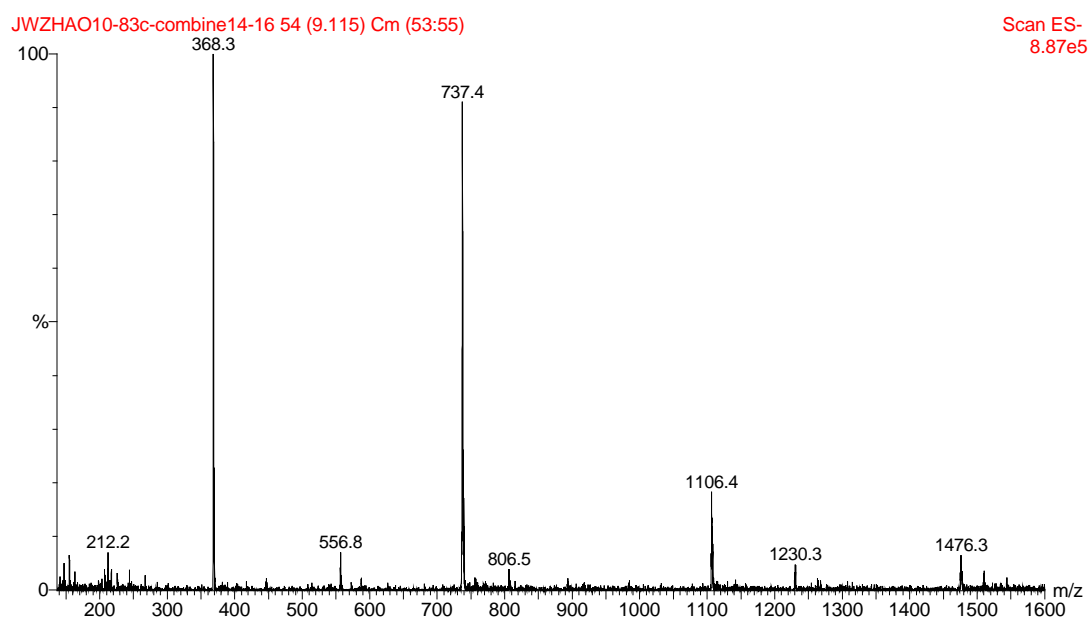**Figure 2-26.** LC-MS of crude linear dimer **28** using amidite/H-thiophosphonate monoester method
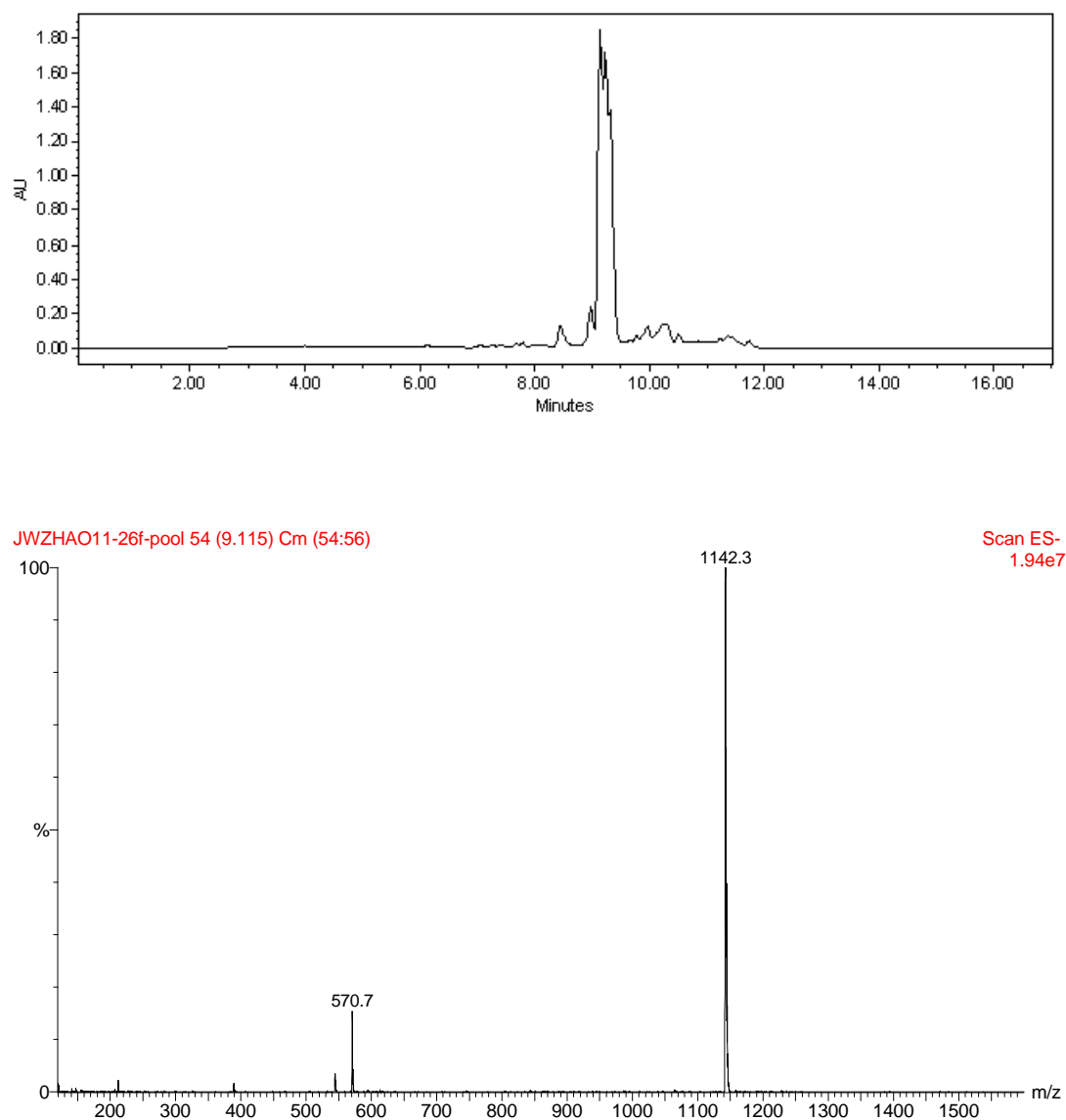
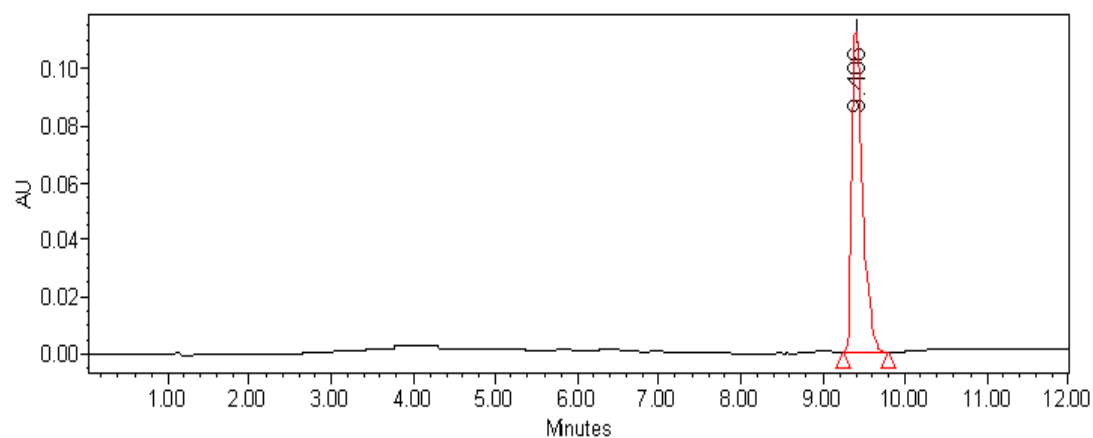**Figure 2-27.** LC-MS of crude protected cyclic dimer **29** using amidite/H-thio-phosphonate monoester method
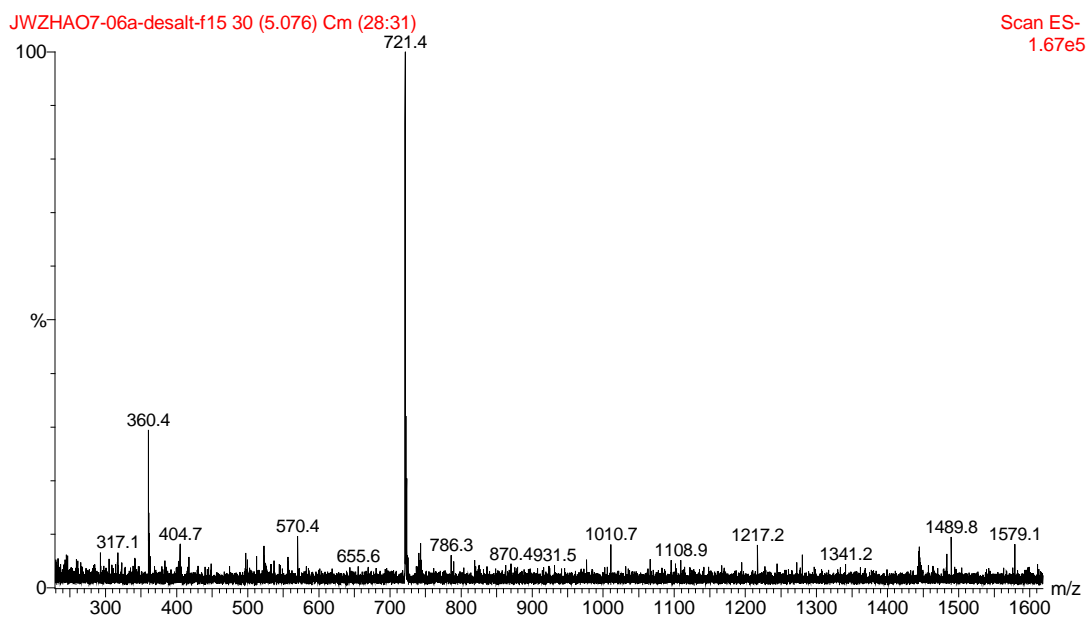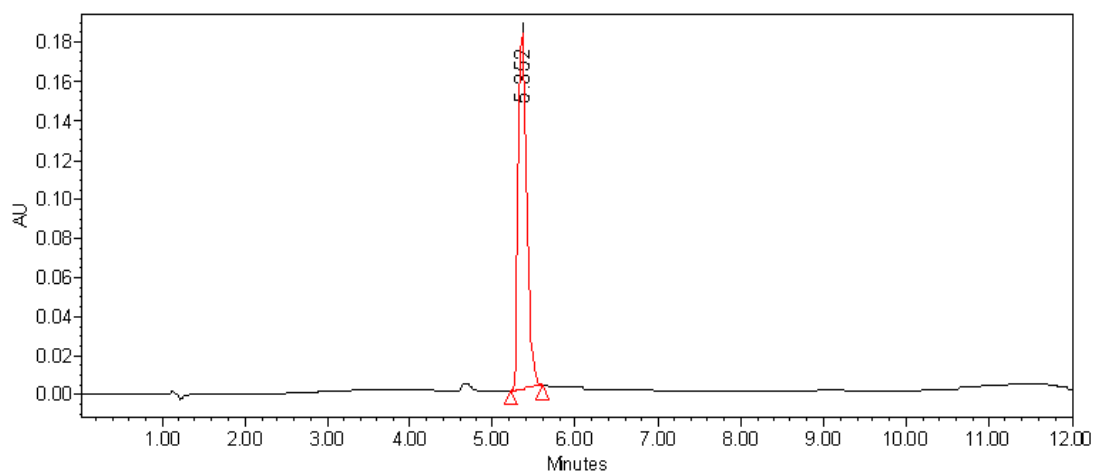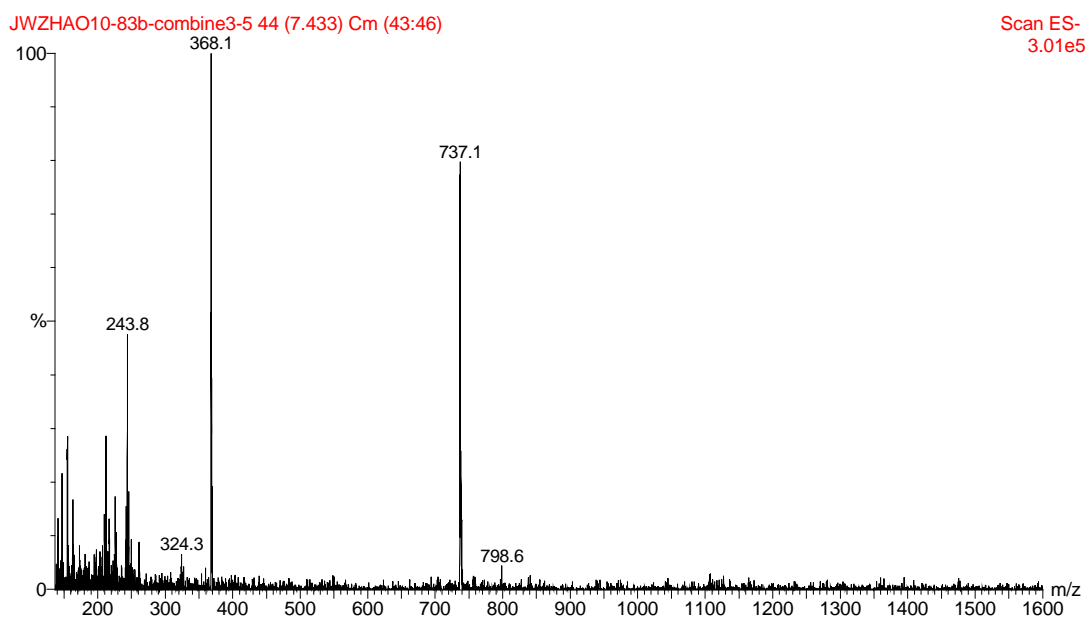
Figure 2-28. LC-MS of dithiophosphate c-di-GMP **23 [*S, S*]**
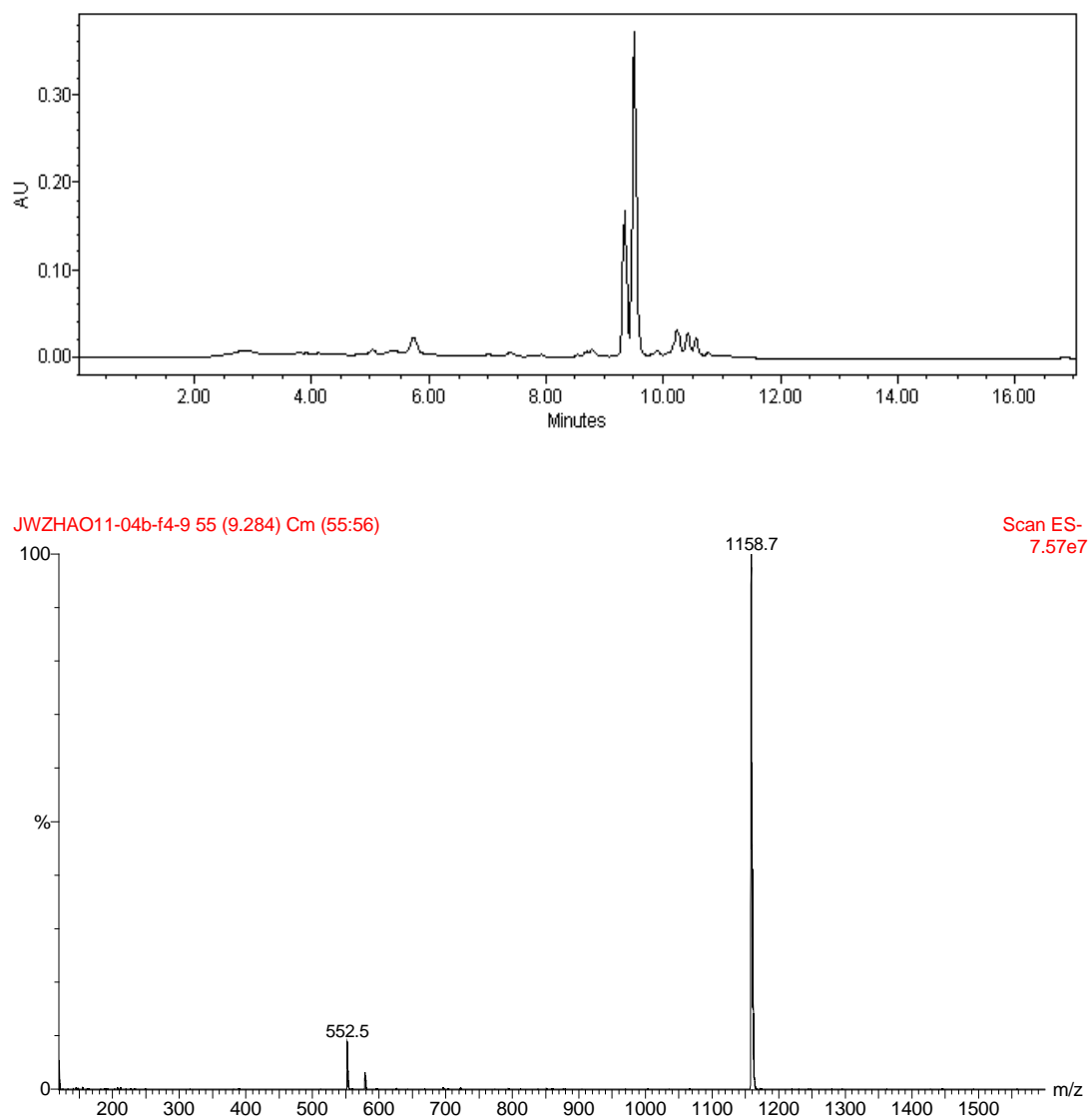
Figure 2-29. LC-MS of crude protected cyclic dimer **30** using amidite/H-thio-phosphonate monoester method

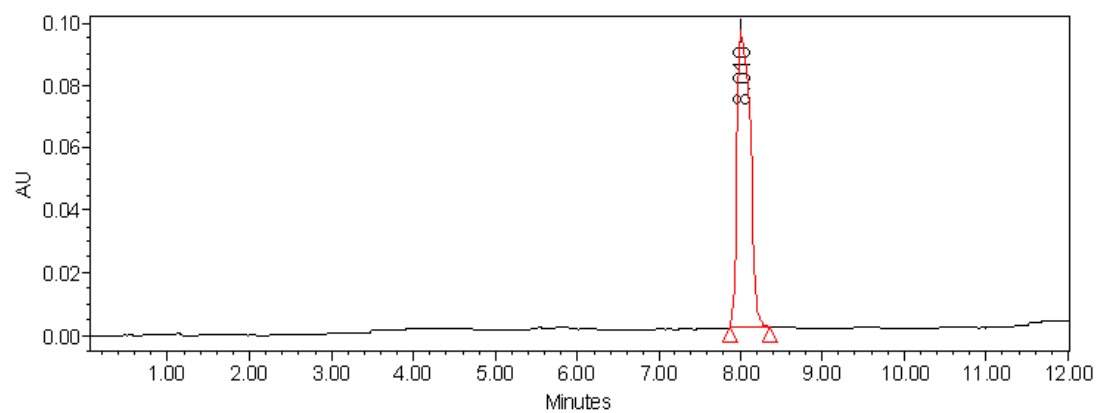**Figure 2-30.** LC-MS of trithiophosphate c-di-GMP **31** [*R*]

Figure 2-31. LC-MS of trithiophosphate c-di-GMP **31** [*S*]

Chapter 3

^{1}H and ^{31}P NMR Studies of Thiophosphate

c-di-GMP Analogs

I. Introduction

NMR is a useful tool for structure analysis and determination of various compounds, including small organic molecules and large biological molecules. One and two dimensional ^{1}H, ^{31}P and ^{15}N NMR have been used in the characterization of DNA and RNA oligonucleotides[1-7] by many groups, including the Jones group.[8, 9]

^{31}P NMR has been used in the determination of stereochemical configurations of thiophosphate analogs[5-7, 10] and the correlation between phosphate backbone and glycosidic torsion angles.[11-13] Stec[5] originally established that in cyclic AMP, the [*R*] thiophosphate analog displayed a more downfield chemical shift (~ 55 ppm) than the [*S*] thiophosphate (~ 53 ppm). Later, Stawinski[7] observed the same trend for various deprotected linear dimers, with the [*R*] diastereomers having more downfield chemical shifts than the [*S*], but the opposite correlation was found for the corresponding protected linear dimers, because of various effects of protecting groups. For the c-di-GMP monothiophosphate analogs, Benziman[6] used Stec's original correlation to assign the stereochemistry of the two fully deprotected diastereomers with [*R*] (56.89 ppm) having a

more downfield chemical shift than [S] (55.35 ppm). However, he did no enzyme degradation work to confirm these assignments. In contrast, Battistini[10] later carried out enzyme degradation of corresponding linear dimer of cyclic-di-TMP thioate analogs and reported that they had the opposite correlation of ^{31}P chemical shift with stereochemistry. The [R] diastereomer displayed a more upfield chemical shift (52.9 ppm), and the [S] diastereomer showed a more downfield value (53.2 ppm). As will be discussed in the next section of this chapter, the results in this thesis are in agreement with Battistini,[10] with the [R] monothiophosphate having a more upfield ^{31}P chemical shift than the [S]. This correlation was then used for assignments of the stereochemistry of the di- and trithiophosphate analogs.

1D ^{1}H NMR was used by Pinnavaia[1] to study 5'-GMP, and he found direct NMR evidence for the regular ordered structure of the G-quartet. The effects of alkali metal ions on G-quartet formation was also studied[14-16] and both K$^+$ and Na$^+$ were found to stabilize the quartet, but a much stronger effect was found with K$^+$. 2D NOSEY NMR has been used for quadruplex structure characterization in guanosine-rich oligonucleotides.[3, 17-19] The formation of G-quartets was confirmed by the signals of hydrogen bonded amido protons. Furthermore, the glycosidic conformation was assigned by the magnitude of the NOE between the guanine H8 and the ribose H1', since those protons are about 4 Å apart in the *anti* conformation, and ~ 2.2 Å in the *syn* conformation. Zhaoying Zhang[20] from the Jones' lab has used 2D NOSEY NMR to study the polymorphism of unmodified c-di-GMP in high concentration solutions. It was found that this molecule displayed five different structures, with most involving G-quartet

formation, and the equilibrium among them was highly temperature and counterion dependent. An all-*anti* bimolecular structure was favored by Li^+ and high temperature, while tetra- and octamolecular complexes in all-*syn* and all-*ant*i conformations were favored by K^+ and lower temperature (See **Figure 1-3** in the Introduction).

In this thesis, 1D ^1H and ^{31}P NMR, as well as 2D NMR, were used to analyze c-di-GMP thiophosphate analogs in solution at high concentration in both Na^+ and K^+ forms. The effects of counterions on the nature of the complexes and the *syn*/*anti* conformational equilibrium will be discussed in the following sections.

II. Stereochemistry assignment by ^{31}P NMR

II1. ^{31}P NMR chemical shift order for monothiophosphate c-di-GMP diastereomers

As discussed in Chapter 2, section **III2**, the absolute configurations of the chiral phosphorus centers of the two monothiophosphate c-di-GMP diastereomers have been assigned by several enzymatic methods. A ^{31}P NMR spectrum of each of these diastereomers was then acquired at a low concentration (~ 0.5 mM) and the chemical shift order of the thiophosphates was used as a standard to extend the stereochemistry assignments to the di- and trithiophosphate c-di-GMP.

It is known that at low concentration, the Na^+ form of c-di-GMP exists mainly in uni- or bimolecular form,[21] and the ^{31}P NMR shows only a single peak for phosphate. **Figure**

3-1a (Appendix) shows the ^{31}P NMR spectrum of [R] monothiophosphate, whose configuration was determined by enzymatic digestion (Chapter 2). It displays two signals, one with a chemical shift around -0.2 ppm, which corresponds to the unmodified phosphate, and another with a chemical shift of ~ 55.6 ppm, which corresponds to the [R] thiophosphate. Similarly, the ^{31}P NMR spectrum of [S] monothiophosphate c-di-GMP, shown in **Figure 3-1b**, also shows two single peaks, one at ~ 0 ppm, corresponding to the unmodified phosphate, and the other one with a chemical shift of ~ 56.9 ppm, corresponding to the [S] thiophosphate. The order of these chemical shifts for the [R] and [S] thiophosphates are consistent with Battistini's work,[10] that [R] is upfield of [S].

II2. Configuration assignment of di- and trithiophosphate c-di-GMP diastereomers

In the di- and trithiophosphate c-di-GMP, both phosphate linkages contain at least one sulfur, which makes selective ring opening of the cyclic dimer to the linear dimer difficult. Thus, the stereochemistry of di- and trithiophosphate c-di-GMP could not be assigned by enzymatic methods.

However, based on the ^{31}P NMR chemical shift difference between the [R] and the [S] monothiophosphate, it is convenient to use this information to assign the configurations of the three diastereomers of dithioate c-di-GMP. **Figure 3-2a** (Appendix) shows the ^{31}P NMR spectrum of the diastereomer with a retention time of 8.0 min in the HPLC. Because it has only a single peak at ~ 55.0 ppm, this diastereomer is symmetrical and contains the same configuration at both thiophosphate linkages. Because this

chemical shift is most similar to that of the known [R] monothiophosphate c-di-GMP (55.6 ppm), it can be concluded that the diastereomer with retention time of 8.0 min is [R, R]. **Figure 3-2c** shows a major peak at ~ 57.5 ppm, similar to that of the [S] monothiophosphate (56.9 ppm). The two minor peaks, which are in accordance with neither the [R] nor the [S], are most likely the result of complexes. Therefore, this diastereomer with retention time of 5.4 min was assigned as the [S, S] diastereomer. The diastereomer with a retention time in between the other two at 6.2 min, shows two peaks in the ^{31}P NMR, as shown in **Figure 3-2b**. Their chemical shifts of 55.4 and 56.7 ppm are similar to those of the [R] and [S] monothiophosphates, respectively, indicating that this diastereomer is the unsymmetrical molecule, [R, S] dithiophosphate c-di-GMP.

The trithiophosphates are not symmetrical, since one of the phosphorus centers contains two sulfurs, which eliminates the chiralty of this linkage. As expected, the thiophosphate with two sulfurs shows a more downfield chemical shift of ~ 114 ppm in the ^{31}P NMR, as shown in both spectra in **Figure 3-3**. The spectrum in **Figure 3-3a** displays an additional peak at ~ 55.5 corresponding to the [R] monothiophosphate. This diastereomer with a longer retention time of 9.1 min in the HPLC is therefore assigned the [R] configuration. The ^{31}P NMR spectrum of the shorter retention time diastereomer (8.0 min) is shown in **Figure 3-3b**, and displays a peak at ~ 57.4 ppm, similar to the [S] monothiophosphate, as well as the peak at ~ 114.6 ppm for the dithiophosphate. This diastereomer is therefore assigned the [S] configuration.

The stereochemistry of the diastereomers of the mono-, di- and trithiophosphate c-di-GMP has thus been assigned, and the results are summarized in **Table 3-1** with ^{31}P NMR chemical shifts and HPLC retention times. Within each family of thiophosphates, the diastereomer with the longer retention time [*R*] or [*R, R*] always has a more upfield chemical shift.

Table 3-1. Summary of HPLC retention times and ^{31}P chemical shifts of the seven thiophosphate analogs of c-di-GMP

Analogs	Configuration assignment	Retention time (min)	^{31}P NMR chemical shifts (ppm)
Monothiophosphate c-di-GMP	*R*	6.1	-0.5, 55.4
	S	4.8	-0.4, 56.7
Dithiophosphate c-di-GMP	*R, R*	8.0	55.4
	R, S	6.2	55.9, 57.4
	S, S	5.4	57.2
Trithiophosphate c-di-GMP	*R*	9.1	55.3, 114.1
	S	8.0	57.2, 114.4

III. One-dimensional ^{1}H and ^{31}P NMR studies

According to previous studies from the Jones lab, the unmodified c-di-GMP at higher concentration (~ 30 mM) formed five different structures.[20] The 1D ^{1}H NMR spectrum of the K$^+$ form at 5 °C showed several sets of resonances, including the N1H in a hydrogen-bonded form, H-bonded and non-H-bonded NH$_2$ protons, and H8 protons. These resonances were shown to reflect all-*syn* and all-*anti* tetra- and octamolecular complexes.

In the work described in this thesis for thiophosphate c-di-GMP analogs, major differences were found for the Na^+ and K^+ forms, so they will be described separately in the following sections. Although samples for the previous work on unmodified c-di-GMP included 0.1 M LiCl, NaCl, or KCl, the work described here had only the appropriate counterion, with no additional salt. A test sample that did have 0.1 M KCl showed extreme aggregation, so this method was not used.

III1. ^{1}H and ^{31}P NMR of monothiophosphate c-di-GMP in Na^+ form

Four 1D ^{1}H NMR spectra of [*R*] monothiophosphate c-di-GMP in Na^+ form are shown in **Figure 3-4**. These spectra were acquired at increasing temperatures from 5 °C to 55 °C in order to observe the breakdown of complexes. The signals near 11 ppm are correlated to the hydrogen-bonded N1 protons. As expected, these N1H signals, which are associated with guanine quartet structures, gradually decrease with increasing temperature, in agreement with dissociation of the higher complexes. In the H8 region a central peak near 7.7 ppm at 5 °C moves downfield with increasing relative intensity upon heating. This signal is therefore most likely associated with the bimolecular structure and is consistent with the earlier work.[20] Since the cyclic dimer appears to exist as a mixture of all complexes at 30 °C, it is reasonable to study the spectrum at 30 °C in detail. As opposed to unmodified c-di-GMP, this unsymmetrical monothiophosphate analog contains two different H8s, which explains the broadness of the central H8 signal. In addition to this central broad resonance, two sets of H8 resonances are present, one upfield and one downfield. Based on comparison to the earlier work,[20] these are likely to

represent all-*syn* and all-*anti* higher order complexes, respectively. This conclusion is verified by 2D NMR, described in section **IV1**.

In the previous work with unmodified c-di-GMP,[20] the *syn/anti* conformational assignments for the higher order H8 signals were consistent with a similar but reversed pattern in the ^{31}P NMR spectra. The latter displayed a central peak at -0.8 ppm assigned to the bimolecular structure, and groups of upfield and downfield signals that represented the *anti* and *syn* higher order complexes, respectively. All the ^{31}P signals corresponding to the higher order complexes disappeared upon heating, indicating the dissociation of guanine quartet structures. This ^{31}P pattern is consistent with previous studies on 5' AMP and GMP analogs,[11-13] for which the downfield resonances were correlated to a *syn* conformation and upfield resonances to an *anti* conformation.

The ^{31}P NMR spectrum of [*R*] monothiophosphate c-di-GMP is shown in **Figure 3-5**. There are two separate clusters of ^{31}P resonances, one around 0 ppm corresponding to the unmodified phosphate, and one near 55 ppm corresponding to the thiophosphate. These two clusters show very similar patterns of peak distribution with changing temperatures. For example, at 5 °C, the unmodified phosphate resonances contain a large central peak around –0.8 ppm, corresponding to the bimolecular structure; a downfield peak at ~ 1 ppm corresponding to the higher order complexes with a *syn* conformation; and a group of upfield peaks corresponding to higher order complexes with an *anti* conformation. The same size cluster near 55 ppm display a similar pattern, indicating the formation of all-*syn* and all-*anti* complexes. These results are consistent with the ^{1}H NMR data, described

above. The integration of ^{31}P NMR resonances at 30 °C is summarized in **Table 3-2** for this and all other diastereomers, showing the distribution of bimolecular and higher order *syn* and *anti* complexes.

In the case of [*S*] monothiophosphate c-di-GMP in Na$^+$ form, a different pattern was observed in both ^{1}H NMR and ^{31}P NMR. As shown in **Figure 3-6**, the ^{1}H NMR spectra displayed the same loss of H-bonded N1H signals with increasing temperature, but completely different H8 signals. There are two equal, well-separated H8 signals that increase with temperature, so can be assigned to the two different H8 atoms in the bimolecular structure. There are also two sets of H8 signals that increase with decreasing temperature, indicating they are correlated with higher order complexes. However, since each one is downfield of one of the bimolecular H8 signals, they are likely to reflect an all-*anti* complex, with no *syn* signals present. Thus, it appears that the Na$^+$ form of [*S*] monothiophosphate c-di-GMP only forms higher order complexes in an all-*anti* conformation.

The ^{31}P NMR spectra of the Na$^+$ form of the [*S*] monothiophosphate shown in **Figure 3-7** support this tentative conclusion. Again, two clusters of signals that have similar pattern are present, corresponding to the unmodified phosphate and the thiophosphate. The main peaks at 55 °C (~ 0 ppm and ~ 57 ppm) are assigned to the phosphate and thiophosphate, respectively, of the bimolecular structure. These peaks gradually decrease with decreasing temperature, and new peaks form, but only upfield of the bimolecular signals. As mentioned earlier, these upfield ^{31}P peaks are correlated with *anti* complexes,

thus supporting the ^{1}H data. Thus, the [S] thioate apparently provides special stabilizations of the higher order *anti* complexes, and/or destabilizes the *syn* complex.

Also, both the ^{1}H and ^{31}P NMR clearly show that the [S] diastereomer complexes are more stable than the [R] diastereomer complexes. At 5 °C, the ^{31}P NMR of the [S] diastereomer displays mainly the *anti* higher order complexes, with little of the bimolecular structure. On the other hand, the [R] diastereomer has more than 30% of the bimolecular structure at 5 °C. At 55°C, all the higher order complexes of the [R] diastereomer have dissociated, while a significant amount of the higher order complexes of the [S] diastereomer are still present.

III2. ^{1}H and ^{31}P NMR of dithiophosphate c-di-GMP in Na$^+$ form

All three diastereomers of dithiophosphate c-di-GMP were studied using ^{1}H and ^{31}P NMR as for the mono-substituted analogs.

The [R, R] diastereomer in Na$^+$ form might be expected to mimic the properties of [R] monothiophosphate, since it has no [S] thioate. As shown in **Figure 3-8**, the ^{1}H spectra of the [R, R] diastereomer do in fact show a very similar pattern as that of [R] monothiophosphate. At 55°C, the H-bonded N1H signal near 11 ppm is greatly diminished, and a broad H8 signal is observed. With decreasing temperature, the likely *syn* and *anti* higher order complexes start to form, indicated by the appearance of both up- and downfield H8 signals. The ^{31}P NMR spectra, shown in **Figure 3-9**, support these

assignments, with appearance upon decreasing temperature of both up- and downfield peaks relative to a central signal for the bimolecular structure.

The ^{1}H NMR spectra of [*S, S*] diastereomer shown in **Figure 3-10** shows a different pattern than the [*R, R*] analog. At 55 °C, the major H8 signal near 8.4 ppm correlates with the bimolecular structure. A small downfield signal is also present, which is likely due to an *anti* higher order complex. With decreasing temperature, the bimolecular structure decreases and the *anti* complex increases. However, at 15 °C, the baseline has an unusually low signal/noise ratio and several very broad peaks appear. At 5 °C, there are signs of extensive aggregation, with extreme line broadening. Thus the single sharp peak at 5 °C for the *anti* complex in fact represents only a small amount of the sample. The extreme aggregation of the [*S, S*] diastereomer is confirmed by ^{31}P NMR, which is shown in **Figure 3-11**. Even the 30 °C spectrum shows a lowered signal/noise ratio, and the 5 °C spectrum shows only a broad ill-defined region. It is concluded that the combination of two [*S*] thiophosphates not only provides specific stabilization of the *anti* conformation, as in the [*S*] monothiophosphate c-di-GMP, but also leads to extensive aggregation of the sample at lower temperatures.

Figure 3-12 shows ^{1}H spectra of the [*R, S*] dithiophosphate c-di-GMP in Na$^+$ form, which are very similar to those of the [*S*] monothiophosphate analog. At 55 °C, there is no H-bonded N1H, and only two single peaks in the H8 region, corresponding to the two different H8s of the bimolecular structure. With decreasing temperature, two new clusters of resonances appear, each one downfield to one of the bimolecular signals. The two

different H8s in this molecule apparently have quite different magnetic environments. No upfield H8 signals were found with decreasing temperature, indicating again that just one [*S*] thiophosphate seems to effectively provide special stabilization of the *anti* conformation. Formation of only all-*anti* complexes in the [*R, S*] diastereomer was again supported by ^{31}P NMR. As shown in **Figure 3-13**, two peaks at ~55.5 ppm and ~ 56.9 ppm are observed at 55 °C, corresponding to the [*R*] and [*S*] thiophosphates, respectively. The intensity of these two peaks decreases with decreasing temperature, while a new cluster of upfield signals appears. The lack of any downfield signals supports the conclusion that only all-*anti* complexes are present.

III3. ^{1}H and ^{31}P NMR of trithiophosphate c-di-GMP in Na^{+} form

The ^{1}H spectra of the [*R*] trithiophosphate c-di-GMP, Na^{+} form, shown in **Figure 3-14**, display a similar temperature dependence as those of [*S*] mono- and [*R, S*] dithiophosphate, presumably because they all have one sulfur in the [*S*] position. Two single H8 signals at 55 °C decrease with decreasing temperature, and two new downfield signals appear (one major and one minor), consistent with all-*anti* complexes. ^{31}P NMR, illustrated in **Figure 3-15**, shows two signals at 55 °C near 55 ppm and 114 ppm, corresponding to [*R*] monothioate and dithioate, respectively. These two signals are consistent with the bimolecular structure and decrease with decreasing temperature, while clusters of upfield signals appear, supporting the presence of all-*anti* complexes, but no *syn* complexes. Since one of the two sulfurs in the dithiophosphate group is in an [*S*]

position, it is apparently sufficient to provide special stabilization of the *anti* complexes, as seen before.

Because the [*S*] trithiophosphate has two sulfurs in the [*S*] position, it has much in common with the [*S, S*] dithiophosphate. The ^{1}H NMR spectra shown in **Figure 3-16** is similar, except that there are two different kinds of H8s in the molecule, so there are two different H8 signals for the bimolecular structure at 55 °C. Just as there are only downfield H8 signals in the ^{1}H NMR at lower temperature, there are only upfield signals in the ^{31}P NMR, shown in **Figure 3-17**, consistent with only all-*anti* complexes. Furthermore, the ^{31}P NMR spectra in particular show low signal/noise ratios, again indicating extensive aggregation.

In summary, of all seven thiophosphate analogs of c-di-GMP in the Na$^+$ forms, those with at least one [*S*] sulfur seem to specifically have special stabilization of the *anti* complexes relative to the *syn* complexes. Furthermore, those with two [*S*] sulfurs form highly aggregated species that cannot be observed by NMR under these conditions. As mentioned in Chapter 2, this extensive aggregation partially explains the difficulties in separation and purification of these compounds after their synthesis.

III4. ^{1}H and ^{31}P NMR of the seven analogs in K$^+$ form

As shown in **Figure 3-18** and **Figure 3-19**, the 1D ^{1}H and ^{31}P NMR spectra of the [*R*] monothiophosphate c-di-GMP in K$^+$ form display a similar pattern as those of the Na$^+$

form, with the bimolecular structure dominant at 55 °C, and the higher order complexes in all-*syn* and all-*anti* conformations increasing with decreasing temperatures. However, these complexes are much more stable in the K^+ form than in the Na^+ form, which is consistent with the fact that K^+ stabilizes guanine quartets more than Na^+ does.[22, 23]

However, the [*S*] monothiophosphate in the K^+ form is very different from the Na^+ form. **Figure 3-20** shows that its ^{1}H NMR is much more complicated than that for the Na^+ form (**Figure 3-6**). As seen by the H-bonded N1H, the higher order complexes are present even at 55 °C. The H8 region shows two dominant signals consistent with the bimolecular structure, and additional small clusters of signals both upfield and downfield, suggesting that both *syn* and *anti* complexes are present. The ^{31}P NMR shown in **Figure 3-21**, is in agreement at 55 °C, with dominant central peaks near 0 ppm and 57.0 ppm, corresponding to the bimolecular structure, and both downfield and upfield signals corresponding to *syn* and *anti* higher order complexes. At 30 °C, the central peak is greatly diminished, and higher order complexes are dominant.

The ^{1}H and ^{31}P NMR spectra of the K^+ forms of dithiophosphate c-di-GMP diastereomers are shown in **Figure 3-22** to **Figure 3-27**. In the case of the [*R, R*] diastereomer, both ^{1}H and ^{31}P spectra display a similar pattern to the Na^+ form, but with more stable higher order complexes, because of the special stabilization of the guanine quartets provided by K^+. Both ^{1}H and ^{31}P spectra show downfield and upfield resonances relative to the bimolecular structure signals even at 55 °C, indicating the presence of both *syn* and *anti* complexes.

Extensive aggregation was found for the [*R, S*] diastereomer, shown by the lower S/N ratio in the ^{31}P NMR spectra. None-the-less, at 5 °C, the ^{1}H NMR shows a major H8 peak at ~ 8.2 ppm, and a minor one at ~ 7.5 ppm, consistent with *anti* and *syn* complexes, respectively. The ^{31}P spectra at 55 °C and 30 °C also show upfield and downfield signals.

Table 3-2. Distribution of complexes at 30 °C based on integration of ^{31}P NMR spectra

		Na$^+$ forms			K$^+$ forms		
	#*S* sulfurs^a	% B/U^b	% *anti* T/O^c	% *syn* T/O^c	% B/U^b	% *anti* T/O^c	% *syn* T/O^c
Monothioate *R*	0	50	33	17	5	60	35
Monothioate *S*	1	12	88	0	2	56	42
Dithioate *RR*	0	49	35	16	7	60	33
Dithioate *RS*	1	22	78	0	4	76	20
Dithioate *SS*	2	ND^d			ND^d		
Trithioate *R*	1	26	74	0	5	64	31
Trithioate *S*	2	ND^d			ND^d		

^{a} Number of sulfurs in the [*S*] position
^{b} Bimolecular and/or unimolecular structures
^{c} Tetramolecular and/or octamolecular complexes
^{d} Not determined due to extensive aggregation

The [*S, S*] diastereomer shows extensive aggregation in both its ^{1}H and particularly its ^{31}P spectra at 5 °C. The ^{1}H and ^{31}P spectra at higher temperatures are difficult to interpret, but none-the-less, are consistent with the presence of both *syn* and *anti* complexes.

Figure 3-28 through **Figure 3-31** display ^{1}H and ^{31}P NMR spectra of the [*R*] and [*S*] trithiophosphate c-di-GMP diastereomers in the K^{+} form. These samples also show extensive aggregation with low S/N ratios, particularly the [*S*] diastereomer. Again, the spectra at higher temperatures show signals consistent with *syn* and *anti* complexes.

Integration of all the ^{31}P spectra is summarized in **Table 3-2**, which shows the distribution of varies complexes in the different samples.

IV. Two-dimensional proton NMR studies of all analogs in Na^{+} and K^{+} forms

To provide more definitive evidence for the effects of stereochemistry on complex formation in the Na^{+} and K^{+} forms, two-dimensional (2D) ^{1}H NOSEY and DOSY NMR experiments, were carried out at 30 °C. The extreme aggregation found with the [*S, S*] dithioate and [*S*] trithioate in Na^{+} and K^{+} forms prevented sufficient signals in the NOSEY experiments at 30 °C, so they were carried out at 45 °C.

IV1. 2D NOSEY of all seven thioate analogs in Na^{+} and K^{+} forms

2D NOSEY has been used for many years to study the *syn*/*anti* conformation of nucleotides and oligonucleotides. The intensity of the cross peak between a guanine H8 and its H1' is a good measure of its *syn*/*anti* orientation. 2D NOSEY was used in the earlier work in the Jones lab on unmodified c-di-GMP,[20] and helped to elucidate the identity of the five different complexes that formed, including the bimolecular structure, the all-*syn* and all-*anti* tetramolecular complexes, and the all-*syn* and all-*anti* octamolecular complexes. As already discussed in the previous sections, the 1D ^{1}H and ^{31}P NMR results tentatively show that the K^{+} forms of all seven analogs appear to form both *syn* and *anti* complexes, but the Na^{+} forms of the analogs with at least one [*S*] sulfur stabilize the *anti* complexes to the exclusion of any *syn* complexes. 2D NOSEY spectra were acquired for all samples to obtain direct evidence for their *syn*/*an*ti conformation.

2D NOSEY spectra of all seven analogs in the Na^{+} form are illustrated in **Figure 3-32** through **Figure 3-38**, all at 30 °C, with the exception of the [*S, S*] dithioate and the [*S*] trithioate analogs, which are at 45 °C. 1D spectra are shown across the top and the side of the 2D plots. No detectable cross peaks are observed in the H8/H1' region for any of the Na^{+} form analogs, except the [*R*] mono- and the [*R, R*] dithiophosphate. Expanded sections of the H8/H1' region for these two analogs are shown in **Figures 3-32** and **3-34**. According to the literature, strong H8/H1' cross peaks are observed for *syn* conformations of the glycosidic bond, and much weaker cross peaks for *anti* conformations. The lack of strong cross peaks in the H8/H1' region for all Na^{+} form analogs with at least one sulfur in the [*S*] configuration confirms the tentative conclusion described earlier for the 1D ^{1}H and ^{31}P NMR. Thus, the presence of one or two sulfurs in

the [S] position results in special stabilization for the all-*anti* higher order complexes and/or destabilization of the all-*syn* complexes. Since the [R] monothioate and [R, R] dithioate have no sulfurs in the [S] position, they form both all-*syn* and all-*anti* complexes.

2D NOSEY spectra of all seven analogs in the K$^+$ form are illustrated in **Figure 3-39** through **Figure 3-45**, with the corresponding H8/H1' sections expanded. These expanded regions demonstrate that in all the K$^+$ form analogs, there are at least two strong H8/H1' cross peaks. For example, in the [R] monothioate analog (**Figure 3-39**), there are strong H8/H1' cross peaks for the resonances at 7.6 and 7.7 ppm, which reflect different all-*syn* higher order complexes. The much weaker H8/H1' cross peaks at ~ 8.1 ppm reflect all-*anti* complexes. There is no detectable cross peak around 7.8 ppm, previously assigned to the bimolecular structure, which is known to adopt an *anti* conformation. Similarly, the [S] monothioate analog (**Figure 3-40**) shows a strong cross peak for the resonance at ~ 7.7 ppm, showing it reflects an all-*syn* complex, but no cross peaks from 8.0-8.2 ppm, showing that region reflects all-*anti* complex. The other NOESY spectra for the di- and trithiophosphate analogs show very similar patterns, confirming our previous tentative conclusion that all the K$^+$ form analogs exist as both all-*syn* and all-*anti* complexes.

IV2. 2D DOSY of all analogs in Na$^+$ and K$^+$ forms

Diffusion ordered spectroscopy (DOSY) is a new 2D NMR technique, which was first introduced in 1992[24] to obtain information about translational diffusion rates of a

given molecule or mixture. In a DOSY spectrum, NMR chemical shift is displayed in one dimension, and diffusion coefficients (or particle sizes derived from diffusion rates) are displayed in the other dimension. In a mixture of complexes, it is possible to study the supramolecular structures by measuring their translational diffusion coefficients (D), since this property is closely related to the size and shape of the complexes. The self-aggregation of 5'-GMP, involving G-quartet formation and stacking, was studied using 2D DOSY, and the authors were able to obtain information about the aggregate size from diffusion coefficients both for the monomer 5'-GMP and the G-quartet complex.[25] Recently, a DNA base hybrid, named G^C, was studied using 2D DOSY,[26] and the measured diffusion rates were in agreement with ESI-MS data, showing a tetrameric higher order complex in addition to the monomer and dimer.

As discussed in previous sections, all thiophosphates described in this thesis, as well as unmodified c-di-GMP, form higher order complexes due to G-quartet formation. After the 2006 publication of the original 2D NMR of the unmodified c-di-GMP,[20] 2D DOSY spectra of unmodified c-di-GMP in Li^+, Na^+, and K^+ salts were obtained at 30 °C in the Jones's lab using upgraded software and hardware.[27] In addition to the bimolecular structure with a diffusion coefficient of 3.0-4.0, the previously assigned tetramolecular complexes were all seen to have a D of 2.0-2.1, and the octamolecular complexes a D of 1.8-1.9, irrespective of salt. The D values for the tetra- and octamolecular complexes are relatively close, because the octamolecular complex is not twice the size of the tetramolecular complex, but rather consists of two intercalated tetramolecular complexes and is thus more compact. For this reason, no attempt was made to convert diffusion

coefficient to molecular weight. The same DOSY experiments used for the unmodified c-di-GMP were carried out as part of this thesis for all seven thiophosphate analogs, and the results are summarized below.

The 2D DOSY spectra focusing on the H8 region of the Na$^+$ forms of all seven thioate analogs are shown in **Figure 3-46** through **Figure 3-52**. In all Na$^+$ analogs, except for those containing two [*S*] sulfurs ([*S, S*] dithioate and [*S*] trithioate), there are signals with a D of 3.0-4.0, corresponding to the bimolecular structure, and signals with D around 2.0-2.2, previously assigned as unspecified higher order complexes. By comparison to the results for the unmodified c-di-GMP, the higher order complexes in these samples most likely are tetramolecular. In both cases without any [*S*] sulfur ([*R*] monothioate and [*R, R*] dithioate), both *syn* and *anti* tetramolecular complexes are present. In the cases with one [*S*] sulfur, only *anti* complexes are present, as discussed previously. For the [*S, S*] dithioate and [*S*] trithioate, that have two [*S*] sulfurs, there are mainly signals with a D of 1.2-1.6, which are smaller than that of an octamolecular complex. These results are consistent with the presence of large fragment from extensive aggregation previously described for these samples. This aggregation may result from end-to-end stacking of the tetramolecular and/or octamolecular complexes.

The 2D DOSY spectra of the K$^+$ forms of all seven analogs are shown in **Figure 3-53** through **Figure 3-59**. For the samples containing zero or one [*S*] sulfur, the spectra show mostly octamolecular complexes (D around 1.7-1.9), with a small amount of the bimolecular structure in some cases. In all these samples, both *syn* and *anti* octamolecular

complexes are present, as discussed previously. For the [*S, S*] dithio and [*S*] trithio samples, the signals primarily have a D smaller than that of an octamolecular complex, again consistent with the extensive aggregation described previously for these samples.

In summary, 1D ^{1}H and ^{31}P NMR, along with 2D NOSEY and DOSY, were used to characterize seven thiophosphate analogs of c-di-GMP in both Na^+ and K^+ forms. The results demonstrate the dramatic effects of [*S*] sulfurs, as well as the major differences between Na^+ and K^+ forms. Supported by 2D NOESY and DOSY, it is concluded that: 1) in all cases, the presence of an [*S*] sulfur promotes more extensive complex formation than [*R*], illustrated by the smaller percentage of the bimolecular structure in these [*S*] samples (**Table 3-2**); 2) in both K^+ and Na^+ forms, the presence of two sulfurs in the [*S*] position promotes extensive aggregation, forming large aggregates that cannot be observed in the NMR spectra, as well as somewhat smaller aggregates that are still larger than octamolecular complexes; 3) as expected for its stronger stabilization of guanine quartets, K^+ promotes more extensive complex formation than Na^+, resulting in primarily octamolecular complexes in the K^+ forms but tetramolecular complexes in the Na^+ forms; and 4) in all Na^+ cases, the presence of one [*S*] sulfur stabilizes *anti* complexes and/or destabilizes *syn* complexes, excluding the latter.

V. NMR Experimental methods

Instrumentation: All seven thiophosphate analogs were quantified by OD measurement at 260 nm using a Varian Cary 4000. All NMR spectra were acquired on a Varian Inova 500 MHz spectrometer.

^{31}P NMR at low concentration

About 10 OD (0.38 µmol) thioate was dissolved in 700 µL D_2O to give samples with a concentration of ~ 0.5 mM. These solutions were transferred to standard 5 mm NMR tubes. All seven spectra were recorded at 30 °C.

1D ^{1}H and ^{31}P NMR at higher concentration

About 240 OD (9.2 µmol) of all fourteen samples (seven analogs each in Na^+ and K^+ forms) was dissolved in 270 µL H_2O and 30 µL D_2O, to make samples with a concentration of ~ 31 mM. The pH of these samples was adjusted to 6.8 with aqueous HCl and/or either NaOH or KOH. They were then transferred into Shigemi NMR tubes. One day before the NMR acquisition, samples were heated at 60 °C for 30 min, allowed to cool slowly to room temperature, and then placed in a refrigerator overnight. ^{31}P NMR was acquired with a relaxation delay of 1.5 or 2 seconds and referenced to neat phosphoric acid.

2D NOSEY

The same NMR samples from the 1D experiments were used for the 2D experiments. 2D NOSEY spectra were collected at 30 °C (45 °C for [*S, S*] dithio and [*S*] trithio both in Na$^+$ and K$^+$ forms), using 4096 (t2) times 512 (t1) complex data points with spectral widths of 8000 Hz in both dimensions. The relaxation delay for each scan was 2 seconds with a mixing time of 150 ms, and the number of scans per each t1 increment was 16.

2D DOSY

The same higher concentration samples were used for the 2D DOSY experiments. All spectra were acquired at 30 °C, using 20 increments, with a diffusion delay of 0.1 second. The gradient strength was set from 400 to 20,000.

VI. References:

1.   Pinnavaia, T. J., Miles, H. T., and Becker, E. D., "Self-assembled 5'-guanosine monophosphate. Nuclear magnetic resonance evidence for a regular, ordered structure and slow chemical exchange" *J. Am. Chem. Soc*, **1975**, 97, 7198-7200

2.   Pinnavaia, T. J., Marshall, C. L., Mettler, C. M., Fisk, H. T., Miles, H. T., and Becker, E. D., "Alkali metal ion specificity in the solution ordering of a nucleotide, 5'-guanosine monophosphate" *J. Am. Chem. Soc*, **1978**, 100, 3625-3627

3.   Smith, F. W. and Feigon, J., "Quadruplex structure of Oxytricha telomeric DNA oligonucleotides" *Nature (London)*, **1992**, 356, 164-168

4.   Smith, F. W. and Feigon, J., "Strand orientation in the DNA quadruplex formed from the Oxytricha telomere repeat oligonucleotide d(G4T4G4) in solution" *Biochemistry*, **1993**, 32, 8682-8692

5.   Baranick, J., Kinas, R. W., Lesiak, K., and Stec, W. J., "Stereospecific synthesis of adenosine 3',5'-(Sp)- and -(Rp)-cyclic phosphorothioates (cAMPs)" *Journal of the Chemical Society, Chemical communications*, **1979**, 940-941

6.   Ross, P., Mayer, R., Weinhouse, H., Amikam, D., Huggirat, Y., Benziman, M., Vroom, E. d., Fidder, A., Paus, P. d., Sliedregt, L. A. J. M., Marel, G. A. v. d., and Boom, J. H. v., "The cyclic diguanylic acid regulatory system of cellulose synthesis in *Acetobacter xylinum*. Chemical synthesis and biological activity of cyclic nucleotide dimer, trimer, and phosphothioate derivatives" *J. Biol. Chem.*, **1990**, 265, 18933-18943

7.   Almer, H., Stawinski, J., Stromberg, R., and Thelin, M., "Synthesis of diribonucleoside phosphorothioates via stereospecific sulfurization of H-phosphonate diesters" *J. Org. Chem.*, **1992**, 57, 6163-6169

8.   Zhang, X., Gaffney, B. L., and Jones, R. A., "^{15}N NMR of a specifically labeled RNA fragment containing intrahelical GU wobble pairs" *J. Am. Chem. Soc.*, **1997**, 119, 6432-6433

9.   Wang, G., Gaffney, B. L., and Jones, R. A., "Differential binding of Mg^{2+}, Zn^{2+}, and Cd^{2+} at two sites in a hammerhead ribozyme motif, determined by ^{15}N NMR" *J. Am. Chem. Soc.*, **2004**, 126, 8908-8909

10. Battistini, C., Fustinoni, S., Brasca, M. G., and Borghi, D., "Stereoselective synthesis of cyclic dinucleotide phosphorothioates" *Tetrahedron*, **1993**, 49, 1115-1132

11. Evans, F. E. and Kaplan, N. O., "Probing the sensitivity of ^{31}P NMR chemical shifts to hydrogen bonding and to stereochemistry" *FEBS Lett.*, **1979**, 105, 11-14

12. Evans, F. E. and Wright, J. M., "Proton and phosphorus-31 nuclear magnetic resonance study on the stabilization of the *anti* conformation about the glycosyl bond of 8-alkylamino adenyl nucleotides" *Biochemistry*, **1980**, 19, 2113-2117

13. Lee, C. H., Evans, F. E., and Sarma, R. H., "Interrelation between glycosidic torsion, sugar pucker, and backbone conformation in 5'-β-nucleotides" *J. Biol. Chem.*, **1975**, 250, 1290-1296

14. Bouhoutsos-Brown, E., Marshall, C. L., and Pinnavaia, T. J., "Structure-directing properties of Na^+ in the solution ordering of guanosine 5'-monophosphate. Stoichiometry of aggregation, binding to ethidium, and modes of Na^+ complexation" *J. Am. Chem. Soc.*, **1982**, 104, 6576-6584

15. Marlow, A. L., Mezzina, E., Spada, G. P., Masiero, S., Davis, J. T., and Gottarelli, G., "Cation-templated self-assembly of a lipophilic deoxyguanosine: Solution structure of a K^+-dG_8 octamer" *J. Org. Chem.*, **1999**, 64, 5116-5123

16. Detellier, C. D. and Laszlo, P., "Role of alkali metal and ammonium cations in the self-assembly of 5'-guanosine monophosphate dianion" *J. Am. Chem. Soc*, **1980**, 102, 1135-1141

17. Phan, A. T. and Patel, D. J., "Two-repeat human telomeric d(TAGGGTTAGGGT) sequence forms interconverting parallel and antiparallel G-quadruplexes in solution: Distinct topologies thermodynamic properties, and folding/unfolding kinetics" *J. Am. Chem. Soc.*, **2003**, 125, 15021-15027

18. Dias, E., Battiste, L., and Williamson, J. R., "Chemical probe for glycosidic conformation in telomeric DNAs" *J. Am. Chem. Soc.*, **1994**, 116, 4479-7780

19. Wang, K. Y., McCurdy, S., Shea, R. G., Swaminathan, S., and Bolton, P. H., "A DNA aptamer which binds to and inhibits thrombin exhibits a new structural motif for DNA" *Biochemistry*, **1993**, 32, 1899-1904

20. Zhang, Z., Kim, S., Gaffney, B. L., and Jones, R. A., "Polymorphism of signaling molecule c-di-GMP" *J. Am. Chem. Soc*, **2006**, 128, 7015-7024

21. Zhang, Z., Gaffney, B. L., and Jones, R., "c-di-GMP displays a monovalent metal ion-dependent polymorphism" *J. Am. Chem. Soc*, **2004**, 126, 16700-16701

22. Williamson, J. R., "Guanine quartets" *Curr. Opin. Struct. Biol.*, **1993**, 3, 357-362

23. Williamson, J. R., Raghuraman, M. K., and Cech, T. R., "Monovalent cation-induced structure of telomeric DNA: The G-quartet model" *Cell*, **1989**, 59, 871-880

24. Morris, K. F. and Johnson, C. S., Jr., "Diffusion-ordered two-dimensional nuclear magnetic resonance spectroscopy" *J. Am. Chem. Soc.*, **1992**, 114, 3139-3141

25. Wong, A., Ida, R., Spindler, L., and Wu, G., "Disodium guanosine 5'-monophosphate self-associates into nanoscale cylinders at pH 8: A combined diffusion NMR spectroscopy and dynamic light scattering study" *J. Am. Chem. Soc.*, **2005**, 127, 6990-6998

26. Asadi, A., Patrick, B. O., and Perrin, D. M., "G^C quartet - a DNA-inspired Janus-GC heterocycle: Synthesis, structural analysis, and self-organization" *J. Am. Chem. Soc.*, **2008**, 130, 12860-12861

27. Veliath, E., Zhang, Z., Gaffney, B. L., and Jones, R. A., unpublished data

Appendix
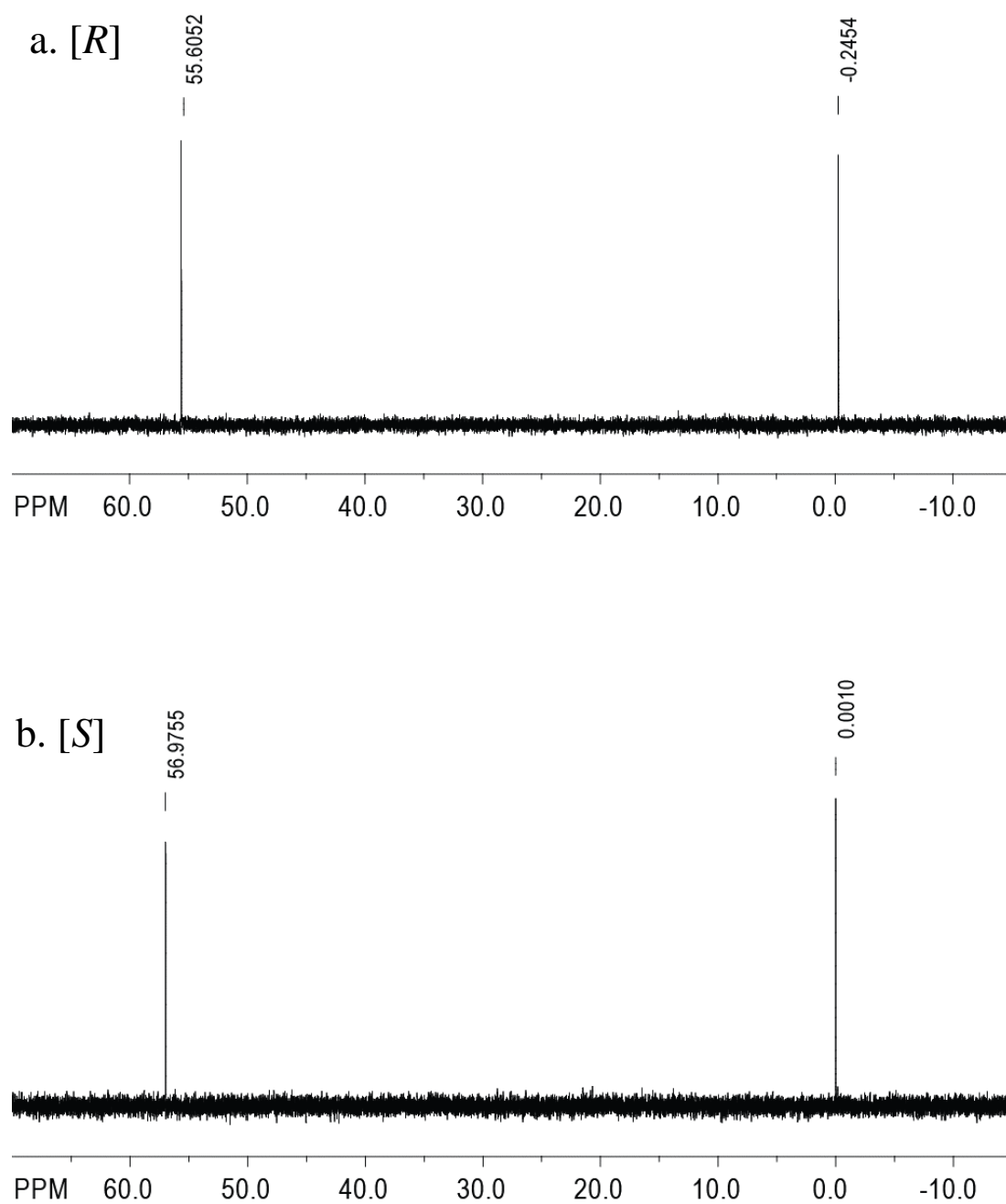
Figure 3-1. ^{31}P NMR of the two diastereomers of monothioate c-di-GMP at 0.5 mM
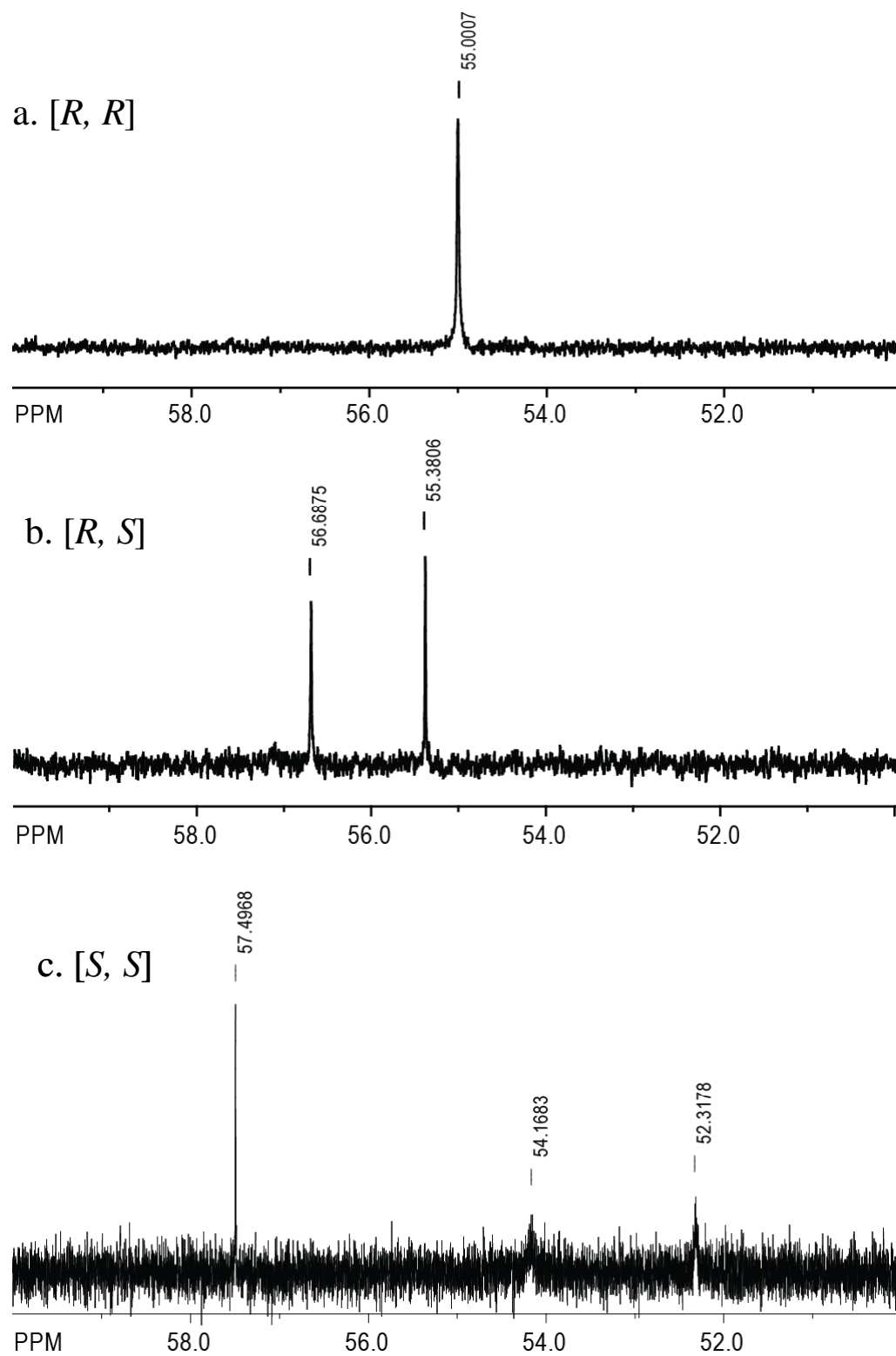
Figure 3-2. ^{31}P NMR of the three diastereomers of dithioate c-di-GMP at 0.5 mM
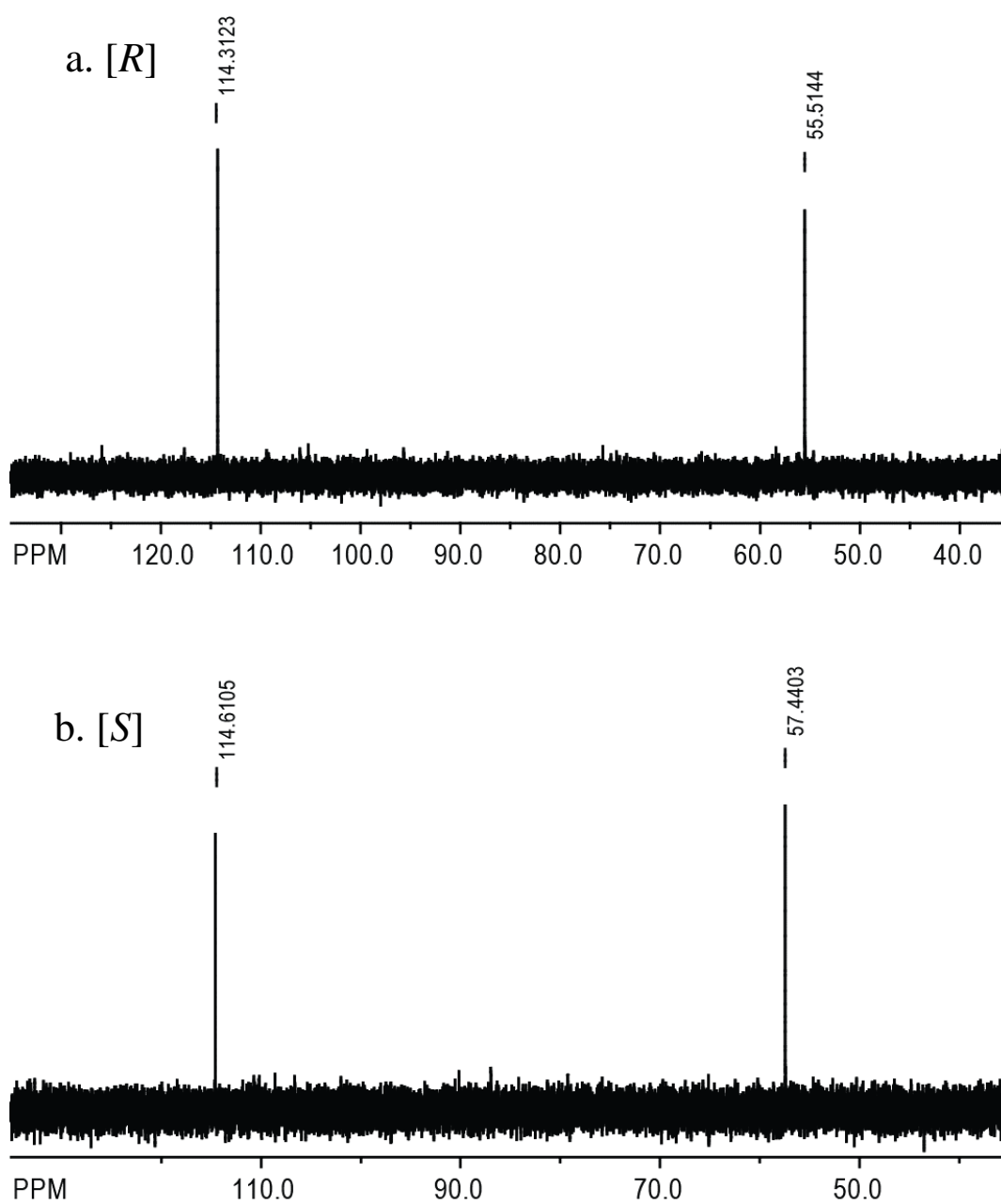
Figure 3-3. ^{31}P NMR of the two diastereomers of trithioate c-di-GMP at 0.5 mM
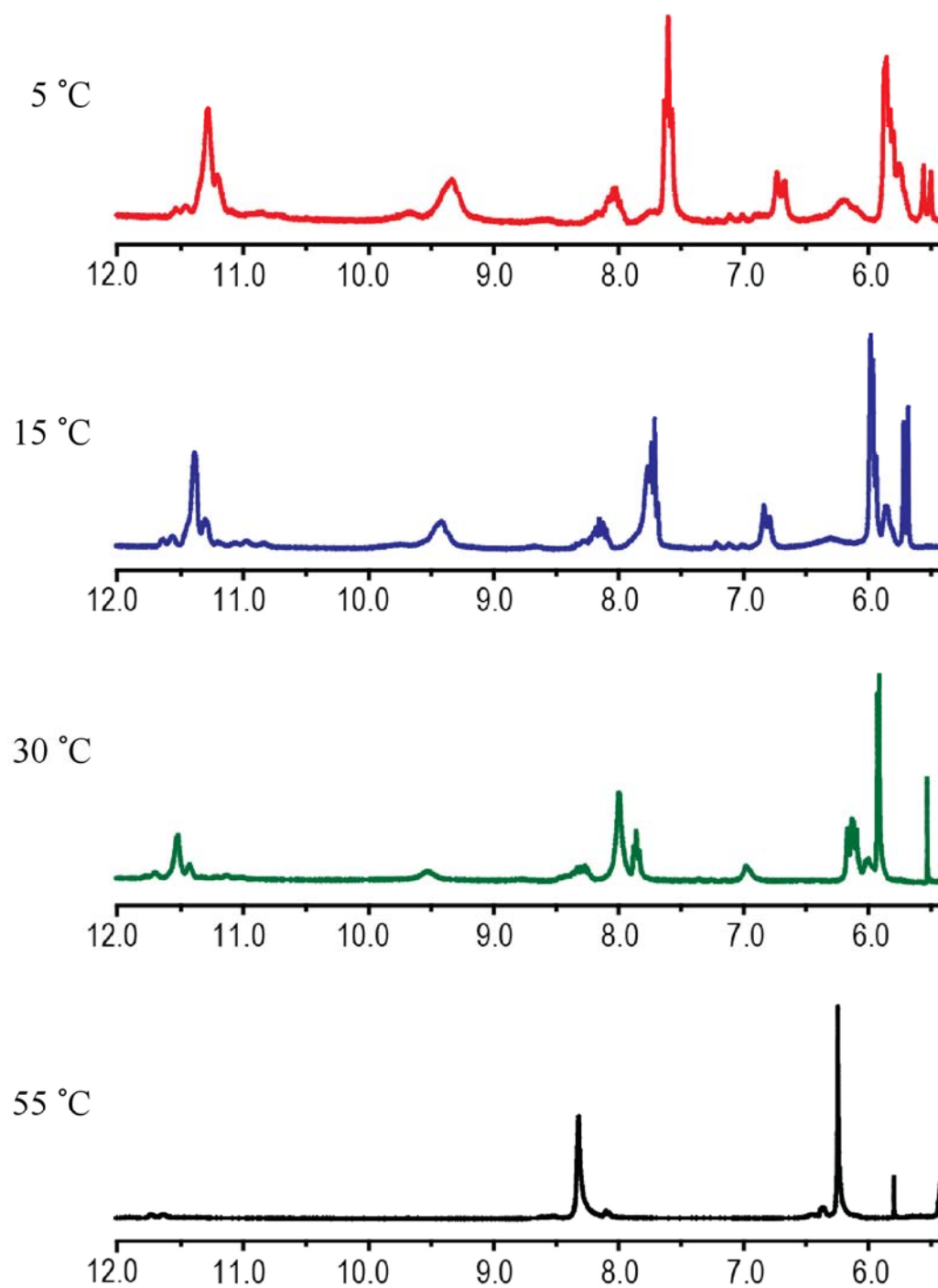
Figure 3-4. ^{1}H NMR of [*R*] monothiophosphate c-di-GMP in Na^{+} form
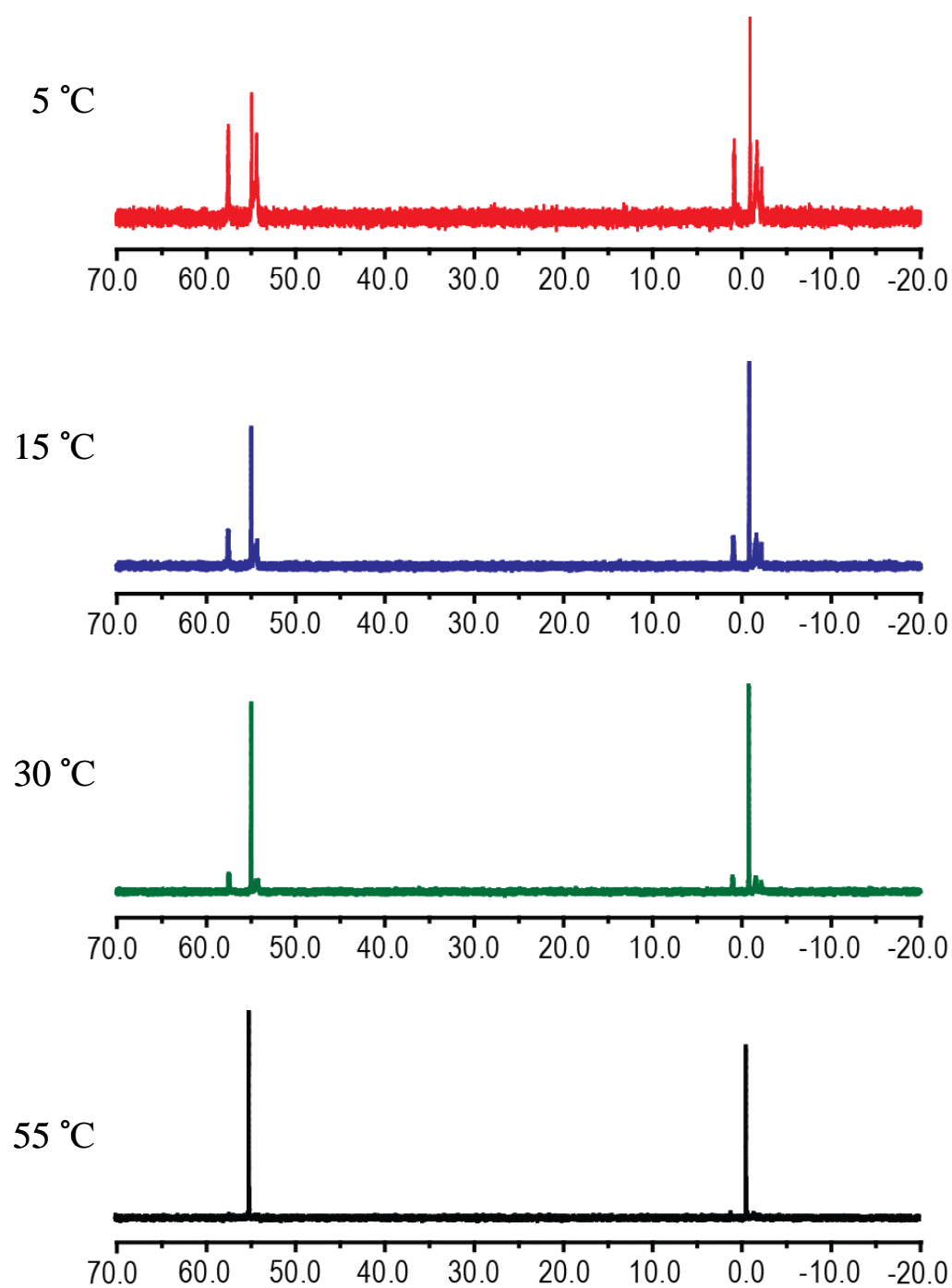
Figure 3-5. ^{31}P NMR of [*R*] monothiophosphate c-di-GMP in Na$^+$ form
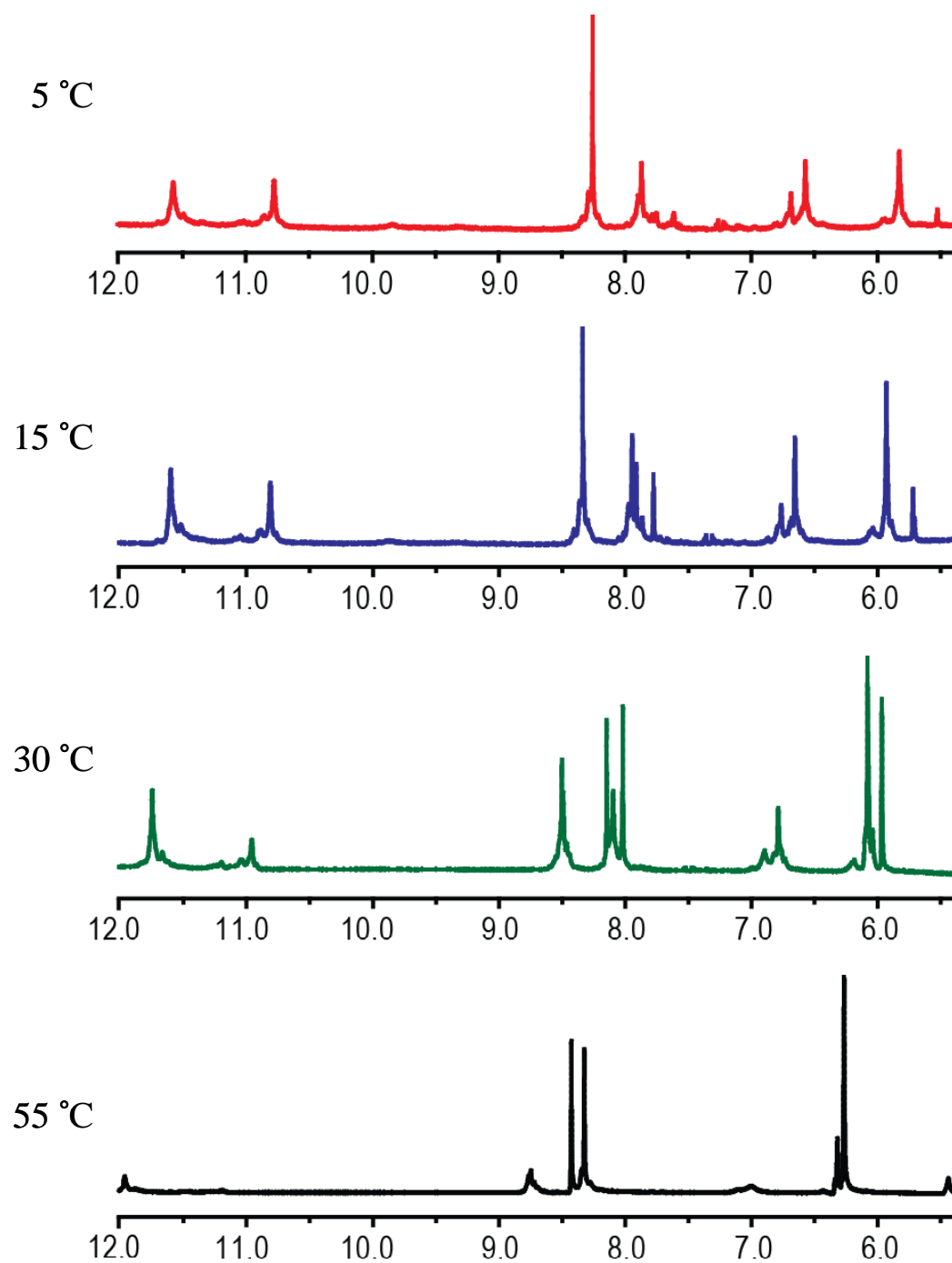
Figure 3-6 . ^{1}H NMR of [*S*] monothiophosphate c-di-GMP in Na^{+} form
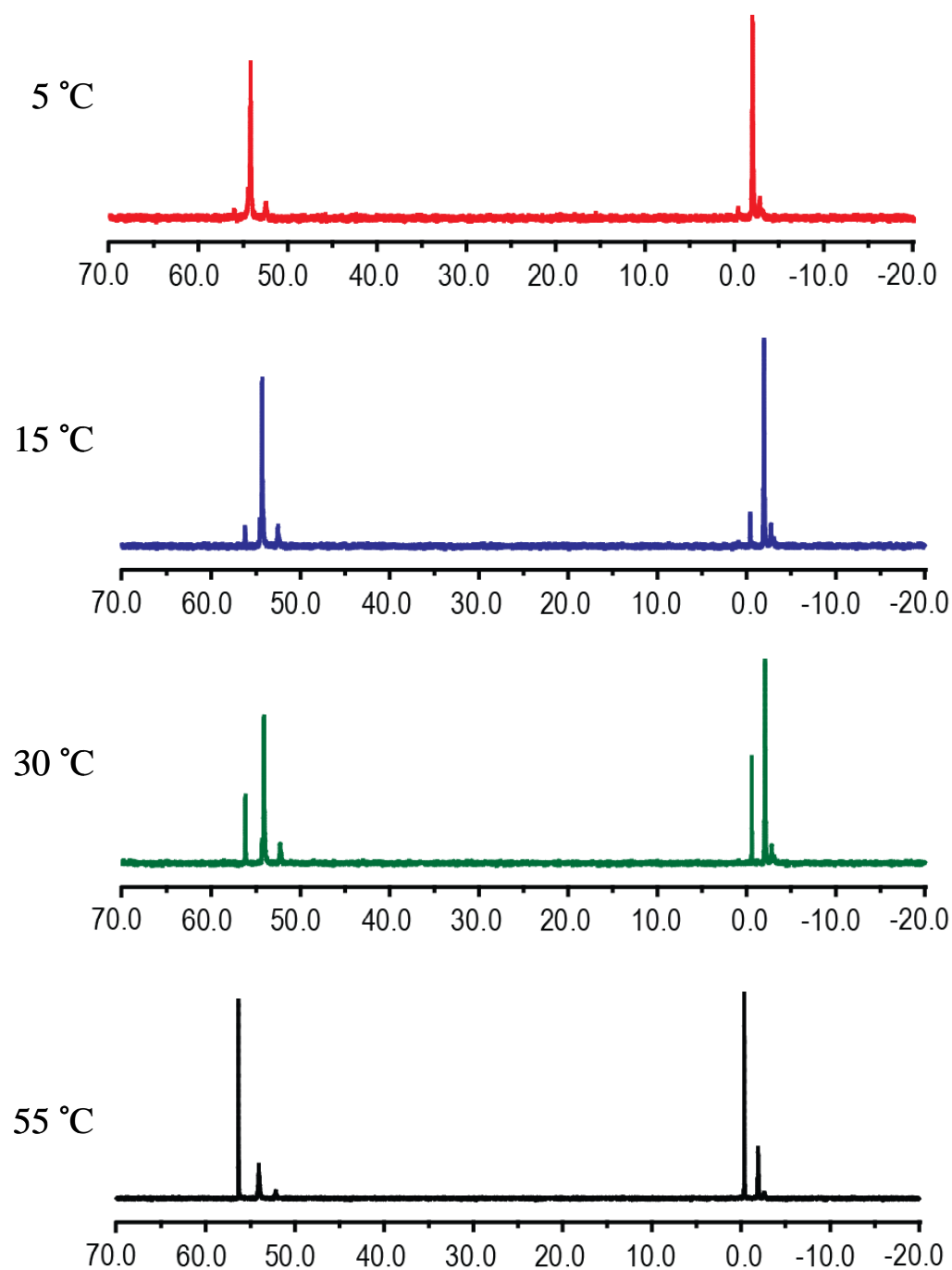
Figure 3-7 . ^{31}P NMR of [*S*] monothiophosphate c-di-GMP in Na$^+$ form

5 ℃

15 ℃

30 ℃

55 ℃
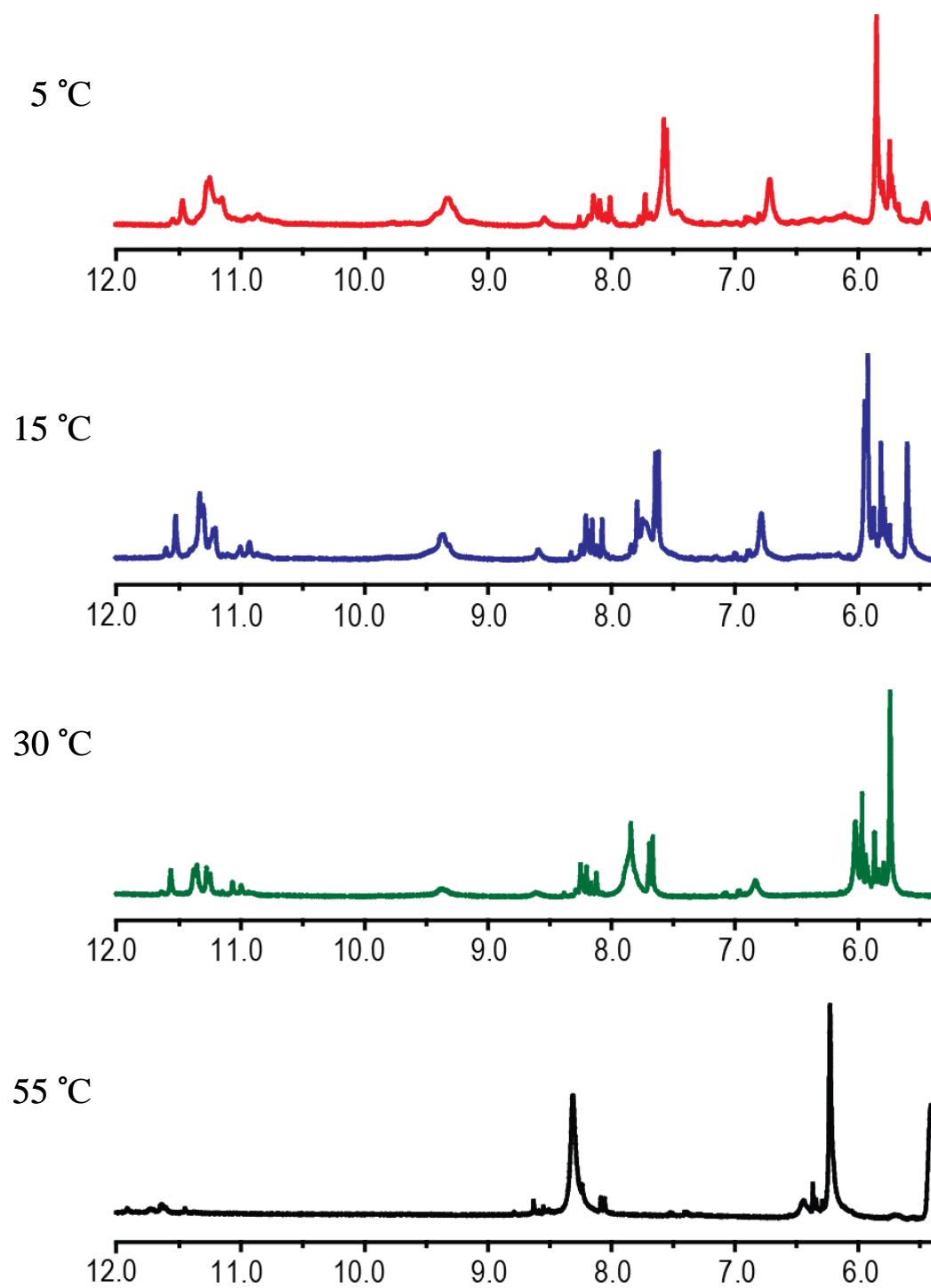
Figure 3-8 . ^{1}H NMR of [*R, R*] dithiophosphate c-di-GMP in Na^{+} form
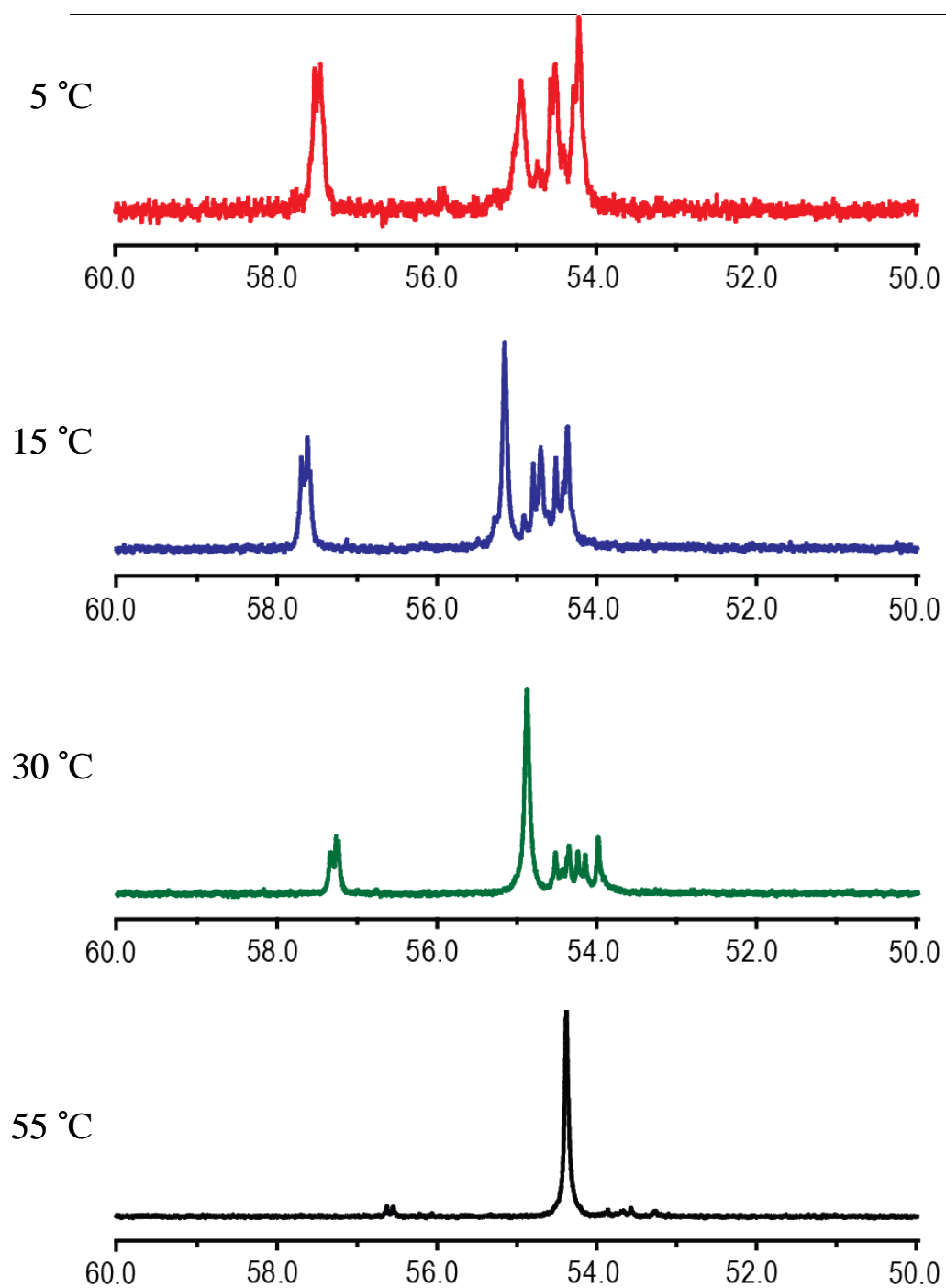
Figure 3-9 . ^{31}P NMR of [*R, R*] dithiophosphate c-di-GMP in Na^{+} form
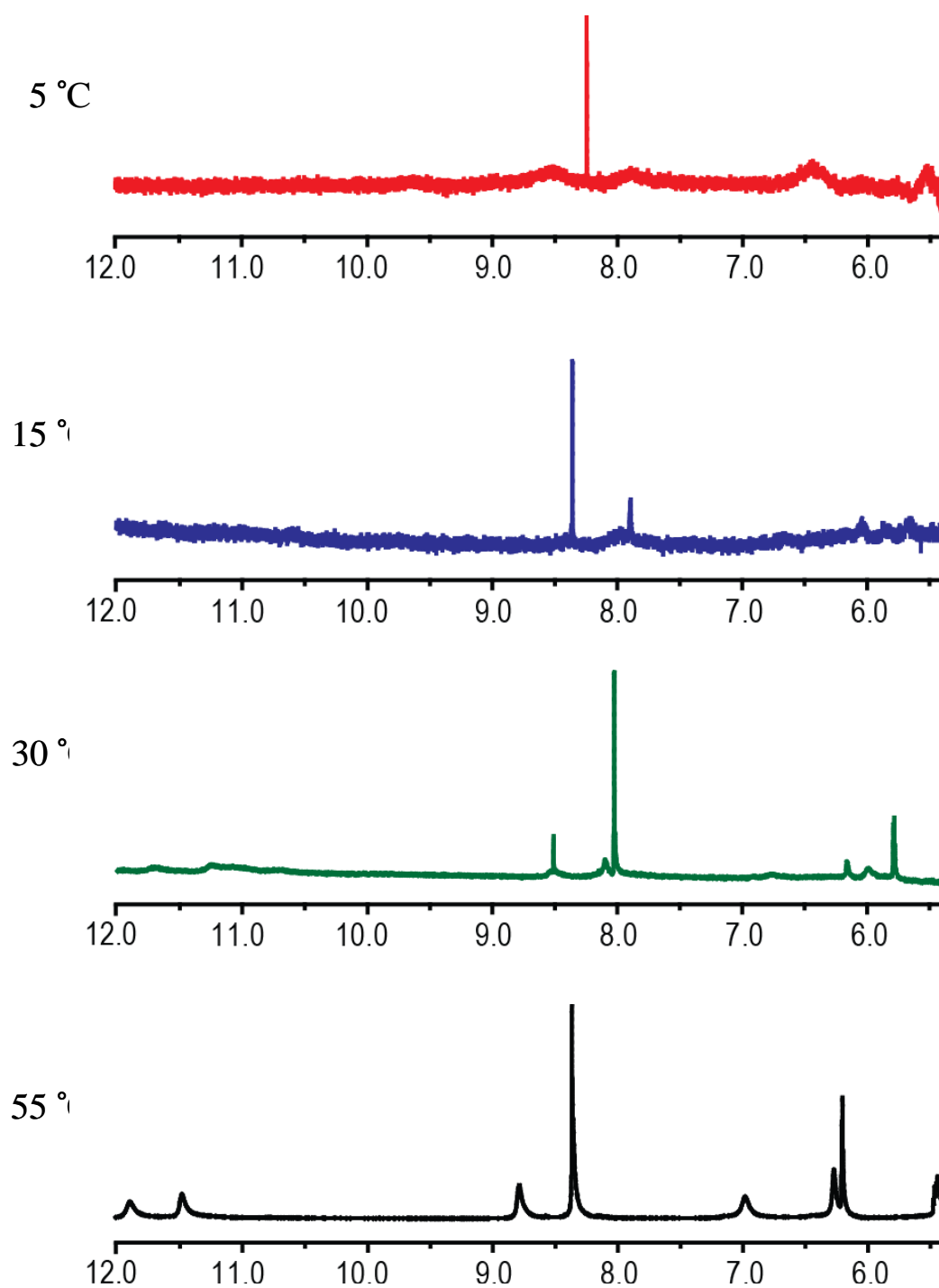
Figure 3-10 . ^{1}H NMR of [*S, S*] dithiophosphate c-di-GMP in Na^{+} form
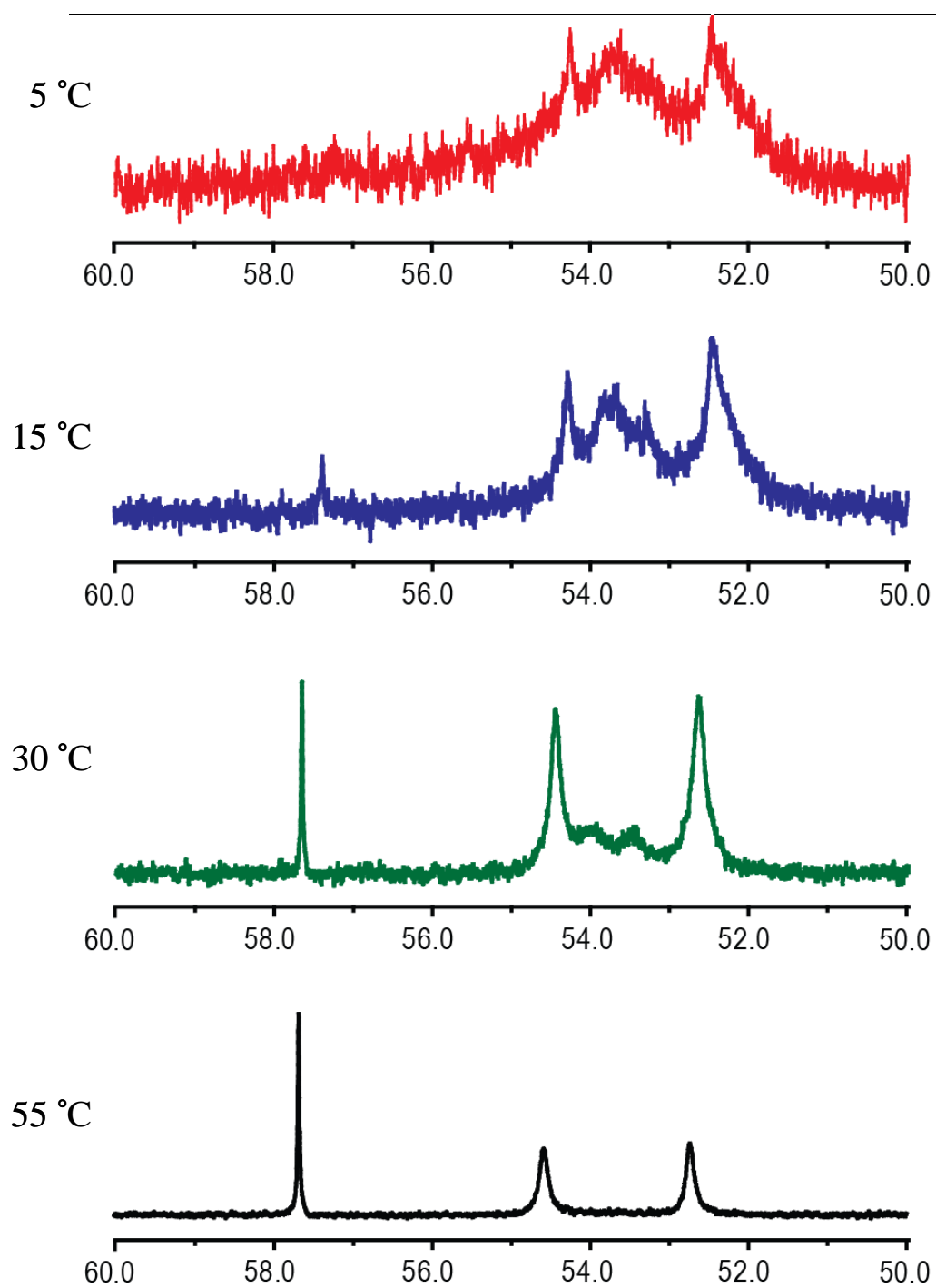
Figure 3-11 . ^{31}P NMR of [*S, S*] dithiophosphate c-di-GMP in Na^{+} form
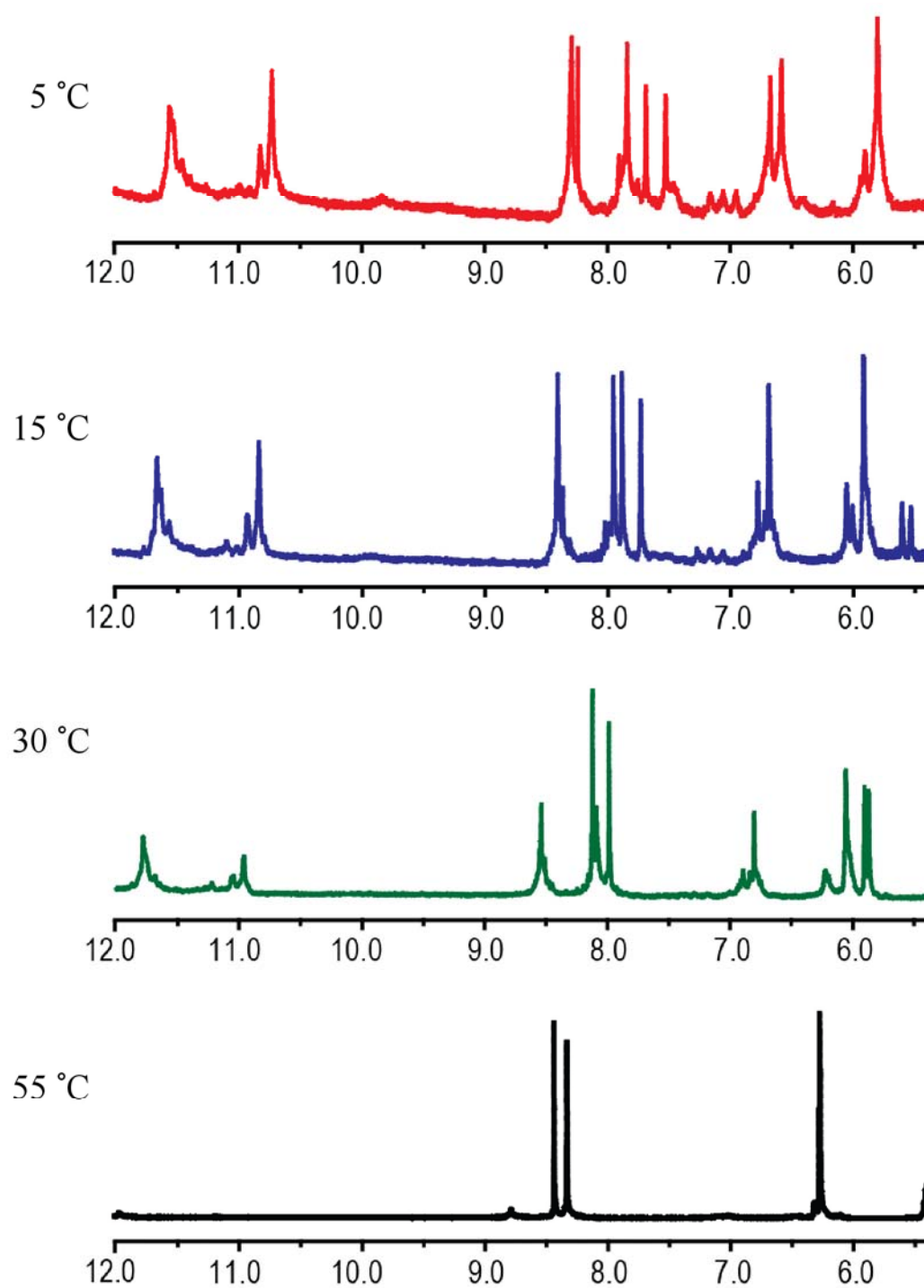
Figure 3-12 . ^{1}H NMR of [*R, S*] dithiophosphate c-di-GMP in Na^{+} form
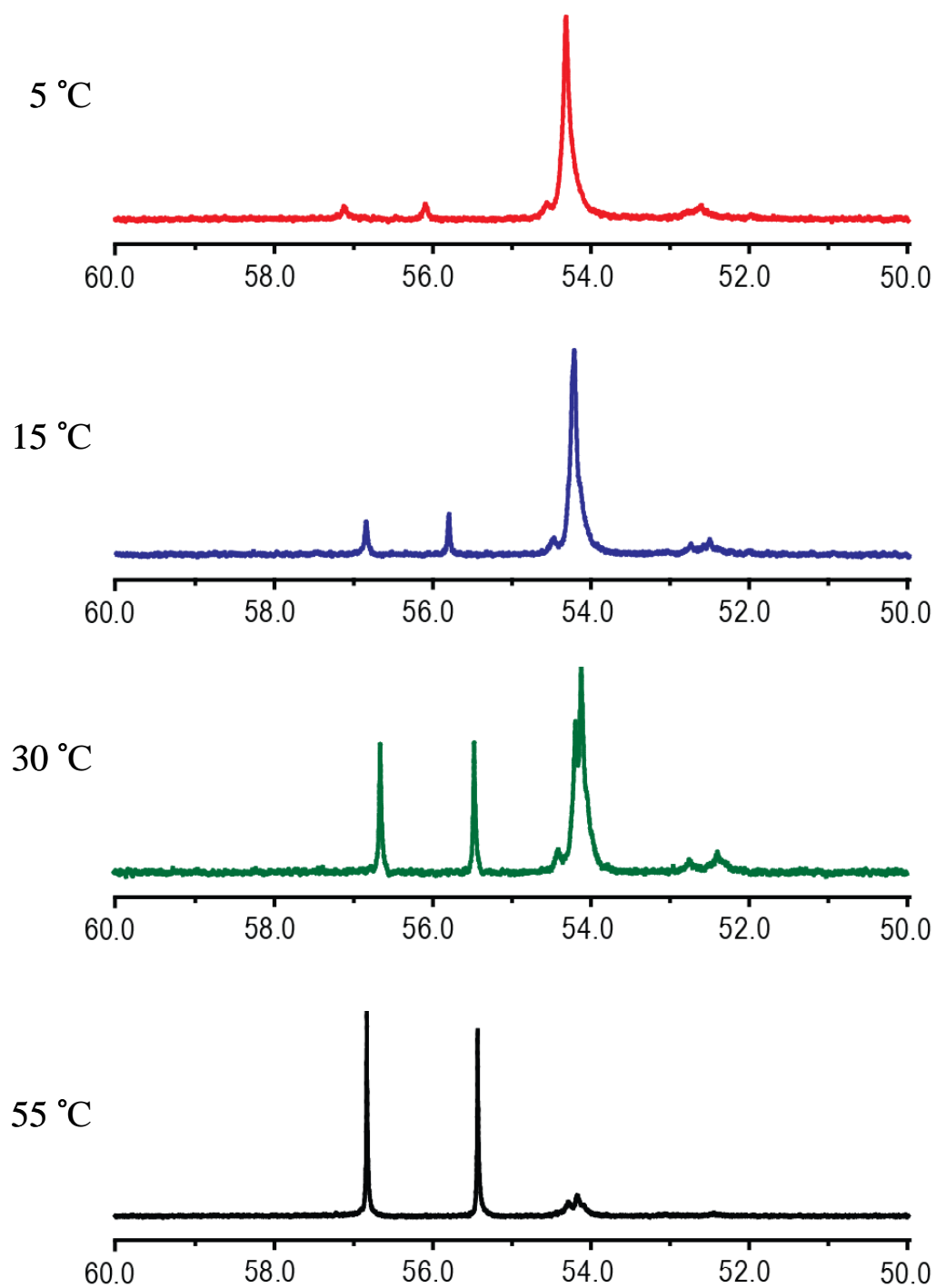
Figure 3-13 . ^{31}P NMR of [*R, S*] dithiophosphate c-di-GMP in Na^{+} form

5 °C

15 °

30 °

55 °

12.0 11.0 10.0 9.0 8.0 7.0 6.0
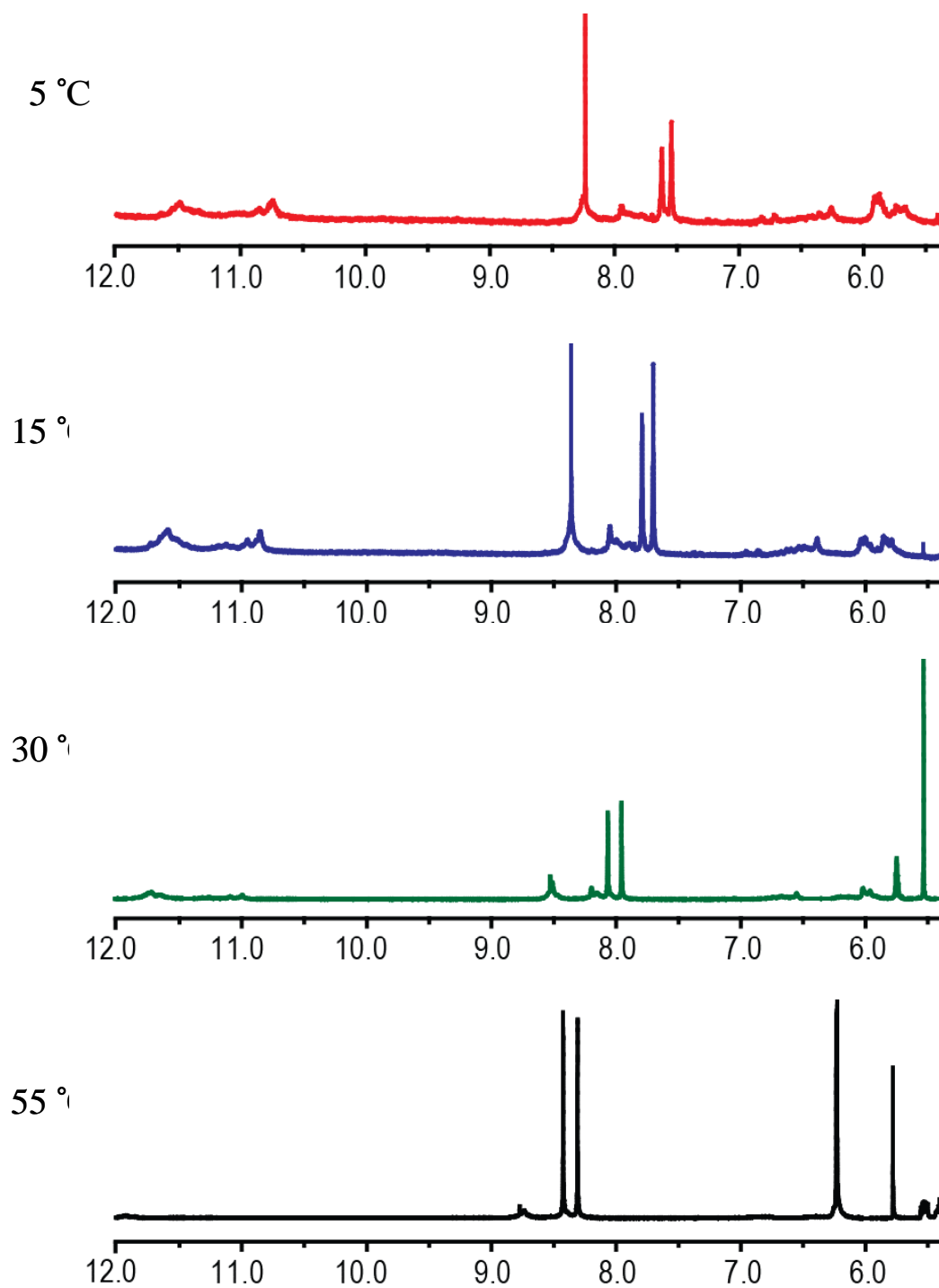
Figure 3-14 . ^{1}H NMR of [*R*] trithiophosphate c-di-GMP in Na^{+} form
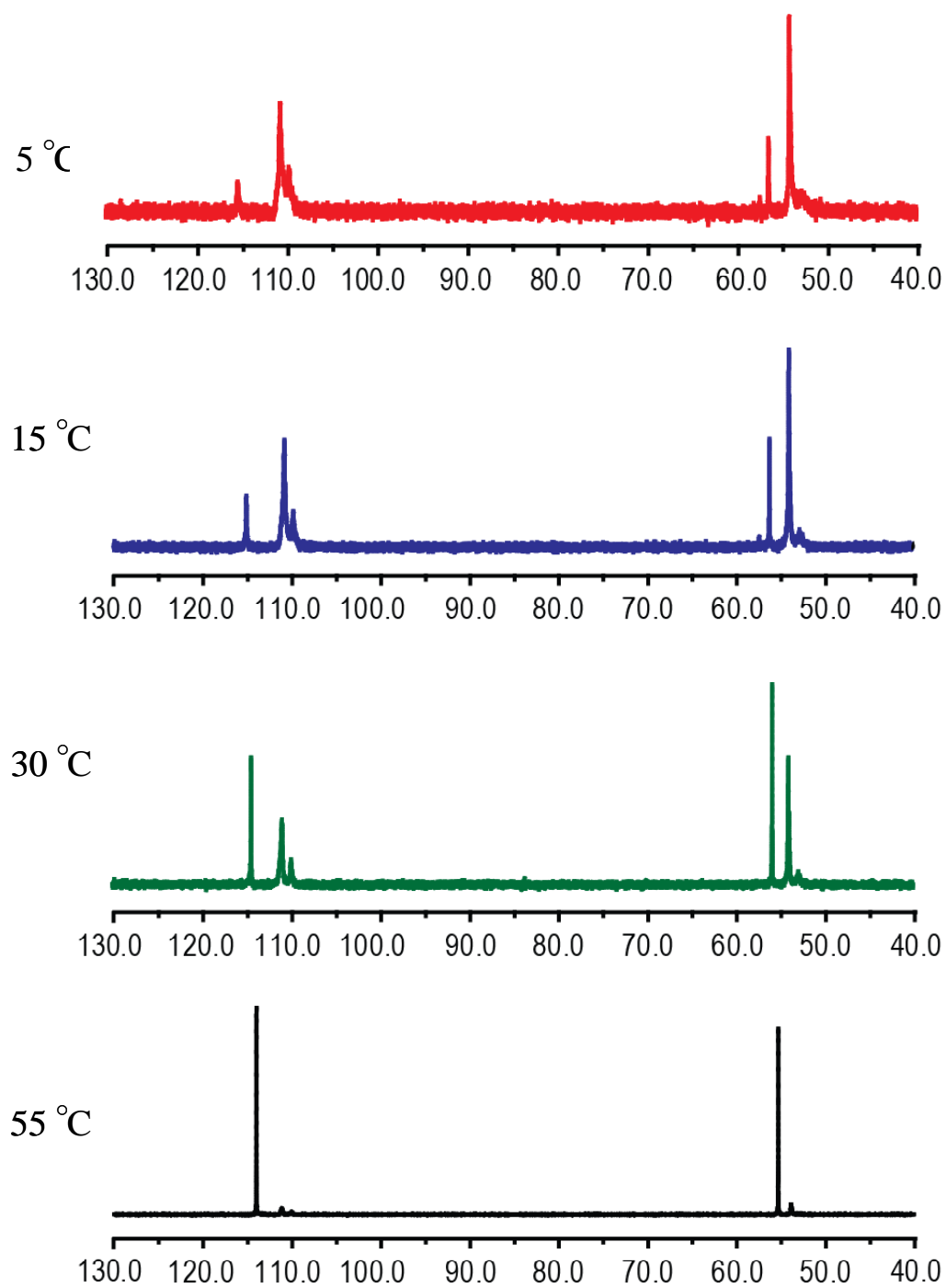
Figure 3-15 . ^{31}P NMR of [*R*] trithiophosphate c-di-GMP in Na$^+$ form
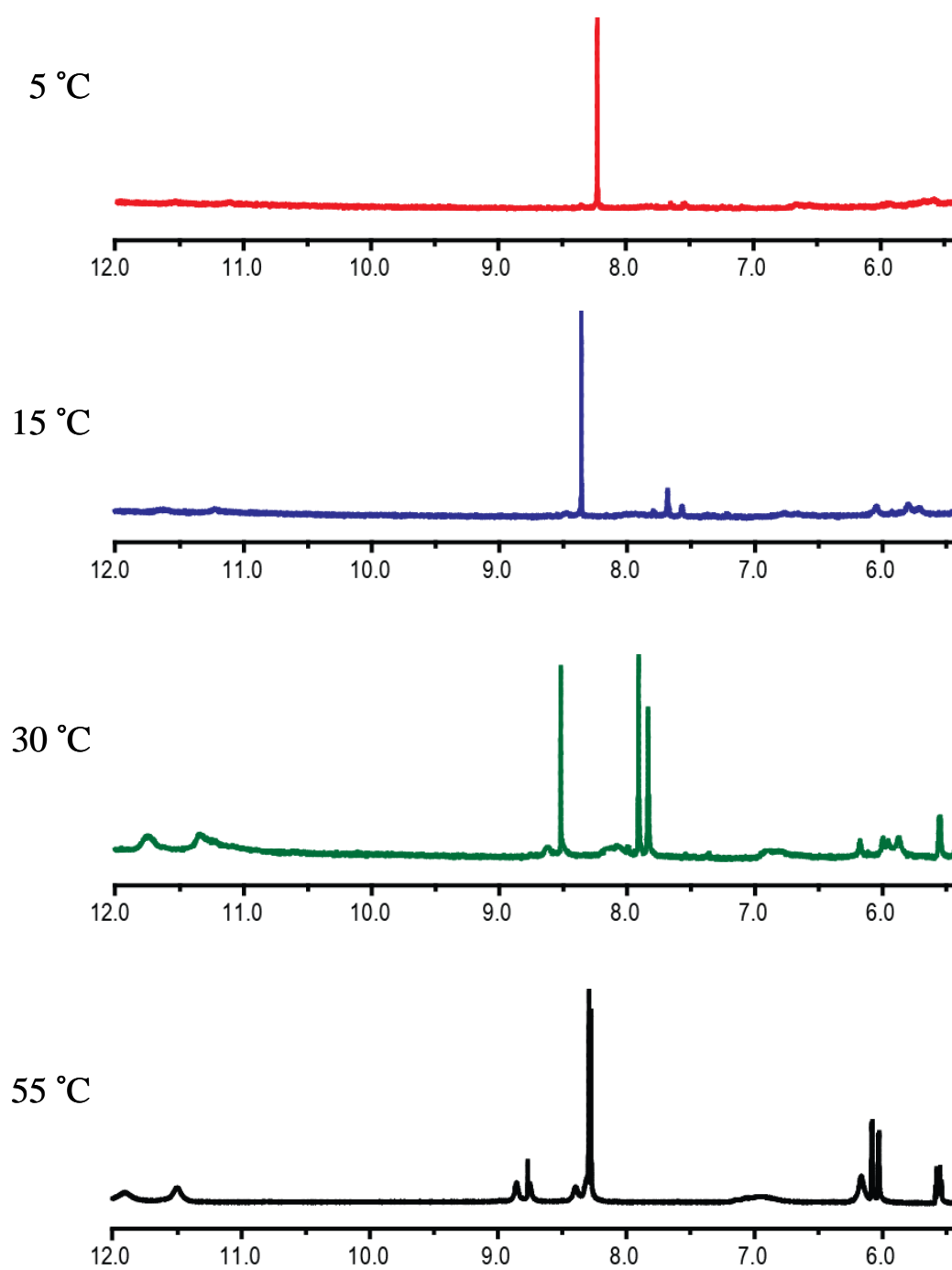
Figure 3-16 . ^{1}H NMR of [*S*] trithiophosphate c-di-GMP in Na^{+} form
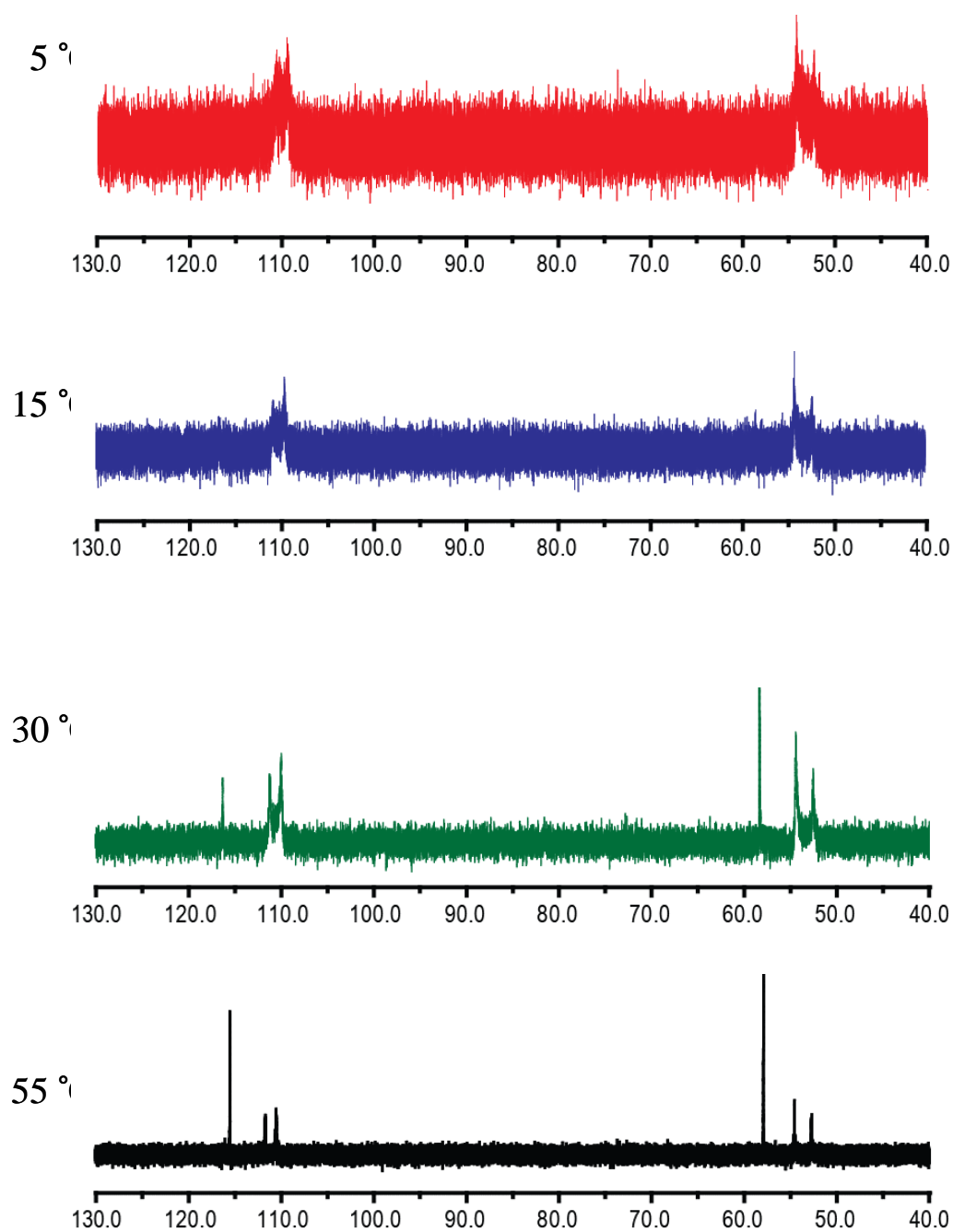
Figure 3-17 . ^{31}P NMR of [*S*] trithiophosphate c-di-GMP in Na$^+$ form
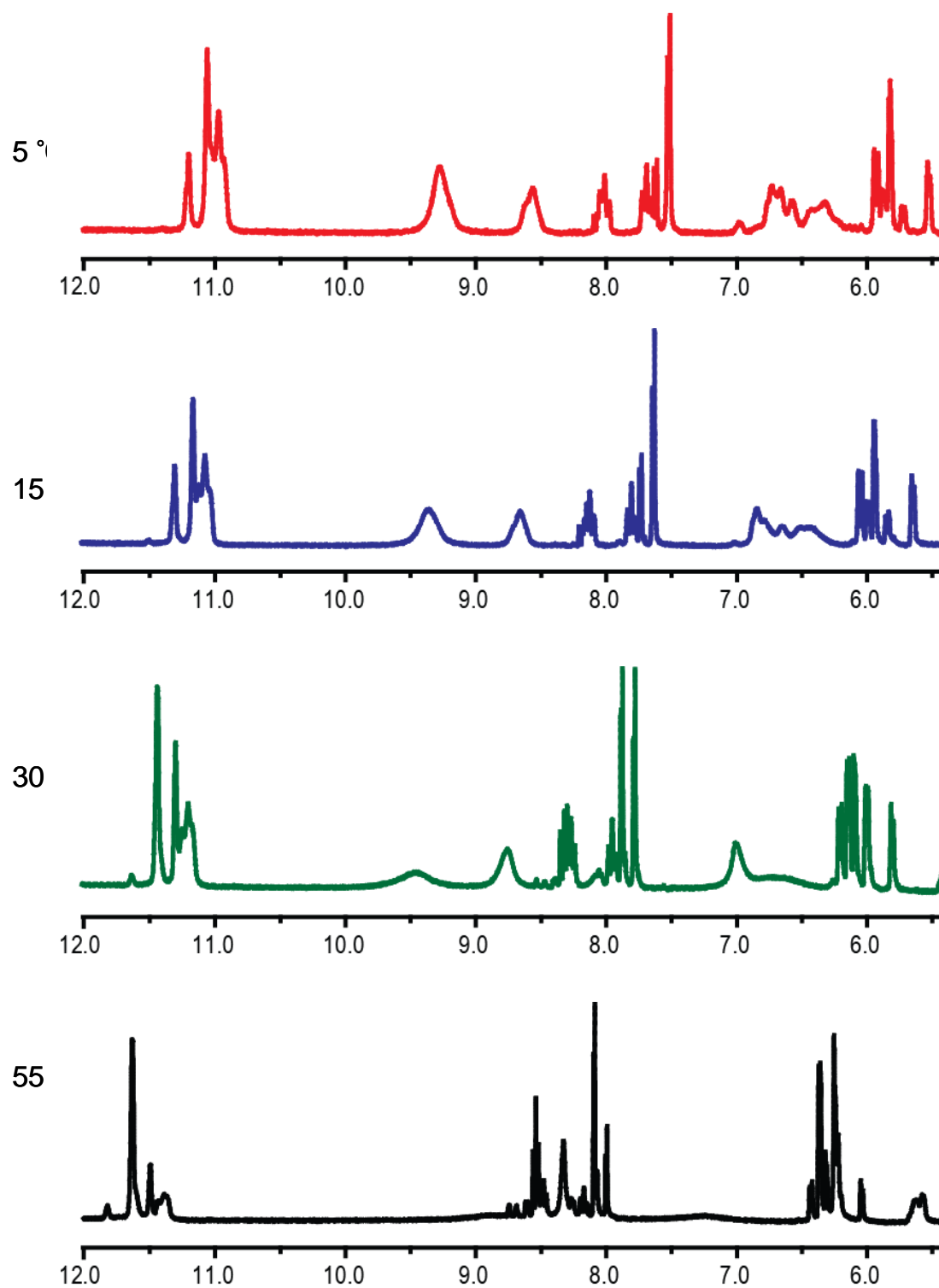
Figure 3-18 . ^{1}H NMR of [*R*] monothiophosphate c-di-GMP in K^{+} form
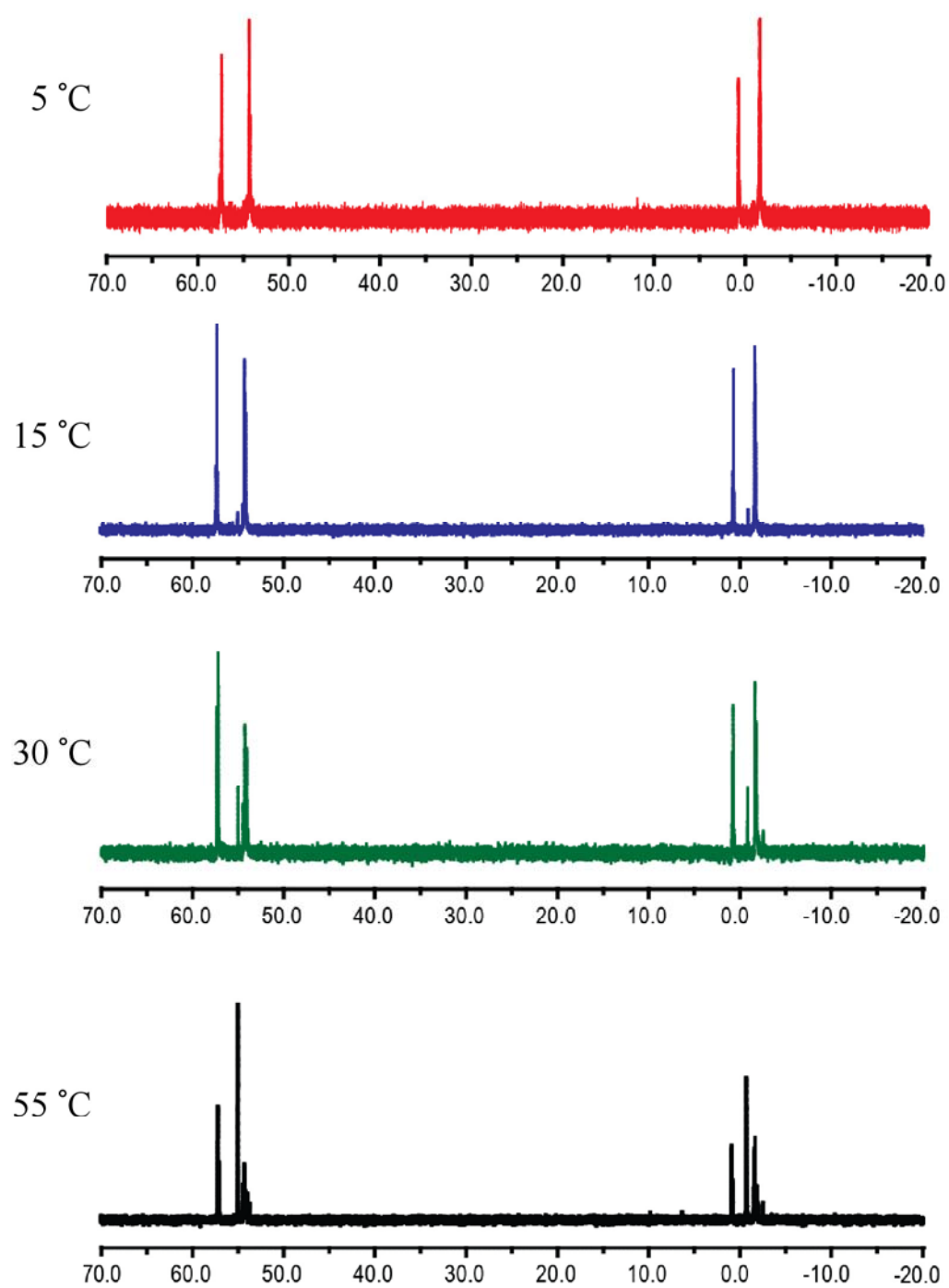
Figure 3-19 . ^{31}P NMR of [*R*] monothiophosphate c-di-GMP in K$^+$ form

5 °(

15

30

55
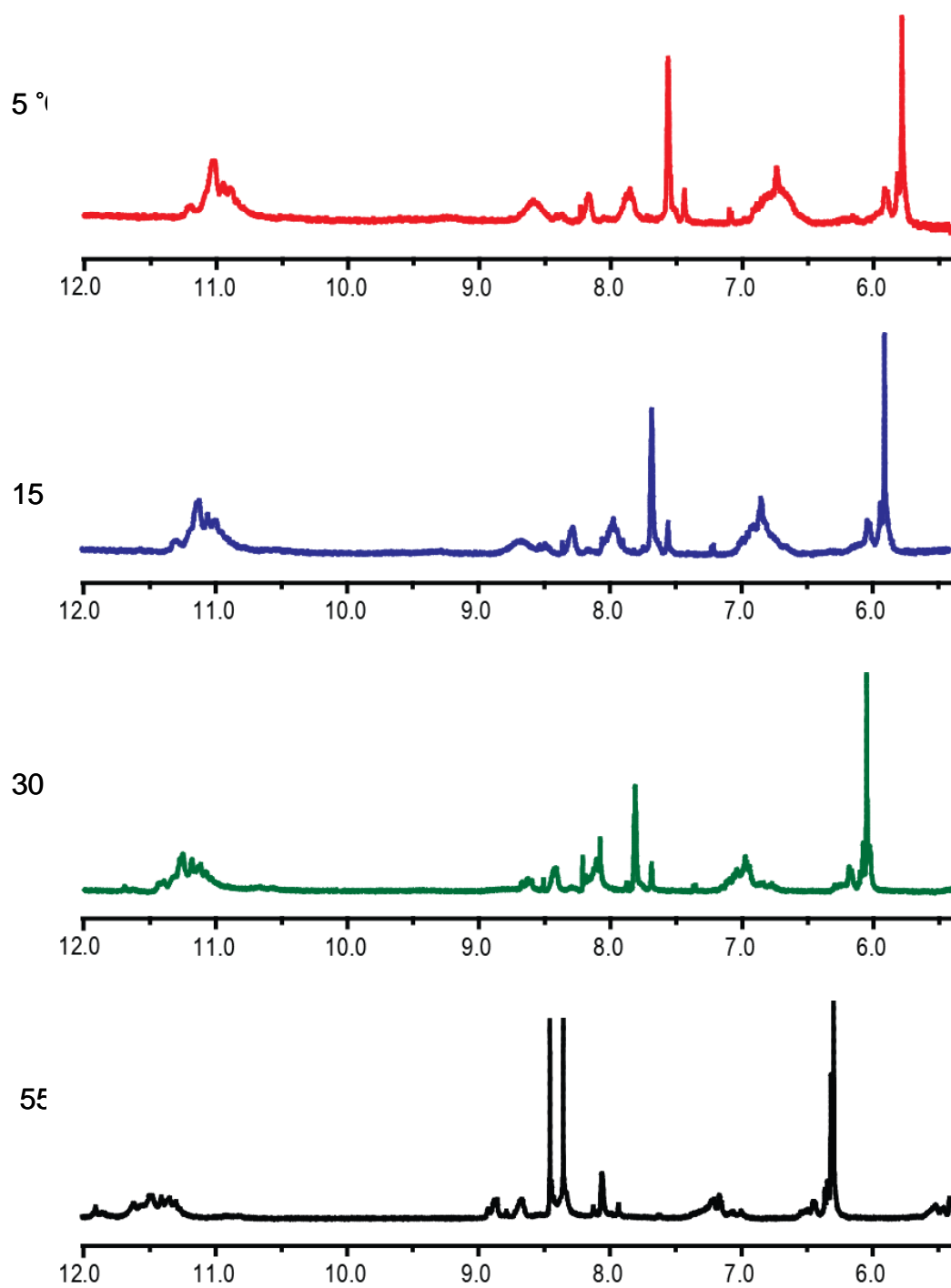
Figure 3-20 . ^{1}H NMR of [*S*] monothiophosphate c-di-GMP in K^{+} form
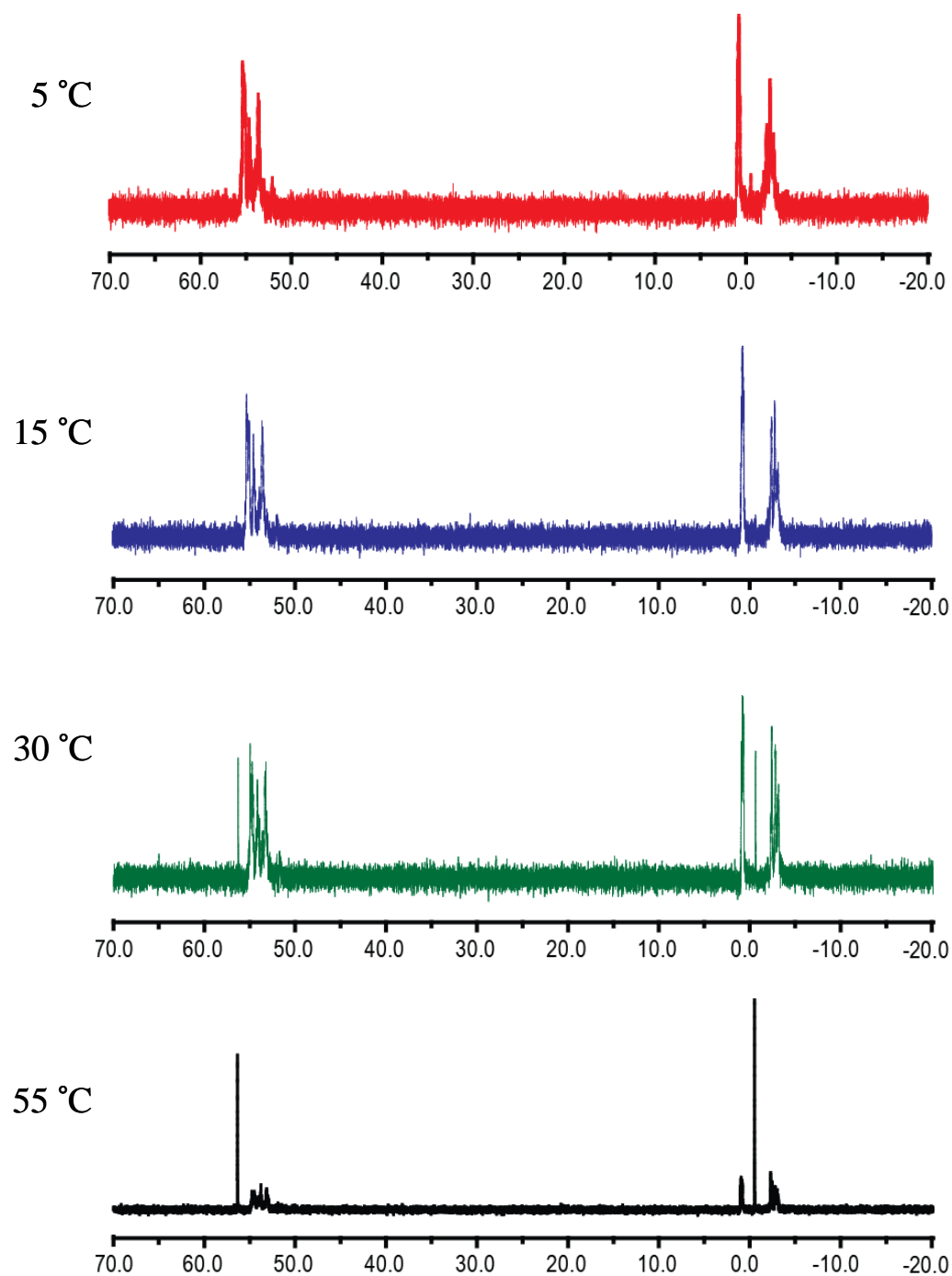
Figure 3-21 . ^{31}P NMR of [*S*] monothiophosphate c-di-GMP in K^{+} form
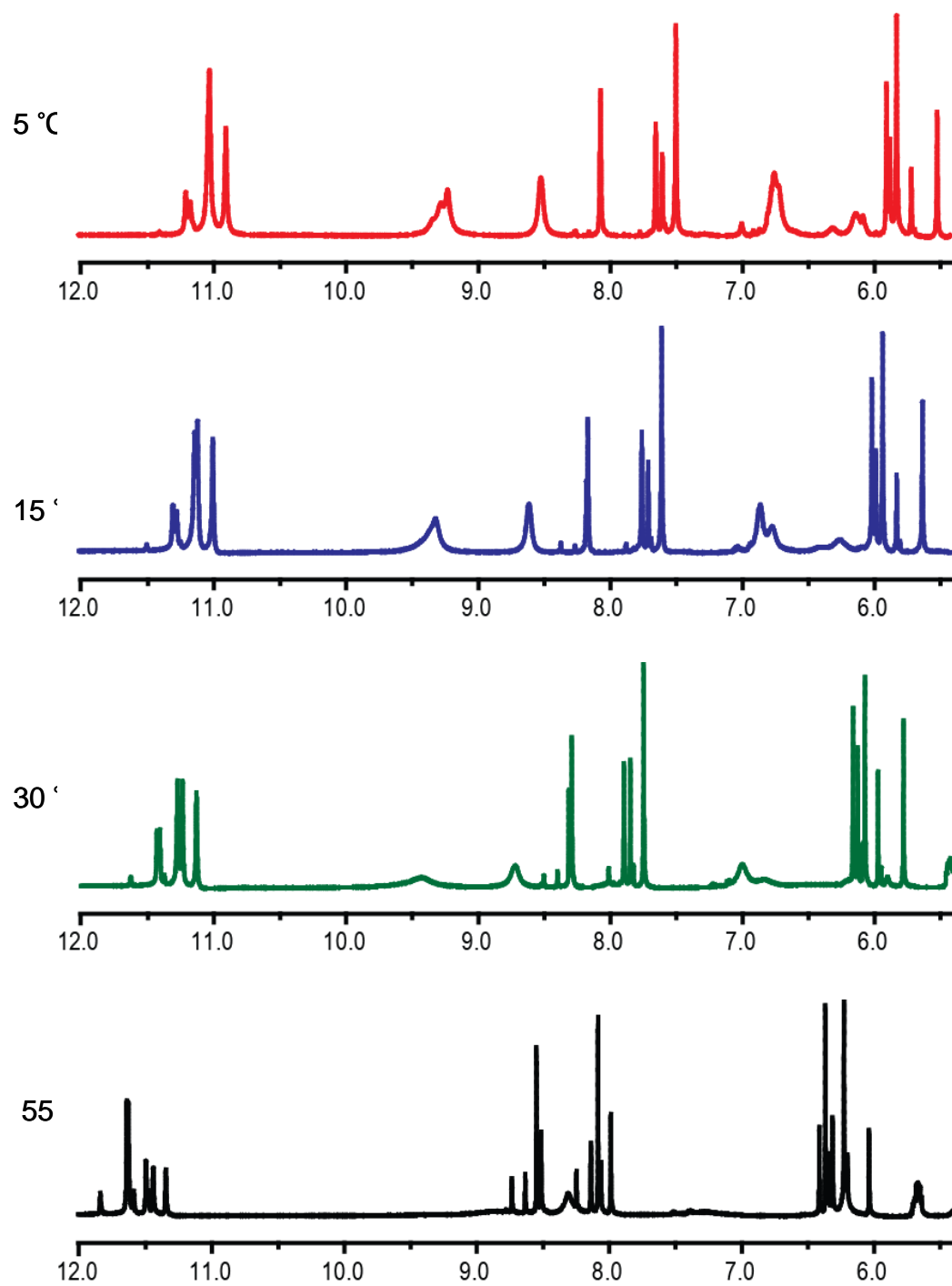
Figure 3-22 . ^{1}H NMR of [*R, R*] dithiophosphate c-di-GMP in K^{+} form
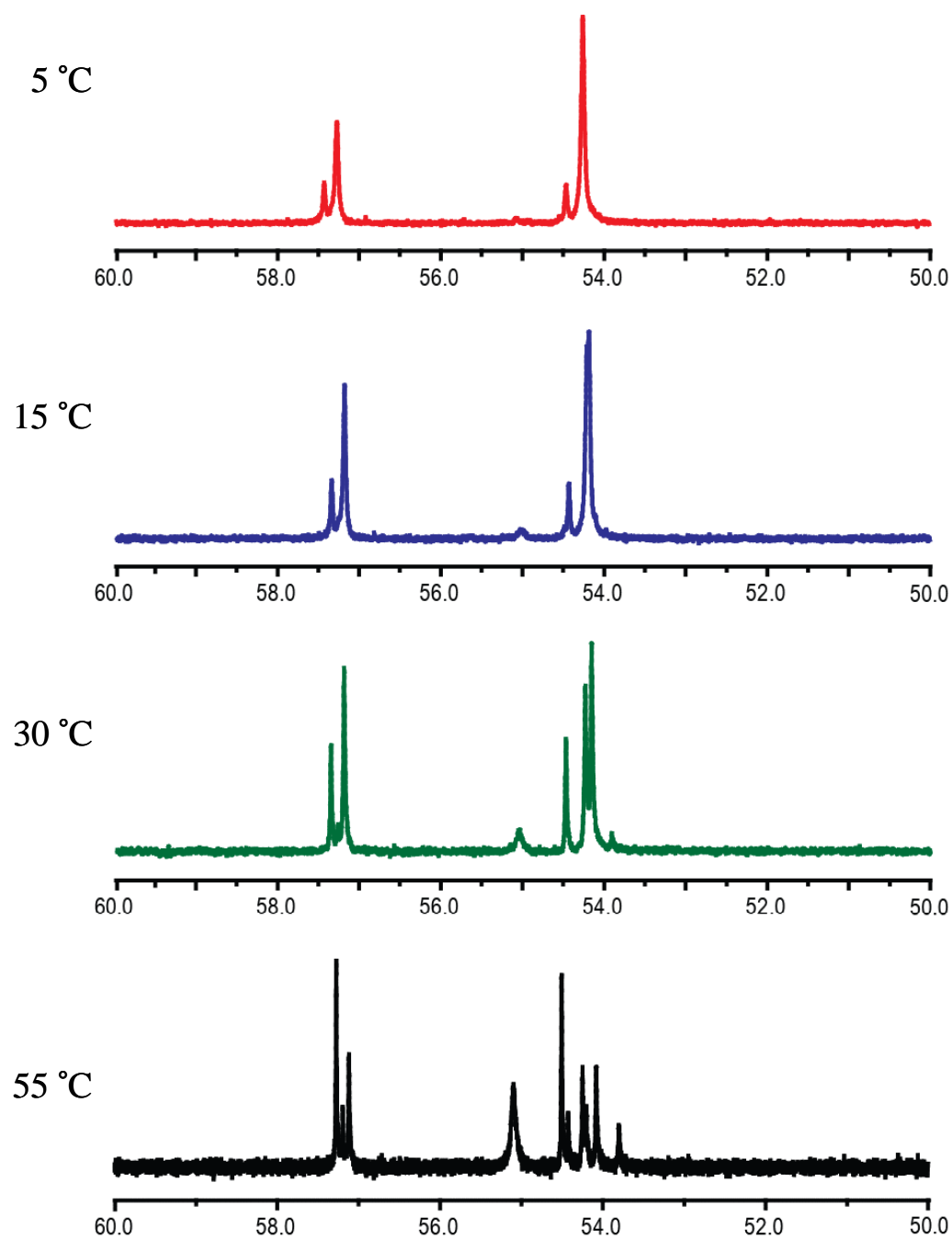
Figure 3-23 . ^{31}P NMR of [*R, R*] dithiophosphate c-di-GMP in K$^+$ form

151
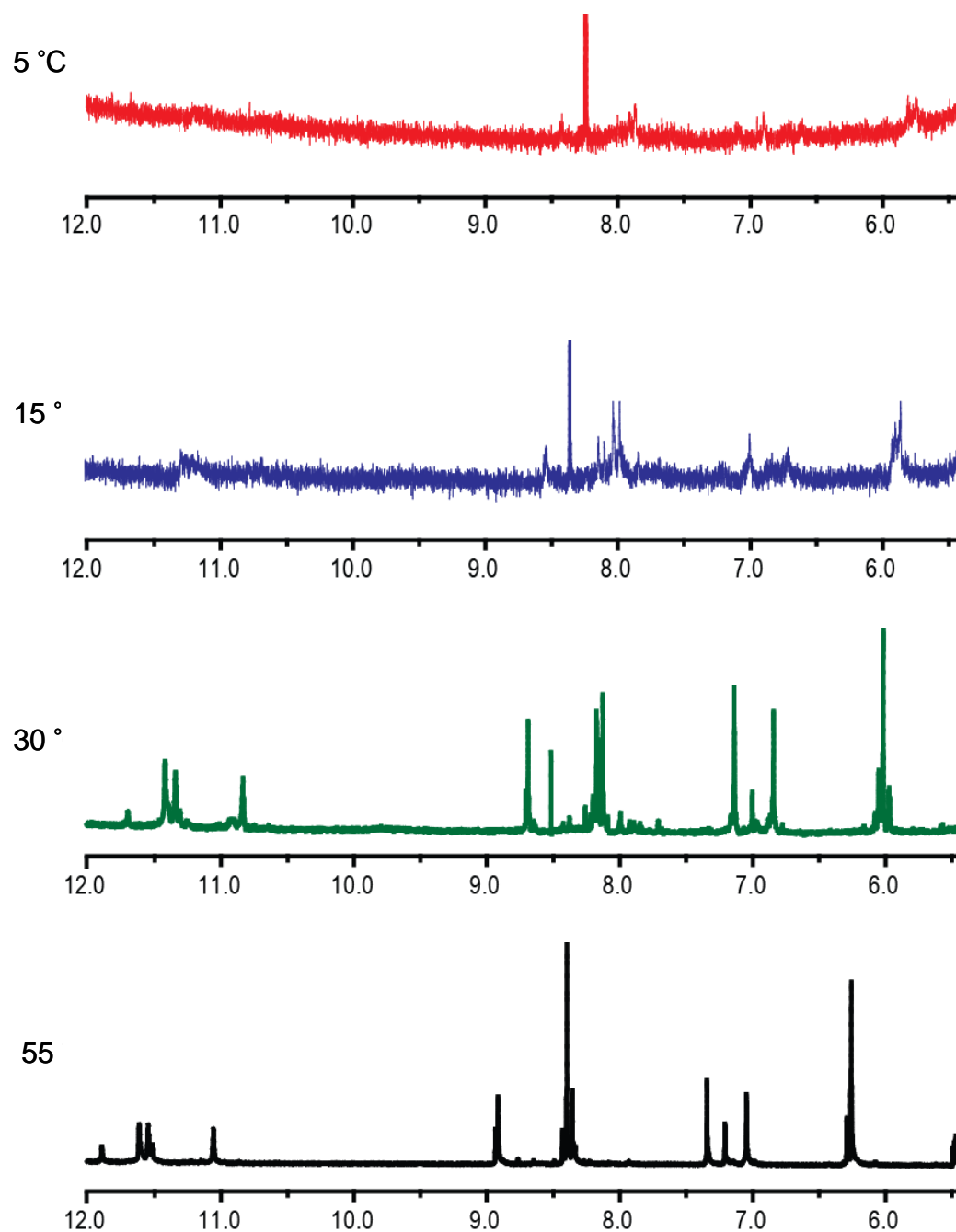
Figure 3-24 . ¹H NMR of [*S, S*] dithiophosphate c-di-GMP in K⁺ form
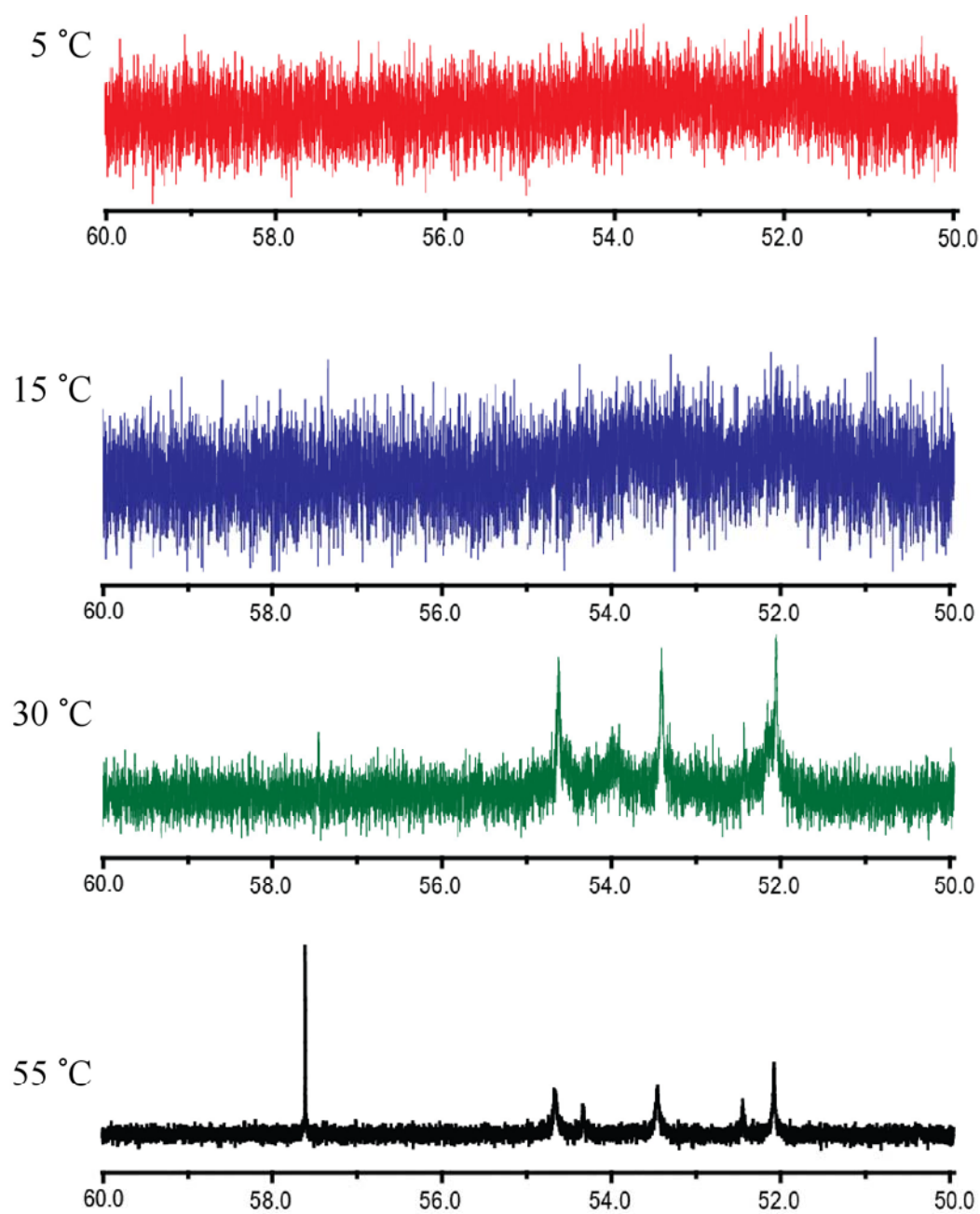
Figure 3-25 . ^{31}P NMR of [*S, S*] dithiophosphate c-di-GMP in K^{+} form
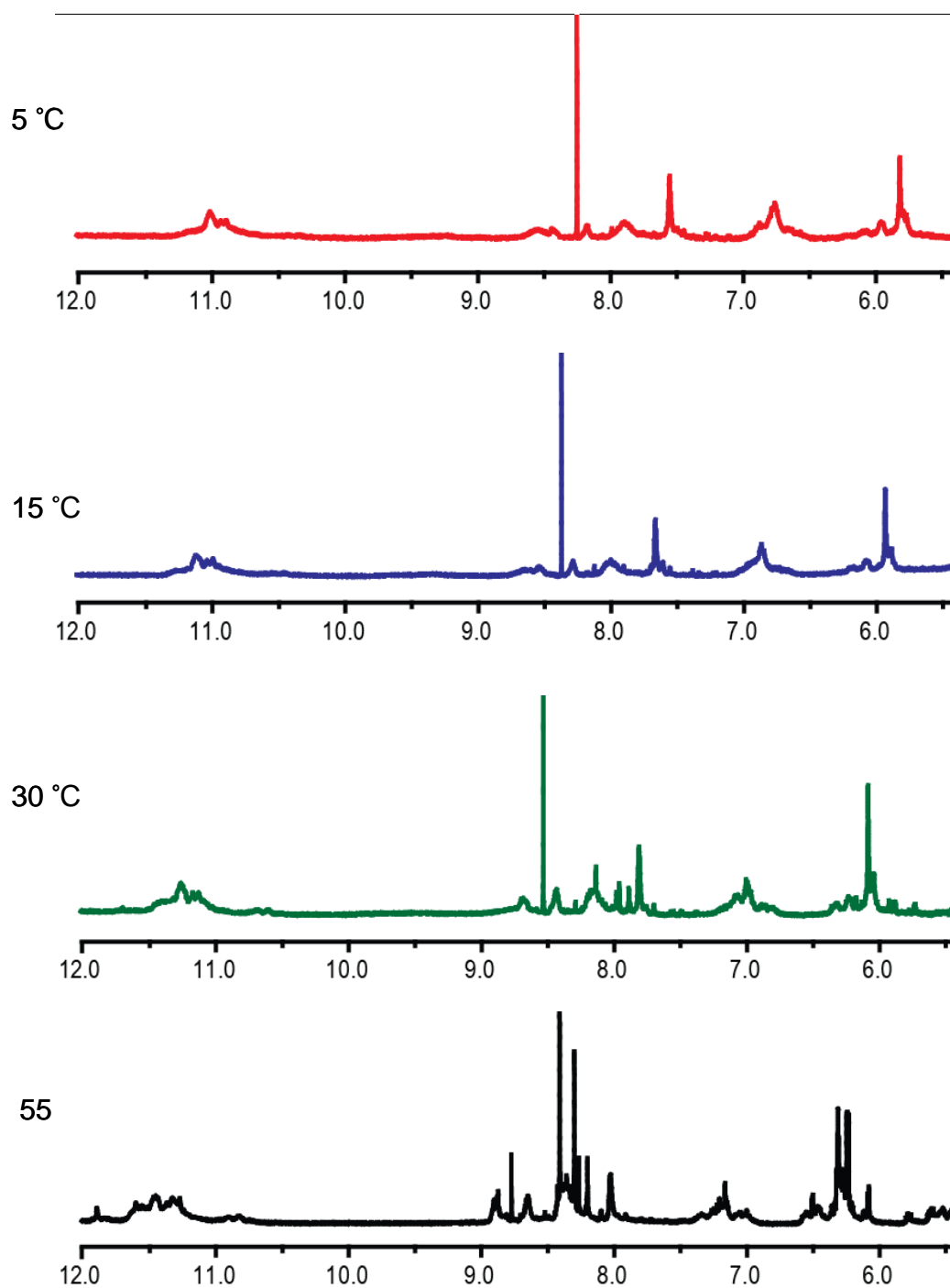
Figure 3-26 . ^{1}H NMR of [*R, S*] dithiophosphate c-di-GMP in K^{+} form
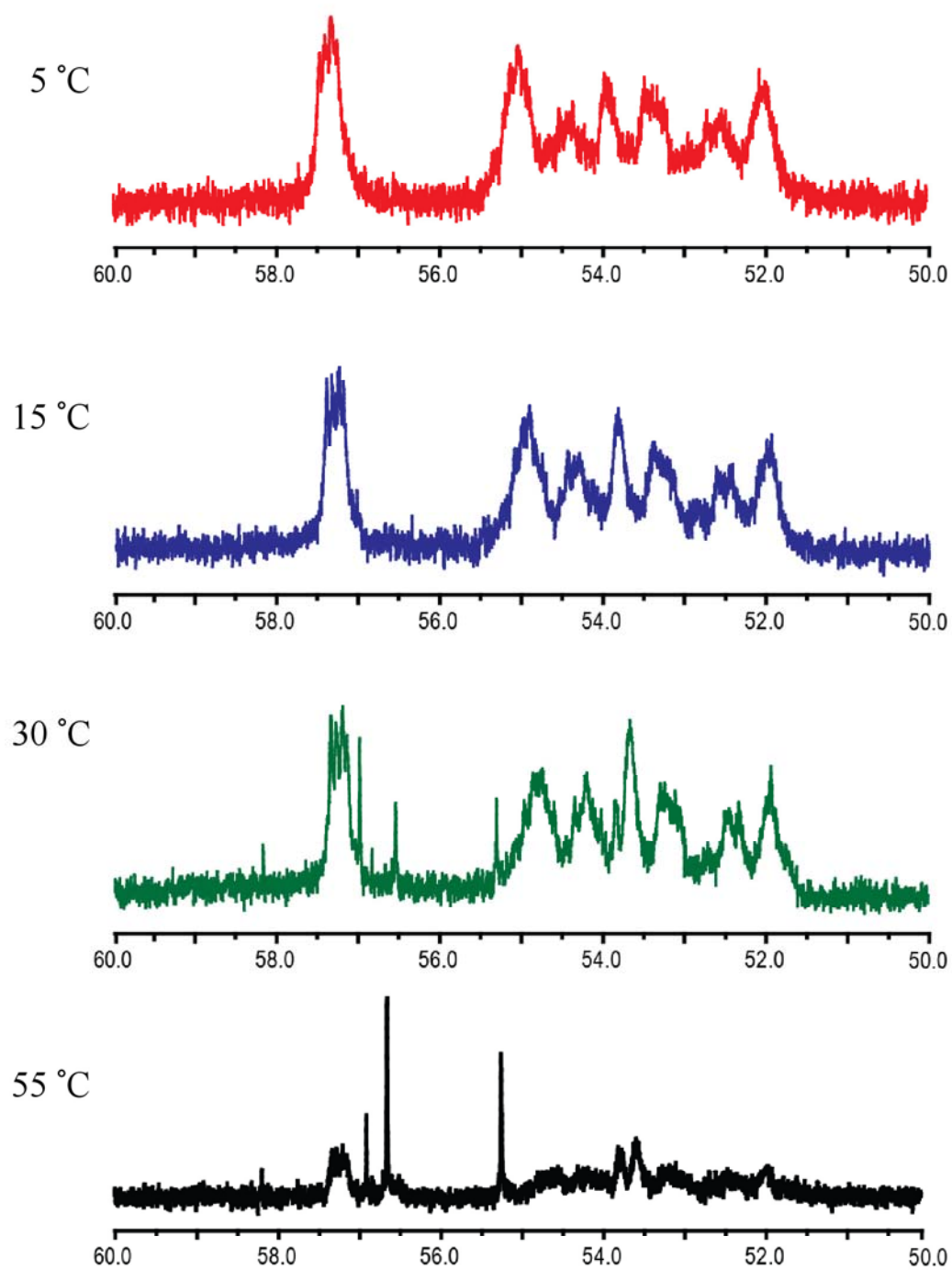
Figure 3-27 . ^{31}P NMR of [*R, S*] dithiophosphate c-di-GMP in K^{+} form
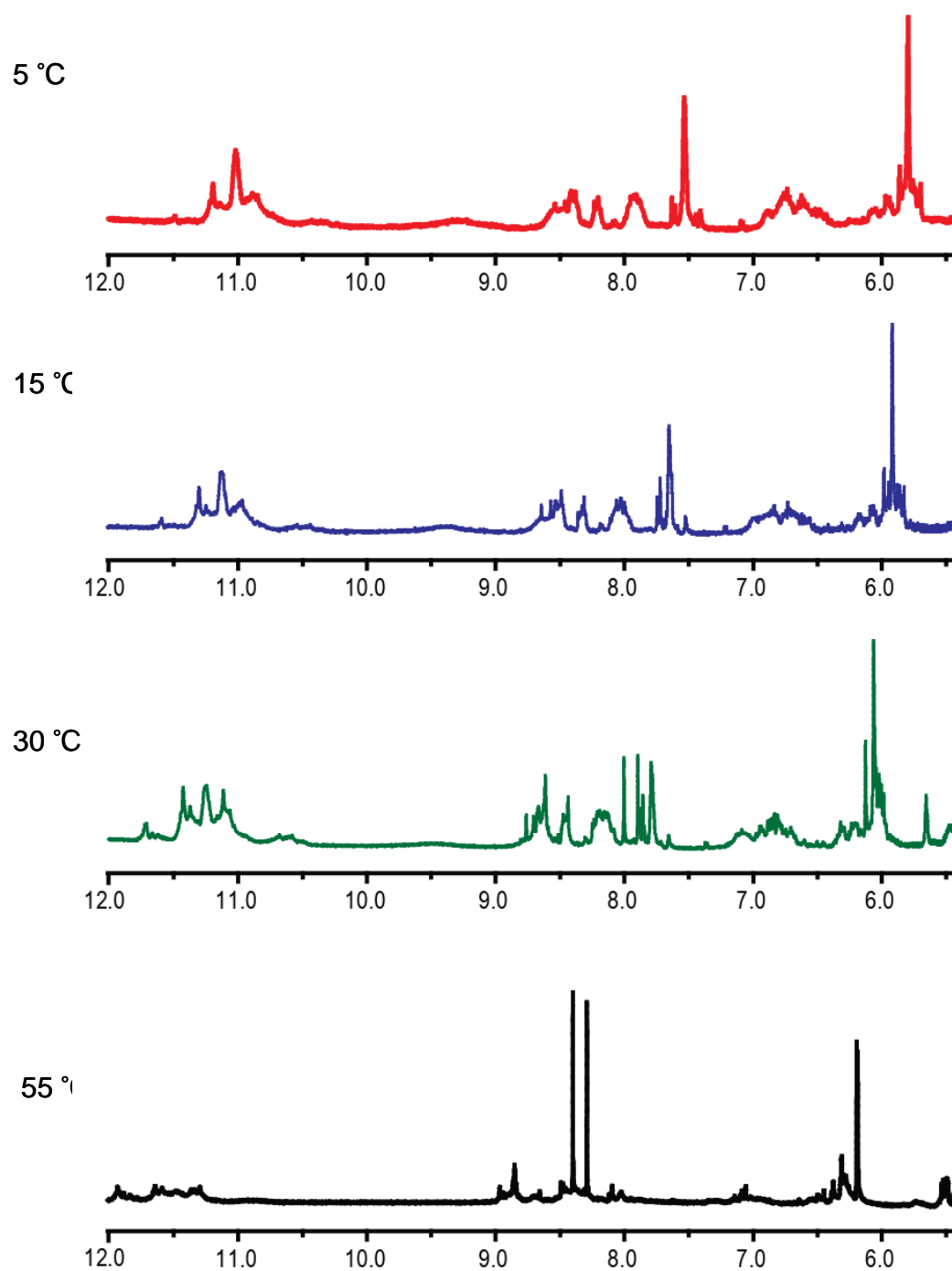
Figure 3-28 . ^{1}H NMR of [*R*] trithiophosphate c-di-GMP in K$^+$ form
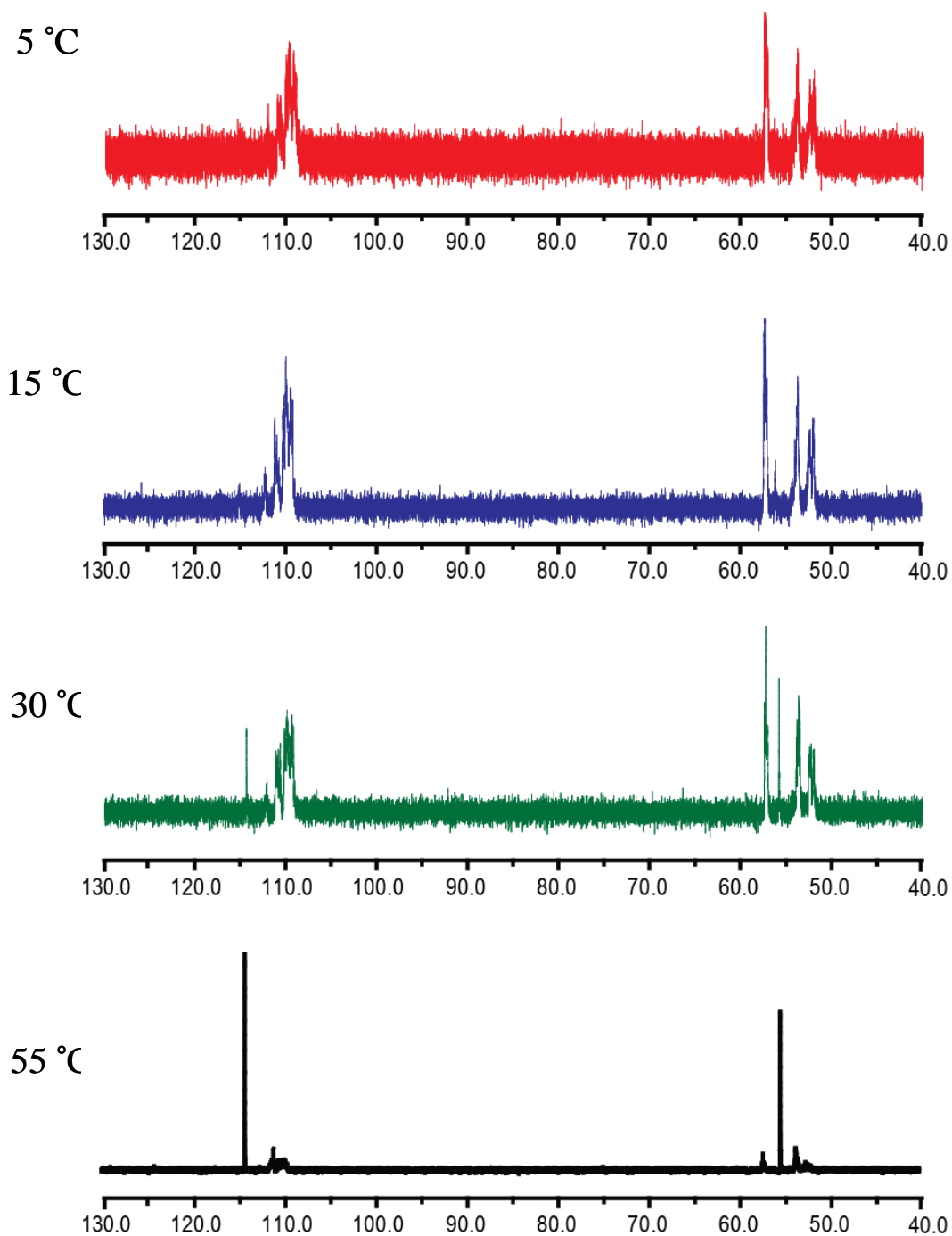
Figure 3-29 . ^{31}P NMR of [*R*] trithiophosphate c-di-GMP in K$^+$ form

5 ℃

15 ℃

30 ℃

55 ℃
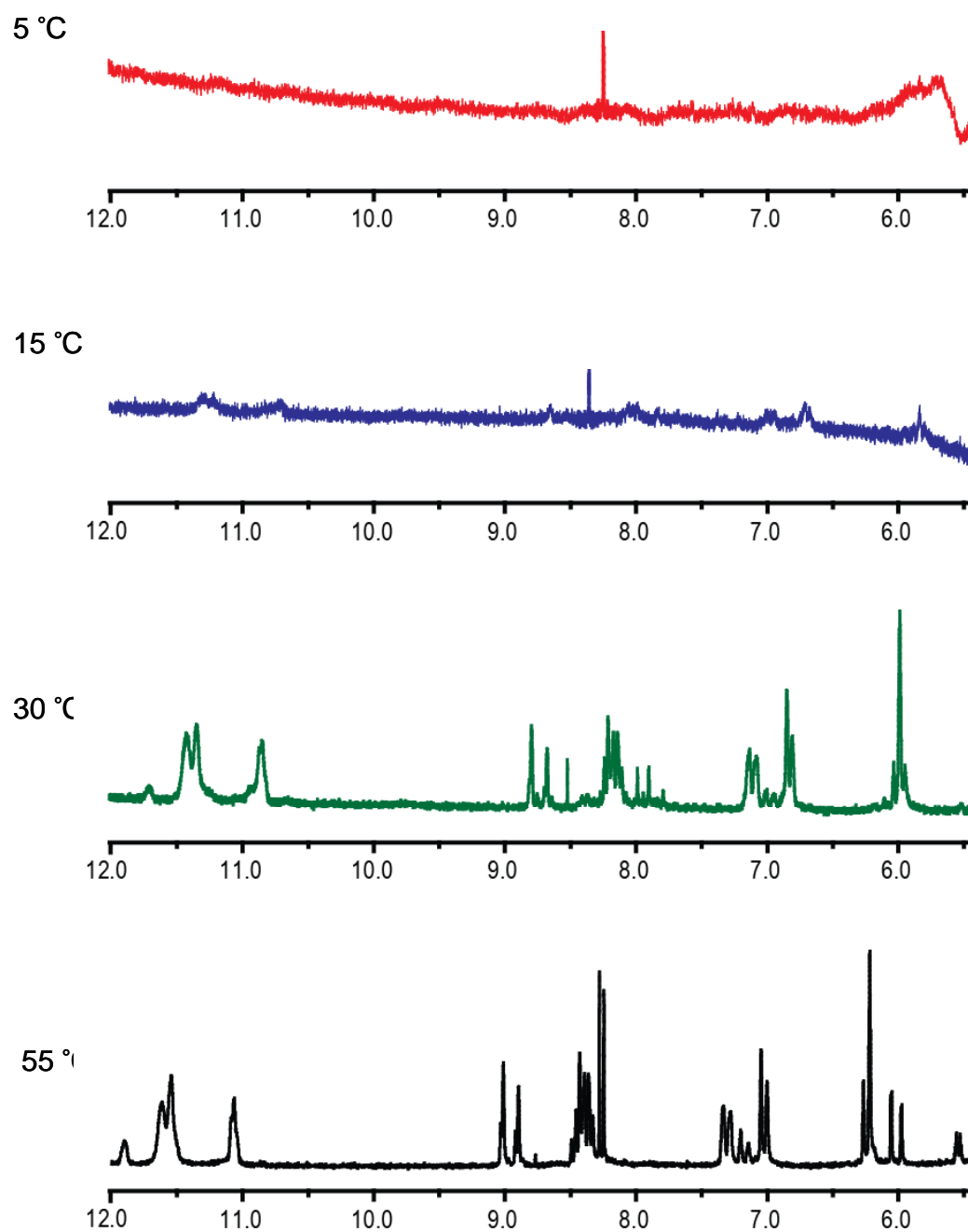
Figure 3-30 . ^{1}H NMR of [*S*] trithiophosphate c-di-GMP in K$^+$ form
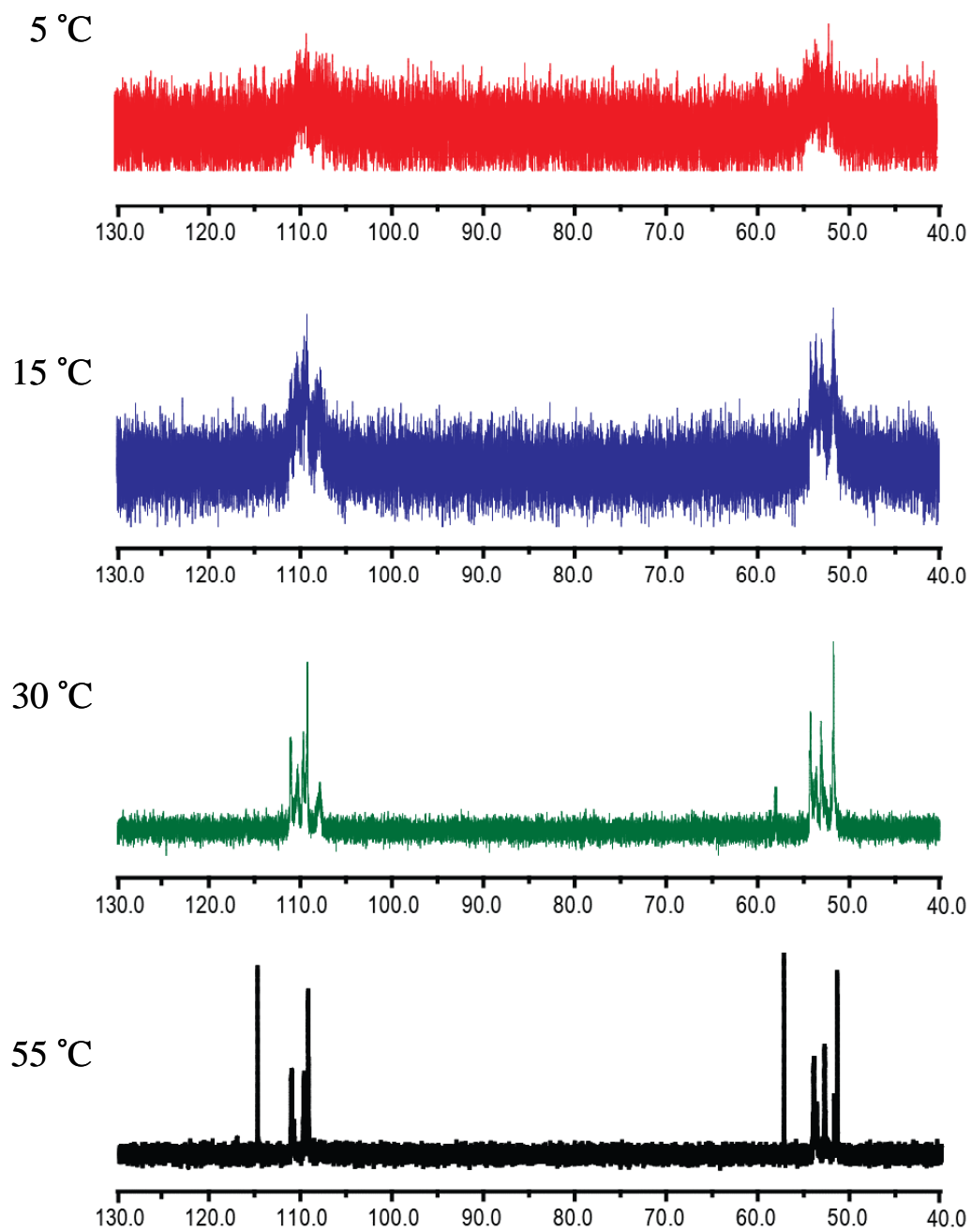
Figure 3-31 . ^{31}P NMR of [*S*] trithiophosphate c-di-GMP in K^{+} form
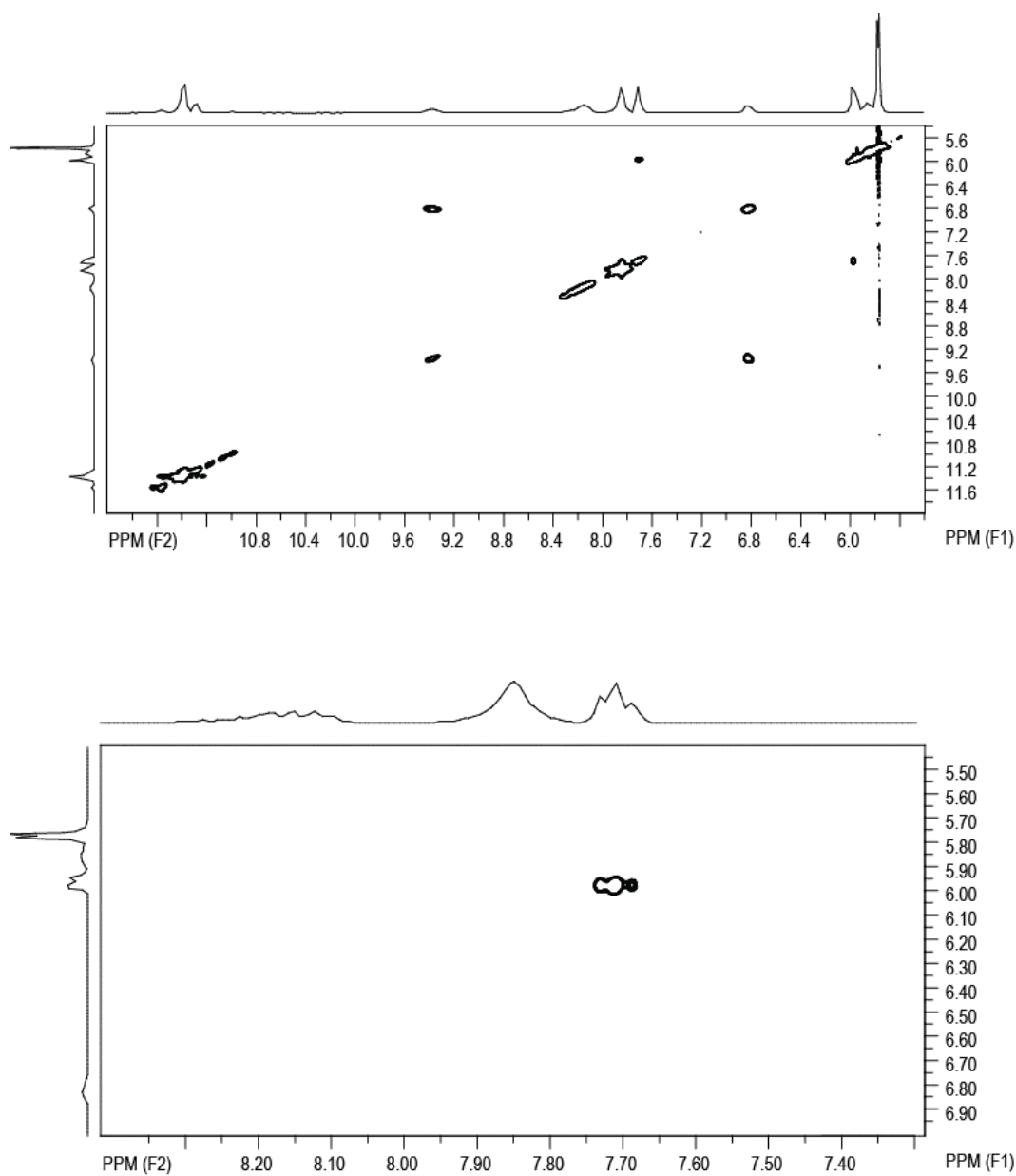
Figure 3-32 . 2D NOSEY spectra of the Na$^+$ form of [*R*] monothioate c-di-GMP. Above: 5.4 ppm to 12.0 ppm. Bottom: expanded H8/H1' region.
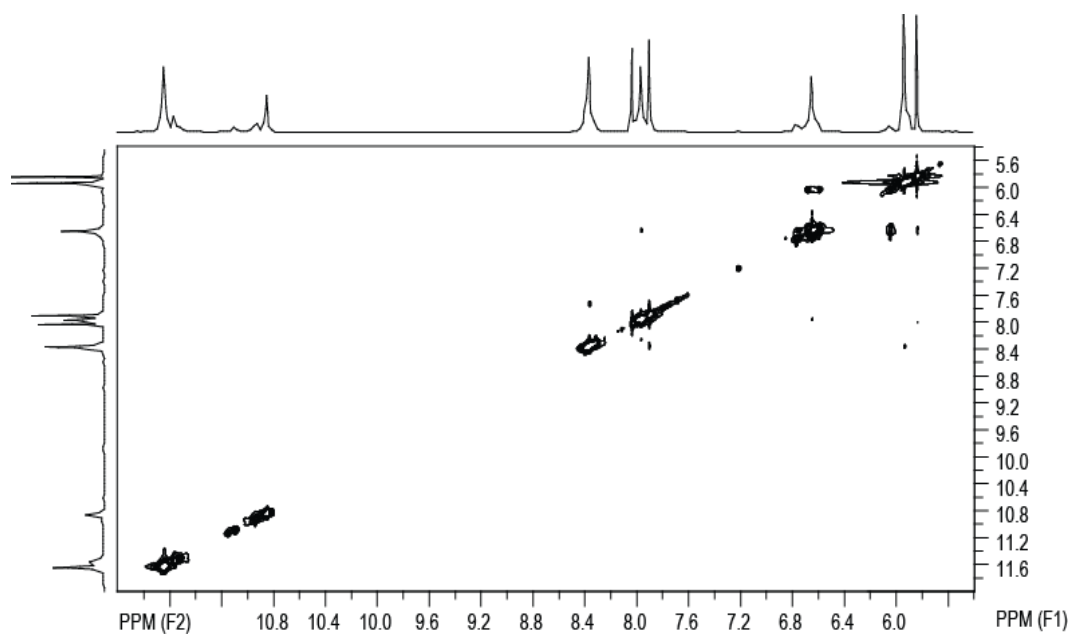
Figure 3-33 . 2D NOSEY spectrum of the Na$^+$ form of [*S*] monothioate c-di-GMP at 5.4 ppm to 12.0 ppm range. No strong signals found in expanded H8/H1'.
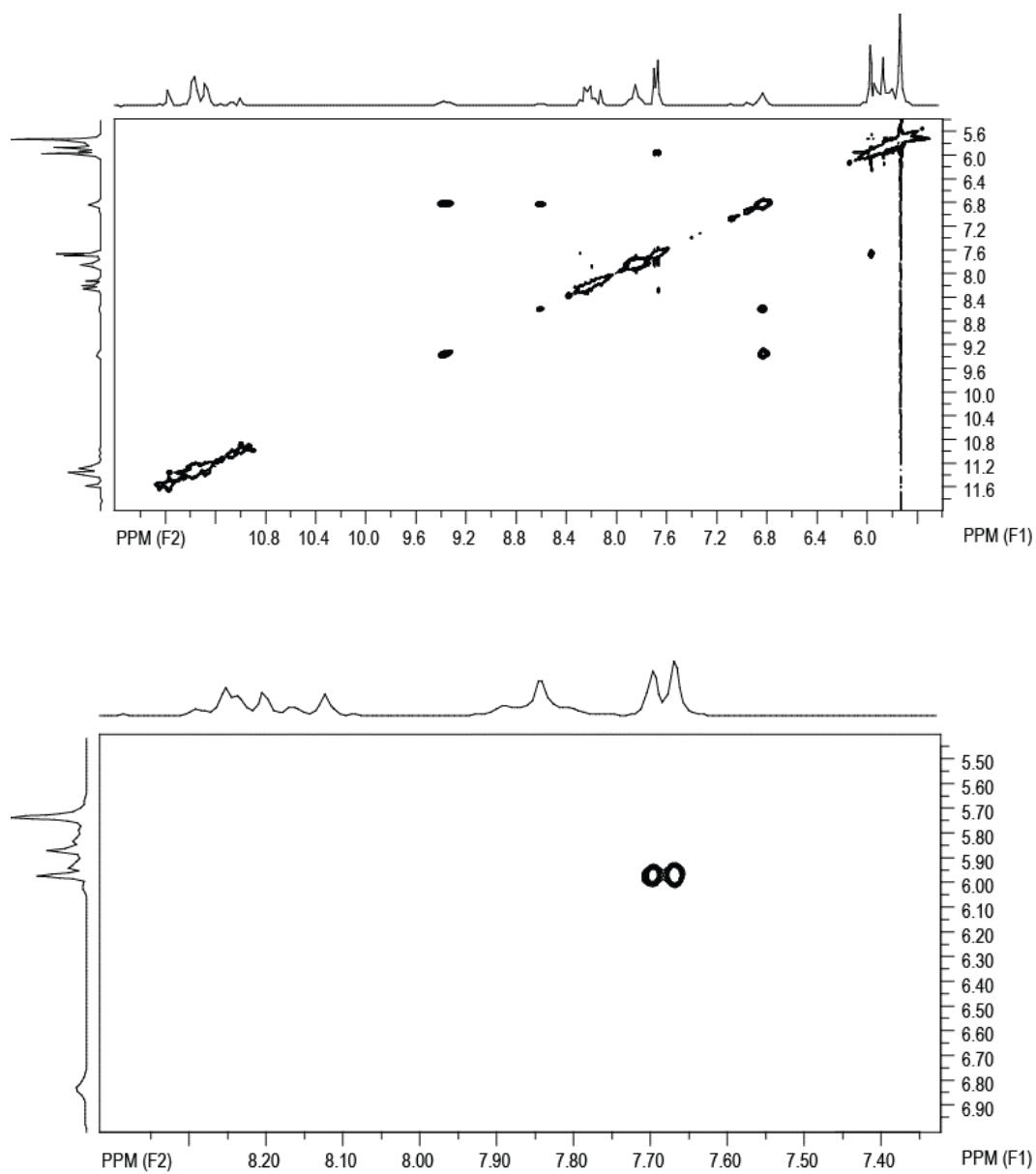
Figure 3-34 . 2D NOSEY spectra of the Na^{+} form of [*R, R*] dithioate c-di-GMP. Above: 5.4 ppm to 12.0 ppm. Bottom: expanded H8/H1' region.
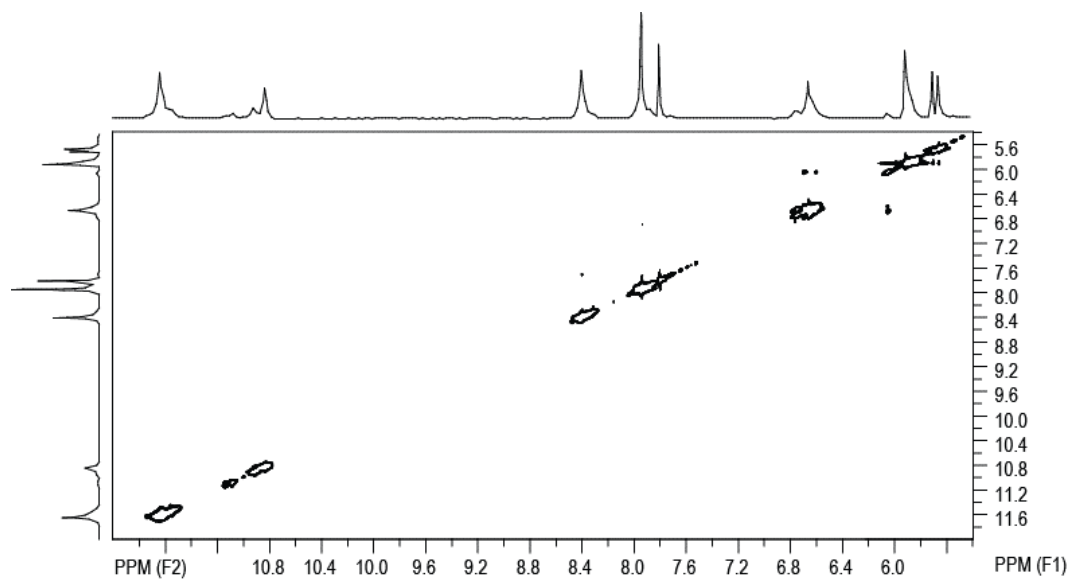
Figure 3-35 . 2D NOSEY spectrum of the Na⁺ form of [*R, S*] dithioate c-di-GMP in Na⁺ at 5.4 ppm to 12.0 ppm range. No strong signals found in expanded H8/H1'.
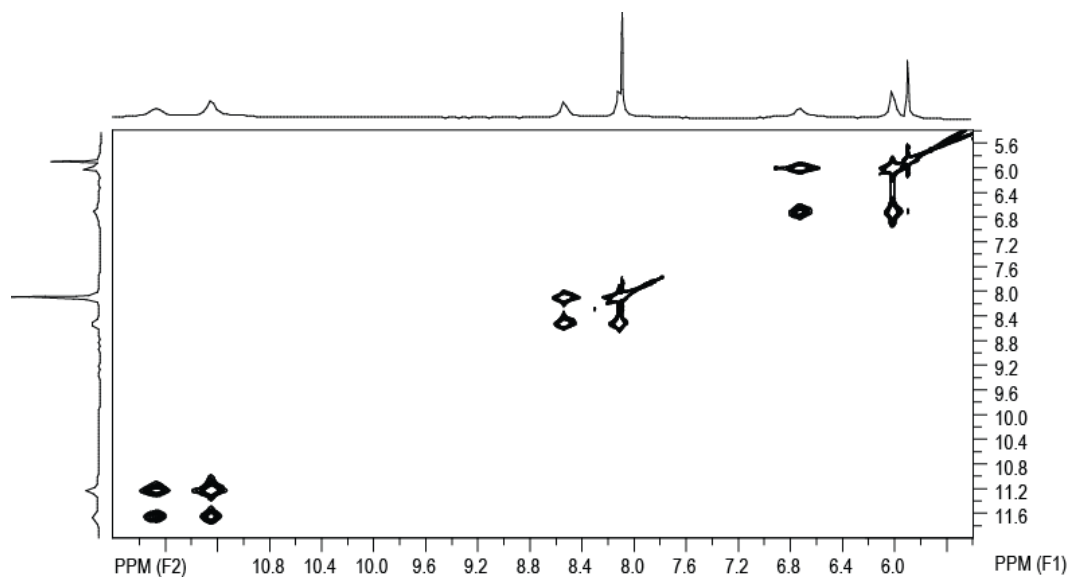
Figure 3-36 . 2D NOSEY spectrum of the Na⁺ form of [*S, S*] dithioate c-di-GMP at 5.4 ppm to 12.0 ppm range at 45 °C. No strong signals found in expanded H8/H1'.
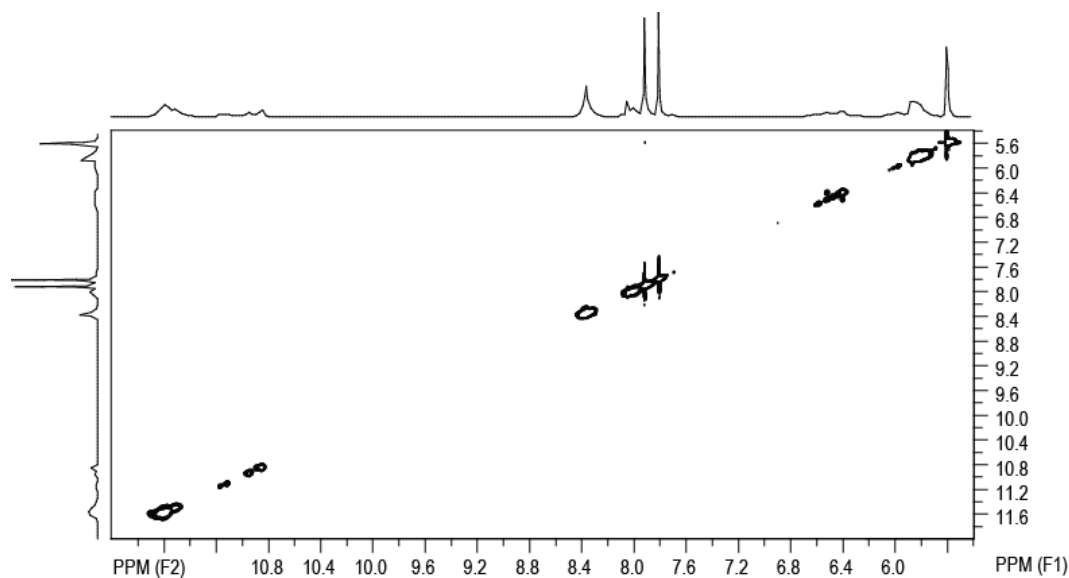
Figure 3-37 . 2D NOSEY spectrum of the Na$^+$ form of [*R*] trithioate c-di-GMP at 5.4 ppm to 12.0 ppm range. No strong signals found in expanded H8/H1'.
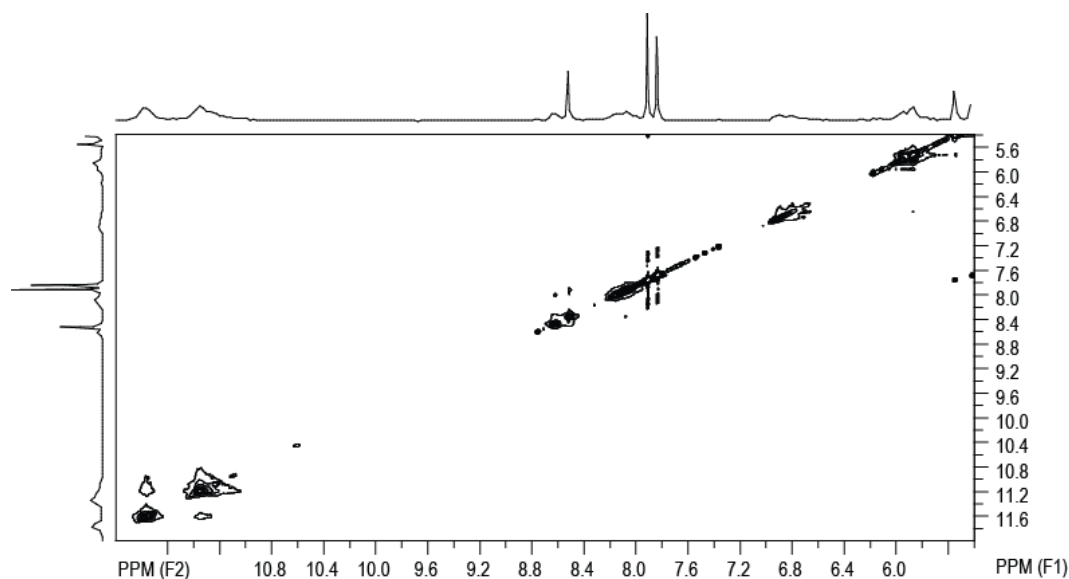
Figure 3-38 . 2D NOSEY spectrum of the Na$^+$ form of [*S*] trithioate c-di-GMP at 5.4 ppm to 12.0 ppm range at 45 °C. No strong signals found in expanded H8/H1'.
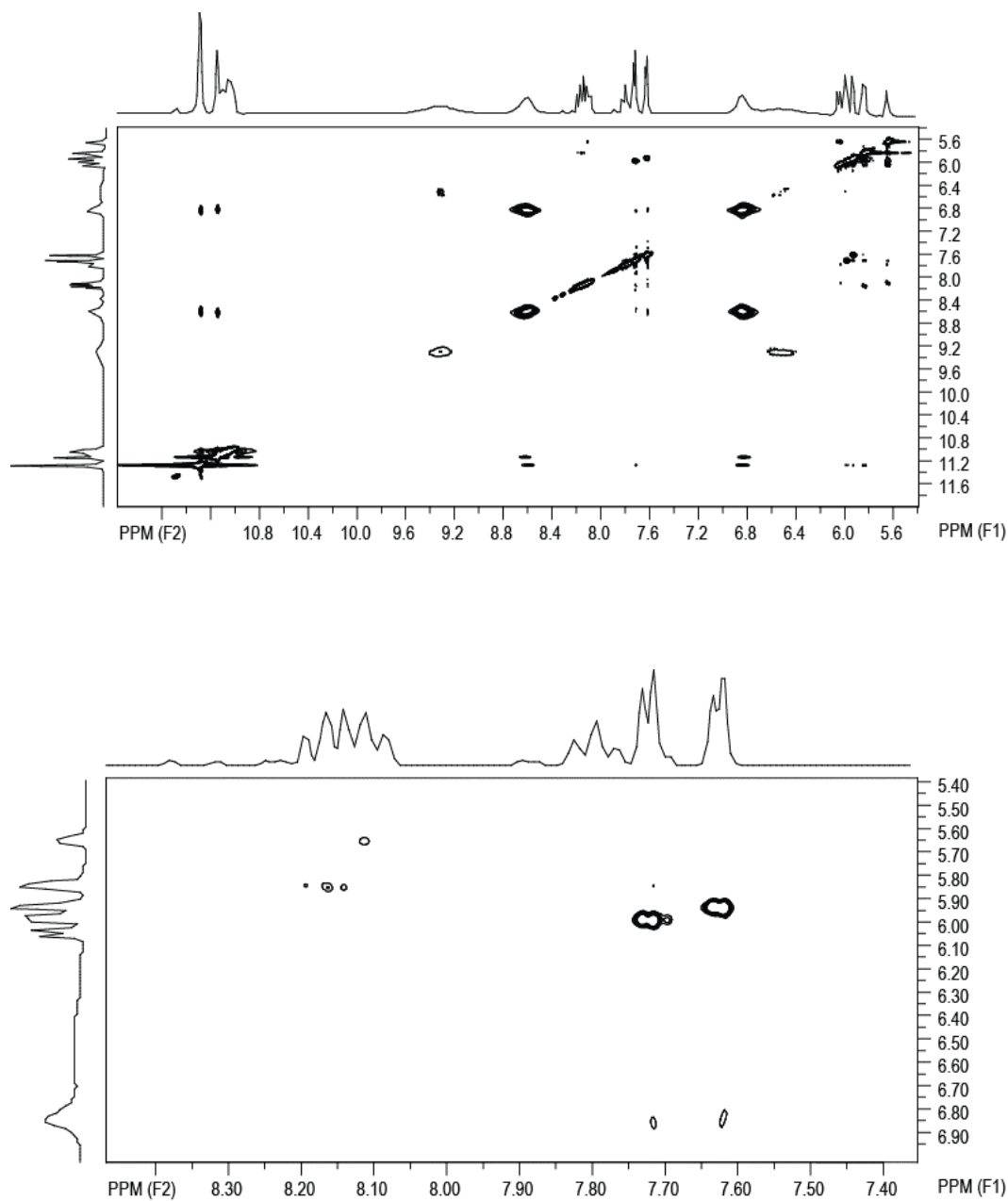
Figure 3-39 . 2D NOSEY spectra of the K$^+$ form of [*R*] monothioate c-di-GMP. Above: 5.4 ppm to 12.0 ppm. Bottom: expanded H8/H1' region.
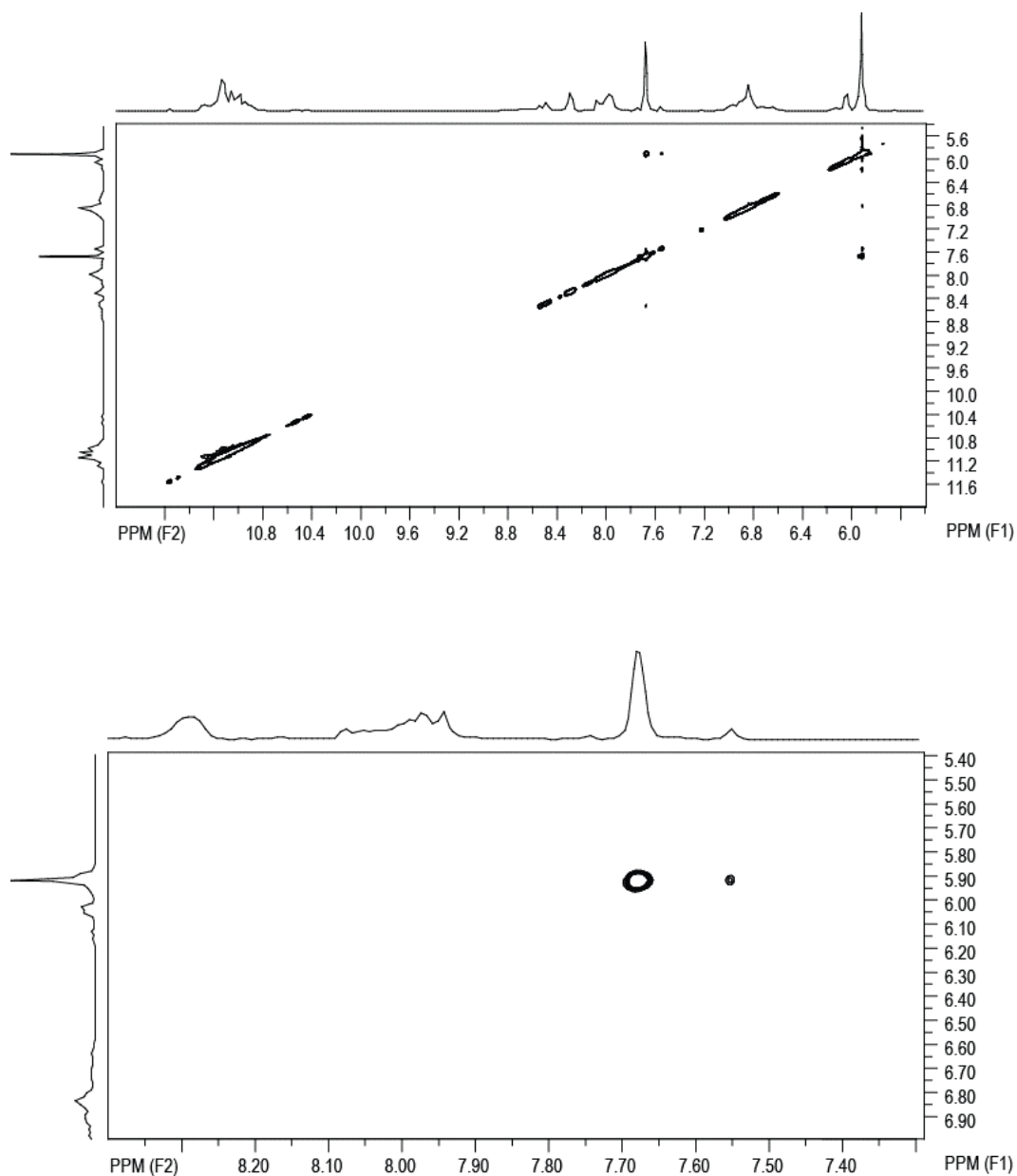
Figure 3-40 . 2D NOSEY spectra of the K^+ form of [*S*] monothioate c-di-GMP. Above: 5.4 ppm to 12.0 ppm. Bottom: expanded H8/H1' region.
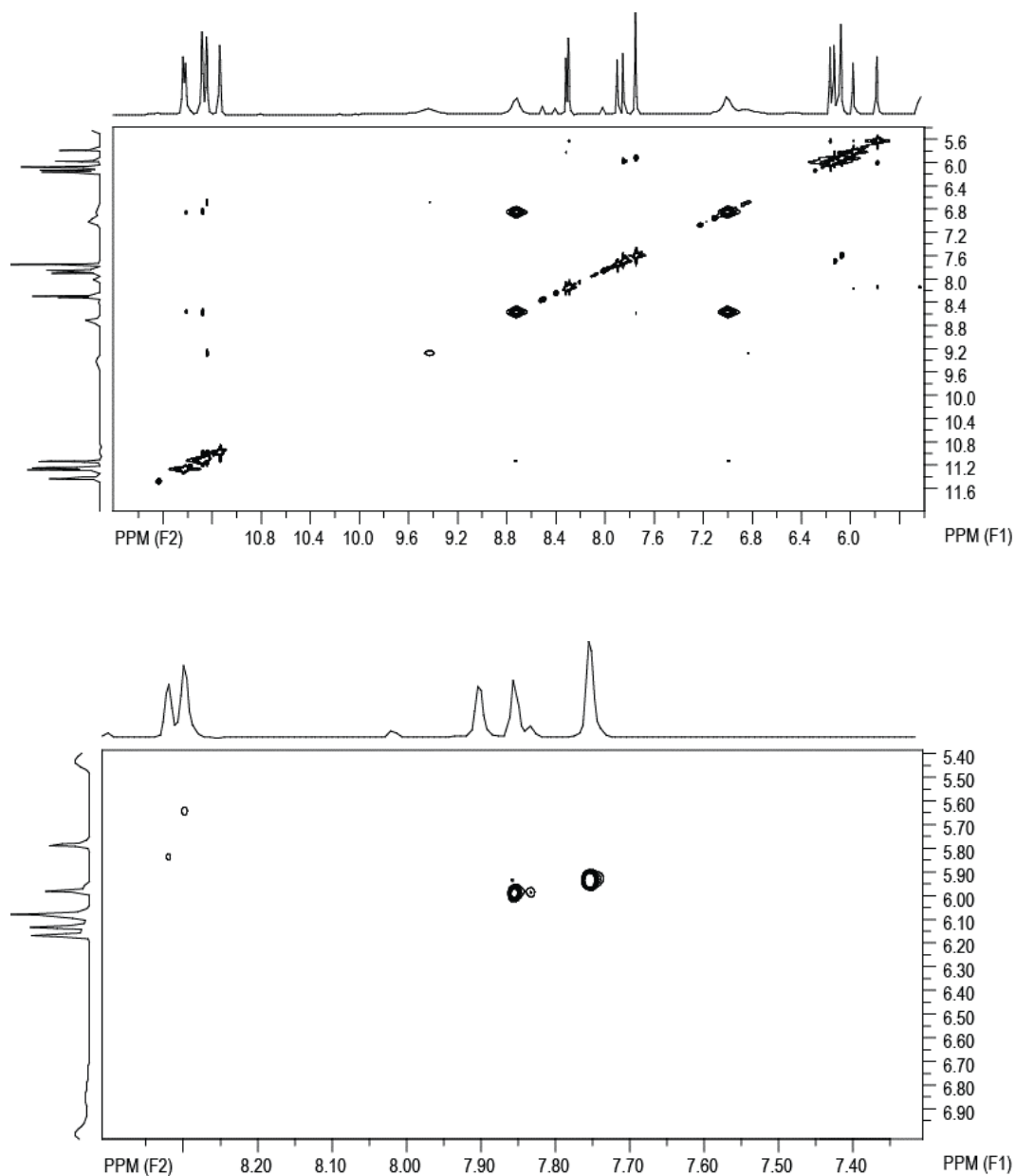
Figure 3-41 . 2D NOSEY spectra of the K$^+$ form of [*R, R*] dithioate c-di-GMP. Above: 5.4 ppm to 12.0 ppm. Bottom: expanded H8/H1' region.
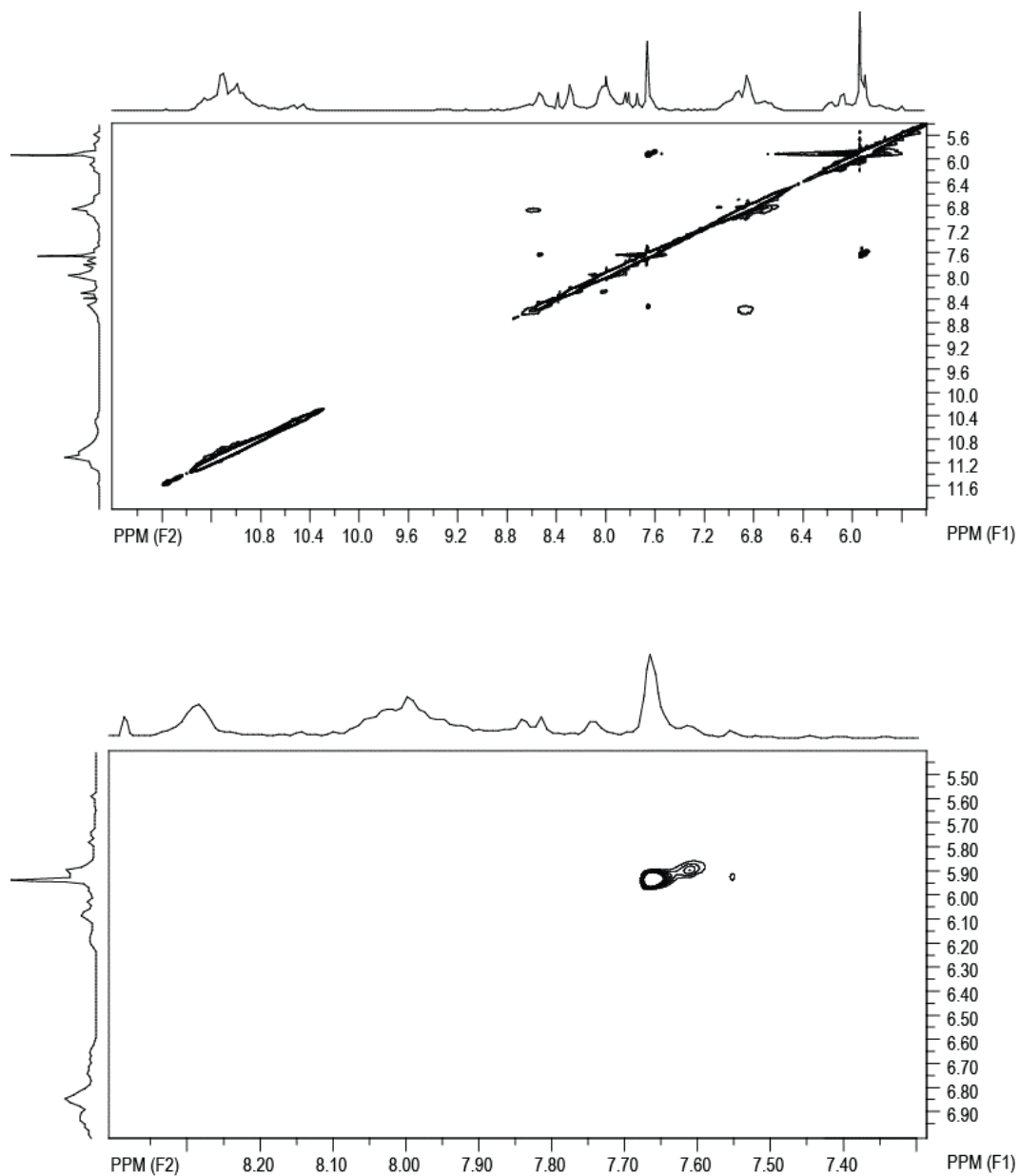
Figure 3-42 . 2D NOSEY spectra of the K$^+$ form of [*R, S*] dithioate c-di-GMP. Above: 5.4 ppm to 12.0 ppm. Bottom: expanded H8/H1' region.
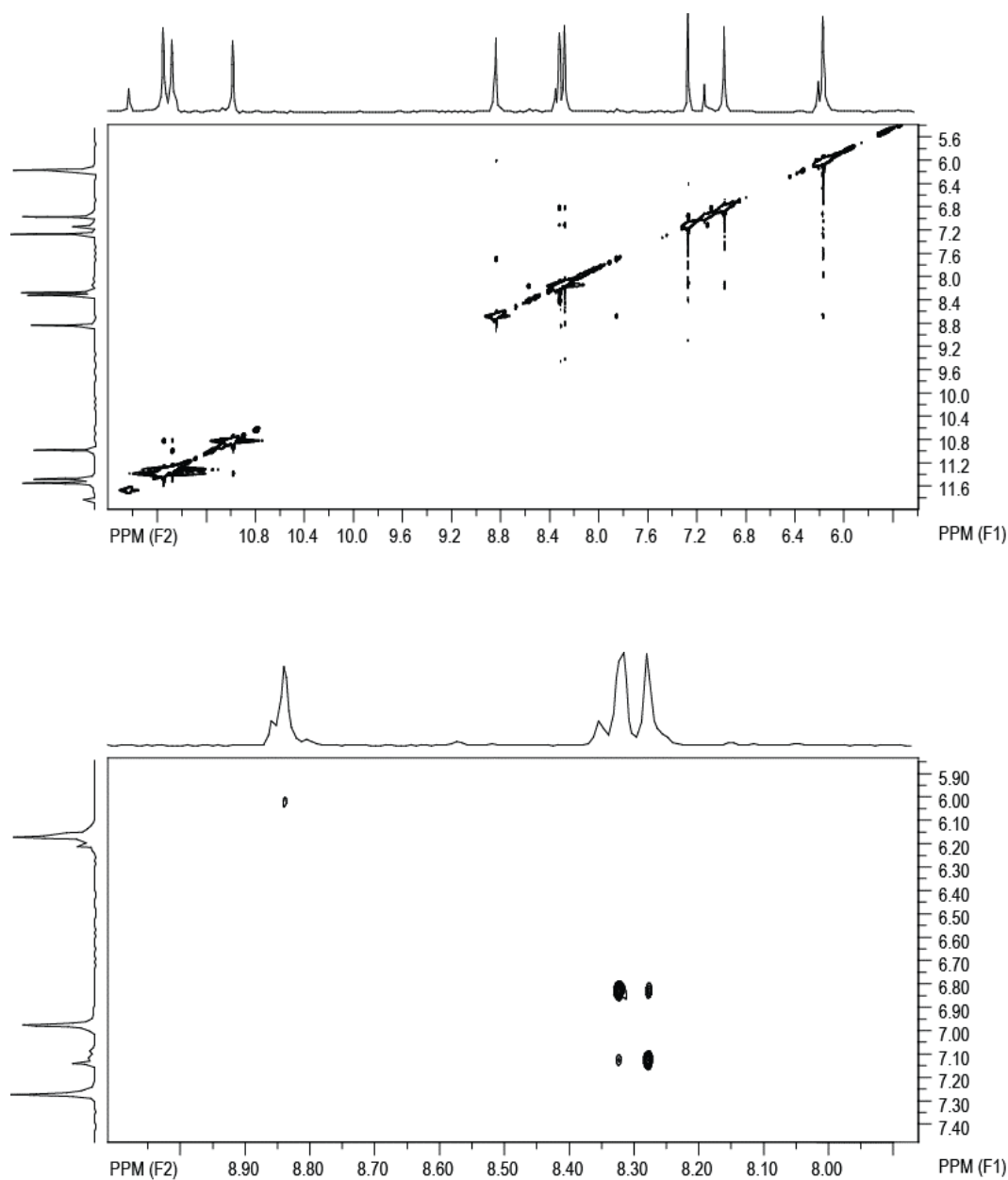
Figure 3-43 . 2D NOSEY spectra of the K$^+$ form of [*S, S*] dithioate c-di-GMP at 45 °C. Above: 5.4 ppm to 12.0 ppm. Bottom: expanded H8/H1' region.
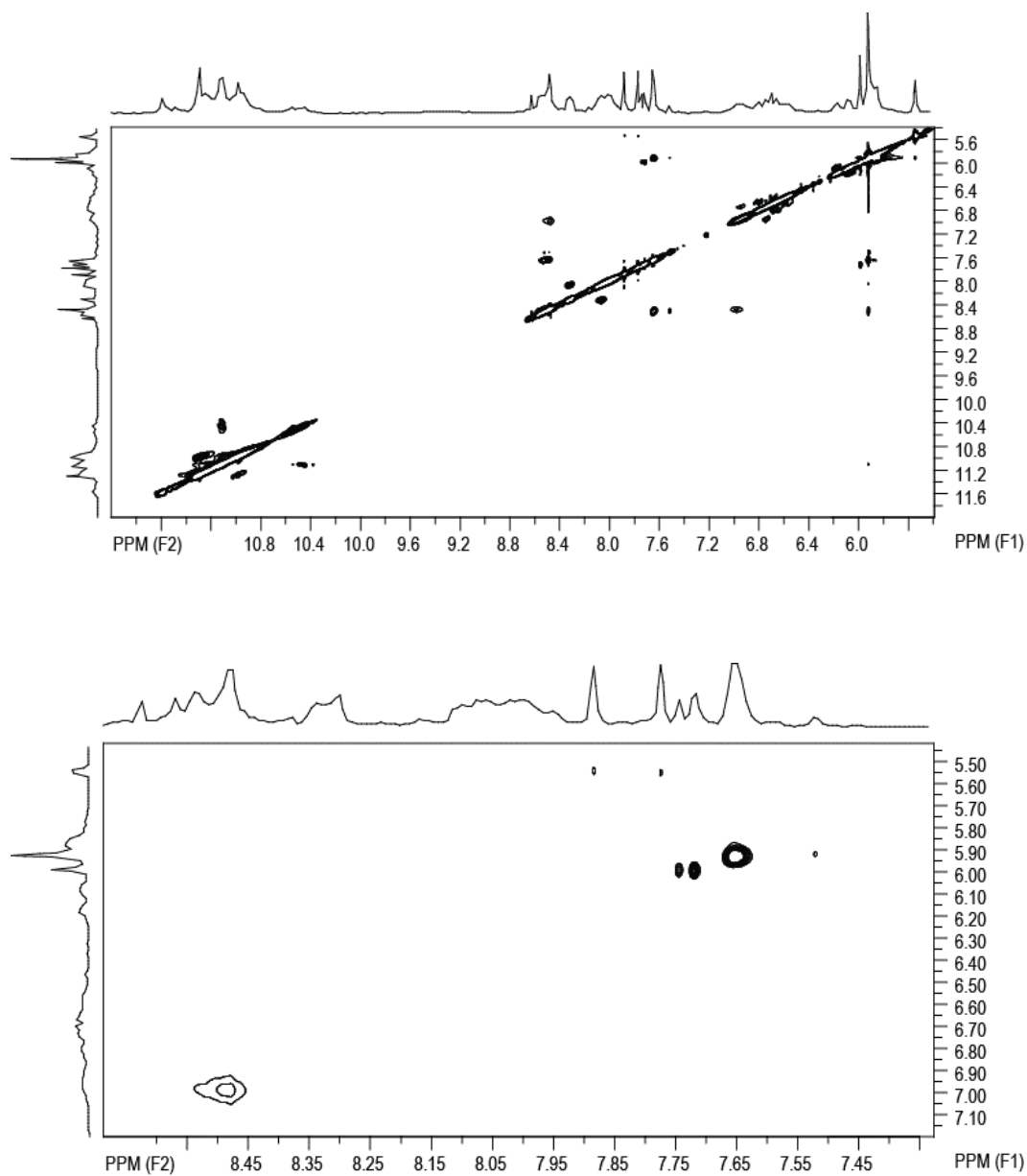
Figure 3-44 . 2D NOSEY spectra of the K$^+$ form of [*R*] trithioate c-di-GMP. Above: 5.4 ppm to 12.0 ppm. Bottom: expanded H8/H1' region.
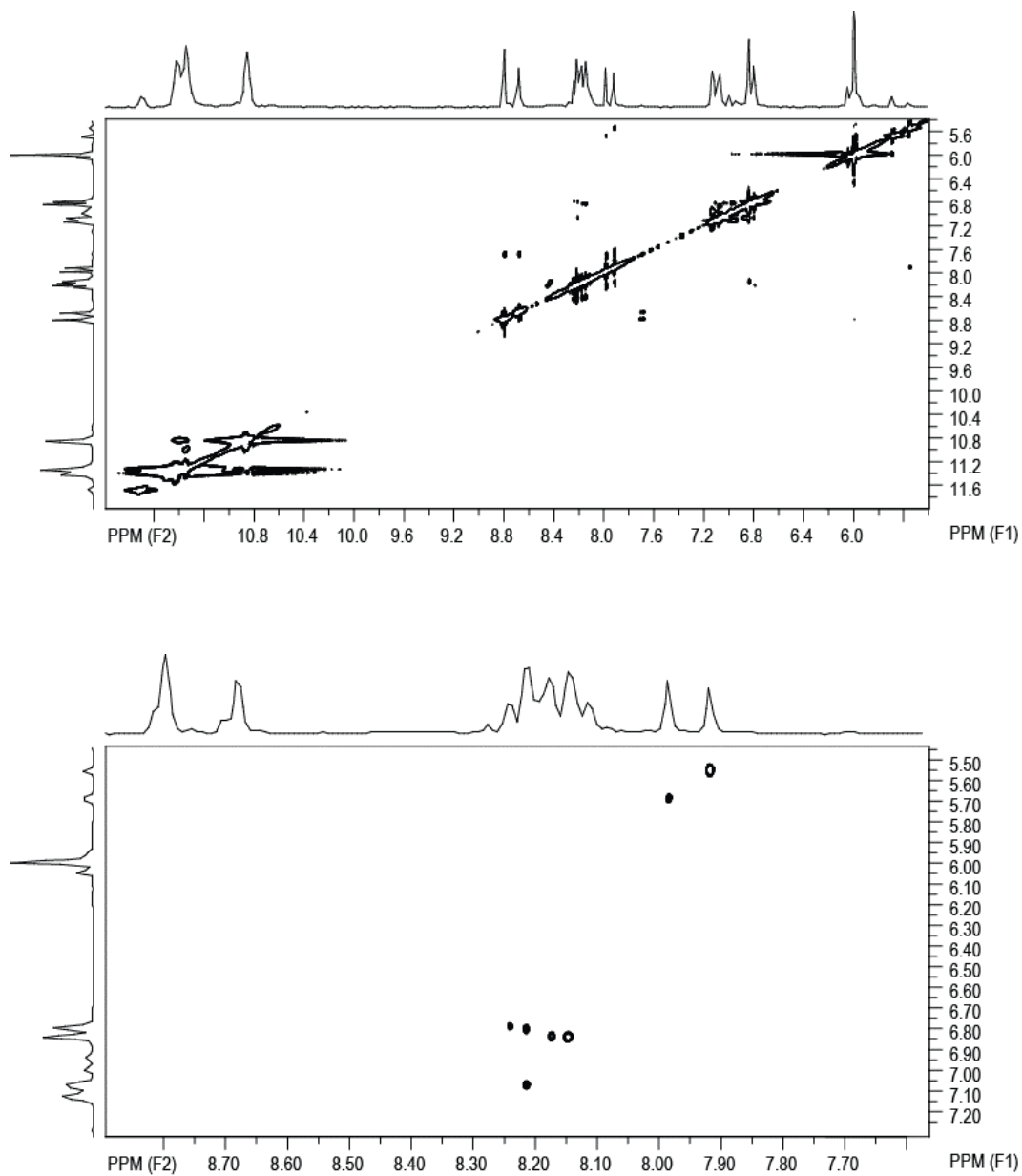
Figure 3-45 . 2D NOSEY spectra of the K$^+$ form of [*S*] trithioate c-di-GMP at 45 °C. Above: 5.4 ppm to 12.0 ppm. Bottom: expanded H8/H1' region.
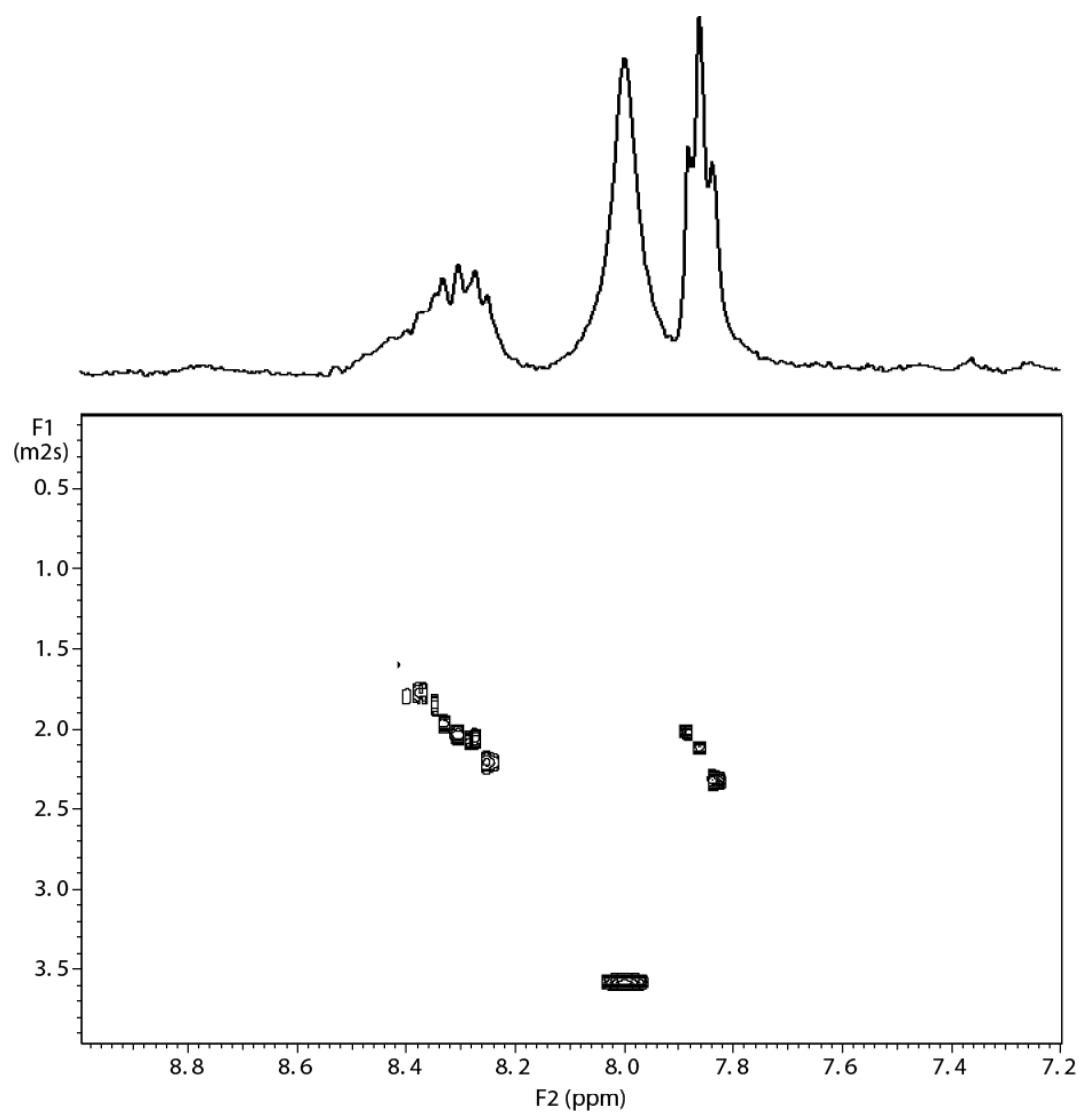
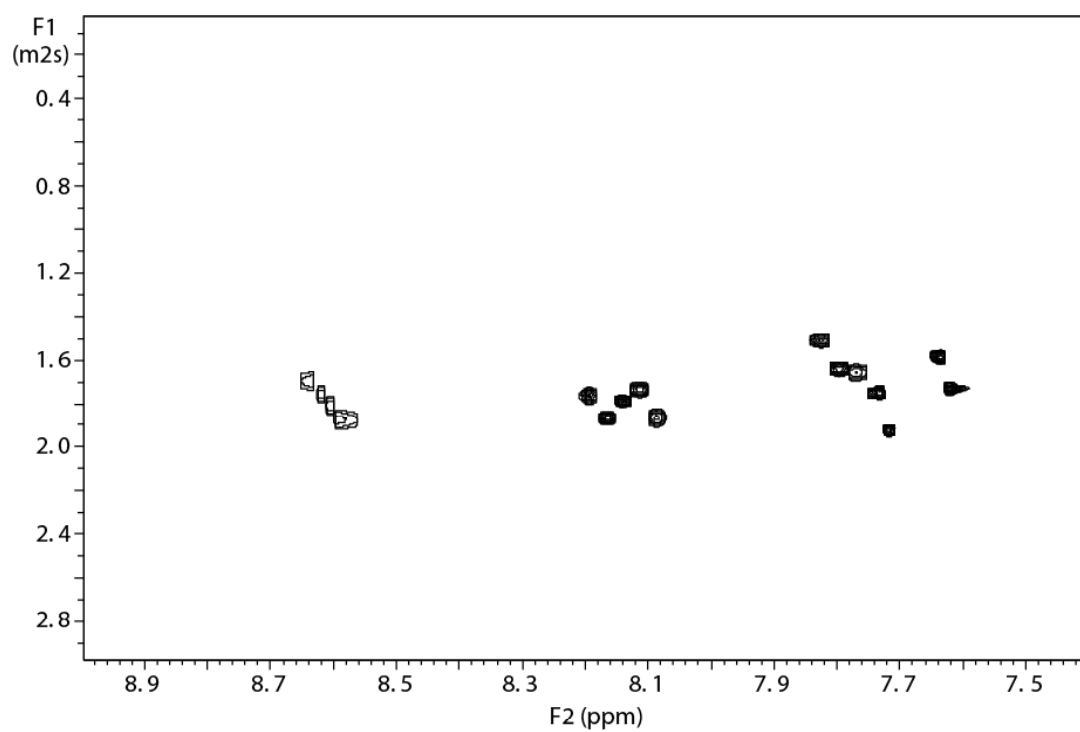**Figure 3-46.** 2D DOSY of [*R*] monothiophosphate in Na$^+$ form at 30 °C
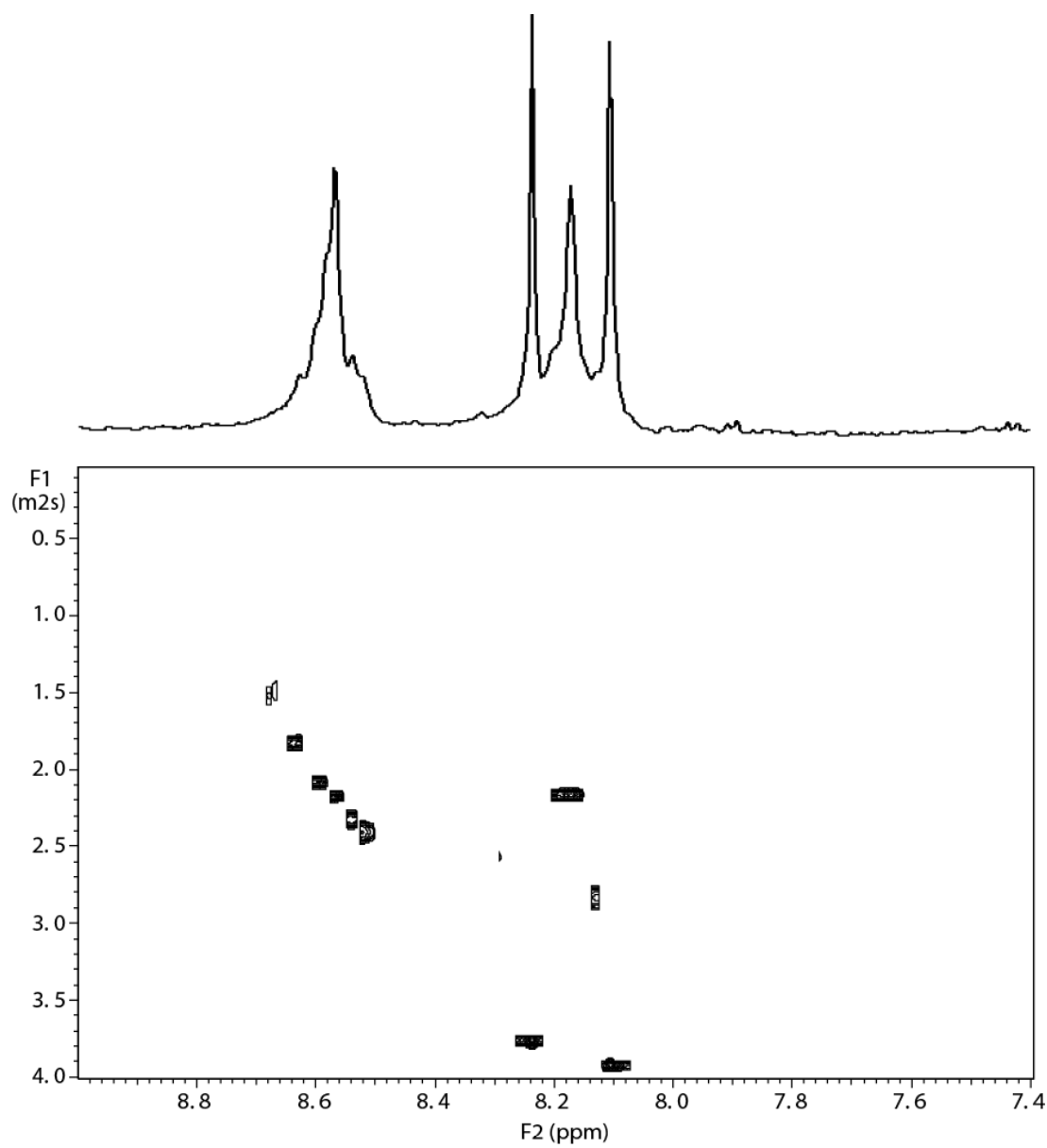
Figure 3-47. 2D DOSY of [*S*] monothiophosphate in Na$^+$ form at 30 °C
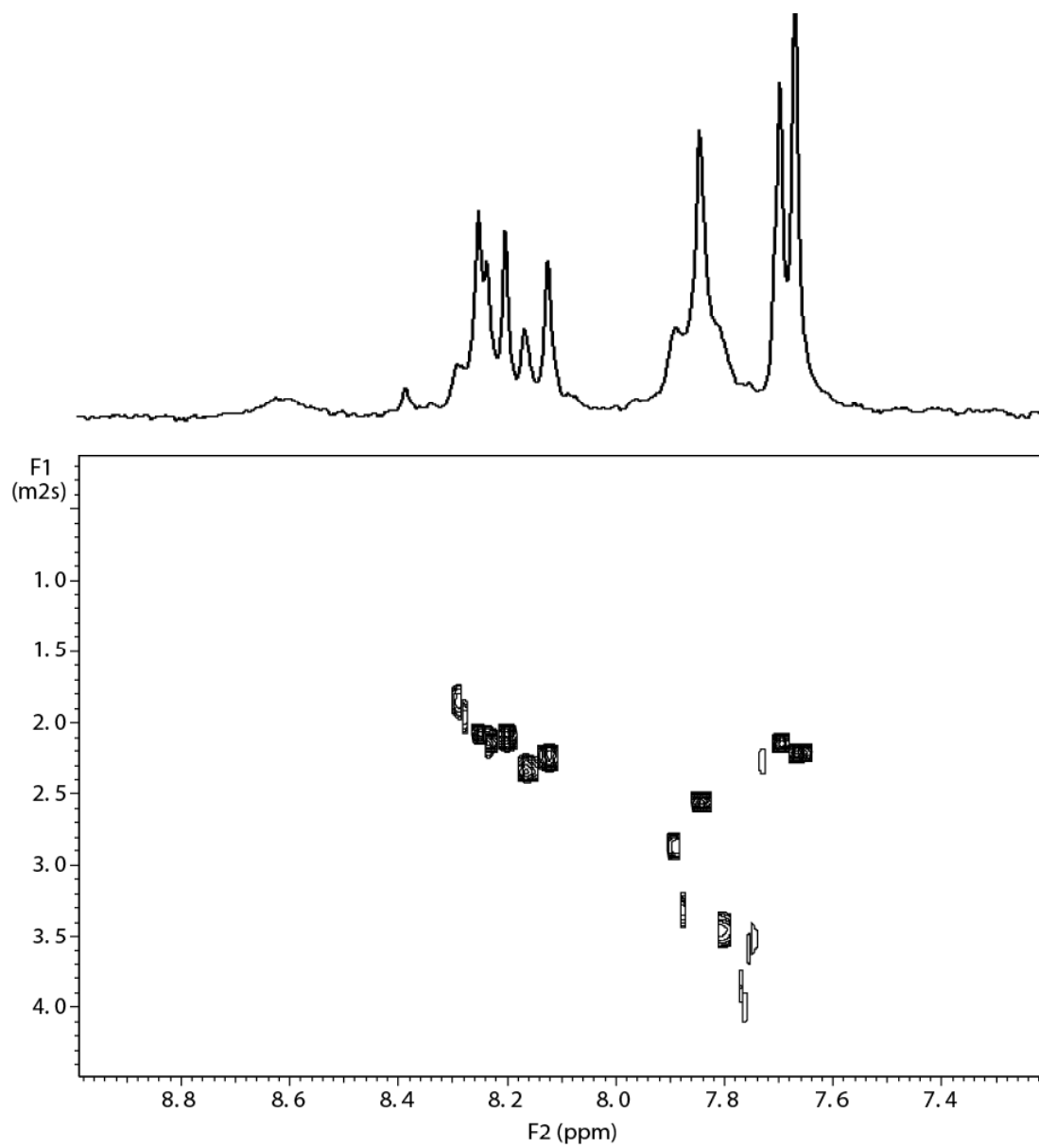
Figure 3-48. 2D DOSY of [*R, R*] dithiophosphate in Na⁺ form at 30 °C
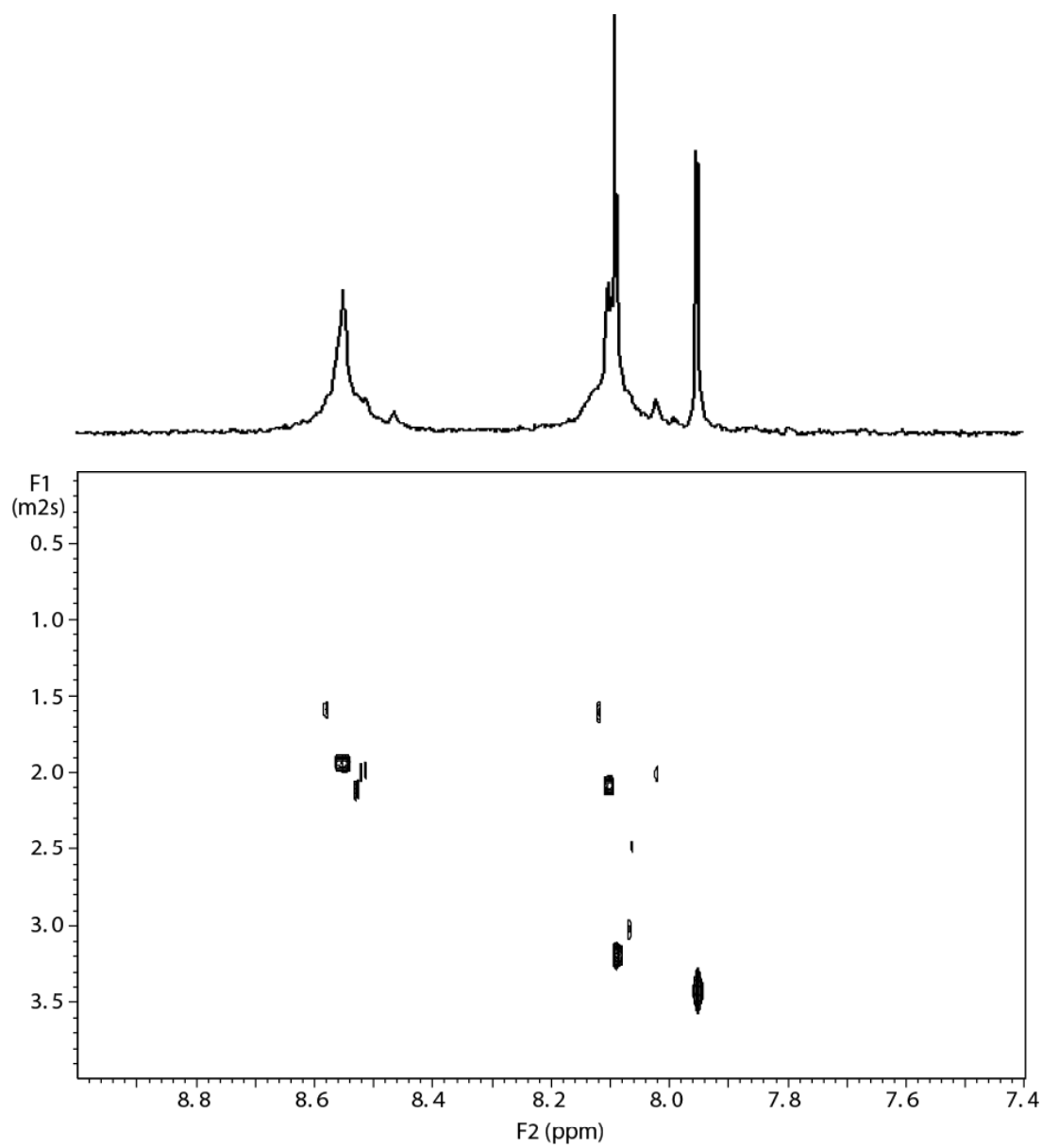
Figure 3-49. 2D DOSY of [*R, S*] dithiophosphate in Na$^+$ form at 30 °C
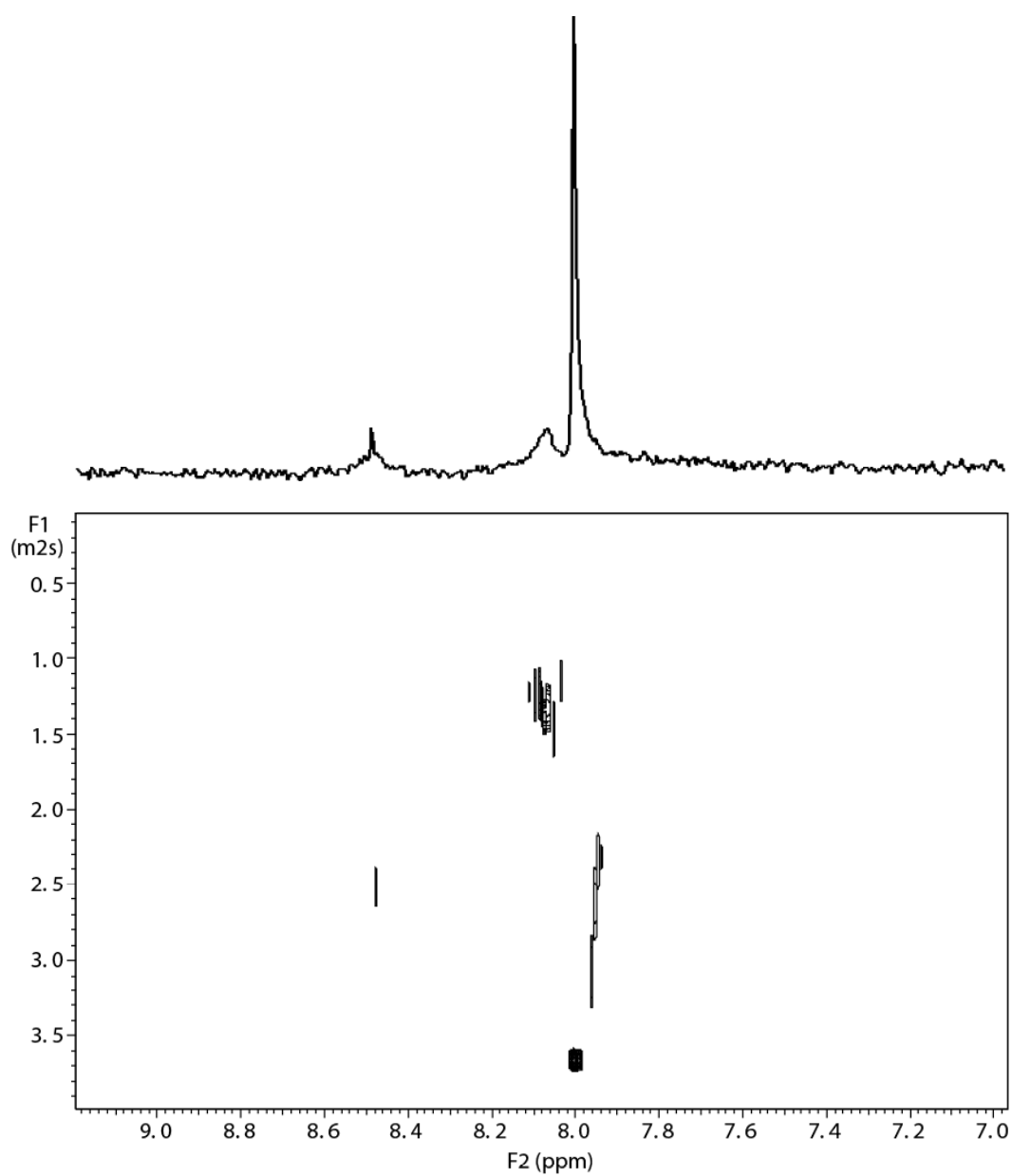
Figure 3-50. 2D DOSY of [*S, S*] dithiophosphate in Na$^+$ form at 30 °C
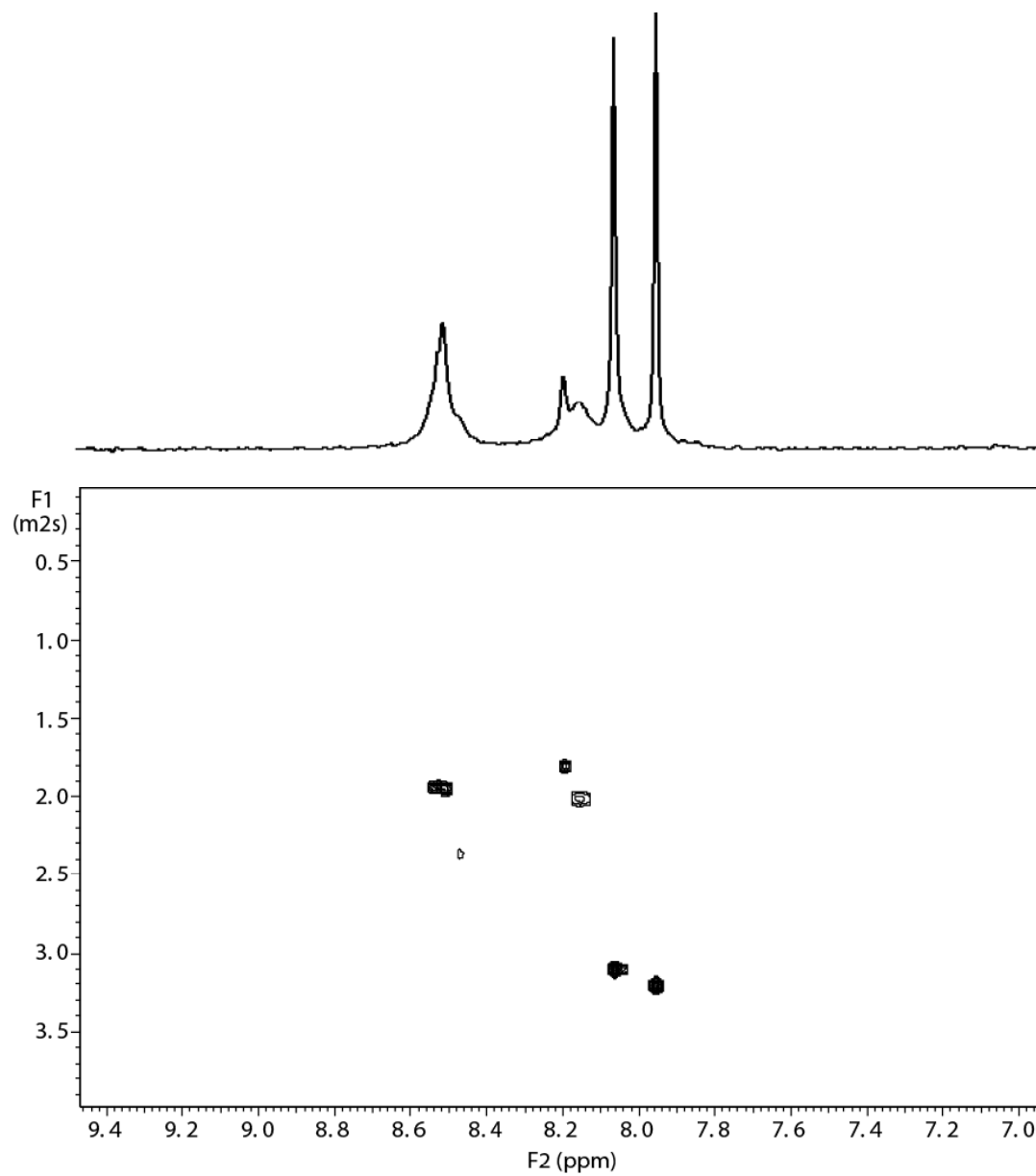
Figure 3-51. 2D DOSY of [*R*] trithiophosphate in Na$^+$ form at 30 °C
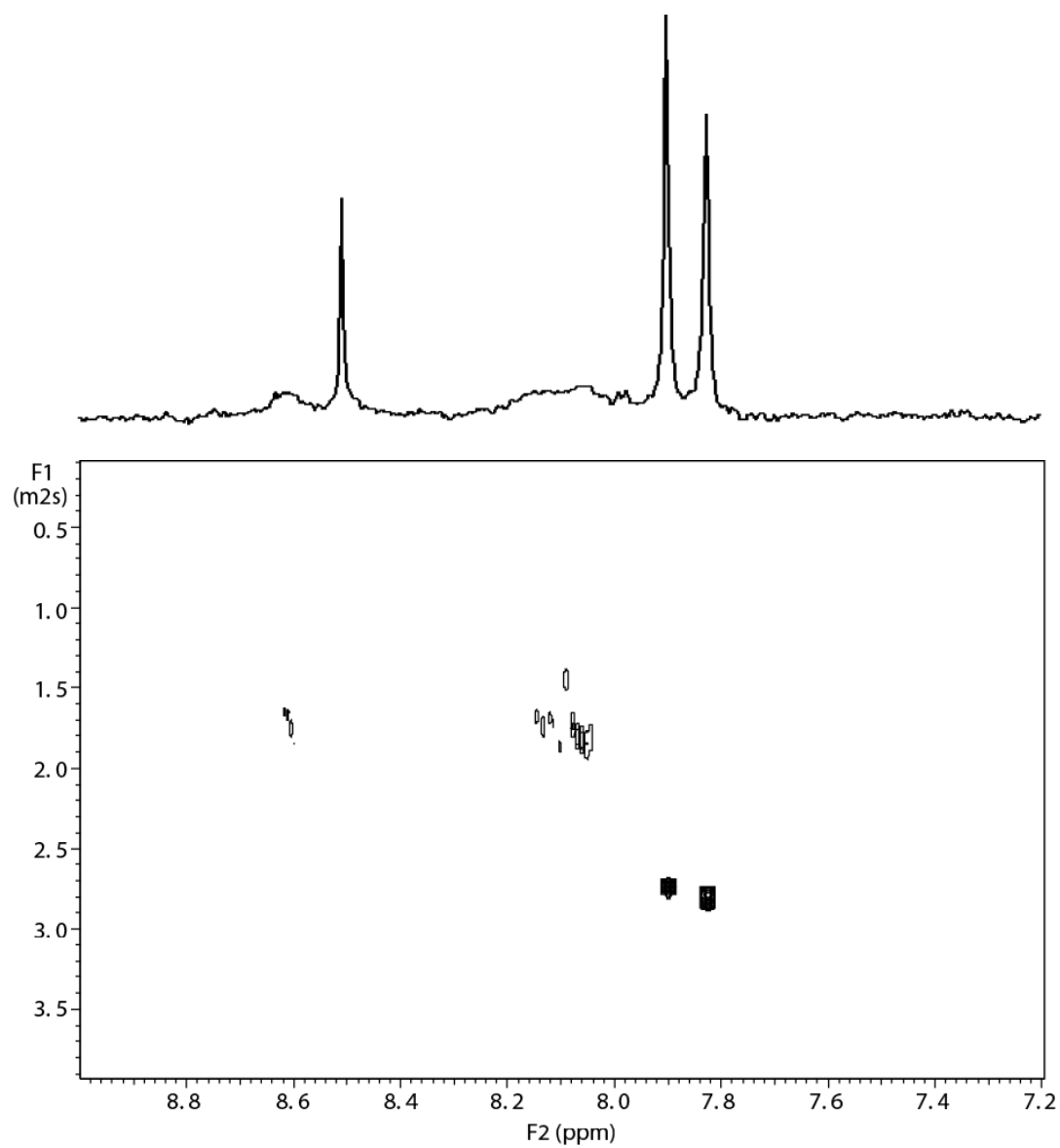
Figure 3-52. 2D DOSY of [*S*] trithiophosphate in Na$^+$ form at 30 °C

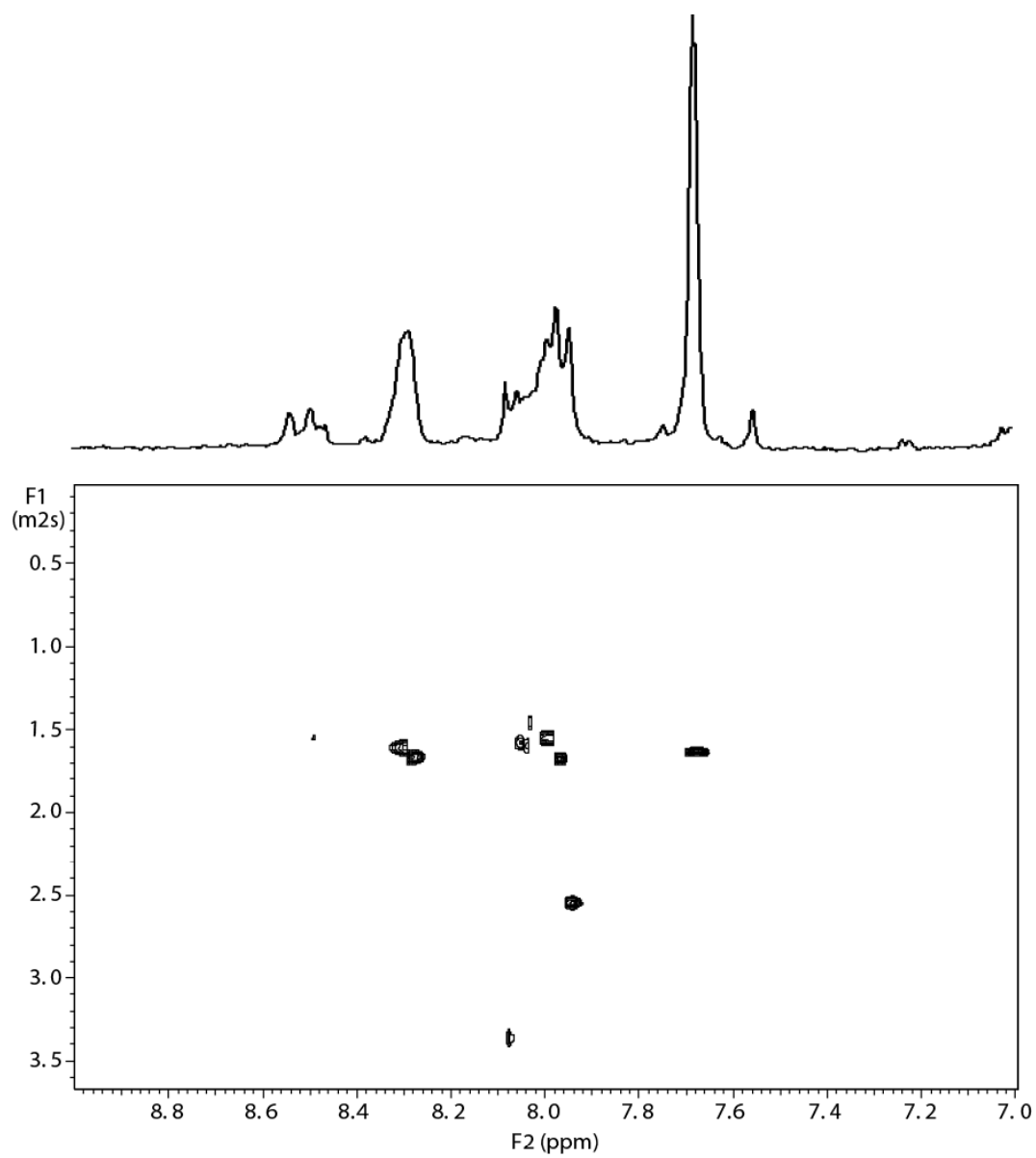**Figure 3-53.** 2D DOSY of [*R*] monothiophosphate in K⁺ form at 30 °C

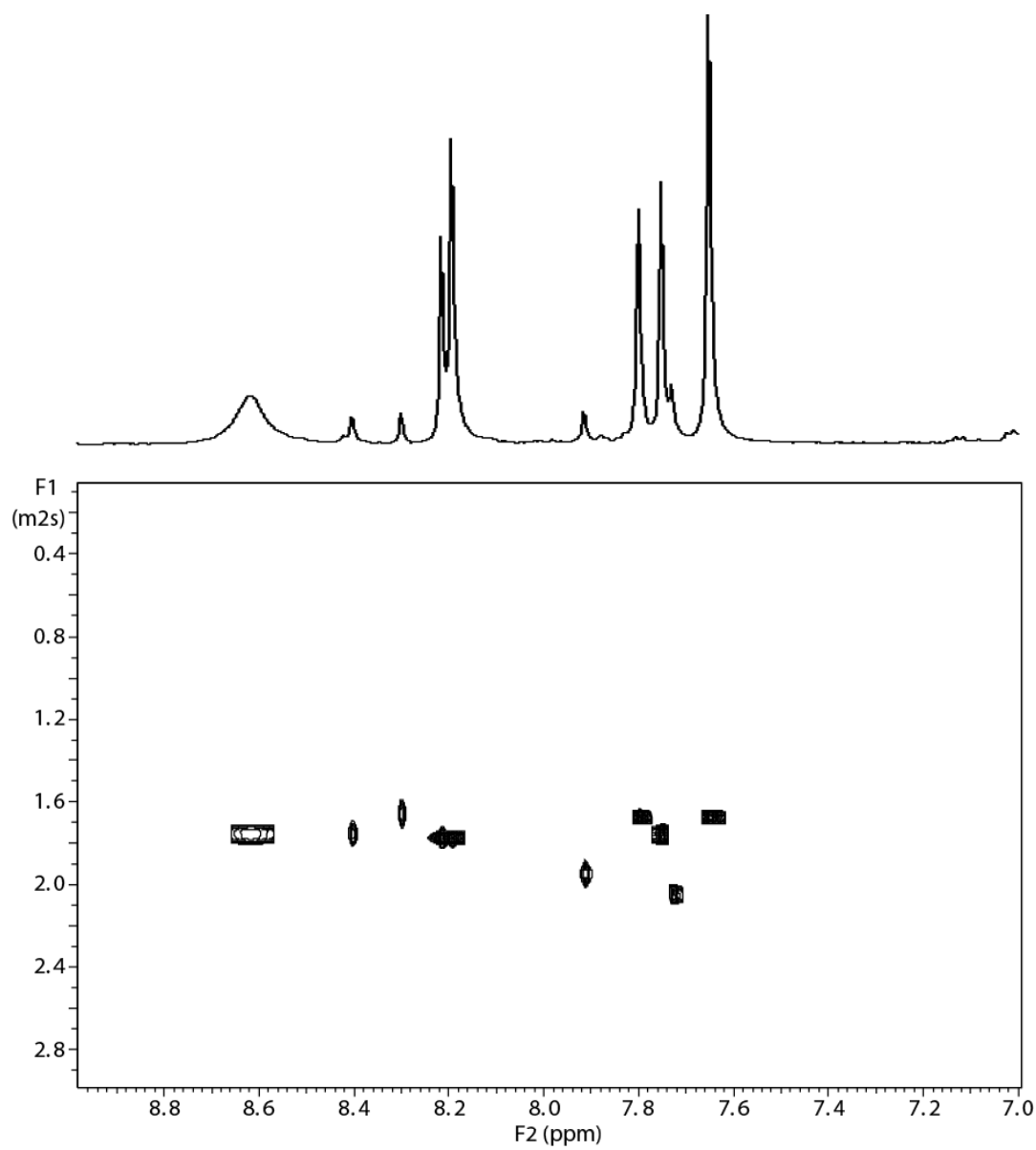**Figure 3-54.** 2D DOSY of [*S*] monothiophosphate in K$^+$ form at 30 °C

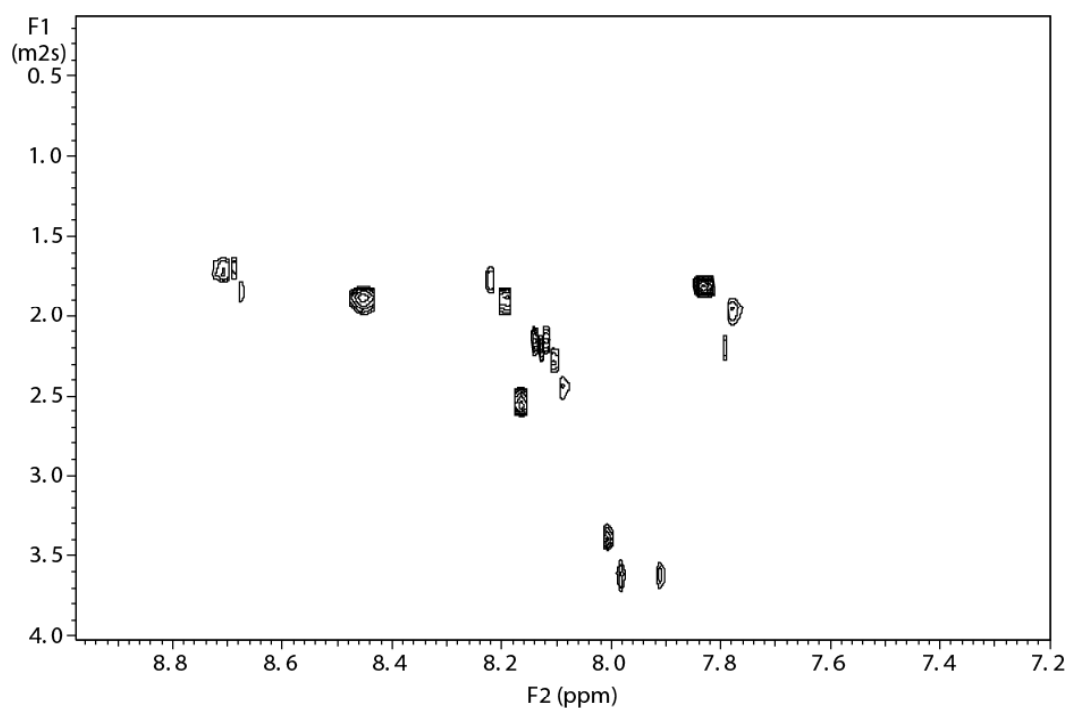**Figure 3-55.** 2D DOSY of [*R, R*] dithiophosphate in K⁺ form at 30 °C

Figure 3-56. 2D DOSY of [*R, S*] dithiophosphate in K⁺ form at 30 °C
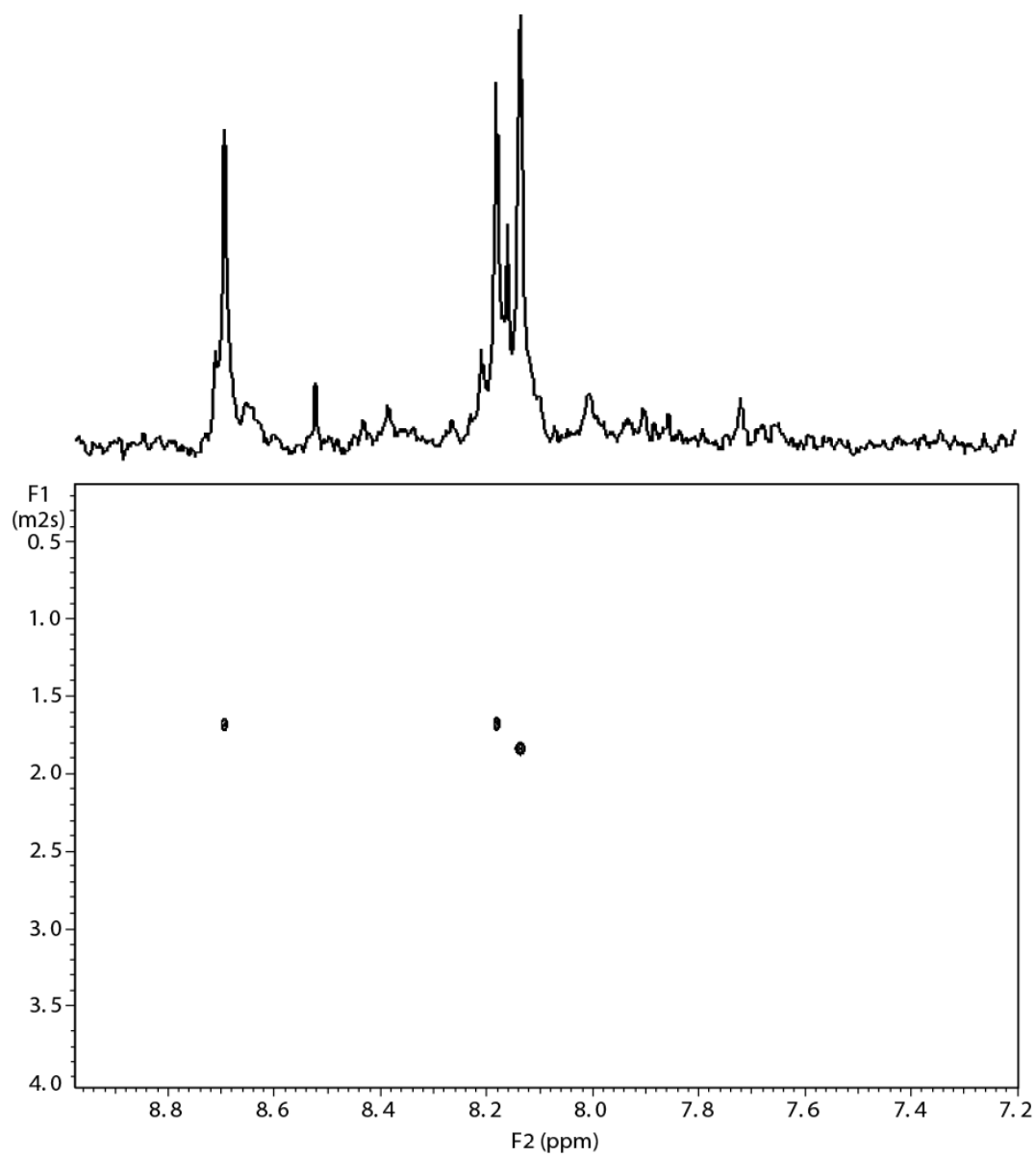
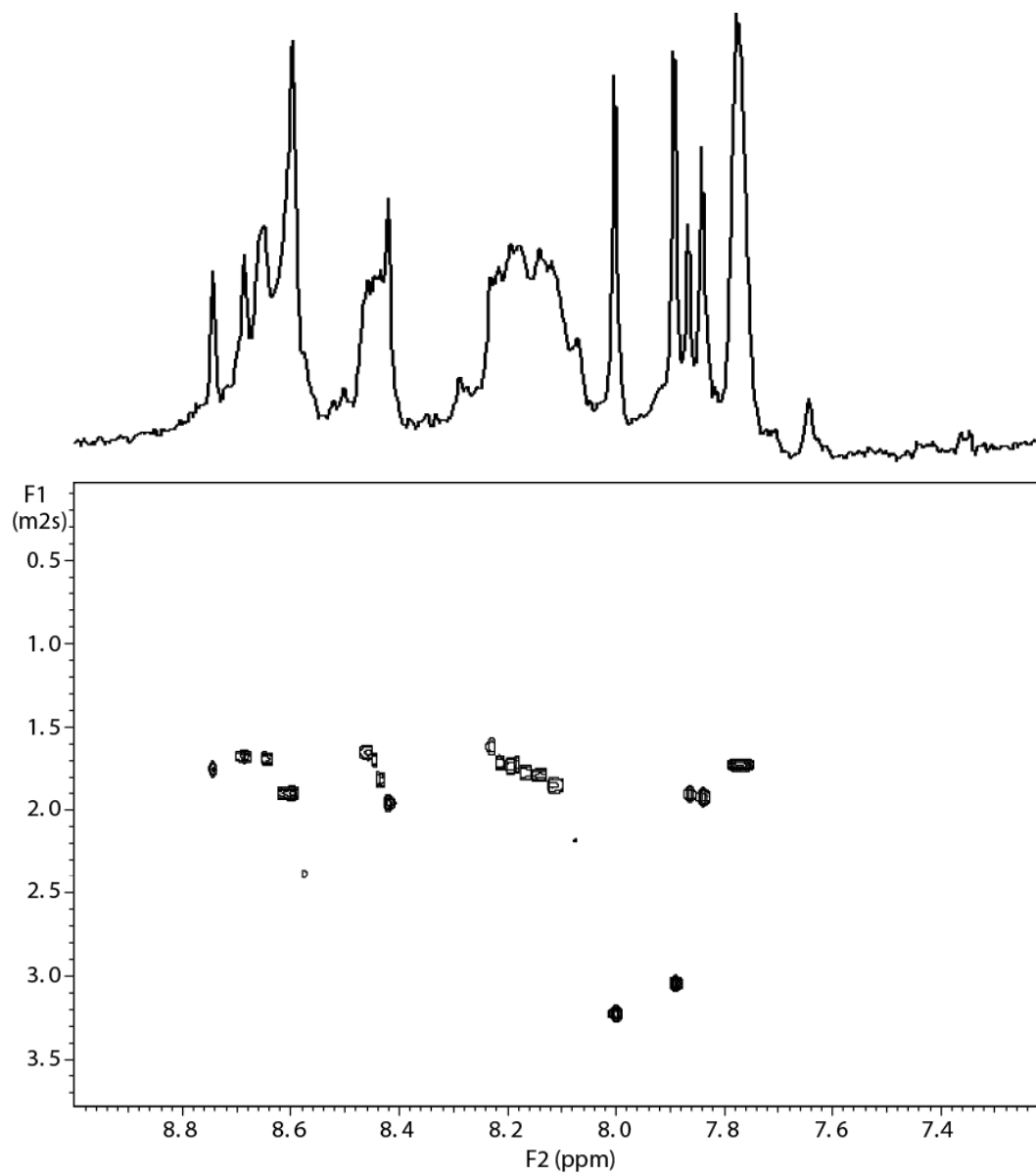**Figure 3-57.** 2D DOSY of [*S, S*] dithiophosphate in K$^+$ form at 30 °C

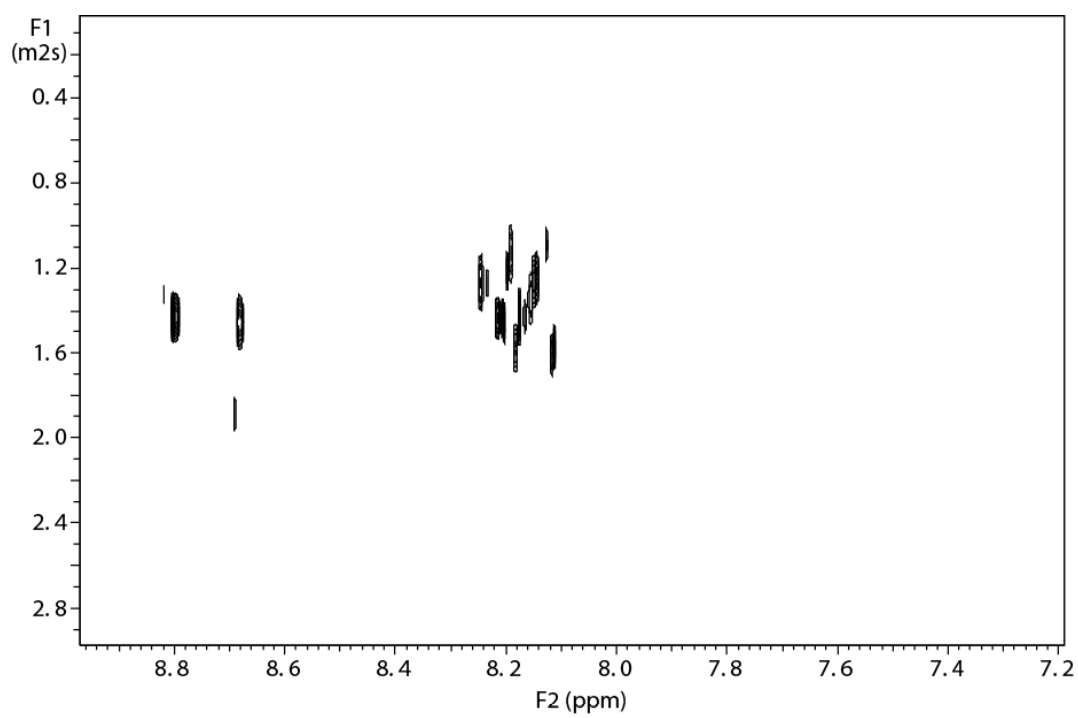**Figure 3-58.** 2D DOSY of [*R*] trithiophosphate in K$^+$ form at 30 °C

Figure 3-59. 2D DOSY of [*S*] trithiophosphate in K$^+$ form at 30 °C

CURRICULUM VITAE

Jianwei Zhao

Education:

1995 - 1999	B.S., Chemistry Fudan University, Shanghai, P. R. China
1999 - 2002	M.S., Analytical Chemistry Fudan University, Shanghai, P. R. China
2002 - 2009	Ph.D., in Organic Chemistry Rutgers, The State University of New Jersey

Publications:

Jianwei Zhao, Elizabeth Veliath, Seho Kim, Barbara L. Gaffney, and Roger A. Jones, "Impact of Thiophosphate Linkages on c-di-GMP Polymorphism" submitted to *Nucleosides, nucleotides & nucleic acids*

Weimin Wang, **Jianwei Zhao**, *et al.* "Modulation of RNA Metal Binding by Flanking Bases: ^{15}N NMR Evaluation of GC, Tandem GU, and Tandem GA Sites" submitted to *Nucleosides, nucleotides & nucleic acids*

Brock Matter, Rebecca Guza, **Jianwei Zhao**, Zhong-ze Li, Roger A. Jones, *et al.* "Sequence Distribution of Acetaldehyde-Derived N2-Ethyl-dG Adducts along Duplex DNA." *Chem. Res. Toxicol.* **2007**, 20, 1379–1387

Jianwei Zhao, Pengyuan Yang, *et al.* "Biomolecule Separation Using Large Pore Mesoporous SBA-15 as a Substrate in High Performance Liquid Chromatography" *Chem. Commun.*, **2002**, 752-753

Feng Gao, **Jianwei Zhao**, *et al.* "Using of C_{18}-Modified Mesoporous SBA-15 as the Substrate for High Performance Liquid Chromatography" *Chem. J. Chin. Univ.* (Chinese) **2002**, 23 (8): 1494-1497

Song Zhang, Fang Huang, **Jianwei Zhao**, *et al.* "Determination of thiols in urinary sample by capillary-column liquid chromatography with amperometric detection at a carbon electrode" *TALANTA* **2002**, 58 (3): 451-458

Jianwei Zhao, Feng Gao, *et al.* "Application of Mesoporous SBA-15 in Liquid Chromatography" *Chemical Word* (Supplement, Chinese), **2001**, 26-27